



WJG

World Journal of Gastroenterology®

Indexed and Abstracted in:

Current Contents®/Clinical Medicine, Science Citation Index Expanded (also known as SciSearch®), Journal Citation Reports/Science Edition, Index Medicus, MEDLINE, PubMed, Chemical Abstracts, EMBASE/Excerpta Medica, Abstracts Journals, PubMed Central, Digital Object Identifier, CAB Abstracts, and Global Health. ISI, Thomson Reuters, 2008 Impact Factor: 2.081 (32/55 Gastroenterology and Hepatology).

Volume 15 Number 46

December 14, 2009

World J Gastroenterol

2009 December 14; 15(46): 5761-5888

Online Submissions

wjg.wjgnet.com

www.wjgnet.com

Printed on Acid-free Paper

世界胃肠病学杂志

World Journal of Gastroenterology®

Editorial Board

2007-2009



Editorial Office: *World Journal of Gastroenterology*
Room 903, Building D, Ocean International Center

No. 62 Dongsihuan Zhonglu, Chaoyang District, Beijing 100025, China
E-mail: wjg@wjgnet.com http://www.wjgnet.com Telephone: 0086-10-5908-0039 Fax: 0086-10-8538-1893

The *World Journal of Gastroenterology* Editorial Board consists of 1126 members, representing a team of worldwide experts in gastroenterology and hepatology. They are from 60 countries, including Albania (1), Argentina (4), Australia (39), Austria (10), Belarus (1), Belgium (15), Brazil (2), Bulgaria (1), Canada (24), Chile (1), China (36), Croatia (2), Cuba (1), Czech (3), Denmark (7), Egypt (3), Estonia (1), Finland (4), France (42), Germany (104), Greece (8), Hungary (2), Iceland (1), India (11), Iran (4), Ireland (3), Israel (8), Italy (95), Japan (164), Lebanon (3), Lithuania (1), Macedonia (1), Malaysia (3), Mexico (5), Monaco (1), Morocco (1), The Netherlands (26), New Zealand (1), Nigeria (1), Norway (3), Pakistan (2), Peru (1), Poland (7), Portugal (1), Russia (3), Saudi Arabia (2), Serbia (1), Singapore (5), Slovakia (2), Slovenia (1), South Africa (2), South Korea (14), Spain (36), Sweden (15), Switzerland (14), Turkey (8), United Arab Emirates (1), United Kingdom (77), United States (290), and Uruguay (1).

HONORARY EDITORS-IN-CHIEF

Montgomery Bissell, San Francisco
James L Boyer, New Haven
Ke-Ji Chen, Beijing
Jacques Van Dam, Stanford
Martin H Floch, New Haven
Guadalupe Garcia-Tsao, New Haven
Zhi-Qiang Huang, Beijing
Ira M Jacobson, New York
Derek Jewell, Oxford
Emmet B Keeffe, Palo Alto
Nicholas F LaRusso, Rochester
Jie-Shou Li, Nanjing
Geng-Tao Liu, Beijing
Bo-Rong Pan, Xi'an
Fa-Zu Qiu, Wuhan^[2]
Eamonn M Quigley, Cork
David S Rampton, London
Rafiq A Sheikh, Sacramento
Rudi Schmid, Kentfield^[1]
Nicholas J Talley, Rochester
Guido NJ Tytgat, Amsterdam
Meng-Chao Wu, Shanghai
Jia-Yu Xu, Shanghai

PRESIDENT AND EDITOR-IN-CHIEF

Lian-Sheng Ma, Beijing

STRATEGY ASSOCIATE EDITORS-IN-CHIEF

Peter Draganov, Florida
Ronnie Fass, Tucson
Hugh J Freeman, Vancouver
John P Geibel, New Haven

MARIA CONCEPCIÓN GUTIÉRREZ-RUIZ, MÉXICO

Kazuhiro Hanazaki, Kochi
Akio Inui, Kagoshima
Kalpesh Jani, Baroda
Sanaa M Kamal, Cairo
Ioannis E Koutroubakis, Heraklion
Jose JG Marin, Salamanca
Javier S Martin, Punta del Este
Natalia A Osna, Omaha
Jose Sahel, Marseille
Ned Snyder, Galveston
Nathan Subramaniam, Brisbane
Wei Tang, Tokyo
Alan BR Thomson, Edmonton
Paul Joseph Thuluvath, Baltimore
James F Trotter, Denver
Shingo Tsuji, Osaka
Harry HX Xia, Hanover
Yoshio Yamaoka, Houston
Jesus K Yamamoto-Furusho, Mexico

ASSOCIATE EDITORS-IN-CHIEF

Gianfranco D Alpini, Temple
Bruno Annibale, Roma
Roger W Chapman, Oxford
Chi-Hin Cho, Hong Kong
Alexander L Gerbes, Munich
Shou-Dong Lee, Taipei
Walter E Longo, New Haven
You-Yong Lu, Beijing
Masao Omata, Tokyo

BIOSTATISTICAL EDITOR

Liang-Ping Hu, Beijing

GUEST EDITORIAL BOARD MEMBERS

Chao-Long Chen, Kaohsiung
Li-Fang Chou, Taipei
Kevin Cheng-Wen Hsiao, Taipei
Shinn-Jang Hwang, Taipei
Ira M Jacobson, New York
Min-Liang Kuo, Taipei
Lein-Ray Mo, Tainan
Sun-Lung Tsai, Young-Kang City
Hsiu-Po Wang, Taipei
Ta-Sen Yeh, Tao yuan
Ming-Lung Yu, Kaohsiung

MEMBERS OF THE EDITORIAL BOARD



Albania

Bashkim Resuli, Tirana



Argentina

Julio H Carri, Córdoba
Carlos J Pirola, Buenos Aires
Silvia Sookoian, Buenos Aires
Adriana M Torres, Rosario



Australia

Leon Anton Adams, Nedlands
Minoti V Apte, Liverpool

Richard B Banati, *Lidcombe*
 Michael R Beard, *Adelaide*
 Patrick Bertolino, *Sydney*
 Andrew V Biankin, *Sydney*
 Filip Braet, *Sydney*
 Andrew D Clouston, *Sydney*
 Graham Cooksley, *Queensland*
 Darrell HG Crawford, *Brisbane*
 Adrian G Cummins, *Woodville South*
 Guy D Eslick, *Sydney*
 Michael A Fink, *Melbourne*
 Robert JL Fraser, *Daw Park*
 Peter Raymond Gibson, *Victoria*
 Jacob George, *Westmead*
 Mark D Gorrell, *Sydney*
 Yik-Hong Ho, *Townsville*
 Gerald J Holtmann, *Adelaide*
 Michael Horowitz, *Adelaide*
 John E Kellow, *Sydney*
 Rupert Leong, *Concord*
 Geoffrey W McCaughan, *Sydney*
 Finlay A Macrae, *Victoria*
 Daniel Markovich, *Brisbane*
 Phillip S Oates, *Perth*
 Jacqui Richmond, *Victoria*
 Stephen M Riordan, *Sydney*
 Ian C Roberts-Thomson, *Adelaide*
 Devanshi Seth, *Campdown*
 Arthur Shulkes, *Melbourne*
 Ross C Smith, *Sydney*
 Kevin J Spring, *Brisbane*
 Herbert Tilg, *Innsbruck*
 Huy A Tran, *New South Wales*
 Debbie Trinder, *Fremantle*
 Martin J Veysey, *Gosford*
 Daniel L Worthley, *Bedford*
 David Ian Watson, *South Australia*



Austria

Peter Ferenci, *Vienna*
 Valentin Fuhrmann, *Vienna*
 Alfred Gangl, *Vienna*
 Christoph Gasche, *Vienna*
 Kurt Lenz, *Linz*
 Markus Peck-Radosavljevic, *Vienna*
 Rudolf E Stauber, *Auenbruggerplatz*
 Michael Trauner, *Graz*
 Harald Vogelsang, *Vienna*
 Guenter Weiss, *Innsbruck*



Belarus

Yury K Marakhouski, *Minsk*



Belgium

Rudi Beyaert, *Gent*
 Bart Rik De Geest, *Leuven*
 Inge I Depoortere, *Leuven*
 Olivier Detry, *Liège*
 Benedictie Y De Winter, *Antwerp*
 Karel Geboes, *Leuven*
 Thierry Gustot, *Brussels*
 Yves J Horsmans, *Brussels*
 Geert G Leroux-Roels, *Ghent*
 Louis Libbrecht, *Leuven*
 Etienne M Sokal, *Brussels*
 Marc Peeters, *De Pintelaan*
 Gert A Van Assche, *Leuven*
 Yvan Vandenplas, *Brussels*
 Eddie Wisse, *Keerbergen*



Brazil

Heitor Rosa, *Goiania*
 Ana Cristina Simões e Silva, *Belo Horizonte*



Bulgaria

Zahariy Krastev, *Sofia*



Canada

Fernando Alvarez, *Québec*
 David Armstrong, *Ontario*
 Jeffrey P Baker, *Toronto*
 Olivier Barbier, *Québec*
 Nancy Baxter, *Toronto*
 Frank J Burczynski, *Manitoba*
 Michael F Byrne, *Vancouver*
 Wang-Xue Chen, *Ottawa*
 Samuel S Lee, *Calgary*
 Gary A Levy, *Toronto*
 Andrew L Mason, *Alberta*
 John K Marshall, *Ontario*
 Donna-Marie McCafferty, *Calgary*
 Thomas I Michalak, *St. John's*
 Gerald Y Minuk, *Manitoba*
 Paul Moayyedi, *Hamilton*
 Kostas Pantopoulos, *Quebec*
 William G Paterson, *Kingston*
 Eldon Shaffer, *Calgary*
 Martin Storr, *Calgary*
 E F Verdu, *Ontario*
 Walilul Khan, *Ontario*
 John L Wallace, *Calgary*
 Eric M Yoshida, *Vancouver*



Chile

Silvana Zanolungo, *Santiago*



China

Henry LY Chan, *Hong Kong*
 Xiao-Ping Chen, *Wuhan*
 Zong-Jie Cui, *Beijing*
 Da-Jun Deng, *Beijing*
 Er-Dan Dong, *Beijing*
 Sheung-Tat Fan, *Hong Kong*
 Jin Gu, *Beijing*
 Xin-Yuan Guan, *Pokfulam*
 De-Wu Han, *Taiyuan*
 Ming-Liang He, *Hong Kong*
 Wayne HC Hu, *Hong Kong*
 Chee-Kin Hui, *Hong Kong*
 Ching-Lung Lai, *Hong Kong*
 Kam Chuen Lai, *Hong Kong*
 James YW Lau, *Hong Kong*
 Yuk-Tong Lee, *Hong Kong*
 Suet-Yi Leung, *Hong Kong*
 Wai-Keung Leung, *Hong Kong*
 John M Luk, *Pokfulam*
 Chung-Mau Lo, *Hong Kong*
 Jing-Yun Ma, *Beijing*
 Ronnie Tung Ping Poon, *Hong Kong*
 Lun-Xiu Qin, *Shanghai*
 Yu-Gang Song, *Guangzhou*
 Qin Su, *Beijing*
 Wai-Man Wong, *Hong Kong*
 Hong Xiao, *Shanghai*

Dong-Liang Yang, *Wuhan*
 Winnie Yeo, *Hong Kong*
 Yuan Yuan, *Shenyang*
 Man-Fung Yuen, *Hong Kong*
 Jian-Zhong Zhang, *Beijing*
 Xin-Xin Zhang, *Shanghai*
 Bo-Jian Zheng, *Hong Kong*
 Shu Zheng, *Hangzhou*
 Xiao-Peng Zhang, *Beijing*



Croatia

Tamara Cacev, *Zagreb*
 Marko Duvnjak, *Zagreb*



Cuba

Damian C Rodriguez, *Havana*



Czech

Milan Jirsa, *Praha*
 Pavel Trunečka, *Prague*
 Marcela Kopacova, *Hradec Kralove*



Denmark

Peter Bytzer, *Copenhagen*
 Asbjørn M Drewes, *Aalborg*
 Hans Gregersen, *Aalborg*
 Jens H Henriksen, *Hvidovre*
 Claus P Hovendal, *Odense*
 Fin S Larsen, *Copenhagen*
 SØren Møller, *Hvidovre*



Egypt

Abdel-Rahman El-Zayadi, *Giza*
 Amr M Helmy, *Cairo*
 Ayman Yosry, *Cairo*



Estonia

Riina Salupere, *Tartu*



Finland

Irma E Jarvela, *Helsinki*
 Katri M Kaukinen, *Tampere*
 Minna Nyström, *Helsinki*
 Pentti Sipponen, *Espoo*



France

Bettaiib Ali, *Dijon*
 Anne Corlu, *Rennes*
 Denis Ardid, *Clermont-Ferrand*
 Charles P Balabaud, *Bordeaux*
 Soumeya Bekri, *Rouen*
 Jacques Belghiti, *Clichy*
 Jacques Bernauau, *Clichy Cedex*
 Pierre Brissot, *Rennes*
 Patrice P Cacoub, *Paris*
 Franck Carbonnel, *Besançon*
 Laurent Castera, *Pessac*
 Bruno Clément, *Rennes*
 Benoit Coffin, *Colombes*
 Thomas Decaens, *Cedex*
 Francoise L Fabiani, *Angers*

Gérard Feldmann, *Paris*
 Jean Fioramonti, *Toulouse*
 Jean-Noël Freund, *Strasbourg*
 Catherine Guettier, *Villejuif*
 Chantal Housset, *Paris*
 Juan L Iovanna, *Marseille*
 Rene Lambert, *Lyon*
 Patrick Marcellin, *Paris*
 Philippe Mathurin, *Lille*
 Tamara Matysiak-Budnik, *Paris*
 Francis Mégraud, *Bordeaux*
 Richard Moreau, *Clichy*
 Thierry Piche, *Nice*
 Raoul Poupon, *Paris*
 Jean Rosenbaum, *Bordeaux*
 Dominique Marie Roulot, *Bobigny*
 Thierry Poynard, *Paris*
 Jean-Philippe Salier, *Rouen*
 Didier Samuel, *Villejuif*
 Jean-Yves Scoazec, *Lyon*
 Alain L Servin, *Châtenay-Malabry*
 Khalid A Tazi, *Clichy*
 Emmanuel Tiret, *Paris*
 Baumert F Thomas, *Strasbourg*
 Jean-Pierre H Zarski, *Grenoble*
 Jessica Zucman-Rossi, *Paris*
 Boris Guiu, *Dijon*



Germany

Hans-Dieter Allescher, *G-Partenkirchen*
 Martin Anlauf, *Kiel*
 Rudolf Arnold, *Marburg*
 Max G Bachem, *Ulm*
 Thomas F Baumert, *Freiburg*
 Daniel C Baumgart, *Berlin*
 Hubert Blum, *Freiburg*
 Thomas Bock, *Tuebingen*
 Katja Breitkopf, *Mannheim*
 Dunja Bruder, *Braunschweig*
 Markus W Büchler, *Heidelberg*
 Christa Buechler, *Regensburg*
 Reinhard Buettner, *Bonn*
 Elke Cario, *Essen*
 Uta Dahmen, *Essen*
 Christoph F Dietrich, *Bad Mergentheim*
 Arno J Dormann, *Koeln*
 Rainer J Duchmann, *Berlin*
 Volker F Eckardt, *Wiesbaden*
 Fred Fändrich, *Kiel*
 Ulrich R Fölsch, *Kiel*
 Helmut Friess, *Heidelberg*
 Peter R Galle, *Mainz*
 Nikolaus Gassler, *Aachen*
 Markus Gerhard, *Munich*
 Wolfram H Gerlich, *Giessen*
 Dieter Glebe, *Giessen*
 Burkhard Göke, *Munich*
 Florian Graepler, *Tuebingen*
 Axel M Gressner, *Aachen*
 Veit Güllberg, *Munich*
 Rainer Haas, *Munich*
 Eckhart G Hahn, *Erlangen*
 Stephan Hellwig, *Kiel*
 Martin Hennenberg, *Bonn*
 Johannes Herkel, *Hamburg*
 Klaus R Herrlinger, *Stuttgart*
 Eva Herrmann, *Homburg/Saar*
 Eberhard Hildt, *Berlin*
 Jörg C Hoffmann, *Berlin*
 Ferdinand Hofstaedter, *Regensburg*
 Werner Hohenberger, *Erlangen*
 Jörg C Kalff, *Bonn*

Ralf Jakobs, *Ludwigshafen*
 Jutta Keller, *Hamburg*
 Andrej Khandoga, *Munich*
 Sibylle Koletzko, *München*
 Stefan Kubicka, *Hannover*
 Joachim Labenz, *Siegen*
 Frank Lammert, *Bonn*
 Thomas Langmann, *Regensburg*
 Christian Liedtke, *Aachen*
 Matthias Löhr, *Stockholm*
 Christian Maaser, *Muenster*
 Ahmed Madisch, *Dresden*
 Peter Malfertheiner, *Magdeburg*
 Michael P Manns, *Hannover*
 Helmut Messmann, *Augsburg*
 Stephan Miehlke, *Dresden*
 Sabine Mihm, *Göttingen*
 Silvio Nadalin, *Tuebingen*
 Markus F Neurath, *Mainz*
 Johann Ockenga, *Berlin*
 Florian Obermeier, *Regensburg*
 Gustav Paumgartner, *Munich*
 Ulrich KS Peitz, *Magdeburg*
 Markus Reiser, *Bochum*
 Emil C Reisinger, *Rostock*
 Steffen Rickes, *Magdeburg*
 Tilman Sauerbruch, *Bonn*
 Dieter Saur, *Munich*
 Hans Scherübl, *Berlin*
 Joerg Schirra, *Munich*
 Roland M Schmid, *München*
 Volker Schmitz, *Bonn*
 Andreas G Schreyer, *Regensburg*
 Tobias Schroeder, *Essen*
 Henning Schulze-Bergkamen, *Mainz*
 Norbert Senninger, *Muenster*
 Hans Seifert, *Oldenburg*
 Manfred V Singer, *Mannheim*
 Gisela Sparmann, *Rostock*
 Christian J Steib, *München*
 Jurgen M Stein, *Frankfurt*
 Ulrike S Stein, *Berlin*
 Manfred Stolte, *Bayreuth*
 Christian P Strassburg, *Hannover*
 Wolfgang R Stremmel, *Heidelberg*
 Harald F Teutsch, *Ulm*
 Robert Thimme, *Freiburg*
 Hans L Tillmann, *Leipzig*
 Tung-Yu Tsui, *Regensburg*
 Axel Ulsenheimer, *Munich*
 Patrick Veit-Haibach, *Essen*
 Claudia Veltkamp, *Heidelberg*
 Siegfried Wagner, *Deggendorf*
 Henning Walczak, *Heidelberg*
 Heiner Wedemeyer, *Hannover*
 Fritz von Weizsäcker, *Berlin*
 Jens Werner, *Heidelberg*
 Bertram Wiedemann, *Berlin*
 Reiner Wiest, *Regensburg*
 Stefan Wirth, *Wuppertal*
 Stefan JP Zeuzem, *Homburg*



Greece

Alexandra A Alexopoulou, *Athens*
 George N Dalekos, *Larissa*
 Christos Dervenis, *Athens*
 Melanier Maria Deutsch, *Athens*
 Tsianos Epameinondas, *Ioannina*
 Elias A Kouroumalis, *Heraklion*
 George Papatheodoridis, *Athens*
 Spiros Sgouros, *Athens*



Hungary

Peter L Lakatos, *Budapest*
 Szuzsa Szondy, *Debrecen*



Iceland

Hallgrimur Gudjonsson, *Reykjavik*



India

Philip Abraham, *Mumbai*
 Rakesh Aggarwal, *Lucknow*
 Kunissery A Balasubramanian, *Vellore*
 Deepak Kumar Bhasin, *Chandigarh*
 Sujit K Bhattacharya, *Kolkata*
 Yogesh K Chawla, *Chandigarh*
 Radha K Dhiman, *Chandigarh*
 Sri P Misra, *Allahabad*
 Ramesh Roop Rai, *Jaipur*
 Nageshwar D Reddy, *Hyderabad*
 Rakesh Kumar Tandon, *New Delhi*



Iran

Mohammad Abdollahi, *Tehran*
 Seyed-Moayed Alavian, *Tehran*
 Reza Malekzadeh, *Tehran*
 Seyed A Taghavi, *Shiraz*



Ireland

Billy Bourke, *Dublin*
 Ronan A Cahill, *Cork*
 Anthony P Moran, *Galway*



Israel

Simon Bar-Meir, *Hashomer*
 Abraham R Eliakim, *Haifa*
 Zvi Fireman, *Hadera*
 Yaron Ilan, *Jerusalem*
 Avidan U Neumann, *Ramat-Gan*
 Yaron Niv, *Pardesia*
 Ran Oren, *Tel Aviv*
 Ami D Sperber, *Beer-Sheva*



Italy

Giovanni Addolorato, *Roma*
 Luigi E Adinolfi, *Naples*
 Domenico Alvaro, *Rome*
 Vito Annese, *San Giovanni Rotond*
 Filippo Ansaldi, *Genoa*
 Adolfo F Attili, *Roma*
 Giovanni Barbara, *Bologna*
 Claudio Bassi, *Verona*
 Gabrio Bassotti, *Perugia*
 Pier M Battezzati, *Milan*
 Stefano Bellentani, *Carp*
 Antonio Benedetti, *Ancona*
 Mauro Bernardi, *Bologna*
 Livia Biancone, *Rome*
 Luigi Bonavina, *Milano*
 Flavia Bortolotti, *Padova*
 Giuseppe Brisinda, *Rome*
 Elisabetta Buscarini, *Crema*
 Giovanni Cammarota, *Roma*

Antonino Cavallari, *Bologna*
 Giuseppe Chiaroni, *Valeggio*
 Michele Cicala, *Rome*
 Massimo Colombo, *Milan*
 Amedeo Columbano, *Cagliari*
 Massimo Conio, *Sanremo*
 Dario Conte, *Milano*
 Gino R Corazza, *Pavia*
 Francesco Costa, *Pisa*
 Antonio Craxi, *Palermo*
 Silvio Danese, *Milan*
 Roberto de Franchis, *Milano*
 Roberto De Giorgio, *Bologna*
 Maria Stella De Mitteri, *Bologna*
 Giovanni D De Palma, *Naples*
 Fabio Farinati, *Padua*
 Giammarco Fava, *Ancona*
 Francesco Feo, *Sassari*
 Fiorucci Stefano, *Perugia*
 Andrea Galli, *Firenze*
 Valeria Ghisetti, *Turin*
 Gianluigi Giannelli, *Bari*
 Edoardo G Giannini, *Genoa*
 Paolo Gionchetti, *Bologna*
 Fabio Grizzi, *Milan*
 Salvatore Gruttaduria, *Palermo*
 Mario Guslandi, *Milano*
 Pietro Invernizzi, *Milan*
 Ezio Laconi, *Cagliari*
 Giacomo Laffi, *Firenze*
 Giovanni Maconi, *Milan*
 Lucia Malaguarnera, *Catania*
 Emanuele D Mangoni, *Napoli*
 Paolo Manzoni, *Torino*
 Giulio Marchesini, *Bologna*
 Fabio Marra, *Florence*
 Marco Marzioni, *Ancona*
 Roberto Mazzanti, *Florence*
 Giuseppe Mazzella, *Bologna*
 Giuseppe Montalto, *Palermo*
 Giovanni Monteleone, *Rome*
 Giovanni Musso, *Torino*
 Gerardo Nardone, *Napoli*
 Valerio Nobili, *Rome*
 Fabio Pace, *Milano*
 Luisi Pagliaro, *Palermo*
 Francesco Pallone, *Rome*
 Fabrizio R Parente, *Milan*
 Maurizio Parola, *Torino*
 Francesco Perri, *San Giovanni Rotondo*
 Raffaele Pezzilli, *Bologna*
 Alberto Pilotto, *San Giovanni Rotondo*
 Alberto Piperno, *Monza*
 Mario Pirisi, *Novara*
 Anna C Piscaglia, *Roma*
 Paolo Del Poggio, *Treviglio*
 Gabriele B Porro, *Milano*
 Piero Portincasa, *Bari*
 Cosimo Prantero, *Roma*
 Bernardino Rampone, *Siena*
 Oliviero Riggio, *Romer*
 Claudio Romano, *Messina*
 Marco Romano, *Napoli*
 Gerardo Rosati, *Potenza*
 Mario Del Tacca, *Pisa*
 Gloria Taliani, *Rome*
 Pier A Testoni, *Milan*
 Enrico Roda, *Bologna*
 Domenico Sansonno, *Bari*
 Vincenzo Savarino, *Genova*
 Vincenzo Stanghellini, *Bologna*
 Giovanni Tarantino, *Naples*
 Roberto Testa, *Genoa*
 Dino Vaira, *Bologna*
 Roberto Berni Canani, *Naples*
 Gianlorenzo Dionigi, *Varese*



Japan

Kyoichi Adachi, *Izumo*
 Yasushi Adachi, *Sapporo*
 Taiji Akamatsu, *Matsumoto*
 Sk Md Fazle Akbar, *Ehime*
 Takafumi Ando, *Nagoya*
 Akira Andoh, *Otsu*
 Taku Aoki, *Tokyo*
 Masahiro Arai, *Tokyo*
 Tetsuo Arakawa, *Osaka*
 Yasuji Arase, *Tokyo*
 Hitoshi Asakura, *Tokyo*
 Takeshi Azuma, *Fukui*
 Takahiro Fujimori, *Tochigi*
 Jiro Fujimoto, *Hyogo*
 Kazuma Fujimoto, *Saga*
 Mitsuhiro Fujishiro, *Tokyo*
 Yoshihide Fujiyama, *Otsu*
 Hirokazu Fukui, *Tochigi*
 Hiroyuki Hanai, *Hamamatsu*
 Naohiko Harada, *Fukuoka*
 Makoto Hashizume, *Fukuoka*
 Tetsuo Hayakawa, *Nagoya*
 Toru Hiyama, *Higashitiroshima*
 Kazuhide Higuchi, *Osaka*
 Keisuke Hino, *Ube*
 Keiji Hirata, *Kitakyushu*
 Yuji Iimuro, *Nishinomiya*
 Kenji Ikeda, *Tokyo*
 Kenichi Ikejima, *Bunkyo-ku*
 Fumio Imazeki, *Chiba*
 Yutaka Inagaki, *Kanagawa*
 Yasuhiro Inokuchi, *Yokohama*
 Haruhiro Inoue, *Yokohama*
 Masayasu Inoue, *Osaka*
 Hiromi Ishibashi, *Nagasaki*
 Shunji Ishihara, *Izumo*
 Toru Ishikawa, *Niigata*
 Kei Ito, *Sendai*
 Masayoshi Ito, *Tokyo*
 Toru Ikegami, *Fukuoka*
 Hiroaki Itoh, *Akita*
 Ryuichi Iwakiri, *Saga*
 Yoshiaki Iwasaki, *Okayama*
 Terumi Kamisawa, *Tokyo*
 Hiroshi Kaneko, *Aichi-gun*
 Shuichi Kaneko, *Kanazawa*
 Takashi Kanematsu, *Nagasaki*
 Mitsuo Katano, *Fukuoka*
 Mototsugu Kato, *Sapporo*
 Shinzo Kato, *Tokyo*
 Norifumi Kawada, *Osaka*
 Sunao Kawano, *Osaka*
 Mitsuhiro Kida, *Kanagawa*
 Yoshikazu Kinoshita, *Izumo*
 Tsuneo Kitamura, *Chiba*
 Seigo Kitano, *Oita*
 Kazuhiko Koike, *Tokyo*
 Norihiro Kokudo, *Tokyo*
 Shoji Kubo, *Osaka*
 Masatoshi Kudo, *Osaka*
 Katsunori Iijima, *Sendai*
 Shin Maeda, *Tokyo*
 Shigeru Marubashi, *Suita*
 Masatoshi Makuuchi, *Tokyo*
 Osamu Matsui, *Kanazawa*
 Yasuhiro Matsumura, *Kashiwa*
 Yasushi Matsuzaki, *Tsukuba*
 Kiyoshi Migita, *Omura*
 Kenji Miki, *Tokyo*
 Tetsuya Mine, *Kanagawa*
 Hiroto Miwa, *Hyogo*

Masashi Mizokami, *Nagoya*
 Yoshiaki Mizuguchi, *Tokyo*
 Motoivo Mizuno, *Hiroshima*
 Morito Monden, *Suita*
 Hisataka Moriawaki, *Gifu*
 Yasuaki Motomura, *Izuka*
 Yoshiharu Motoo, *Kanazawa*
 Naofumi Mukaida, *Kanazawa*
 Kazunari Murakami, *Oita*
 Kunihiko Murase, *Tusima*
 Hiroaki Nagano, *Suita*
 Masahito Nagaki, *Gifu*
 Atsushi Nakajima, *Yokohama*
 Yuji Naito, *Kyoto*
 Hisato Nakajima, *Tokyo*
 Hiroki Nakamura, *Yamaguchi*
 Shotaro Nakamura, *Fukuoka*
 Mikio Nishioka, *Niihama*
 Shuji Nomoto, *Nagoya*
 Susumu Ohmada, *Maebashi*
 Hirohide Ohnishi, *Akita*
 Masayuki Ohta, *Oita*
 Tetsuo Ohta, *Kanazawa*
 Kazuichi Okazaki, *Osaka*
 Katsuhisa Omagari, *Nagasaki*
 Saburo Onishi, *Nankoku*
 Morikazu Onji, *Ehime*
 Satoshi Osawa, *Hamamatsu*
 Masanobu Oshima, *Kanazawa*
 Hiromitsu Saisho, *Chiba*
 Hidetsugu Saito, *Tokyo*
 Yutaka Saito, *Tokyo*
 Michiie Sakamoto, *Tokyo*
 Yasushi Sano, *Chiba*
 Hiroki Sasaki, *Tokyo*
 Iwao Sasaki, *Sendai*
 Motoko Sasaki, *Kanazawa*
 Chifumi Sato, *Tokyo*
 Shuichi Seki, *Osaka*
 Hiroshi Shimada, *Yokohama*
 Mitsuo Shimada, *Tokushima*
 Tomohiko Shimatan, *Hiroshima*
 Hiroaki Shimizu, *Chiba*
 Ichiro Shimizu, *Tokushima*
 Yukihiro Shimizu, *Kyoto*
 Shinji Shimoda, *Fukuoka*
 Tooru Shimosegawa, *Sendai*
 Tadashi Shimoyama, *Hirosaki*
 Ken Shirabe, *Izuka City*
 Yoshio Shirai, *Niigata*
 Katsuya Shiraki, *Mie*
 Yasushi Shiratori, *Okayama*
 Masayuki Sho, *Nara*
 Yasuhiko Sugawara, *Tokyo*
 Hidekazu Suzuki, *Tokyo*
 Minoru Tada, *Tokyo*
 Tadatoshi Takayama, *Tokyo*
 Tadashi Takeda, *Osaka*
 Kiichi Tamada, *Tochigi*
 Akira Tanaka, *Kyoto*
 Eiji Tanaka, *Matsumoto*
 Noriaki Tanaka, *Okayama*
 Shinji Tanaka, *Hiroshima*
 Hideki Taniguchi, *Yokohama*
 Kyuichi Tanikawa, *Kurume*
 Akira Terano, *Shimotsugun*
 Hitoshi Togash, *Yamagata*
 Shinji Togo, *Yokohama*
 Kazunari Tominaga, *Osaka*
 Takuji Torimura, *Fukuoka*
 Minoru Toyota, *Sapporo*
 Akihito Tsubota, *Chiba*
 Takato Ueno, *Kurume*

Shinichi Wada, *Tochigi*
 Hiroyuki Watanabe, *Kanazawa*
 Toshio Watanabe, *Osaka*
 Yuji Watanabe, *Ehime*
 Toshiaki Watanabe, *Tokyo*
 Chun-Yang Wen, *Nagasaki*
 Satoshi Yamagiwa, *Niigata*
 Koji Yamaguchi, *Fukuoka*
 Takayuki Yamamoto, *Yokkaichi*
 Takashi Yao, *Fukuoka*
 Masashi Yoneda, *Tochigi*
 Hiroshi Yoshida, *Tokyo*
 Masashi Yoshida, *Tokyo*
 Norimasa Yoshida, *Kyoto*
 Hitoshi Yoshiiji, *Nara*
 Kentaro Yoshika, *Toyooka*
 Masahide Yoshikawa, *Kashihara*
 Katsutoshi Yoshizato, *Higashihiroshima*
 Yoshiaki Murakami, *Hiroshima*
 Masahiro Tajika, *Nagoya*



Lebanon

Bassam N Abboud, *Beirut*
 Ala I Sharara, *Beirut*
 Joseph D Boujaoude, *Beirut*



Lithuania

Limas Kupcinskas, *Kaunas*



Macedonia

Vladimir C Serafimoski, *Skopje*



Malaysia

Andrew Seng Boon Chua, *Ipooh*
 Khean-Lee Goh, *Kuala Lumpur*
 Jayaram Menon, *Sabah*



Mexico

Diego Garcia-Compean, *Monterrey*
 Eduardo R Marín-López, *Puebla*
 Nahum Méndez-Sánchez, *Mexico City*
 Saúl Villa-Trevio, *México*
 Omar Vergara-Fernandez, *México*



Monaco

Patrick Rampal, *Monaco*



Morocco

Abdellah Essaid, *Rabat*



The Netherlands

Ulrich Beuers, *Amsterdam*
 Gerd Bouma, *Amsterdam*
 Lee Bouwman, *Leiden*
 J Bart A Crusius, *Amsterdam*
 NKH de Boer, *Amsterdam*
 Koert P de Jong, *Groningen*
 Henrike Hamer, *Maastricht*
 Frank Hoentjen, *Haarlem*
 Janine K Kruit, *Groningen*

Ernst J Kuipers, *Rotterdam*
 CBHW Lamers, *Leiden*
 Ton Lisman, *Utrecht*
 Yi Liu, *Amsterdam*
 Jeroen Maljaars, *Maastricht*
 Servaas Morré, *Amsterdam*
 Chris JJ Mulder, *Amsterdam*
 Michael Müller, *Wageningen*
 Amado S Peña, *Amsterdam*
 Robert J Porte, *Groningen*
 Ingrid B Renes, *Rotterdam*
 Paul E Sijens, *Groningen*
 Reinhold W Stockbrugger, *Maastricht*
 Luc JW van der Laan, *Rotterdam*
 Karel van Erpecum, *Utrecht*
 Gerard P VanBerge-Henegouwen, *Utrecht*
 Albert Frederik Pull ter Gunne, *Tilburg*



New Zealand

Ian D Wallace, *Auckland*



Nigeria

Samuel B Olaleye, *Ibadan*



Norway

Trond Berg, *Oslo*
 Tom H Karlsen, *Oslo*
 Helge L Waldum, *Trondheim*



Pakistan

Muhammad S Khokhar, *Lahore*
 Syed MW Jafri, *Karachi*



Peru

Hector H Garcia, *Lima*



Poland

Tomasz Brzozowski, *Cracow*
 Robert Flisiak, *Bialystok*
 Hanna Gregorek, *Warsaw*
 Dariusz M Lebentsztein, *Bialystok*
 Wojciech G Polak, *Wroclaw*
 Marek Hartleb, *Katowice*
 Beata Jolanta Jabłońska, *Katowice*



Portugal

Miguel C De Moura, *Lisbon*



Russia

Vladimir T Ivashkin, *Moscow*
 Leonid Lazebnik, *Moscow*
 Vasiliy I Reshetnyak, *Moscow*



Saudi Arabia

Ibrahim A Al Mofleh, *Riyadh*
 Ahmed Helmy, *Riyadh*



Serbia

Dusan M Jovanovic, *Sremska Kamenica*



Singapore

Bow Ho, *Singapore*
 Khek-Yu Ho, *Singapore*
 Fock Kwong Ming, *Singapore*
 Francis Seow-Choen, *Singapore*
 Brian Kim Poh Goh, *Singapore*



Slovakia

Silvia Pastorekova, *Bratislava*
 Anton Vavrecka, *Bratislava*



Slovenia

Sasa Markovic, *Ljubljana*



South Africa

Michael C Kew, *Cape Town*
 Rosemary Joyce Burnett, *Pretoria*



South Korea

Byung Ihn Choi, *Seoul*
 Ho Soon Choi, *Seoul*
 Marie Yeo, *Suwon*
 Sun Pyo Hong, *Gyeonggi-do*
 Jae J Kim, *Seoul*
 Jin-Hong Kim, *Suwon*
 Myung-Hwan Kim, *Seoul*
 Chang Hong Lee, *Seoul*
 Jeong Min Lee, *Seoul*
 Jong Kyun Lee, *Seoul*
 Eun-Yi Moon, *Seoul*
 Jae-Gahb Park, *Seoul*
 Dong Wan Seo, *Seoul*
 Byung Chul Yoo, *Seoul*



Spain

Juan G Abraldes, *Barcelona*
 Agustin Albillos, *Madrid*
 Raul J Andrade, *Málaga*
 Luis Aparisi, *Valencia*
 Fernando Azpiroz, *Barcelona*
 Ramon Bataller, *Barcelona*
 Josep M Bordas, *Barcelona*
 Jordi Camps, *Catalunya*
 Andres Cardenas, *Barcelona*
 Vicente Carreño, *Madrid*
 Jose Castellote, *Barcelona*
 Antoni Castells, *Barcelona*
 Vicente Felipo, *Valencia*
 Juan C Garcia-Pagán, *Barcelona*
 Jaime B Genover, *Barcelona*
 Ignacio Gil-Bazo, *Pamplona*
 Javier P Gisbert, *Madrid*
 Jaime Guardia, *Barcelona*
 Isabel Fabregat, *Barcelona*
 Mercedes Fernandez, *Barcelona*
 Angel Lanas, *Zaragoza*
 Juan-Ramón Larrubia, *Guadalajara*
 Laura Lladó, *Barcelona*
 María IT López, *Jaén*
 José M Mato, *Derio*
 Juan F Medina, *Pamplona*
 Miguel A Muñoz-Navas, *Pamplona*
 Julian Panes, *Barcelona*
 Miguel M Perez, *Valencia*
 Miguel Perez-Mateo, *Alicante*

Josep M Pique, *Barcelona*
Jesús M Prieto, *Pamplona*
Sabino Riestra, *Pola De Siero*
Luis Rodrigo, *Oviedo*
Manuel Romero-Gómez, *Sevilla*
Joan Roselló-Catafau, *Barcelona*



Sweden

Einar S Björnsson, *Gothenburg*
Curt Einarsson, *Huddinge*
Per M Hellström, *Stockholm*
Ulf Hindorf, *Lund*
Elisabeth Hultgren-Hörnquist, *Örebro*
Anders Lehmann, *Mölnadal*
Hanns-Ulrich Marschall, *Stockholm*
Lars C Olbe, *Molndal*
Lars A Pahlman, *Uppsala*
Matti Sallberg, *Stockholm*
Magnus Simrén, *Göteborg*
Xiao-Feng Sun, *Linköping*
Ervin Tóth, *Malmö*
Weimin Ye, *Stockholm*
Christer S von Holstein, *Lund*



Switzerland

Christoph Beglinger, *Basel*
Pierre-Alain Clavien, *Zürich*
Jean-Francois Dufour, *Bern*
Franco Fortunato, *Zürich*
Jean L Frossard, *Geneva*
Andreas Geier, *Zürich*
Gerd A Kullak-Ublick, *Zurich*
Pierre Michetti, *Lausanne*
Francesco Negro, *Genève*
Bruno Stieger, *Zürich*
Radu Tutuian, *Zürich*
Stephan R Vavricka, *Zürich*
Gerhard Rogler, *Zürich*
Arthur Zimmermann, *Berne*



Turkey

Yusuf Bayraktar, *Ankara*
Figen Gurakan, *Ankara*
Aydin Karabacakoglu, *Konya*
Serdar Karakose, *Konya*
Hizir Kurtel, *Istanbul*
Osman C Ozdogan, *Istanbul*
Özlem Yilmaz, *Izmir*
Cihan Yurdaydin, *Ankara*



United Arab Emirates

Sherif M Karam, *Al-Ain*



United Kingdom

David H Adams, *Birmingham*
Simon Afford, *Birmingham*
Navneet K Ahluwalia, *Stockport*
Ahmed Alzaraa, *Manchester*
Lesley A Anderson, *Belfast*
Charalambos G Antoniades, *London*
Anthony TR Axon, *Leeds*
Qasim Aziz, *London*
Nicholas M Barnes, *Birmingham*
Jim D Bell, *London*

Mairi Brittan, *London*
Alastair D Burt, *Newcastle*
Simon S Campbell, *Manchester*
Simon R Carding, *Leeds*
Paul J Ciclitira, *London*
Eithne Costello, *Liverpool*
Tatjana Crnogorac-Jurcevic, *London*
Harry Dalton, *Truro*
Amar P Dhillon, *London*
William Dickey, *Londonderry*
James E East, *London*
Emad M El-Omar, *Aberdeen*
Ahmed M Elsharkawy, *Newcastle Upon Tyne*
Annette Fristscher-Ravens, *London*
Elizabeth Furrie, *Dundee*
Daniel R Gaya, *Edinburgh*
Subrata Ghosh, *London*
William Greenhalf, *Liverpool*
Indra N Guha, *Southampton*
Gwo-Tzer Ho, *Edinburgh*
Anthony R Hobson, *Salford*
Lesley A Houghton, *Manchester*
Stefan G Hübscher, *Birmingham*
Robin Hughes, *London*
Pali Hungin, *Stockton*
David P Hurlstone, *Sheffield*
Rajiv Jalan, *London*
Janusz AZ Jankowski, *Oxford*
Brian T Johnston, *Belfast*
David EJ Jones, *Newcastle*
Roger Jones, *London*
Michael A Kamm, *Harrow*
Peter Karayiannis, *London*
Laurens Kruidenier, *Harlow*
Patricia F Lalor, *Birmingham*
Chee Hooi Lim, *Midlands*
Hong-Xiang Liu, *Cambridge*
Yun Ma, *London*
K E L McColl, *Glasgow*
Stuart A C McDonald, *London*
Dermot P McGovern, *Oxford*
Giorgina Mieli-Vergani, *London*
Nikolai V Naoumov, *London*
John P Neoptolemos, *Liverpool*
James Neuberger, *Birmingham*
Philip Noel Newsome, *Birmingham*
Mark S Pearce, *Newcastle Upon Tyne*
D Mark Pritchard, *Liverpool*
Sakhwat Rahman, *England*
Stephen E Roberts, *Swansea*
Marco Senzolo, *Padova*
Soraya Shirazi-Beechey, *Liverpool*
Robert Sutton, *Liverpool*
Simon D Taylor-Robinson, *London*
Paris P Tekkis, *London*
Ulrich Thalheimer, *London*
David G Thompson, *Salford*
Nick P Thompson, *Newcastle*
Frank I Tovey, *London*
Chris Tselepis, *Birmingham*
Diego Vergani, *London*
Geoffrey Warhurst, *Salford*
Alastair John Watson, *Liverpool*
Peter J Whorwell, *Manchester*
Roger Williams, *London*
Karen L Wright, *Bath*
Min Zhao, *Foresterhill*



United States

Manal F Abdelmalek, *Durham*
Gary A Abrams, *Birmingham*
Maria T Abreu, *New York*
Reid B Adams, *Virginia*

Golo Ahlenstielf, *Bethesda*
BS Anand, *Houston*
M Ananthanarayanan, *New York*
Gavin E Arteel, *Louisville*
Jasmohan S Bajaj, *Milwaukee*
Shashi Bala, *Worcester*
Subhas Banerjee, *Palo Alto*
Jamie S Barkin, *Miami Beach*
Kim E Barrett, *San Diego*
Marc D Basson, *Lansing*
Anthony J Bauer, *Pittsburgh*
Wallace F Berman, *Durham*
Timothy R Billiar, *Pittsburgh*
Edmund J Bini, *New York*
David G Binion, *Milwaukee*
Jennifer D Black, *Buffalo*
Herbert L Bonkovsky, *Charlotte*
Carla W Brady, *Durham*
Andrea D Branch, *New York*
Robert S Bresalier, *Houston*
Alan L Buchman, *Chicago*
Ronald W Busuttil, *Los Angeles*
Alan Cahill, *Philadelphia*
John M Carethers, *San Diego*
David L Carr-Locke, *Boston*
Maurice A Cerulli, *New York*
Ravi S Chari, *Nashville*
Anping Chen, *St. Louis*
Jiande Chen, *Galveston*
Xian-Ming Chen, *Omaha*
Xin Chen, *San Francisco*
Ramsey Chi-man Cheung, *Palo Alto*
William D Chey, *Ann Arbor*
John Y Chiang, *Rootstown*
Parimal Chowdhury, *Arkansas*
Raymond T Chung, *Boston*
James M Church, *Cleveland*
Ram Chuttani, *Boston*
Mark G Clemens, *Charlotte*
Ana J Coito, *Los Angeles*
Vincent Coghlann, *Beaverton*
David Cronin II, *New Haven*
John Cuppoletti, *Cincinnati*
Mark J Czaja, *New York*
Peter V Danenberg, *Los Angeles*
Kiron M Das, *New Brunswick*
Conor P Delaney, *Cleveland*
Jose L del Pozo, *Rochester*
Sharon DeMorrow, *Temple*
Deborah L Diamond, *Seattle*
Douglas A Drossman, *Chapel Hill*
Katerina Dvorak, *Tucson*
Bijan Eghtesad, *Cleveland*
Hala El-Zimaity, *Houston*
Michelle Embree-Ku, *Providence*
Sukru Emre, *New Haven*
Douglas G Farmer, *Los Angeles*
Alessio Fasano, *Baltimore*
Mark A Feitelson, *Philadelphia*
Ariel E Feldstein, *Cleveland*
Alessandro Fichera, *Chicago*
Robert L Fine, *New York*
Chris E Forsmark, *Gainesville*
Glenn T Furuta, *Aurora*
Chandrashekhar R Gandhi, *Pittsburgh*
Susan L Gearhart, *Baltimore*
Xupeng Ge, *Stockholm*
Xin Geng, *New Brunswick*
M Eric Gershwin, *Suite*
Jean-Francois Geschwind, *Baltimore*
Shannon S Glaser, *Temple*
Ajay Goel, *Dallas*
Richard M Green, *Chicago*
Julia B Greer, *Pittsburgh*

James H Grendell, MD, *New York*
 David R Gretch, *Seattle*
 Stefano Guandalini, *Chicago*
 Anna S Gukovskaya, *Los Angeles*
 Sanjeev Gupta, *Bronx*
 David J Hackam, *Pittsburgh*
 Stephen B Hanauer, *Chicago*
 Gavin Harewood, *Rochester*
 Margaret M Heitkemper, *Washington*
 Alan W Hemming, *Gainesville*
 Samuel B Ho, *San Diego*
 Peter R Holt, *New York*
 Colin W Howden, *Chicago*
 Hongjin Huang, *Alameda*
 Jamal A Ibdah, *Columbia*
 Atif Iqbal, *Omaha*
 Hajime Isomoto, *Rochester*
 Ira M Jacobson, *New York*
 Hartmut Jaeschke, *Tucson*
 Cheng Ji, *Los Angeles*
 Leonard R Johnson, *Memphis*
 Michael P Jones, *Chicago*
 Peter J Kahrilas, *Chicago*
 Anthony N cBaltimore
 Marshall M Kaplan, *Boston*
 Neil Kaplowitz, *Los Angeles*
 Serhan Karvar, *Los Angeles*
 Rashmi Kaul, *Tulsa*
 Jonathan D Kaunitz, *Los Angeles*
 Ali Keshavarzian, *Chicago*
 Miran Kim, *Providence*
 Joseph B Kirsner, *Chicago*
 Leonidas G Koniaris, *Miami*
 Burton I Korelitz, *New York*
 Robert J Korst, *New York*
 Richard A Kozarek, *Seattle*
 Alyssa M Krasinskas, *Pittsburgh*
 Michael Kremer, *Chapel Hill*
 Shiu-Ming Kuo, *Buffalo*
 Paul Y Kwo, *Indianapolis*
 Daryl Tan Yeung Lau, *Galveston*
 Stephen J Lanspa, *Omaha*
 Joel E Levine, *San Diego*
 Bret Lashner, *Cleveland*
 Dirk J van Leeuwen, *Lebanon*
 Glen A Lehman, *Indianapolis*
 Alex B Lentsch, *Cincinnati*
 Andreas Leodolter, *La Jolla*
 Gene LeSage, *Houston*
 Josh Levitsky, *Chicago*
 Cynthia Levy, *Gainesville*
 Ming Li, *New Orleans*
 Zhiping Li, *Baltimore*
 Zhe-Xiong Lian, *Davis*
 Lenard M Lichtenberger, *Houston*
 Gary R Lichtenstein, *Philadelphia*
 Otto Schiueh-Tzang Lin, *Seattle*
 Martin Lipkin, *New York*
 Chen Liu, *Gainesville*
 Robin G Lorenz, *Birmingham*
 Michael R Lucey, *Madison*
 James D Luketich, *Pittsburgh*
 Guangbin Luo, *Cheveland*
 Henry Thomson Lynch, *Omaha*
 Patrick M Lynch, *Houston*
 John S Macdonald, *New York*
 Bruce V MacFadyen, *Augusta*
 Willis C Maddrey, *Dallas*
 Ashok Malani, *Los Angeles*
 Mercedes Susan Mandell, *Aurora*
 Peter J Mannon, *Bethesda*
 Charles M Mansbach, *Tennessee*
 John F Di Mari, *Texas*
 John M Mariadason, *Bronx*
 Jorge A Marrero, *Ann Arbor*
 Paul Martin, *New York*
 Paulo Ney Aguiar Martins, *Boston*
 Wendy M Mars, *Pittsburgh*
 Laura E Matarese, *Pittsburgh*
 Richard W McCallum, *Kansas*
 Beth A McCormick, *Charlestown*
 Lynne V McFarland, *Washington*
 Kevin McGrath, *Pittsburgh*
 Harihara Mehendale, *Monroe*
 Ali Mencin, *New York*
 Fanyin Meng, *Ohio*
 Stephan Menne, *New York*
 Didier Merlin, *Atlanta*
 Howard Mertz, *Nashville*
 George W Meyer, *Sacramento*
 George Michalopoulos, *Pittsburgh*
 James M Millis, *Chicago*
 Albert D Min, *New York*
 Pramod K Mistry, *New Haven*
 Emiko Mizoguchi, *Boston*
 Smruti R Mohanty, *Chicago*
 Satdarshan S Monga, *Pittsburgh*
 Timothy H Moran, *Baltimore*
 Peter L Moses, *Burlington*
 Steven F Moss, *Providence*
 Andrew J Muir, *Durham*
 Milton G Mutchnick, *Detroit*
 Masaki Nagaya, *Boston*
 Victor Navarro, *Philadelphia*
 Laura E Nagy, *Cleveland*
 Hiroshi Nakagawa, *Philadelphia*
 Douglas B Nelson, *Minneapolis*
 Justin H Nguyen, *Florida*
 Christopher O'Brien, *Miami*
 Robert D Odze, *Boston*
 Brant K Oelschlager, *Washington*
 Curtis T Okamoto, *Los Angeles*
 Stephen JD O'Keefe, *Pittsburgh*
 Dimitry Oleynikov, *Omaha*
 Stephen J Pandol, *Los Angeles*
 Georgios Papachristou, *Pittsburgh*
 Pankaj J Pasricha, *Galveston*
 Zhiheng Pei, *New York*
 CS Pitchumoni, *New Brunswiuc*
 Paul J Pockros, *La Jolla*
 Jay Pravda, *Gainesville*
 Massimo Raimondo, *Jacksonville*
 GS Raju, *Galveston*
 Raymund R Razonable, *Minnesota*
 Adrian Reuben, *Charleston*
 Douglas K Rex, *Indianapolis*
 Victor E Reyes, *Galveston*
 Basil Rigas, *New York*
 Yehuda Ringel, *Chapel Hill*
 Richard A Rippe, *Chapel Hill*
 Maribel Rodriguez-Torres, *Santurce*
 Marcos Rojkind, *Washington*
 Philip Rosenthal, *San Francisco*
 Barry Rosser, *Jacksonville Florida*
 Hemant K Roy, *Evanston*
 Sammy Saab, *Los Angeles*
 Shawn D Safford, *Norfolk*
 Dushyant V Sahani, *Boston*
 James M Scheiman, *Ann Arbor*
 Eugene R Schiff, *Miami*
 Nicholas J Shaheen, *Chapel Hill*
 Vanessa M Shami, *Charlottesville*
 Prateek Sharma, *Kansas City*
 Harvey L Sharp, *Minneapolis*
 Stuart Sherman, *Indianapolis*
 Shrivendra Shukla, *Columbia*
 Alphonse E Sirica, *Virginia*
 Shanthi V Sitaraman, *Atlanta*
 Bronislaw L Slomiany, *Newark*
 Stuart J Spechler, *Dallas*
 Subbaramiah Sridhar, *Augusta*
 Shanthi Srinivasan, *Atlanta*
 Peter D Stevens, *New York*
 Charmaine A Stewart, *Rochester*
 Christian D Stone, *Saint Louis*
 Gary D Stoner, *Columbus*
 R Todd Stravitz, *Richmond*
 Liping Su, *Chicago*
 Christina Surawicz, *Seattle*
 Robert W Summers, *Iowa City*
 Wing-Kin Syn, *Durham*
 Gyongyi Szabo, *Worcester*
 Yvette Taché, *Los Angeles*
 Toku Takahashi, *Milwaukee*
 Andrzej S Tarnawski, *Orange*
 K-M Tchou-Wong, *New York*
 Christopher C Thompson, *Boston*
 Swan N Thung, *New York*
 Michael Torbenson, *Baltimore*
 Natalie J Tork, *Sacramento*
 Travagli, *Baton Rouge*
 George Triadafilopoulos, *Stanford*
 Chung-Jyi Tsai, *Lexington*
 Janet Elizabeth Tuttle-Newhall, *Durham*
 Andrew Ukleja, *Florida*
 Michael F Vaezi, *Nashville*
 Hugo E Vargas, *Phoenix*
 Arnold Wald, *Wisconsin*
 Scott A Waldman, *Philadelphia*
 Jian-Ying Wang, *Baltimore*
 Junru Wang, *Little Rock*
 Timothy C Wang, *New York*
 Irving Waxman, *Chicago*
 Steven A Weinman, *Galveston*
 Steven D Wexner, *Weston*
 Keith T Wilson, *Baltimore*
 Jacqueline L Wolf, *Boston*
 Jackie Wood, *Ohio*
 George Y Wu, *Farmington*
 Jian Wu, *Sacramento*
 Samuel Wyllie, *Houston*
 Wen Xie, *Pittsburgh*
 Vijay Yajnik, *Boston*
 Vincent W Yang, *Atlanta*
 Francis Y Yao, *San Francisco*
 Hal F Yee, *San Francisco*
 Xiao-Ming Yin, *Pittsburgh*
 Min You, *Tampa*
 Zobair M Younossi, *Virginia*
 Liqing Yu, *Winston-Salem*
 David Yule, *Rochester*
 Ruben Zamora, *Pittsburgh*
 Michael E Zenilman, *New York*
 Zhi Zhong, *Chapel Hill*
 Michael A Zimmerman, *Colorado*
 Stephen D Zucker, *Cincinnati*
 Robert CG Martin, *Louisville*
 Imran Hassan, *Springfield*
 Klaus Thaler, *Columbia*
 Luca Stocchi, *Cleveland*
 Kevin Michael Reavis, *Orange*
 Mark Bloomston, *Columbus*



Uruguay

Henry Cohen, *Montevideo*

[¹]Passed away on October 20, 2007

[²]Passed away on June 14, 2008



World Journal of Gastroenterology®

Weekly Established in October 1995



Volume 15 Number 46
December 14, 2009

Contents

EDITORIAL	5761 Clinical relevance and public health significance of hepatitis B virus genomic variations <i>Cao GW</i>
TOPIC HIGHLIGHT	5770 Confocal laser endomicroscopy in the "in vivo" histological diagnosis of the gastrointestinal tract <i>De Palma GD</i>
REVIEW	5776 Signal molecule-mediated hepatic cell communication during liver regeneration <i>Zheng ZY, Weng SY, Yu Y</i> 5784 Potential role of Th17 cells in the pathogenesis of inflammatory bowel disease <i>Liu ZJ, Yadav PK, Su JL, Wang JS, Fei K</i>
ORIGINAL ARTICLE	5789 Role of the receptor for advanced glycation end products in hepatic fibrosis <i>Lohwasser C, Neureiter D, Popov Y, Bauer M, Schuppan D</i> 5799 Identification of TRPM7 channels in human intestinal interstitial cells of Cajal <i>Kim BJ, Park KJ, Kim HW, Choi S, Jun JY, Chang IY, Jeon JH, So I, Kim SJ</i> 5805 Role of diffusion-weighted magnetic resonance imaging in the differential diagnosis of focal hepatic lesions <i>Koike N, Cho A, Nasu K, Seto K, Nagaya S, Ohshima Y, Ohkohchi N</i> 5813 NT4(Si)-p53(N15)-antennapedia induces cell death in a human hepatocellular carcinoma cell line <i>Song LP, Li YP, Wang N, Li WW, Ren J, Qiu SD, Wang QY, Yang GX</i>
BRIEF ARTICLE	5821 Separate basolateral and apical phosphatidylcholine secretion routes in intestinally differentiated tumor cells <i>Gotthardt D, Braun A, Tietje A, Weiss KH, Ehehalt R, Stremmel WR</i> 5827 Value of three-dimensional reconstructions in pancreatic carcinoma using multidetector CT: Initial results <i>Klauß M, Schöbinger M, Wolf I, Werner J, Meinzer HP, Kauczor HU, Grenacher L</i> 5833 Iodized oil uptake assessment with cone-beam CT in chemoembolization of small hepatocellular carcinomas <i>Jeon UB, Lee JW, Choo KS, Kim CW, Kim S, Lee TH, Jeong YJ, Kang DH</i> 5838 Image-guided conservative management of right colonic diverticulitis <i>Park SJ, Choi SI, Lee SH, Lee KY</i>

Contents

World Journal of Gastroenterology
Volume 15 Number 46 December 14, 2009

5843	Changes in intestinal mucosal immune barrier in rats with endotoxemia <i>Liu C, Li A, Weng YB, Duan ML, Wang BE, Zhang SW</i>
5851	Effect of implanting fibrin sealant with ropivacaine on pain after laparoscopic cholecystectomy <i>Fu JZ, Li J, Yu ZL</i>
5855	Multidrug resistance protein 3 R652G may reduce susceptibility to idiopathic infant cholestasis <i>Chen XQ, Wang LL, Shan QW, Tang Q, Lian SJ</i>
 CASE REPORT	
5859	Two synchronous somatostatinomas of the duodenum and pancreatic head in one patient <i>Čolović RB, Matić SV, Micev MT, Grubor NM, Atkinson HD, Latinčić SM</i>
5864	Is iron overload in alcohol-related cirrhosis mediated by hepcidin? <i>Iqbal T, Diab A, Ward DG, Brookes MJ, Tselepis C, Murray J, Elias E</i>
5867	Neoadjuvant peptide receptor radionuclide therapy for an inoperable neuroendocrine pancreatic tumor <i>Kaemmerer D, Prasad V, Daffner W, Hörsch D, Klöppel G, Hommann M, Baum RP</i>
5871	Cronkhite-Canada syndrome associated with myelodysplastic syndrome <i>Suzuki R, Irisawa A, Hikichi T, Takahashi Y, Kobayashi H, Kumakawa H, Ohira H</i>
5875	Spontaneous liver rupture in hypereosinophilic syndrome: A rare but fatal complication <i>Cheung YS, Wong S, Lam PKN, Lee KF, Wong J, Lai PBS</i>
5879	Surgery for rare aneurysm associated with colorectal cancer <i>Lu PH, Tao GQ, Shen W, Cai B, Jiang ZY, Sun J</i>
 LETTERS TO THE EDITOR 5882 Lethal neuroendocrine carcinoma in ulcerative colitis <i>Freeman HJ, Berean K</i>	
 ACKNOWLEDGMENTS 5884 Acknowledgments to reviewers of <i>World Journal of Gastroenterology</i>	
 APPENDIX 5885 Meetings	
5886 Instructions to authors	
 FLYLEAF I-VII Editorial Board	
 INSIDE BACK COVER Online Submissions	
 INSIDE FRONT COVER Online Submissions	

Contents

World Journal of Gastroenterology
Volume 15 Number 46 December 14, 2009

INTRODUCTION

World Journal of Gastroenterology is an international, open-access, peer-reviewed, and multi-disciplinary weekly journal that serves gastroenterologists and hepatologists. The biggest advantage of the open access model is that it provides free, full-text articles in PDF and other formats for experts and the public without registration, which eliminates the obstacle that traditional journals possess and usually delays the speed of the propagation and communication of scientific research results. The open access model has been proven to be a true approach that may achieve the ultimate goal of the journals, i.e. the maximization of the values of the readers, the authors and the society.

Maximization of the value of the readers can be comprehended in two ways. First, the journal publishes articles that can be directly read or downloaded free of charge at any time, which attracts more readers. Second, the readers can apply the knowledge in clinical practice without delay after reading and understanding the information in their fields. In addition, the readers are encouraged to propose new ideas based on those of the authors, or to provide viewpoints that are different from those of the authors. Such discussions or debates among different schools of thought will definitely boost advancements and developments in the fields. Maximization of the value of the authors refers to the fact that these journals provide a platform that promotes the speed of propagation and communication to a maximum extent. This is also what the authors really need. Maximization of the value of the society refers to the maximal extent of the social influences and impacts produced by the high quality original articles published in the journal. This is also the main purpose of many journals around the world.

EDITORS FOR THIS ISSUE

Responsible Assistant Editor: *Xiao-Fang Liu*
Responsible Electronic Editor: *Wen-Hua Ma*
Proofing Editor-in-Chief: *Lian-Sheng Ma*

Responsible Science Editor: *Lin Tian*
Proofing Editorial Office Director: *Jian-Xia Cheng*

NAME OF JOURNAL

World Journal of Gastroenterology

RESPONSIBLE INSTITUTION

Department of Science and Technology of Shanxi Province

SPONSOR

Taiyuan Research and Treatment Center for Digestive Diseases, 77 Shuangta Xijie, Taiyuan 030001, Shanxi Province, China

EDITING

Editorial Board of *World Journal of Gastroenterology*, Room 903, Building D, Ocean International Center, No.62 Dongsihuan Zhonglu, Chaoyang District, Beijing 100025, China
Telephone: +86-10-59080039
Fax: +86-10-85381893
E-mail: wjg@wjgnet.com
<http://www.wjgnet.com>

PUBLISHING

The WJG Press and Beijing Baishideng BioMed Scientific Co., Ltd. Room 903, Building D, Ocean International Center, No.62 Dongsihuan Zhonglu, Chaoyang District, Beijing 100025, China
Telephone: +86-10-59080039
Fax: +86-10-85381893
E-mail: wjg@wjgnet.com
<http://www.wjgnet.com>

PRINTING

Beijing Kexin Printing House

OVERSEAS DISTRIBUTOR

Beijing Bureau for Distribution of Newspapers and Journals (Code No. 82-261)
China International Book Trading Corporation PO Box 399, Beijing, China (Code No. M4481)

PUBLICATION DATE

December 14, 2009

EDITOR-IN-CHIEF

Lian-Sheng Ma, *Beijing*

SUBSCRIPTION

RMB 50 Yuan for each issue, RMB 2400 Yuan for one year

ISSN

ISSN 1007-9327
CN 14-1219/R

HONORARY EDITORS-IN-CHIEF

Montgomery Bissell, *San Francisco*
James L Boyer, *New Haven*
Chao-Long Chen, *Kaohsiung*
Ke-Ji Chen, *Beijing*
Li-Fang Chou, *Taipei*
Jacques V Dam, *Stanford*
Martin H Floch, *New Haven*
Guadalupe Garcia-Tsao, *New Haven*
Zhi-Qiang Huang, *Beijing*
Shinn-Jang Hwang, *Taipei*
Ira M Jacobson, *New York*
Derek Jewell, *Oxford*
Emmet B Keeffe, *Palo Alto*
Min-Liang Kuo, *Taipei*
Nicholas F LaRusso, *Rochester*
Jie-Shou Li, *Nanjing*
Geng-Tao Liu, *Beijing*
Lein-Ray Mo, *Tainan*
Bo-Rong Pan, *Xi'an*
Fa-Zu Qiu, *Wuhan*
Eamonn M Quigley, *Cork*
David S Rampton, *London*
Rafiq A Sheikh, *Sacramento*
Rudi Schmid, *Kentfield*¹⁾
Nicholas J Talley, *Rochester*
Sun-Lung Tsai, *Young-Kang City*
Guido NJ Tytgat, *Amsterdam*
Hsiu-Po Wang, *Taipei*
Jaw-Ching Wu, *Taipei*
Meng-Chao Wu, *Shanghai*
Ming-Shiang Wu, *Taipei*
Jia-Yu Xu, *Shanghai*
Ta-Sen Yeh, *Taoyuan*
Ming-Lung Yu, *Kaohsiung*

STRATEGY ASSOCIATE EDITORS-IN-CHIEF

Peter Dragovan, *Florida*
Ronnie Fass, *Tucson*
Hugh J Freeman, *Vancouver*
John P Geibel, *New Haven*
Maria C Gutierrez-Ruiz, *México*

Kazuhiko Hanazaki, *Kochi*

Akio Inui, *Kagoshima*
Kalpesh Jani, *Vadodara*
Sanaa M Kamal, *Cairo*
Ioannis E Koutroubakis, *Heraklion*
Jose JG Marin, *Salamanca*
Javier S Martin, *Punta del Este*
Natalia A Osna, *Omaha*
Jose Sahel, *Marseille*
Ned Snyder, *Galveston*
Nathan Subramaniam, *Brisbane*
Wei Tang, *Tokyo*
Alan BR Thomson, *Edmonton*
Paul Joseph Thuluvath, *Baltimore*
James F Trotter, *Denver*
Shingo Tsuji, *Osaka*
Harry HX Xia, *Hanover*
Yoshio Yamaoka, *Houston*
Jesus K Yamamoto-Furusho, *México*

ASSOCIATE EDITORS-IN-CHIEF

Gianfranco D Alpini, *Temple*
Bruno Annibale, *Roma*
Roger William Chapman, *Oxford*
Chi-Hin Cho, *Hong Kong*
Alexander L Gerbes, *Munich*
Shou-Dong Lee, *Taipei*
Walter Edwin Longo, *New Haven*
You-Yong Lu, *Beijing*
Masao Omata, *Tokyo*

EDITORIAL OFFICE

Director: Jian-Xia Cheng, *Beijing*
Deputy Director: Jian-Zhong Zhang, *Beijing*

LANGUAGE EDITORS

Director: Jing-Yun Ma, *Beijing*
Deputy Director: Xian-Lin Wang, *Beijing*

MEMBERS

Gianfranco D Alpini, *Temple*
BS Anand, *Houston*
Manoj Kumar, *Nepal*
Patricia F Lalor, *Birmingham*
Ming Li, *New Orleans*
Margaret Lutze, *Chicago*
Sabine Mihm, *Göttingen*
Francesco Negro, *Genève*
Bernardino Ramponi, *Siena*
Richard A Rippe, *Chapel Hill*
Stephen E Roberts, *Swansea*

COPY EDITORS

Gianfranco D Alpini, *Temple*
Sujit Kumar Bhattacharya, *Kolkata*
Filip Braet, *Sydney*
Kirsteen N Browning, *Baton Rouge*
Radha K Dhiman, *Chandigarh*
John Frank Di Mari, *Texas*
Shannon S Glaser, *Temple*
Eberhard Hildt, *Berlin*
Patricia F Lalor, *Birmingham*
Ming Li, *New Orleans*
Margaret Lutze, *Chicago*
MI Torrs, *Jaén*
Sri Prakash Misra, *Allahabad*
Giovanni Monteleone, *Rome*
Giovanni Musso, *Torino*
Valerio Nobili, *Rome*
Osman Cavit Ozdogan, *Istanbul*
Francesco Perri, *San Giovanni Rotondo*
Thierry Piche, *Nice*
Bernardino Ramponi, *Siena*
Richard A Rippe, *Chapel Hill*
Ross C Smith, *Sydney*
Daniel Lindsay Worthley, *Bedford*
George Y Wu, *Farmington*
Jian Wu, *Sacramento*

COPYRIGHT

© 2009 Published by The WJG Press and Baishideng. All rights reserved; no part of this publication may be reproduced, stored in a retrieval system, or transmitted in any form or by any means, electronic, mechanical, photocopying, recording, or otherwise without the prior permission of *WJG*. Authors are required to grant *WJG* an exclusive licence to publish.

SPECIAL STATEMENT

All articles published in this journal represent the viewpoints of the authors except where indicated otherwise.

INSTRUCTIONS TO AUTHORS

Full instructions are available online at <http://www.wjgnet.com/wjg/help/instructions.jsp>. If you do not have web access please contact the editorial office.

ONLINE SUBMISSION

<http://wjg.wjgnet.com>



Clinical relevance and public health significance of hepatitis B virus genomic variations

Guang-Wen Cao

Guang-Wen Cao, Department of Epidemiology, Second Military Medical University, Shanghai 200433, China

Author contributions: Cao GW solely contributed to this paper. Supported by Ministry of Health of China, No. 2008ZX10002-15; National Natural Science Foundation of China, No. 30921006; Shanghai Science & Technology Committee, No. 08XD14001; Shanghai Board of Health, No. 08GWD02; 08GWZX0201

Correspondence to: Guang-Wen Cao, MD, PhD, Professor of Medicine, Chairman, Department of Epidemiology, Second Military Medical University, 800 Xiangyin Road, Shanghai 200433, China. gcao@smmu.edu.cn

Telephone: +86-21-81871060 **Fax:** +86-21-81871060

Received: October 22, 2009 **Revised:** November 5, 2009

Accepted: November 12, 2009

Published online: December 14, 2009

tibility will be helpful in classifying the HBV-infected subjects who will develop HCC and need active anti-viral treatments.

© 2009 The WJG Press and Baishideng. All rights reserved.

Key words: Hepatitis B virus; Genotype; Subgenotype; Mutation; Clinical; Public health; Evolution

Peer reviewers: Rakesh Aggarwal, Additional Professor, Department of Gastroenterology, Sanjay Gandhi Postgraduate Institute of Medical Sciences, Lucknow 226014, India; Rosemary Joyce Burnett, MPH, Department of Epidemiology National School of Public Health, University of Limpopo, Medunsa Campus PO Box 173, MEDUNSA, Pretoria 0204, South Africa

Cao GW. Clinical relevance and public health significance of hepatitis B virus genomic variations. *World J Gastroenterol* 2009; 15(46): 5761-5769 Available from: URL: <http://www.wjgnet.com/1007-9327/15/5761.asp> DOI: <http://dx.doi.org/10.3748/wjg.15.5761>

Abstract

Ten hepatitis B virus (HBV) genotypes (A-J) and 34 HBV subgenotypes have been identified so far. HBV genotypes and subgenotypes have distinct geographical distributions, and have been shown to differ with regard to clinical outcome, prognosis, and response to interferon treatment. Infection with subgenotype A2 is frequently associated with high viral load, resulting in acute infection *via* horizontal transmission. Genotypes A and B are more sensitive to interferon treatment than genotypes D and C, respectively. Genotype B is more frequent in acute hepatitis than genotype C, whereas genotype C (C2) is more frequently associated with an increased risk of hepatocellular carcinoma (HCC), mostly cirrhotic, as compared with genotype B (B2). Genotype mixture is associated with high viral load and worse outcome of HBV infection. HBV mutations in the S genes, especially amino acids substitution at position 145 (G145R), are associated with immune escape, whereas mutations in the PreS or S genes which impair HBsAg secretion could present a risk to blood safety. HBV variants harboring mutations in the viral polymerase gene that confer resistance to nucleoside analogs may be selected during antiviral therapy. Different genotypes have distinct mutation patterns in the PreS and Enh II /BCP/Precore regions. PreS deletions, C1653T, T1753V, and A1762T/G1764A are associated with an increased risk of HCC. HCC-associated HBV mutants may not transmit *via* mother-to-child transmission, and are likely generated during HBV-induced pathogenesis. Examination of HBV mutations alone or in combination and host genetic suscep-

INTRODUCTION

Hepatitis B virus (HBV) belongs to the hepadnaviridae, a family of enveloped viruses with an incomplete double-stranded DNA genome of 3.2 kb. The double-stranded DNA genome of HBV contains four overlapping open reading frames that encode the surface protein, the core protein, a polymerase, and a multifunctional nonstructural protein called X. The PreS region, which consists of PreS1 (nucleotides 2848-3204) and PreS2 (nucleotides 3205-154) domains, overlaps a region encoding the polymerase gene. The enhancer II (Enh II; nucleotides 1636-1744) and basic core promoter (BCP; nucleotides 1751-1769) regions overlap with the X gene (nucleotides 1374-1835).

Infection with HBV is a major public health problem. Approximately 45% of the world's population lives in regions where HBV infection is endemic. Approximately 2 billion people have been exposed to HBV, and more than 300 million are chronically infected with HBV^[1]. In Asia and most of Africa, chronic HBV infection is common and usually acquired perinatally or in childhood^[2]. Chronic HBV infection is one of the most important determinants of the occurrence of liver cirrhosis (LC) and hepatocellular carcinoma (HCC). Most HCC

cases (> 80%) occur in either Eastern Asia or in sub-Saharan Africa where HBV is endemic^[3]. HBV infection contributes to more than 50% of HCC cases worldwide and 70%-80% of HCC cases in highly HBV endemic regions. The relative risks of HCC among people infected with HBV ranges from 5 to 49 in case-control studies and from 7 to 98 in cohort studies^[4]. The incidence of HCC (per 100 000 person/year) among people with chronic HBV infection ranges from 400 to 800 in males and from 120 to 180 in females^[4]. Standard HBV vaccination dramatically decreases HCC prevalence among vaccinees aged 6-19 years^[5]. HBV genomic variations, including genotypes, subgenotypes, and HBV mutations in the PreS region and the Enh II /BCP/Precore region are associated with the development of LC and HCC in different HBV replication and hepatitis B e antigen (HBeAg) status.

HBV GENOTYPES/SUBGENOTYPES AND THEIR CLINICAL RELEVANCE

Distribution of HBV genotypes and subgenotypes

Eight genotypes (genotypes A-H) have been identified by a sequence divergence greater than 8% in the entire HBV genome or a sequence divergence greater than 4% in the S region^[6]. HBV isolated in Vietnam and Laos has been suggested to form a ninth genotype I^[7,8]. The designation has been questioned due to complex recombination. Recently, a HBV strain isolated from a Japanese patient has been provisionally designated HBV genotype J. HBV genotype J is closer to gibbon/orangutan genotypes than to human genotypes in the P and large S genes and closest to Australian aboriginal strains and orangutan-derived strains in the S gene, whereas it is closer to human than ape genotypes in the C gene^[9]. Genotypes have further been separated into subgenotypes if the divergence in whole nucleotide sequence is between 4% and 8%^[10]. Currently, subgenotypes 1-5 of genotype A, subgenotypes 1-8 of genotype B, subgenotypes 1-8 of genotype C, and subgenotypes 1-7 of genotype D have been identified^[11-37]. HBV genotypes and subgenotypes have distinct geographical distributions (Table 1), and often present demographic characteristics. HBV genotype A1, A3, A4, and A5 are endemic in Africa, especially in West Africa, whereas genotype A2 is endemic in Europe^[11-15]. Genotypes B and C are predominant in Asian and Pacific islanders^[6,10,16-22,28]. Of HBV genotypes B and C, subgenotypes B2 and C2 are endemic in most parts of Asia. Subgenotype B1 is endemic in Japan^[16]. Subgenotype C4 is encountered in Aborigines from Australia, and frequently termed as the Australian aboriginal strain^[9,19]. Subgenotypes B3-B8, C1, C3, and C5-C8 have been isolated in South Asia, especially in Indonesia and the Philippines^[17-22,28]. Genotype D is endemic in the entire Old World including Africa, Northern and South Eastern Asia, the Mediterranean area, and most European countries^[13,23-26,32-34,37]. Subgenotype D1 is predominant in Moslem ethnicity. Subgenotype D2 is endemic in Russia and the Baltic region^[26,32]. Subgenotypes D2, D3, and D5 have been found in In-

dia^[32]. Subgenotypes D4 and D6 are endemic in Oceania and Indonesia, respectively^[19,33]. A new subgenotype D7 has been found in Tunisia^[34]. HBV genotype E is endemic in Western and Central Africa^[13,27,35]. HBV genotypes F, G, and H are endemic in America^[29-31,36]. More subgenotypes have been found in South Asia, Oceania, and Africa than other areas in the world, probably indicating evolutionary history of HBV. The distribution of HBV genotypes often provides clues about human migration. HBV genotype B is more frequent than genotype C in Taiwan^[38,39]. Although genotype C is more frequent than genotype B in Mainland China^[40], HBV genotype B accounts for more than 80% in Zhangzhou (our unpublished data), a city at the coastal line of Fujian Province of Mainland China where early Taiwan residents had migrated from. Subgenotype C1 is endemic in Southern Guangdong Province of Mainland China^[41], this subgenotype is also endemic in Hong Kong^[42]. Hong Kong residents are mostly from Southern Guangdong Province of Mainland China. HBV genotype E is endemic in Africa. As genotype E is essentially absent from the Americas despite the Afro-American slave trade until at least the beginning of the 19th century, genotype E strains may have been introduced into the general African population only within the past 200 years^[14,35]. The genetic diversity of HBV and the geographical distribution of its subgenotypes provide a tool to reconstruct the evolutionary history of HBV and may help to complement genetic data in the understanding of the evolution and past migrations of man^[19].

Genotype mixture and its clinical relevance

In an HBV endemic area, infection with more than one HBV genotype often results in genotype recombination and genotype mixture (co-infection or super-infection with multiple HBV genotype in an infected person). With the use of multiplex PCR, a genotype mixture has been frequently identified in the HBV-infected subjects^[43,44]. HBV genotype mixture has been associated with high viral load in patients with chronic hepatitis B (CHB) as compared with patients with a single genotype, also associated with increased *in vitro* HBV replication^[45]. In our recent study, the prevalence of genotype mixture in asymptomatic hepatitis B surface antigen (HBsAg) carriers (ASC), patients with HCC, and patients with CHB is 5.4%, 10.6%, and 13.7%, respectively. Genotype mixture (mostly mixed genotype B with genotype C) is associated with higher viral load and more severe course of the disease than HBV genotype C alone^[40]. These results indicate that co-infection or superinfection with multiple genotypes is associated with worse prognosis of HBV infection.

Clinical relevance of HBV genotypes/subgenotypes

HBV genotypes and subgenotypes have been shown to differ with regard to clinical outcome, prognosis, and response to antiviral treatment. Infection with HBV genotype A is associated with high viral load which facilitates viral transmission. High replication rates of genotype A

Table 1 Geographic distribution and important clinical relevance of HBV genotypes and subgenotypes

Genotype	Subgenotype	Geographic distribution	Important clinical relevance	Ref.
A	A1	Africa	ND	[13-15]
	A2	Europe	Acute infection, chronicification, more sensitive to interferon treatment than genotype D	[11,12,47,48]
	A3	West Africa	ND	[13-15]
	A4	West Africa	ND	[15]
	A5	West Africa	ND	[14,15]
B	B1	Japan	Fulminant hepatitis	[16]
	B2	Most of Asia, except Korea	Acute hepatitis, HCC in mostly those younger than 50 years	[6,10]
	B3	Indonesia	ND	[17,18]
	B4	Indonesia, Vietnam	ND	[18,19]
	B5	Indonesia, Philippines	ND	[17,18,22]
	B6	Indonesia	ND	[28]
	B7	Indonesia	ND	[17,18]
	B8	Indonesia	ND	[17]
C	C1	South Asia, Southern China	HCC and LC	[18]
	C2	Northeast Asia, China	HCC and LC mostly in those older than 50 years	[6,10]
	C3	Indonesia, Oceania	ND	[18,19]
	C4	Australia	ND	[19]
	C5	Indonesia, Philippines	ND	[17,22]
	C6	Indonesia, Philippines	ND	[17,21]
	C7	Indonesia	ND	[17]
	C8	Philippines	ND	[20,21]
	C9	Tibet, China	ND	Unpublished [13,23-25, 37,81]
D	D1 (mainly D)	Middle East, the Mediterranean area	Chronic liver disease, HCC	[26,32]
	D2	Russia, the Baltic region, India	No apparent clinical relevance	[17,32]
	D3	Indonesia, India	Occult HBV infection	[19]
	D4	Oceania	ND	[32]
	D5	India	No apparent clinical relevance	[33]
	D6	Indonesia	ND	[34]
	D7	Tunisia	ND	[13,27,35]
E	ND	Western and Central Africa	ND	[29,36,62]
F	F I a	Central America	HCC	[30,31]
	F I b	Chile, Alaska		
	F II	Argentina, Japan, Venezuela, USA		
	F III	Brazil, Venezuela, Nicaragua		
	F IV	Venezuela, Panama, Columbia		
G	ND	Argentina, Bolivia, France		
H	ND	Mexico, Canada	ND	[30]
I	ND	Mexico	ND	[7,8]
J	ND	Vietnam, Laos	ND	[9]
	ND	Japan (might be from Borneo)	HCC	

HBV: Hepatitis B virus; ND: Not determined; HCC: Hepatocellular carcinoma.

in adults lead to an increased risk of horizontal transmission of HBV by sexual activity because a high concentration of HBV DNA in serum is associated with high concentrations in semen and other body fluids of HBV carriers^[46]. Genotype A also tends to cause chronic infection following an acute course. This has been demonstrated in Japan where genotype A introduced from Europe has started to increase sharply in patients with acute infection since 1991, and gradually in those with chronic infection^[47]. As compared with HBV genotype D endemic in Europe, genotype A is more sensitive to interferon α treatment^[48]. Spontaneous HBeAg seroclearance was significantly higher in genotype A carriers than in carriers of genotypes A, B, D, and F. After losing HBeAg, those with genotypes C and F were more likely to revert to the HBeAg-positive state^[49]. Infection with subgenotype B2 is associated with HCC or HCC recurrence in young, mostly noncirrhotic, patients in Mainland China and Taiwan^[39,40,50], whereas infection with subgenotype

B1 is frequently associated with fulminant hepatitis B in Japan^[16]. Infection with HBV genotype C is associated with increased risks of LC and HCC at an older age as compared with infection with the HBV genotype B^[38,51,52]. Although HBV subgenotypes C1 and C2 are associated with the risk of HCC, only HBV subgenotype C2 is independently associated with an increased risk of HCC^[53]. Genotype B has recently been shown by us to be more likely to cause acute hepatitis B, while the serum viral load of ASCs with genotype B is significantly higher than that of ASCs infected with genotype C^[54]. As compared with genotype C, HBV genotype B has been shown to be associated with earlier HBeAg seroconversion, and associated with better response to interferon therapy in HBeAg-positive chronic hepatitis^[55,56]. Early HBeAg seroconversion typically confers a favorable outcome^[57]. In HBeAg-negative patients, detectable HBV DNA and HBV genotype C are associated with more severe liver damage^[58]. Thus, infection with HBV genotype C is as-

sociated with worse clinical outcome as compared with genotype B. Data from India have shown that HBV subgenotype D1 is significantly associated with chronic liver disease, whereas HBV subgenotype D3 is significantly associated with occult HBV infection. No apparent clinical relevance was observed in those infected with HBV subgenotypes D2 and D5^[52]. There are very limited data on the association of genotype E with its clinical relevance. Population-based prospective cohort studies have found that HBV genotypes C and F are associated with the highest risk for HCC or LC^[59]. HBV genotypes E, F, and H appear to be sensitive to IFN- α treatment^[60]. The recombination of two genotypes is frequent in the area where the two genotypes are endemic^[6,15,61], probably due to the selection of viral growth advantage. Lower rates of response to IFN- α treatment in patients with HBV genotype G might be related to the frequent occurrence of double infection^[60].

CLINICAL AND PUBLIC HEALTH SIGNIFICANCE OF HBV MUTATIONS

Association of HBV PreS and S region mutations with immune escape, occult infection, and the development of HCC

HBV genomic variations in the PreS and S regions which are selected during the infection course are of clinical and public health importance. The HBV envelope is composed of 3 forms of HBsAg, the so-called large (L, coded for by the PreS1/S2/S gene), middle (M, the PreS2/S gene), and small (S, the S gene) proteins. The small or major peptide is 226 amino acids in length, and the M and L proteins are assembled by amino-terminal extension of 55 amino acids at the PreS2 domain and of 108-119 amino acids of the PreS1 domain. HBsAg is the main target for viral neutralization, either by natural or vaccine-induced anti-HBs. A central major hydrophilic region (MHR, approximately residues 103-173) exposed at the surface of viral particles. The MHR itself is structured into five regions, including three central loops held together by disulphide bonds. The immunodominant "a" determinant (residues 124-147), against which most neutralizing antibodies are directed and which is the major target of HBsAg detection tests, is formed by loops 2 and 3^[62]. HBV with mutations in the portion of the S gene coding the "a" determinant of hepatitis surface antigen, including a glycine to arginine substitution at position 145 (G145R) and other S gene mutations in the region of amino acids 120-147, can potentially evade neutralizing anti-HBs antibody and infect vaccinated people. G145R is by far the most common immune escape mutant, whereas the most important immune escape mutants with substitutions outside of the "a" determinant is P120S/T. Mutations in the S genes within "a" determinant (but not G145R) are partially responsible for occult HBV infection, which are characterized by the presence of HBV DNA in serum in the absence of detectable HBsAg, and could present a risk to blood safety^[63]. Mutations in PreS are also associated with occult HBV infection^[64], probably due

to the inactivation of the overlapping PreS2/S promoter which causes impaired HBsAg secretion.

The 5' flanking region of the S gene coding the PreS1 and PreS2 domains is overlapped by the region of the P gene coding the spacer domain of the viral polymerase. Genotype D and non-human primate isolates inherently have a 33 nucleotide deletion at or near the beginning of the PreS1 open reading frame^[10,62]. The PreS1 protein contains the hepatocyte binding site (amino acids 21-47) and is known to be essential for virion assembly and for the transporting of virions out of the hepatocyte^[65]. The PreS1 and PreS2 regions play an essential role in the interaction with immune responses because they contain several epitopes for T or B cells^[66]. There is little evidence supporting the idea that PreS mutants are transmissible, therefore, the PreS mutation might generate during the pathological process following the infection. The PreS mutations emerge in chronic infections, often in patients treated with interferon, and seem to represent desperate attempts to escape from host immune surveillance^[62]. Many of the mutations affecting the PreS domains of the envelope proteins are deletions. More recently, PreS deletions are frequently associated with an increased risk of HCC, especially in those infected with HBV genotype C^[66-69]. Our recent meta-analysis showed that the frequencies of the PreS deletion mutation consecutively increased during the progression of chronic HBV infection from ASC states to LC or HCC ($P_{trend} < 0.001$), while the frequencies of mutations at the promoter sites of PreS1 and PreS2 were significantly higher in the patients with HCC than in the patients without HCC ($P < 0.001$, $P = 0.032$, respectively)^[70]. It is suggested that PreS deletion and nucleotide substitution mutations at the promoter sites of PreS1 and PreS2 may serve as useful biomarkers for predicting the clinical outcomes of HBV-infected patients, especially for predicting HCC.

Polymerase mutations associated with drug resistance

HBV variants harboring mutations in the viral polymerase gene that confer resistance to antiviral drugs may be gradually selected during long-term antiviral therapy with nucleoside analogs. The main polymerase gene mutations conferring resistance to nucleoside analogs have been well characterized. Lamivudine resistance mutants harbor a M204V or I substitution in the YMDD motif of the C domain of the polymerase/reverse transcriptase. Adefovir resistance mutants harbor a N236T and/or A181V amino acid substitution in the D and B domains of viral polymerase, respectively^[71,72]. Entecavir resistance mutations occurred on a background of lamivudine resistance, as these patients received entecavir for lamivudine failure, with a combination of substitutions I169T and M250V, or T184G and S202I. These additional mutations clearly conferred an increased level of entecavir resistance compared to the initial lamivudine resistant strain^[62]. Resistance to telbivudine has been associated with a M204I mutation in the viral polymerase^[73]. Table 2 summarizes drug-resistance-associated amino acid substitutions in the 5 domains of HBV polymerase. On the other hand, the reappearance of wild-type virus

Table 2 HBV mutations associated with drug resistance

Nucleoside analogs	Mutations in the polymerase domains (amino acids)				
	A	B	C (YMDD)	D	E
Lamivudine/-	-	V173L	M204I/V	-	-
Emtricitabine		L180M			
Adefovir	-	A181V	I233V	N236T	-
Entecavir	-	I169T	S202I	M250V	-
		T184G			
Telbivudine	-	-	M204I	-	-
Famciclovir	-	L180M	-	-	-

-: Not reported.

as the major viral population after cessation of drug treatment is probably due to persistence of non-mutated cccDNA molecules in hepatocytes even after long-term drug treatment^[62,74]. Naïve patients infected with adefovir resistance mutants have been reported^[71]. In this case, drug resistant mutants transmitted to a naïve subject may be stable since there will be no competition with wild-type virus.

The association of viral mutations in the Enh II /BCP/Precore region with hepatocarcinogenesis

The core promoter, positively and negatively regulated by Enhancer II and to some extent by Enhancer I, controls the transcription of precore mRNA and pregenomic RNA that can be the mRNA for both core protein and the viral polymerase and is the template for viral replication. HBeAg expression indicates active viral replication. There are two classes of mutants that affect HBeAg expression, BCP mutants and precore mutants. Although viral loads are generally several logs lower in HBeAg-negative patients than in HBeAg-positive patients and children born to HBeAg-positive mothers have a much higher risk of contracting chronic HBV infection than children born to HBeAg-negative mothers^[62], some combined mutations in the Enh II /BCP/Precore region like 1766/1768, 1762/1764/1766, 1753/1762/1764, and 1753/1762/1764/1766 mutations have been associated with high HBV DNA production in the *in vitro* transfection studies^[75,76]. HBV core promoter mutations other than those at 1762/1764 appear to upregulate viral DNA replication and, at the same time, greatly reduce HBeAg production. Although expression of HBeAg has been associated with an increased risk of HCC in a prospective study^[77], high viral load in HBeAg-negative patients is often associated with worse outcome of chronic HBV infection, especially in those with HBV carrying mutations at the PreS and Enh II /BCP/Precore regions^[66,78-82].

Several mutations at the Enh II /BCP/Precore region have been recently associated with an increased risk of HCC. These mutations include C1653T, T1753V, T1766/A1768, and A1762T/G1764A^[81-92]. Our recent meta-analysis using published data up to August 31, 2008 has shown that C1653T, T1753V, and A1762T/G1764A are each associated with an increased risk of HCC, whereas precore mutations G1896A and C1858T are not associ-

ated with the risk of HCC, regardless of HBeAg status and HBV genotype^[70]. A1762T/G1764A has been shown to be a valuable biomarker for identifying a subset of male HBsAg carriers who are at extremely high risk of HCC in a prospective study^[92]. In a community-based prospective study, A1762T/G1764A and genotype C have been associated with an increased risk of HCC, whereas G1896A in the precore region has been associated with decreased risk of HCC^[84]. G1896A has been associated with fulminant hepatitis in Japan^[93]. Since the Enh II /BCP/Precore region overlaps with X gene in the HBV genome, mutations in the Enh II /BCP/Precore region should be included in evaluating the role of HBV X protein on the development of HCC. That is to say, the mutated X protein might be more carcinogenic than the wild-type X protein in HBV-induced hepatocarcinogenesis.

C1653T, T1753V, and A1762T/G1764A are increasingly more prevalent as chronic HBV infection progresses from the asymptomatic HBsAg carrier state to liver cirrhosis or HCC, indicating that these mutations accumulate before the diagnosis of HCC^[70]. This finding suggests that these HBV mutations may serve as useful biomarkers for predicting clinical outcomes of the patients with CHB, especially with regard to predicting whether they will develop HCC. Like the PreS mutants, HCC-associated HBV mutants in the Enh II /BCP/Precore region, e.g. A1762T/G1764A mutants, may not transmit *via* mother-to-child vertical transmission because the children whose mothers carrying HBV mutants were mostly found to be infected with wild-type form of the same viruses^[94,95]. These HBV mutations are likely generated during HBV-induced pathogenesis. A1762T/G1764A is frequently detected approximately 10 years before the diagnosis of HCC^[70]. It is therefore necessary to set up likely checkpoints in the life time for the examination of the HCC-associated HBV mutations in HBV-infected subjects. Recent epidemiological studies demonstrated that male sex, old age, high HBV DNA (> 10 000 copies/mL), viral mutations in the PreS and the Enh II /BCP/Precore regions, HBV genotypes (C and F), cirrhosis, and family history were associated with an increased risk of HCC^[50-52,65,79-92,96,97]. Further study should focus on systemic evaluation of these risk factors for the prediction of HCC.

Combined HBV mutations in the PreS and the Enh II /BCP/Precore regions are becoming important in evaluating HCC risk of HBV-infected subjects^[66,69,98]. In a meta-analysis, we have demonstrated that the frequencies of A1762T/G1764A+C1653T (8.6%), A1762T/G1764A+T1753V (14.6%), A1762T/G1764A+PreS mutation (2.2%), and A1762T/G1764A+C1653T+T1753V (3.2%) are low in ASCs, whereas the frequencies of A1762T/G1764A-based combined mutations are statistically significantly higher in patients with HCC than in patients without HCC^[70]. For the prediction of HCC in HBV-infected subjects, A1762T/G1764A alone has a sensitivity and specificity of 70.6% (95% CI = 68.7% to 72.5%) and 60.6% (95% CI = 68.7% to 62.0%), respectively, whereas C1653T+T1753V and A1762T/G1764A+C1653T+T1753V has high specificity [92.6% (95% CI = 89.2% to 96.0%) and 93.9% (95%

CI = 90.5% to 97.2%), respectively] but low sensitivity [20.6% (95% CI = 14.9% to 26.3%) and 24.3% (95% CI = 17.5% to 31.1%), respectively]^[70]. These mutations, alone or in combination, might be reasonably arranged as predictive markers for the prediction of HCC.

INTERACTIONS BETWEEN HBV AND HOST SUSCEPTIBLE GENES

HBV genetic variations are necessary but insufficient for HBV-induced hepatocarcinogenesis. HBV genotype-associated mutations might be selected by the host immune system and in turn promote host hepatocarcinogenesis. It is possible that the mutated X protein could transactivate host oncogenes responsible for the development of HCC or that transactivators encoded by some oncogenes select the specific HBV mutations during HBV-induced hepatocarcinogenesis. There are many important trans-activating nuclear factors binding sites located in the PreS and the Enh II /BCP/Precore regions^[66,69,70]. Mutations in the PreS and the Enh II /BCP/Precore regions might alter the binding ability of some potential trans-activating factors and therefore alter viral replication and/or change expression profiling of some related host genes. The genetic predisposition of some host genes like *MDM2* and *p53* gene polymorphisms, cytokine and TGF-β1 gene polymorphisms, and DNA repair gene polymorphisms have been associated with HBV-induced hepatocarcinogenesis^[99-102]. Our recent study demonstrated that nuclear factor κB1 gene promoter *NFKB1*-94ATTG2 allelic carriage, *IκBα* gene promoter *NFKB1A*-826T and *NFKB1A*-881AG allelic carriage, and HBV genotype C are independently associated with an increased risk of HCC, while the estimated haplotype frequency of *NFKB1A* promoter -881G-826T-519C is significantly higher in the patients with HCC than in the HBV-infected subjects without HCC^[103]. Even so, it is largely unknown so far how HBV variations interact with host genetic susceptibility. Understanding the interactions between HBV genetic variations and host genetic susceptibility is undoubtedly helpful in classifying the HBV-infected subjects who will develop HCC in future and need active anti-viral treatments and extensive surveillance of HCC.

CONCLUSION

Ten HBV genotypes (A-J) and 34 subgenotypes have been identified so far. HBV genotypes and subgenotypes have distinct geographical distributions, and have been shown to differ with regard to clinical outcome, prognosis, and response to interferon treatment. Infection with subgenotype A2 is frequently associated with high viral load, resulting in acute infection via horizontal transmission. Genotypes A and B are more sensitive to interferon treatment than genotypes D and C, respectively. Genotype B is more common in acute hepatitis than genotype C, whereas genotype C (C2) is more frequently associated with an increased risk of HCC, mostly cirrhotic, as compared

with genotype B (B2). Genotypes C and F are frequently associated with the development of HCC. Viral load of the patients with genotype mixture is usually higher than that of those infected with unique genotype. HBV mutations in the S genes, especially amino acid substitutions at position 145 (G145R), are associated with immune escape, whereas the mutations in the PreS or S genes which cause impaired HBsAg secretion could present a risk to blood safety. HBV variants harboring mutations in the viral polymerase gene that confer resistance to antiviral drugs may be selected during antiviral therapy with nucleoside analogs. Genetic diversity of HBV is partly due to virus/host interactions and partly due to parallel evolution in geographically distinct areas. Different genotypes have a distinct pattern of mutations in the PreS and Enh II /BCP/Precore regions. PreS deletions, C1653T, T1753V, and A1762T/G1764A are associated with an increased risk of HCC. HCC-associated HBV mutants may not transmit via mother-to-child vertical transmission, and are likely generated during HBV-induced pathogenesis. Frequent examination of HBV mutation alone or in combination as well as genetic susceptibility will be helpful in classifying the HBV-infected subjects who will develop HCC and need active anti-viral treatments.

REFERENCES

- 1 Lavanchy D. Worldwide epidemiology of HBV infection, disease burden, and vaccine prevention. *J Clin Virol* 2005; **34** Suppl 1: S1-S3
- 2 Lai CL, Ratziu V, Yuen MF, Poynard T. Viral hepatitis B. *Lancet* 2003; **362**: 2089-2094
- 3 El-Serag HB, Rudolph KL. Hepatocellular carcinoma: epidemiology and molecular carcinogenesis. *Gastroenterology* 2007; **132**: 2557-2576
- 4 Nguyen VT, Law MG, Dore GJ. Hepatitis B-related hepatocellular carcinoma: epidemiological characteristics and disease burden. *J Viral Hepat* 2009; **16**: 453-463
- 5 Chang MH, You SL, Chen CJ, Liu CJ, Lee CM, Lin SM, Chu HC, Wu TC, Yang SS, Kuo HS, Chen DS. Decreased incidence of hepatocellular carcinoma in hepatitis B vaccinees: a 20-year follow-up study. *J Natl Cancer Inst* 2009; **101**: 1348-1355
- 6 Schaefer S. Hepatitis B virus taxonomy and hepatitis B virus genotypes. *World J Gastroenterol* 2007; **13**: 14-21
- 7 Tran TT, Trinh TN, Abe K. New complex recombinant genotype of hepatitis B virus identified in Vietnam. *J Virol* 2008; **82**: 5657-5663
- 8 Olinger CM, Jutavijittum P, Hubschen JM, Yousukh A, Samountry B, Thammavong T, Toriyama K, Muller CP. Possible new hepatitis B virus genotype, southeast Asia. *Emerg Infect Dis* 2008; **14**: 1777-1780
- 9 Tatematsu K, Tanaka Y, Kurbanov F, Sugauchi F, Mano S, Maeshiro T, Nakayoshi T, Wakuta M, Miyakawa Y, Mizokami M. A genetic variant of hepatitis B virus divergent from known human and ape genotypes isolated from a Japanese patient and provisionally assigned to new genotype J. *J Virol* 2009; **83**: 10538-10547
- 10 Schaefer S. Hepatitis B virus: significance of genotypes. *J Viral Hepat* 2005; **12**: 111-124
- 11 Deterding K, Constantinescu I, Nedelcu FD, Gervain J, Nemecek V, Srtunecky O, Vince A, Grgurevic I, Bielawski KP, Zalewska M, Bock T, Ambrozaitis A, Stanczak J, Takacs M, Chulanov V, Slusarczyk J, Drazd'akova M, Wiegand J, Cornberg M, Manns MP, Wedemeyer H. Prevalence of HBV genotypes in Central and Eastern Europe. *J Med Virol* 2008;

- 80: 1707-1711
- 12 **Schaefer S.** Hepatitis B virus genotypes in Europe. *Hepatol Res* 2007; **37**: S20-S26
- 13 **Kramvis A,** Kew MC. Epidemiology of hepatitis B virus in Africa, its genotypes and clinical associations of genotypes. *Hepatol Res* 2007; **37**: S9-S19
- 14 **Andernach IE,** Nolte C, Pape JW, Muller CP. Slave trade and hepatitis B virus genotypes and subgenotypes in Haiti and Africa. *Emerg Infect Dis* 2009; **15**: 1222-1228
- 15 **Olinger CM,** Venard V, Njayou M, Oyefolu AO, Maiga I, Kemp AJ, Omilabu SA, le Faou A, Muller CP. Phylogenetic analysis of the precore/core gene of hepatitis B virus genotypes E and A in West Africa: new subtypes, mixed infections and recombinations. *J Gen Virol* 2006; **87**: 1163-1173
- 16 **Kusakabe A,** Tanaka Y, Mochida S, Nakayama N, Inoue K, Sata M, Isoda N, Kang JH, Sumino Y, Yatsuhashi H, Takikawa Y, Kaneko S, Yamada G, Karino Y, Tanaka E, Kato J, Sakaida I, Izumi N, Sugauchi F, Nojiri S, Joh T, Miyakawa Y, Mizokami M. Case-control study for the identification of virological factors associated with fulminant hepatitis B. *Hepatol Res* 2009; **39**: 648-656
- 17 **Mulyanto,** Depamede SN, Surayah K, Tsuda F, Ichiyama K, Takahashi M, Okamoto H. A nationwide molecular epidemiological study on hepatitis B virus in Indonesia: identification of two novel subgenotypes, B8 and C7. *Arch Virol* 2009; **154**: 1047-1059
- 18 **Utama A,** Purwantomo S, Siburian MD, Dhenni R, Gani RA, Hasan I, Sanityoso A, Miskad UA, Akil F, Yusuf I, Achwan WA, Soemohardjo S, Lelosutan SA, Martamala R, Lukito B, Budihusodo U, Lesmana LA, Sulaiman A, Tai S. Hepatitis B virus subgenotypes and basal core promoter mutations in Indonesia. *World J Gastroenterol* 2009; **15**: 4028-4036
- 19 **Norder H,** Courouce AM, Coursaget P, Echevarria JM, Lee SD, Mushahwar IK, Robertson BH, Locarnini S, Magnus LO. Genetic diversity of hepatitis B virus strains derived worldwide: genotypes, subgenotypes, and HBsAg subtypes. *Intervirology* 2004; **47**: 289-309
- 20 **Cavinta L,** Cao G, Schaefer S. Description of a new hepatitis B virus C6 subgenotype found in the Papua province of Indonesia and suggested renaming of a tentative C6 subgenotype found in the Philippines as subgenotype C7. *J Clin Microbiol* 2009; **47**: 3068-3069
- 21 **Cavinta L,** Sun J, May A, Yin J, von Meltzer M, Radtke M, Barzaga NG, Cao G, Schaefer S. A new isolate of hepatitis B virus from the Philippines possibly representing a new subgenotype C6. *J Med Virol* 2009; **81**: 983-987
- 22 **Sakamoto T,** Tanaka Y, Orito E, Co J, Clavio J, Sugauchi F, Ito K, Ozasa A, Quino A, Ueda R, Sollano J, Mizokami M. Novel subtypes (subgenotypes) of hepatitis B virus genotypes B and C among chronic liver disease patients in the Philippines. *J Gen Virol* 2006; **87**: 1873-1882
- 23 **Abdo AA,** Al-Jarallah BM, Sanai FM, Hersi AS, Al-Swat K, Azzam NA, Al-Dukhayil M, Al-Maarik A, Al-Faleh FZ. Hepatitis B genotypes: relation to clinical outcome in patients with chronic hepatitis B in Saudi Arabia. *World J Gastroenterol* 2006; **12**: 7019-7024
- 24 **Mojiri A,** Behzad-Behbahani A, Saberifirozi M, Ardabili M, Beheshti M, Rahsaz M, Banihashemi M, Azarpira N, Geramizadeh B, Khadang B, Moaddeb A, Ghaedi M, Heidari T, Torab A, Salah A, Amirzadeh S, Jowkar Z, Mehrabani D, Amini-Bavil-Olyaei S, Dehyadegari MA. Hepatitis B virus genotypes in southwest Iran: molecular, serological and clinical outcomes. *World J Gastroenterol* 2008; **14**: 1510-1513
- 25 **Bozdayi G,** Turkyilmaz AR, Idilman R, Karatayli E, Rota S, Yurdagdin C, Bozdayi AM. Complete genome sequence and phylogenetic analysis of hepatitis B virus isolated from Turkish patients with chronic HBV infection. *J Med Virol* 2005; **76**: 476-481
- 26 **Tallo T,** Tefanova V, Priimagi L, Schmidt J, Katargina O, Michailov M, Mukomolov S, Magnus L, Norder H. D2: major subgenotype of hepatitis B virus in Russia and the Baltic region. *J Gen Virol* 2008; **89**: 1829-1839
- 27 **Garmiri P,** Loua A, Haba N, Candotti D, Allain JP. Deletions and recombinations in the core region of hepatitis B virus genotype E strains from asymptomatic blood donors in Guinea, west Africa. *J Gen Virol* 2009; **90**: 2442-2451
- 28 **Nurainy N,** Muljono DH, Sudoyo H, Marzuki S. Genetic study of hepatitis B virus in Indonesia reveals a new subgenotype of genotype B in east Nusa Tenggara. *Arch Virol* 2008; **153**: 1057-1065
- 29 **Di Lello FA,** Pineiro Y Leone FG, Munoz G, Campos RH. Diversity of hepatitis B and C viruses in Chile. *J Med Virol* 2009; **81**: 1887-1894
- 30 **Alvarado-Esquivel C,** Sablon E, Conde-Gonzalez CJ, Juarez-Figueroa L, Ruiz-Maya L, Aguilar-Benavides S. Molecular analysis of hepatitis B virus isolates in Mexico: predominant circulation of hepatitis B virus genotype H. *World J Gastroenterol* 2006; **12**: 6540-6545
- 31 **Osiowy C,** Gordon D, Borlang J, Giles E, Villeneuve JP. Hepatitis B virus genotype G epidemiology and co-infection with genotype A in Canada. *J Gen Virol* 2008; **89**: 3009-3015
- 32 **Chandra PK,** Biswas A, Datta S, Banerjee A, Panigrahi R, Chakrabarti S, De BK, Chakravarty R. Subgenotypes of hepatitis B virus genotype D (D1, D2, D3 and D5) in India: differential pattern of mutations, liver injury and occult HBV infection. *J Viral Hepat* 2009; **16**: 749-756
- 33 **Utsumi T,** Lusida MI, Yano Y, Nugrahaputra VE, Amin M, Juniautti, Soetijpto, Hayashi Y, Hotta H. Complete genome sequence and phylogenetic relatedness of hepatitis B virus isolates in Papua, Indonesia. *J Clin Microbiol* 2009; **47**: 1842-1847
- 34 **Meldal BH,** Moula NM, Barnes IH, Boukef K, Allain JP. A novel hepatitis B virus subgenotype, D7, in Tunisian blood donors. *J Gen Virol* 2009; **90**: 1622-1628
- 35 **Hubschen JM,** Andernach IE, Muller CP. Hepatitis B virus genotype E variability in Africa. *J Clin Virol* 2008; **43**: 376-380
- 36 **Livingston SE,** Simonetti JP, McMahon BJ, Bulkow LR, Hurlburt KJ, Homan CE, Snowball MM, Cagle HH, Williams JL, Chulanov VP. Hepatitis B virus genotypes in Alaska Native people with hepatocellular carcinoma: preponderance of genotype F. *J Infect Dis* 2007; **195**: 5-11
- 37 **Masaadeh HA,** Hayajneh WA, Alqudah EA. Hepatitis B virus genotypes and lamivudine resistance mutations in Jordan. *World J Gastroenterol* 2008; **14**: 7231-7234
- 38 **Yu MW,** Yeh SH, Chen PJ, Liaw YF, Lin CL, Liu CJ, Shih WL, Kao JH, Chen DS, Chen CJ. Hepatitis B virus genotype and DNA level and hepatocellular carcinoma: a prospective study in men. *J Natl Cancer Inst* 2005; **97**: 265-272
- 39 **Kao JH,** Chen PJ, Lai MY, Chen DS. Hepatitis B genotypes correlate with clinical outcomes in patients with chronic hepatitis B. *Gastroenterology* 2000; **118**: 554-559
- 40 **Yin J,** Zhang H, Li C, Gao C, He Y, Zhai Y, Zhang P, Xu L, Tan X, Chen J, Cheng S, Schaefer S, Cao G. Role of hepatitis B virus genotype mixture, subgenotypes C2 and B2 on hepatocellular carcinoma: compared with chronic hepatitis B and asymptomatic carrier state in the same area. *Carcinogenesis* 2008; **29**: 1685-1691
- 41 **Yuan J,** Zhou B, Tanaka Y, Kurbanov F, Orito E, Gong Z, Xu L, Lu J, Jiang X, Lai W, Mizokami M. Hepatitis B virus (HBV) genotypes/subgenotypes in China: mutations in core promoter and precore/core and their clinical implications. *J Clin Virol* 2007; **39**: 87-93
- 42 **Orito E,** Mizokami M. Differences of HBV genotypes and hepatocellular carcinoma in Asian countries. *Hepatol Res* 2007; **37**: S33-S35
- 43 **Chen J,** Yin J, Tan X, Zhang H, Zhang H, Chen B, Chang W, Schaefer S, Cao G. Improved multiplex-PCR to identify hepatitis B virus genotypes A-F and subgenotypes B1, B2, C1 and C2. *J Clin Virol* 2007; **38**: 238-243
- 44 **Kirschberg O,** Schuttler C, Repp R, Schaefer S. A multiplex-PCR to identify hepatitis B virus--enotypes A-F. *J Clin Virol* 2004; **29**: 39-43
- 45 **Toan NL,** Song le H, Kremsner PG, Duy DN, Binh VQ, Koeberlein B, Kaiser S, Kandolf R, Torresi J, Bock CT. Impact

- of the hepatitis B virus genotype and genotype mixtures on the course of liver disease in Vietnam. *Hepatology* 2006; **43**: 1375-1384
- 46 **Kidd-Ljunggren K**, Holmberg A, Blackberg J, Lindqvist B. High levels of hepatitis B virus DNA in body fluids from chronic carriers. *J Hosp Infect* 2006; **64**: 352-357
- 47 **Kobayashi M**, Ikeda K, Arase Y, Suzuki F, Akuta N, Hosaka T, Sezaki H, Yatsuji H, Kobayashi M, Suzuki Y, Watahiki S, Mineta R, Iwasaki S, Miyakawa Y, Kumada H. Change of hepatitis B virus genotypes in acute and chronic infections in Japan. *J Med Virol* 2008; **80**: 1880-1884
- 48 **Erhardt A**, Blondin D, Hauck K, Sagir A, Kohnle T, Heintges T, Haussinger D. Response to interferon alfa is hepatitis B virus genotype dependent: genotype A is more sensitive to interferon than genotype D. *Gut* 2005; **54**: 1009-1013
- 49 **Livingston SE**, Simonetti JP, Bulkow LR, Homan CE, Snowball MM, Cagle HH, Negus SE, McMahon BJ. Clearance of hepatitis B e antigen in patients with chronic hepatitis B and genotypes A, B, C, D, and F. *Gastroenterology* 2007; **133**: 1452-1457
- 50 **Ni YH**, Chang MH, Wang KJ, Hsu HY, Chen HL, Kao JH, Yeh SH, Jeng YM, Tsai KS, Chen DS. Clinical relevance of hepatitis B virus genotype in children with chronic infection and hepatocellular carcinoma. *Gastroenterology* 2004; **127**: 1733-1738
- 51 **Chan HL**, Hui AY, Wong ML, Tse AM, Hung LC, Wong VW, Sung JJ. Genotype C hepatitis B virus infection is associated with an increased risk of hepatocellular carcinoma. *Gut* 2004; **53**: 1494-1498
- 52 **Chan HL**, Wong GL, Tse CH, Chim AM, Yiu KK, Chan HY, Sung JJ, Wong VW. Hepatitis B Virus Genotype C Is Associated With More Severe Liver Fibrosis Than Genotype B. *Clin Gastroenterol Hepatol* 2009; Epub ahead of print
- 53 **Chan HL**, Tse CH, Mo F, Koh J, Wong VW, Wong GL, Lam Chan S, Yeo W, Sung JJ, Mok TS. High viral load and hepatitis B virus subgenotype ce are associated with increased risk of hepatocellular carcinoma. *J Clin Oncol* 2008; **26**: 177-182
- 54 **Zhang HW**, Yin JH, Li YT, Li CZ, Ren H, Gu CY, Wu HY, Liang XS, Zhang P, Zhao JF, Tan XJ, Lu W, Schaefer S, Cao GW. Risk factors for acute hepatitis B and its progression to chronic hepatitis in Shanghai, China. *Gut* 2008; **57**: 1713-1720
- 55 **Chu CJ**, Hussain M, Lok AS. Hepatitis B virus genotype B is associated with earlier HBeAg seroconversion compared with hepatitis B virus genotype C. *Gastroenterology* 2002; **122**: 1756-1762
- 56 **Wai CT**, Chu CJ, Hussain M, Lok AS. HBV genotype B is associated with better response to interferon therapy in HBeAg(+) chronic hepatitis than genotype C. *Hepatology* 2002; **36**: 1425-1430
- 57 **Lin CL**, Kao JH. Hepatitis B viral factors and clinical outcomes of chronic hepatitis B. *J Biomed Sci* 2008; **15**: 137-145
- 58 **Chan HL**, Tsang SW, Liew CT, Tse CH, Wong ML, Ching JY, Leung NW, Tam JS, Sung JJ. Viral genotype and hepatitis B virus DNA levels are correlated with histological liver damage in HBeAg-negative chronic hepatitis B virus infection. *Am J Gastroenterol* 2002; **97**: 406-412
- 59 **McMahon BJ**. The natural history of chronic hepatitis B virus infection. *Hepatology* 2009; **49**: S45-S55
- 60 **Erhardt A**, Gobel T, Ludwig A, Lau GK, Marcellin P, van Bommel F, Heinzel-Pleines U, Adams O, Haussinger D. Response to antiviral treatment in patients infected with hepatitis B virus genotypes E-H. *J Med Virol* 2009; **81**: 1716-1720
- 61 **Chauhan R**, Kazim SN, Kumar M, Bhattacharjee J, Krishnamoorthy N, Sarin SK. Identification and characterization of genotype A and D recombinant hepatitis B virus from Indian chronic HBV isolates. *World J Gastroenterol* 2008; **14**: 6228-6236
- 62 **Kay A**, Zoulim F. Hepatitis B virus genetic variability and evolution. *Virus Res* 2007; **127**: 164-176
- 63 **Tabor E**. Infections by hepatitis B surface antigen gene mutants in Europe and North America. *J Med Virol* 2006; **78** Suppl 1: S43-S47
- 64 **Mu SC**, Lin YM, Jow GM, Chen BF. Occult hepatitis B virus infection in hepatitis B vaccinated children in Taiwan. *J Hepatol* 2009; **50**: 264-272
- 65 **Shinkai N**, Tanaka Y, Ito K, Mukaide M, Hasegawa I, Asahina Y, Izumi N, Yatsuhashi H, Orito E, Joh T, Mizokami M. Influence of hepatitis B virus X and core promoter mutations on hepatocellular carcinoma among patients infected with subgenotype C2. *J Clin Microbiol* 2007; **45**: 3191-3197
- 66 **Chen CH**, Hung CH, Lee CM, Hu TH, Wang JH, Wang JC, Lu SN, Changchien CS. Pre-S deletion and complex mutations of hepatitis B virus related to advanced liver disease in HBeAg-negative patients. *Gastroenterology* 2007; **133**: 1466-1474
- 67 **Gao ZY**, Li T, Wang J, Du JM, Li YJ, Li J, Lu FM, Zhuang H. Mutations in preS genes of genotype C hepatitis B virus in patients with chronic hepatitis B and hepatocellular carcinoma. *J Gastroenterol* 2007; **42**: 761-768
- 68 **Mun HS**, Lee SA, Jee Y, Kim H, Park JH, Song BC, Yoon JH, Kim YJ, Lee HS, Hyun JW, Hwang ES, Kook YH, Kim BJ. The prevalence of hepatitis B virus preS deletions occurring naturally in Korean patients infected chronically with genotype C. *J Med Virol* 2008; **80**: 1189-1194
- 69 **Chen BF**, Liu CJ, Jow GM, Chen PJ, Kao JH, Chen DS. High prevalence and mapping of pre-S deletion in hepatitis B virus carriers with progressive liver diseases. *Gastroenterology* 2006; **130**: 1153-1168
- 70 **Liu S**, Zhang H, Gu C, Yin J, He Y, Xie J, Cao G. Associations between hepatitis B virus mutations and the risk of hepatocellular carcinoma: a meta-analysis. *J Natl Cancer Inst* 2009; **101**: 1066-1082
- 71 **Kwon SY**, Choe WH, Lee CH, Yeon JE, Byun KS. Rapid re-emergence of YMDD mutation of hepatitis B virus with hepatic decompensation after lamivudine retreatment. *World J Gastroenterol* 2008; **14**: 4416-4419
- 72 **Schildgen O**, Sirma H, Funk A, Olotu C, Wend UC, Hartmann H, Helm M, Rockstroh JK, Willems WR, Will H, Gerlich WH. Variant of hepatitis B virus with primary resistance to adefovir. *N Engl J Med* 2006; **354**: 1807-1812
- 73 **Lai CL**, Gane E, Liaw YF, Hsu CW, Thongsawat S, Wang Y, Chen Y, Heathcote EJ, Rasenack J, Bzowej N, Naoumov NV, Di Bisceglie AM, Zeuzem S, Moon YM, Goodman Z, Chao G, Constance BF, Brown NA. Telbivudine versus lamivudine in patients with chronic hepatitis B. *N Engl J Med* 2007; **357**: 2576-2588
- 74 **Lu HY**, Zhuang LW, Yu YY, Si CW, Li J, Zhang JJ, Zeng Z, Chen XY, Han ZH, Chen Y. Effects of antiviral agents and HBV genotypes on intrahepatic covalently closed circular DNA in HBeAg-positive chronic hepatitis B patients. *World J Gastroenterol* 2008; **14**: 1268-1273
- 75 **Parekh S**, Zoulim F, Ahn SH, Tsai A, Li J, Kawai S, Khan N, Trepo C, Wands J, Tong S. Genome replication, virion secretion, and e antigen expression of naturally occurring hepatitis B virus core promoter mutants. *J Virol* 2003; **77**: 6601-6612
- 76 **Jammeh S**, Tavner F, Watson R, Thomas HC, Karayannidis P. Effect of basal core promoter and pre-core mutations on hepatitis B virus replication. *J Gen Virol* 2008; **89**: 901-909
- 77 **Yang HI**, Lu SN, Liaw YF, You SL, Sun CA, Wang LY, Hsiao CK, Chen PJ, Chen DS, Chen CJ. Hepatitis B e antigen and the risk of hepatocellular carcinoma. *N Engl J Med* 2002; **347**: 168-174
- 78 **Wong GL**, Wong VW, Choi PC, Chan AW, Chim AM, Yiu KK, Chan HY, Chan FK, Sung JJ, Chan HL. Evaluation of alanine transaminase and hepatitis B virus DNA to predict liver cirrhosis in hepatitis B e antigen-negative chronic hepatitis B using transient elastography. *Am J Gastroenterol* 2008; **103**: 3071-3081
- 79 **Choi CS**, Cho EY, Park R, Kim SJ, Cho JH, Kim HC. X gene mutations in hepatitis B patients with cirrhosis, with and without hepatocellular carcinoma. *J Med Virol* 2009; **81**:

- 1721-1725
- 80 **Tong MJ**, Blatt LM, Kao JH, Cheng JT, Corey WG. Precore/basal core promoter mutants and hepatitis B viral DNA levels as predictors for liver deaths and hepatocellular carcinoma. *World J Gastroenterol* 2006; **12**: 6620-6626
- 81 **Bahramali G**, Sadeghizadeh M, Amini-Bavil-Olyaei S, Alavian SM, Behzad-Behbahani A, Adeli A, Aghasadeghi MR, Amini S, Mahboudi F. Clinical, virologic and phylogenetic features of hepatitis B infection in Iranian patients. *World J Gastroenterol* 2008; **14**: 5448-5453
- 82 **Yuen MF**, Tanaka Y, Fong DY, Fung J, Wong DK, Yuen JC, But DY, Chan AO, Wong BC, Mizokami M, Lai CL. Independent risk factors and predictive score for the development of hepatocellular carcinoma in chronic hepatitis B. *J Hepatol* 2009; **50**: 80-88
- 83 **Guo X**, Jin Y, Qian G, Tu H. Sequential accumulation of the mutations in core promoter of hepatitis B virus is associated with the development of hepatocellular carcinoma in Qidong, China. *J Hepatol* 2008; **49**: 718-725
- 84 **Yang HI**, Yeh SH, Chen PJ, Iloeje UH, Jen CL, Su J, Wang LY, Lu SN, You SL, Chen DS, Liaw YF, Chen CJ. Associations between hepatitis B virus genotype and mutants and the risk of hepatocellular carcinoma. *J Natl Cancer Inst* 2008; **100**: 1134-1143
- 85 **Dong Q**, Chan HL, Liu Z, Chan DP, Zhang B, Chen Y, Kung HF, Sung JJ, He ML. A1762T/G1764A mutations of hepatitis B virus, associated with the increased risk of hepatocellular carcinoma, reduce basal core promoter activities. *Biochem Biophys Res Commun* 2008; **374**: 773-776
- 86 **Sung JJ**, Tsui SK, Tse CH, Ng EY, Leung KS, Lee KH, Mok TS, Bartholomeusz A, Au TC, Tsui KK, Locarnini S, Chan HL. Genotype-specific genomic markers associated with primary hepatomas, based on complete genomic sequencing of hepatitis B virus. *J Virol* 2008; **82**: 3604-3611
- 87 **Ito K**, Tanaka Y, Kato M, Fujiwara K, Suguchi F, Sakamoto T, Shinkai N, Orito E, Mizokami M. Comparison of complete sequences of hepatitis B virus genotype C between inactive carriers and hepatocellular carcinoma patients before and after seroconversion. *J Gastroenterol* 2007; **42**: 837-844
- 88 **Chou YC**, Yu MW, Wu CF, Yang SY, Lin CL, Liu CJ, Shih WL, Chen PJ, Liaw YF, Chen CJ. Temporal relationship between hepatitis B virus enhancer II/basal core promoter sequence variation and risk of hepatocellular carcinoma. *Gut* 2008; **57**: 91-97
- 89 **Yuen MF**, Tanaka Y, Shinkai N, Poon RT, But DY, Fong DY, Fung J, Wong DK, Yuen JC, Mizokami M, Lai CL. Risk for hepatocellular carcinoma with respect to hepatitis B virus genotypes B/C, specific mutations of enhancer II/core promoter/precore regions and HBV DNA levels. *Gut* 2008; **57**: 98-102
- 90 **Kim JK**, Chang HY, Lee JM, Baatarkhuu O, Yoon YJ, Park JY, Kim do Y, Han KH, Chon CY, Ahn SH. Specific mutations in the enhancer II/core promoter/precore regions of hepatitis B virus subgenotype C2 in Korean patients with hepatocellular carcinoma. *J Med Virol* 2009; **81**: 1002-1008
- 91 **Yuan JM**, Ambinder A, Fan Y, Gao YT, Yu MC, Groopman JD. Prospective evaluation of hepatitis B 1762(T)/1764(A) mutations on hepatocellular carcinoma development in Shanghai, China. *Cancer Epidemiol Biomarkers Prev* 2009; **18**: 590-594
- 92 **Fang ZL**, Sabin CA, Dong BQ, Ge LY, Wei SC, Chen QY, Fang KX, Yang JY, Wang XY, Harrison TJ. HBV A1762T, G1764A mutations are a valuable biomarker for identifying a subset of male HBsAg carriers at extremely high risk of hepatocellular carcinoma: a prospective study. *Am J Gastroenterol* 2008; **103**: 2254-2262
- 93 **Ozasa A**, Tanaka Y, Orito E, Sugiyama M, Kang JH, Hige S, Kuramitsu T, Suzuki K, Tanaka E, Okada S, Tokita H, Asahina Y, Inoue K, Kakumu S, Okanoue T, Murawaki Y, Hino K, Onji M, Yatsuhashi H, Sakugawa H, Miyakawa Y, Ueda R, Mizokami M. Influence of genotypes and precore mutations on fulminant or chronic outcome of acute hepatitis B virus infection. *Hepatology* 2006; **44**: 326-334
- 94 **Cheng H**, Su H, Wang S, Shao Z, Men K, Li M, Li S, Zhang J, Xu J, Zhang H, Yan Y, Xu D. Association between genomic heterogeneity of hepatitis B virus and intrauterine infection. *Virology* 2009; **387**: 168-175
- 95 **Shen T**, Yan XM, Zou YL, Gao JM, Dong H. Virologic characteristics of hepatitis B virus in patients infected via maternal-fetal transmission. *World J Gastroenterol* 2008; **14**: 5674-5682
- 96 **Hassan MM**, Spitz MR, Thomas MB, Curley SA, Patt YZ, Vauthey JN, Glover KY, Kaseb A, Lozano RD, El-Deeb AS, Nguyen NT, Wei SH, Chan W, Abbruzzese JL, Li D. The association of family history of liver cancer with hepatocellular carcinoma: a case-control study in the United States. *J Hepatol* 2009; **50**: 334-341
- 97 **Yu MW**, Chang HC, Liaw YF, Lin SM, Lee SD, Liu CJ, Chen PJ, Hsiao TJ, Lee PH, Chen CJ. Familial risk of hepatocellular carcinoma among chronic hepatitis B carriers and their relatives. *J Natl Cancer Inst* 2000; **92**: 1159-1164
- 98 **Chen CH**, Changchien CS, Lee CM, Hung CH, Hu TH, Wang JH, Wang JC, Lu SN. Combined mutations in pre-s/surface and core promoter/precore regions of hepatitis B virus increase the risk of hepatocellular carcinoma: a case-control study. *J Infect Dis* 2008; **198**: 1634-1642
- 99 **Yoon YJ**, Chang HY, Ahn SH, Kim JK, Park YK, Kang DR, Park JY, Myoung SM, Kim do Y, Chon CY, Han KH. MDM2 and p53 polymorphisms are associated with the development of hepatocellular carcinoma in patients with chronic hepatitis B virus infection. *Carcinogenesis* 2008; **29**: 1192-1196
- 100 **Migita K**, Miyazoe S, Maeda Y, Daikoku M, Abiru S, Ueki T, Yano K, Nagaoka S, Matsumoto T, Nakao K, Hamasaki K, Yatsuhashi H, Ishibashi H, Eguchi K. Cytokine gene polymorphisms in Japanese patients with hepatitis B virus infection-association between TGF-beta1 polymorphisms and hepatocellular carcinoma. *J Hepatol* 2005; **42**: 505-510
- 101 **Chen CC**, Yang SY, Liu CJ, Lin CL, Liaw YF, Lin SM, Lee SD, Chen PJ, Chen CJ, Yu MW. Association of cytokine and DNA repair gene polymorphisms with hepatitis B-related hepatocellular carcinoma. *Int J Epidemiol* 2005; **34**: 1310-1318
- 102 **Yu MW**, Yang SY, Pan IJ, Lin CL, Liu CJ, Liaw YF, Lin SM, Chen PJ, Lee SD, Chen CJ. Polymorphisms in XRCC1 and glutathione S-transferase genes and hepatitis B-related hepatocellular carcinoma. *J Natl Cancer Inst* 2003; **95**: 1485-1488
- 103 **He Y**, Zhang H, Yin J, Xie J, Tan X, Liu S, Zhang Q, Li C, Zhao J, Wang H, Cao G. IkappaBalpha gene promoter polymorphisms are associated with hepatocarcinogenesis in patients infected with hepatitis B virus genotype C. *Carcinogenesis* 2009; Epub ahead of print



TOPIC HIGHLIGHT

Giovanni D De Palma, Professor, Series Editor

Confocal laser endomicroscopy in the “*in vivo*” histological diagnosis of the gastrointestinal tract

Giovanni D De Palma

Giovanni D De Palma, Department of Surgery and Advanced Technologies, Center of Excellence for Technical Innovation in Surgery, University of Naples Federico II, School of Medicine, via Pansini 5, 80131 Naples, Italy

Author contributions: De Palma GD contributed solely to this paper.

Correspondence to: Giovanni D De Palma, Professor, Department of Surgery and Advanced Technologies, Center of Excellence for Technical Innovation in Surgery, University of Naples Federico II, School of Medicine, via Pansini 5, 80131 Naples, Italy. giovanni.depalm@unina.it

Telephone: +39-81-7462773 Fax: +39-81-7462752

Received: August 12, 2009 Revised: November 6, 2009

Accepted: November 13, 2009

Published online: December 14, 2009

<http://www.wjgnet.com/1007-9327/15/5770.asp> DOI: <http://dx.doi.org/10.3748/wjg.15.5770>

INTRODUCTION

In recent years, endoscopic image quality has improved as the devices have advanced technologically. Although techniques such as chromoendoscopy, high resolution and magnification endoscopy, narrow band imaging, and auto-fluorescence imaging improve the visualization and detection of mucosal lesions, biopsy of the targeted lesion must still be performed for a formal histological diagnosis of cellular and architectural atypia.

Suspicious areas identified during endoscopy are targeted and biopsied or removed endoscopically. However, there are several disadvantages that may be associated with biopsies or endoscopic resection, including bleeding or perforation. Non-representative biopsies may miss relevant portions of tissue, leading to underestimation of the diagnosis. Random biopsy sampling or endoscopic resection for non-neoplastic lesions can also be time-consuming. It would be ideal if a definite diagnosis could be made during endoscopy without a biopsy.

Recent technological advances in miniaturization have allowed for a confocal scanning microscope to be integrated into a conventional flexible endoscope, or into trans-endoscopic probes, a technique now known as confocal endomicroscopy (CEM) or confocal laser endomicroscopy (CLE). This newly-developed technology has enabled endoscopists to collect real-time *in vivo* histological images or “virtual biopsies” of the gastrointestinal (GI) mucosa during endoscopy, and has stimulated significant interest in the application of this technique in clinical gastroenterology^[1-8].

This report aims to evaluate the current data on the utility of this new technology in clinical gastroenterology and its potential impact in the future, particularly in the screening or surveillance of GI neoplasia.

PRINCIPLES OF CONFOCAL MICROSCOPY

Confocal microscopy has been used in the biological sciences since 1961 when the concept of optical sectioning of a biological specimen was introduced.

Abstract

Recent technological advances in miniaturization have allowed for a confocal scanning microscope to be integrated into a conventional flexible endoscope, or into trans-endoscopic probes, a technique now known as confocal endomicroscopy or confocal laser endomicroscopy. This newly-developed technology has enabled endoscopists to collect real-time *in vivo* histological images or “virtual biopsies” of the gastrointestinal mucosa during endoscopy, and has stimulated significant interest in the application of this technique in clinical gastroenterology. This review aims to evaluate the current data on the technical aspects and the utility of this new technology in clinical gastroenterology and its potential impact in the future, particularly in the screening or surveillance of gastrointestinal neoplasia.

© 2009 The WJG Press and Baishideng. All rights reserved.

Key words: Confocal microscopy; Diagnostic imaging; Gastrointestinal neoplasms; Precancerous conditions; Endoscopy; Virtual histology

Peer reviewer: Dr. William Kemp, MB, BS (Hons), FRACP, Department of Gastroenterology, Alfred Hospital, PO Box 315 Prahran, 55 Commercial Road, Melbourne 3181, Australia

De Palma GD. Confocal laser endomicroscopy in the “*in vivo*” histological diagnosis of the gastrointestinal tract. *World J Gastroenterol* 2009; 15(46): 5770-5775 Available from: URL:

To create confocal images, a low-powered laser (an argon-ion laser that generates an excitation wavelength of 488 nm, blue laser light) is focused by an objective lens into a single point, within a fluorescent specimen. The same lens is used as both the condenser and objective folding. The point of illumination thus coincides with the point of detection within the specimen. Light emanating from that point is focused through a pinhole to a detector, and light emanating from outside the illuminated spot is rejected. The illumination and detection systems are in the same focal plane and are termed “confocal” (Figure 1).

After passing the pinhole, the fluorescent light is detected by a photodetection device (a photomultiplier tube or avalanche photodiode), transforming the light signal into an electrical one that is recorded by a computer. All detected signals from the illuminated spot are captured and measured.

As the laser scans over the plane of interest, a whole image is obtained pixel-by-pixel and line-by-line, whereas the brightness of a resulting image pixel corresponds to the relative intensity of detected fluorescent light.

The gray-scale image created is an optical section representing one focal plane within the examined specimen.

Confocal microscopy provides the capacity for direct, non-invasive, serial optical sectioning of intact, thick, living specimens with a minimum of sample preparation as well as a marginal improvement in lateral resolution. Because confocal images depend on fluorescence, a fluorescent dye (contrast agent) is required to make objects visible.

CONTRAST AGENTS

A fluorescent contrast agent is used and is needed to achieve high contrast images using CEM. Potentially suitable agents in humans are fluorescein, acriflavine, tetracycline or cresyl violet. The contrast agents can be applied systemically (fluorescein, tetracycline) or topically (acriflavine, cresyl violet) by using a spraying catheter. Of these, intravenous fluorescein sodium (10%) and topically applied acriflavine (0.2%) have been most commonly used in humans. No data is so far available on the use of tetracycline and cresyl violet.

Fluorescein is an agent used for diagnostic fluorescein angiography or angioscopy of the retina and iris vasculature.

After intravenous injection, fluorescein binds extensively to serum albumin in the bloodstream. The unbound contrast diffuses across capillaries, entering the tissue and staining the extracellular matrix of the surface epithelium and the lamina propria for up to 30 min^[9]. Cell nuclei and mucin are not stained by fluorescein and therefore appear dark. The mucosal structures that can be identified after fluorescein administration include enterocytes, cellular infiltrate, surface epithelial cells, blood vessels, and red blood cells. Fluorescein is a highly safe agent whose major side effects are short term (1-2 h) and include yellowish skin discoloration and 1-2 d

of bright yellow-colored urine. Nausea and vomiting were reported during angiography and were transient and minor. Serious side effects, such as anaphylaxis or cardiac or respiratory effects, are extremely rare, and to date, have not been recorded in CEM.

Topical acriflavine is highly specific for labeling acidic constituents, and stains the nuclei of superficial layers of the mucosa. The staining provides clear visualization of cell nuclei in the uppermost mucosa and may allow better differentiation between intra-epithelial neoplasia and cancer of the GI tract. Although there has been a hypothetical concern about the risk of mutagenesis, no severe adverse reactions have been reported after the topical use of acriflavine. However, concerns about DNA damage by acriflavine stain have reduced its use in humans.

Fluorescein and acriflavine can also be used simultaneously which adds to the labeling properties.

EQUIPMENT

CLE can be performed currently with 2 devices: (1) integrated into an endoscope (Pentax, Tokio, Japan, herein termed eCLE); and (2) as a stand-alone probe (herein termed pCLE) capable of passage through the accessory channel of most endoscopes (Cellvizio, Mauna Kea Technologies, Paris, France)^[10-14].

The Pentax EG-3870CIK (upper endoscope) and EC-3870CILK (colonoscope)

The components of the confocal laser endoscope are based on the integration of a confocal laser microscope in the distal tip of a conventional video endoscope, which enables confocal microscopy in addition to standard video endoscopy (Figure 2). The diameter of both the distal tip and the insertion tube is 12.8 mm. The distal tip contains an air and water jet nozzle, 2 light guides, an auxiliary water jet channel (used for topical application of the contrast agent) and a 2.8 mm working channel. This imaging system provides confocal imaging using an incident 488 nm wavelength laser, and enables the detection of fluorescence of 505-585 nm wavelength, with reduced image noise compared with the reflectance confocal systems. CLE imaging data are collected at a scan rate of 1.6 frames per second (1024×512 pixels) or 0.8 frames per second (1024×1024 pixels) with an adjustable depth of scanning ranging from 0 to 250 μm , a field of view of $475 \mu\text{m} \times 475 \mu\text{m}$, a lateral resolution of 0.7 μm , and an axial resolution of 7 μm . Confocal images are generated simultaneously with the endoscopic images and the endoscope working channel can still be used.

The Cellvizio® Endomicroscopy System

The Cellvizio® Endomicroscopy System (Figure 3) is based on a different catheter probe with a semiconductor laser that oscillates at 488 nm. The latest model of Cellvizio confocal miniprobes created for GI tract applications include CholangioFlex, GastroFlex, ColoFlex, GastroFlex-UHD, and ColoFlex-UHD. CholangioFlex probes designed for use during endoscopic retrograde

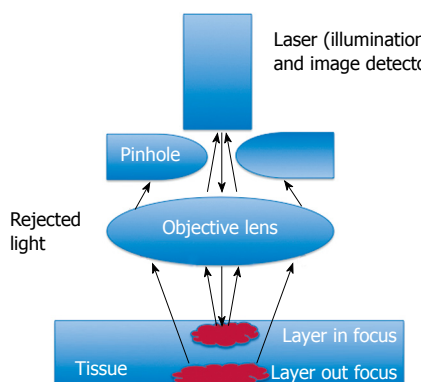


Figure 1 Schematic of confocal endomicroscopy principles.

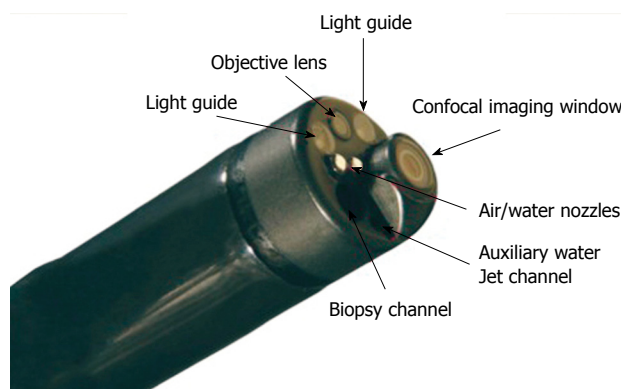


Figure 2 The endoscope-based confocal laser endomicroscopy (eCLE) imaging system: the distal tip.

cholangiopancreatography require an endoscope accessory channel of at least 1.2 mm, whereas the other probes, which are designed for use in esophagogastroduodenoscopy and colonoscopy, require a channel larger than 2.8 mm. All probes generate dynamic (12 frames per second) images with a scanning field of 30 000 pixels.

This system has a field of view of 240–600 µm (CholangioFlex probes: 325 µm; GastroFlex and ColoFlex: 600 µm; GastroFlex-UHD and ColoFlex-UHD: 240 µm) with a lateral resolution of 1–3.5 µm (the lateral resolution for CholangioFlex and for GastroFlex and ColoFlex probes is 3.5 µm; the lateral resolution for GastroFlex-UHD and ColoFlex-UHD is 1 µm). This system has a fixed imaging plane depth, and different confocal miniprobes are required to vary the depth of imaging. The depth of imaging for CholangioFlex probes is 40–70 µm, 70–130 µm for GastroFlex and ColoFlex, and 55–65 µm for GastroFlex-UHD and ColoFlex-UHD.

Single video frames are reconstructed by a special computer algorithm (“mosaicing”) in an image with an enlarged field of view (4 mm × 2 mm).

PROCEDURE

Once a suspicious area of the mucosa is identified, contrast agents (fluorescein and/or acriflavine) can be given, and a CEM examination of the targeted area is performed by placing the distal tip of the endoscope or



Figure 3 The probe-based CLE (pCLE) imaging system.

the distal tip of the catheter probe against the targeted mucosa. Gentle suction and/or an endoscopic cap can be used to stabilize the equipment and minimize excessive movement, which is important to reduce movement artifacts during imaging. At the area of interest, images can be obtained using an image-capture foot pedal and stored digitally.

INTERPRETATION OF CLE IMAGES

The orientation of the “cut” plane of confocal *in vivo* histological images is horizontal whereas in conventional histological specimens it is longitudinal. CLE images cannot display a simultaneous overview of the mucosal and submucosal structures, unlike conventional histology. CLE images provide a thorough view of the mucosal architecture and allow rapid differentiation between normal, regenerative, and neoplastic mucosa of the GI tract. Differentiation between grades of intra-epithelial neoplasm by CEM, however, is not yet possible with the currently available staining techniques.

Endoscopists who perform CEM require a fundamental knowledge of the normal and disease micro-architecture of the GI tract. An onsite pathologist or at least a review of the stored images by a pathologist and correlation with biopsy histology is recommended during the learning process.

Some studies of the learning curve for CLE performed by endoscopists demonstrate that highly accurate, efficient *in vivo* prediction of Barrett’s esophagus can be achieved after approximately 20–30 independently performed CLE procedures.

Normal and pathological aspects of CLE imaging of the upper and lower GI tract are shown in Tables 1–3 and Figures 3–5.

CLINICAL DATA

The current potential indications for CLE imaging are

Table 1 Confocal criteria for squamous cell epithelium and carcinoma

Squamous cell epithelium		Squamous cell neoplasia
Cellular criteria	Dark, homogeneous epithelial cells; regular architecture and clearly visible borders	Dark cells with different sizes; no clearly visible borders; irregular architecture
Vascular criteria	Capillaries directed to luminal epithelium without leakage of fluorescein	Twisted and irregular vessels; elongated capillaries; capillary leakage

Table 2 Confocal laser endomicroscopy (CLE) classification of Barrett's esophagus

Confocal diagnosis	Vessel architecture	Crypt architecture
Gastric-type epithelium	Capillaries with a regular shape only visible in the deeper parts of the mucosal layer	Regular columnar-lined epithelium with round glandular openings and typical cobblestone appearance
Barrett's epithelium	Subepithelial capillaries with a regular shape underneath columnar-lined epithelium visible in the upper and deeper parts of the mucosal layer	Columnar-lined epithelium with intermittent dark mucus in goblet cells in the upper parts of the mucosal layer. In the deeper parts, villous, dark, regular cylindrical Barrett's epithelial cells are present
Neoplasia	Irregular capillaries visible in the upper and deeper parts of the mucosal layer. Leakage of vessels leads to a heterogeneous and brighter signal intensity within the lamina propria	Black cells with irregular apical and distal borders and shapes, with strong dark contrast against the surrounding tissue

Table 3 CLE classification of patterns in colorectal lesions

Grading	Vessel architecture	Crypt architecture
Normal	Hexagonal, honeycomb appearance that presents a network of capillaries outlining the stroma surrounding the luminal openings of the crypts	Regular luminal openings and distribution of crypts covered by a homogeneous layer of epithelial cells, including goblet cells
Regeneration	Hexagonal, honeycomb appearance with no increase or only a slight increase in the number of capillaries	Star-shaped luminal crypt openings or focal aggregation of regular-shaped crypts with a regular or reduced amount of goblet cells
Neoplasia	Dilated and distorted vessels with increased leakage; irregular architecture, with little or no orientation to the adjoining tissue	Ridge-lined irregular epithelial layer with loss of crypts and goblet cells; irregular cell architecture, with little or no mucin

broad and include almost all current applications of endoscopic biopsy.

Unequivocally, this technology is best used in conjunction with other “red-flag” techniques because of its minute scanning area, and thus is only appropriate for classification of tissue at a site already detected by standard or optically enhanced endoscopy. Ideally, the no-dye “red-flag” techniques such as narrow band imaging or auto-fluorescence imaging, should be used to screen the mucosa for “areas of interest”, which can then be interrogated by CEM for a “histological” diagnosis. An example would be use of narrow-band imaging to detect regions of suspicion in Barrett's esophagus, followed by CLE to confirm intraepithelial neoplasia, and guide immediate therapy.

The confocal laser endoscope can be used routinely for screening and surveillance. Suspicious lesions can be examined in a targeted fashion by placing the endomicroscopy window onto the lesion. Confocal images can be graduated according to cellular and vascular changes. The images correlate well with conventional histology after targeted biopsies.

Numerous studies have addressed the clinical applications of CLE, in particular in the study of precancerous

lesions of the upper and lower GI tract^[15,16].

In patients with Barrett's esophagus, CLE can diagnose Barrett's epithelium and Barrett's-associated neoplastic changes with an accuracy > 90% for both e-CLE or p-CLE^[17-23].

CLE in the stomach allows good visualization of normal and pathologic gastric pit patterns, making it a potentially useful tool for diagnosis of gastric cancer and precancerous conditions. Direct *in vivo* identification of *Helicobacter pylori* infection can be obtained^[24-27].

In patients with suspected celiac disease, confocal endomicroscopy can demonstrate villous atrophy and an increased number of intraepithelial lymphocytes, enabling immediate *in vivo* diagnosis of celiac disease^[28].

The presence of neoplastic changes in a colonic mucosa can be predicted with high accuracy (> 95%). CLE has several potential roles in polyp management. The best-studied application is to distinguish between hyperplastic and adenomatous polyps, thus negating the need to remove hyperplastic polyps. In patients with long-term ulcerative colitis, chromoscopy with supplemental CEM, has recently been shown to further increase the yield for intraepithelial neoplasia above and beyond methylene blue. pCLE also has the capacity

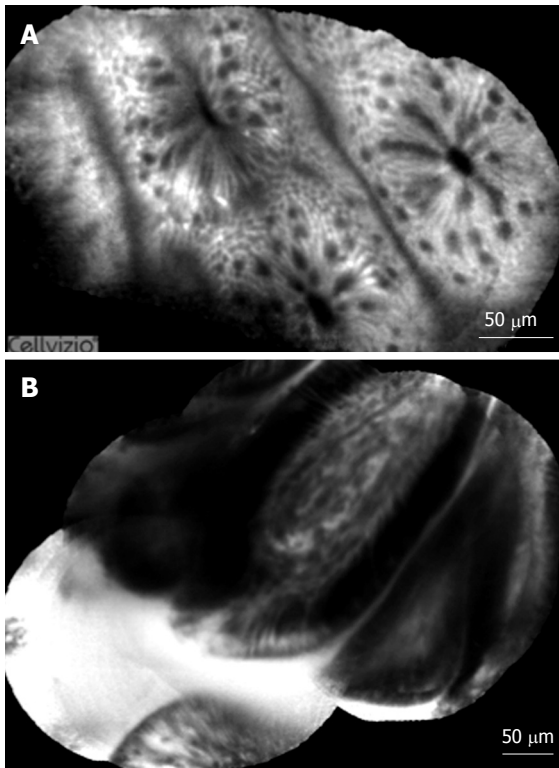


Figure 4 pCLE fluorescein sodium 10% imaging of the normal colon (A) and normal duodenum (B).

to differentiate normal from inflamed tissue, and thus target biopsies for the purpose of grading and mapping the extent of colitis^[29-34].

CEM can also be helpful for the diagnosis of microscopic colitis in patients with chronic diarrhea. In patients with collagenous colitis, it allows direct *in vivo* visualization of collagenous bands under the epithelial layer of the colon, and in patients with lymphocytic colitis, it can demonstrate crypt distortion and an increased distance between the colonic crypt. Thus, CLE has the potential to replace or direct a large number of random biopsies in patients with chronic diarrhea, where the confocal image is normal^[35-37].

Pancreato-biliary applications are under way using the probe-based CLE. The major role of pCLE in the bile duct is likely to detect cancer in indeterminate bile duct and pancreatic strictures^[38,39].

CONCLUSION

CLE is a rapidly emerging field of gastroenterology that bridges the interface between endoscopy and histology. It further expands our ability to image living tissue in real time and to provide therapy in the same setting. The immediate impact will be the ability to target biopsies much more precisely, and eliminate a large number of random biopsies. Currently available devices for CEM have a very narrow field of view and allow only visualization of the superficial mucosal layer of the GI tract. Further technological developments are needed to enlarge the field of view, which will facilitate the use of CEM for cancer screening and surveillance. Increased

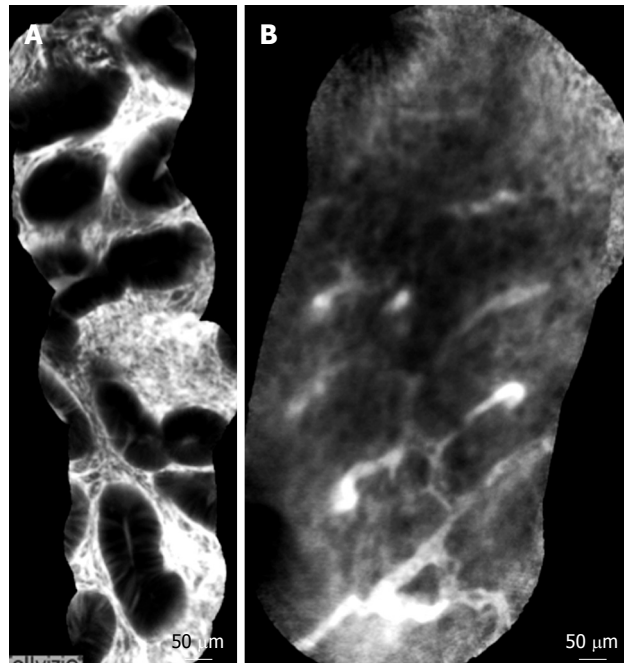


Figure 5 pCLE fluorescein sodium 10% imaging of an adenomatous colonic polyp (A) and colonic adenocarcinoma (B).

depth of penetration is also needed to assess depth of invasion during cancer staging.

REFERENCES

- 1 Wang TD. Confocal microscopy from the bench to the bedside. *Gastrointest Endosc* 2005; **62**: 696-697
- 2 Polglase AL, McLaren WJ, Skinner SA, Kiesslich R, Neurath MF, Delaney PM. A fluorescence confocal endomicroscope for *in vivo* microscopy of the upper- and the lower-GI tract. *Gastrointest Endosc* 2005; **62**: 686-695
- 3 Kiesslich R, Goetz M, Neurath MF. Confocal laser endomicroscopy for gastrointestinal diseases. *Gastrointest Endosc Clin N Am* 2008; **18**: 451-466, viii
- 4 Kantsevoy SV, Adler DG, Conway JD, Diehl DL, Farrey FA, Kaul V, Kethu SR, Kwon RS, Mamula P, Rodriguez SA, Tierney WM. Confocal laser endomicroscopy. *Gastrointest Endosc* 2009; **70**: 197-200
- 5 Venkatesh K, Cohen M, Evans C, Delaney P, Thomas S, Taylor C, Abou-Taleb A, Kiesslich R, Thomson M. Feasibility of confocal endomicroscopy in the diagnosis of pediatric gastrointestinal disorders. *World J Gastroenterol* 2009; **15**: 2214-2219
- 6 Dunbar K, Canto M. Confocal endomicroscopy. *Curr Opin Gastroenterol* 2008; **24**: 631-637
- 7 Kiesslich R, Goetz M, Neurath MF. Virtual histology. *Best Pract Res Clin Gastroenterol* 2008; **22**: 883-897
- 8 Nguyen NQ, Leong RW. Current application of confocal endomicroscopy in gastrointestinal disorders. *J Gastroenterol Hepatol* 2008; **23**: 1483-1491
- 9 Becker V, von Delius S, Bajbouj M, Karagianni A, Schmid RM, Meining A. Intravenous application of fluorescein for confocal laser scanning microscopy: evaluation of contrast dynamics and image quality with increasing injection-to-imaging time. *Gastrointest Endosc* 2008; **68**: 319-323
- 10 Polglase AL, McLaren WJ, Delaney PM. Pentax confocal endomicroscope: a novel imaging device for *in vivo* histology of the upper and lower gastrointestinal tract. *Expert Rev Med Devices* 2006; **3**: 549-556
- 11 Becker V, Vercauteren T, von Weyhern CH, Prinz C, Schmid RM, Meining A. High-resolution miniprobe-based

- confocal microscopy in combination with video mosaicing (with video). *Gastrointest Endosc* 2007; **66**: 1001-1007
- 12 **Meining A**, Saur D, Bajbouj M, Becker V, Peltier E, Hofler H, von Weyhern CH, Schmid RM, Prinz C. In vivo histopathology for detection of gastrointestinal neoplasia with a portable, confocal miniprobe: an examiner blinded analysis. *Clin Gastroenterol Hepatol* 2007; **5**: 1261-1267
- 13 Leeuwenhoek meets Kussmaul: the evolution of endoscopist to endo-pathologist. *Gastroenterology* 2006; **131**: 347-349
- 14 **Wallace MB**, Fockens P. Probe-based confocal laser endomicroscopy. *Gastroenterology* 2009; **136**: 1509-1513
- 15 **Hoffman A**, Goetz M, Vieth M, Galle PR, Neurath MF, Kiesslich R. Confocal laser endomicroscopy: technical status and current indications. *Endoscopy* 2006; **38**: 1275-1283
- 16 **Liu H**, Li YQ, Yu T, Zhao YA, Zhang JP, Zhang JN, Guo YT, Xie XJ, Zhang TG, Desmond PV. Confocal endomicroscopy for in vivo detection of microvascular architecture in normal and malignant lesions of upper gastrointestinal tract. *J Gastroenterol Hepatol* 2008; **23**: 56-61
- 17 **Dunbar KB**, Okolo P 3rd, Montgomery E, Canto MI. Confocal laser endomicroscopy in Barrett's esophagus and endoscopically inappropriate Barrett's neoplasia: a prospective, randomized, double-blind, controlled, crossover trial. *Gastrointest Endosc* 2009; **70**: 645-654
- 18 **Pohl H**, Rosch T, Vieth M, Koch M, Becker V, Anders M, Khalifa AC, Meining A. Miniprobe confocal laser microscopy for the detection of invisible neoplasia in patients with Barrett's oesophagus. *Gut* 2008; **57**: 1648-1653
- 19 **Becker V**, Vieth M, Bajbouj M, Schmid RM, Meining A. Confocal laser scanning fluorescence microscopy for in vivo determination of microvessel density in Barrett's esophagus. *Endoscopy* 2008; **40**: 888-891
- 20 **Liu H**, Li YQ, Yu T, Zhao YA, Zhang JP, Zuo XL, Li CQ, Zhang JN, Guo YT, Zhang TG. Confocal laser endomicroscopy for superficial esophageal squamous cell carcinoma. *Endoscopy* 2009; **41**: 99-106
- 21 **Pech O**, Rabenstein T, Manner H, Petrone MC, Pohl J, Vieth M, Stolte M, Ell C. Confocal laser endomicroscopy for in vivo diagnosis of early squamous cell carcinoma in the esophagus. *Clin Gastroenterol Hepatol* 2008; **6**: 89-94
- 22 **Deinert K**, Kiesslich R, Vieth M, Neurath MF, Neuhaus H. In-vivo microvascular imaging of early squamous-cell cancer of the esophagus by confocal laser endomicroscopy. *Endoscopy* 2007; **39**: 366-368
- 23 **Goetz M**, Hoffman A, Galle PR, Neurath MF, Kiesslich R. Confocal laser endoscopy: new approach to the early diagnosis of tumors of the esophagus and stomach. *Future Oncol* 2006; **2**: 469-476
- 24 **Kakeji Y**, Yamaguchi S, Yoshida D, Tanoue K, Ueda M, Masunari A, Utsunomiya T, Imamura M, Honda H, Maehara Y, Hashizume M. Development and assessment of morphologic criteria for diagnosing gastric cancer using confocal endomicroscopy: an ex vivo and in vivo study. *Endoscopy* 2006; **38**: 886-890
- 25 **Guo YT**, Li YQ, Yu T, Zhang TG, Zhang JN, Liu H, Liu FG, Xie XJ, Zhu Q, Zhao YA. Diagnosis of gastric intestinal metaplasia with confocal laser endomicroscopy in vivo: a prospective study. *Endoscopy* 2008; **40**: 547-553
- 26 **Li WB**, Zuo XL, Zuo F, Gu XM, Yu T, Zhao YA, Zhang TG, Zhang JP, Li YQ. Characterization and identification of gastric hyperplastic polyps and adenomas by confocal laser endomicroscopy. *Surg Endosc* 2009; Epub ahead of print
- 27 **Kiesslich R**, Goetz M, Burg J, Stolte M, Siegel E, Maeurer MJ, Thomas S, Strand D, Galle PR, Neurath MF. Diagnosing Helicobacter pylori in vivo by confocal laser endoscopy. *Gastroenterology* 2005; **128**: 2119-2123
- 28 **Zambelli A**, Villanacci V, Buscarini E, Lupinacci G, De Grazia F, Brambilla G, Menozzi F, La Mantia L, Bassotti G. Confocal laser endomicroscopy in celiac disease: description of findings in two cases. *Endoscopy* 2007; **39**: 1018-1020
- 29 **Kiesslich R**, Goetz M, Vieth M, Galle PR, Neurath MF. Technology insight: confocal laser endoscopy for in vivo diagnosis of colorectal cancer. *Nat Clin Pract Oncol* 2007; **4**: 480-490
- 30 **Hurlstone DP**, Tiffin N, Brown SR, Baraza W, Thomson M, Cross SS. In vivo confocal laser scanning chromo-endomicroscopy of colorectal neoplasia: changing the technological paradigm. *Histopathology* 2008; **52**: 417-426
- 31 **Hurlstone DP**, Baraza W, Brown S, Thomson M, Tiffin N, Cross SS. In vivo real-time confocal laser scanning endomicroscopic colonoscopy for the detection and characterization of colorectal neoplasia. *Br J Surg* 2008; **95**: 636-645
- 32 **Goetz M**, Toermer T, Vieth M, Dunbar K, Hoffman A, Galle PR, Neurath MF, Delaney P, Kiesslich R. Simultaneous confocal laser endomicroscopy and chromoendoscopy with topical cresyl violet. *Gastrointest Endosc* 2009; **70**: 959-968
- 33 **Hurlstone DP**, Brown S. Techniques for targeting screening in ulcerative colitis. *Postgrad Med J* 2007; **83**: 451-460
- 34 **Hurlstone DP**, Thomson M, Brown S, Tiffin N, Cross SS, Hunter MD. Confocal endomicroscopy in ulcerative colitis: differentiating dysplasia-associated lesional mass and adenoma-like mass. *Clin Gastroenterol Hepatol* 2007; **5**: 1235-1241
- 35 **Meining A**, Schwendy S, Becker V, Schmid RM, Prinz C. In vivo histopathology of lymphocytic colitis. *Gastrointest Endosc* 2007; **66**: 398-399, discussion 400
- 36 **Kiesslich R**, Hoffman A, Goetz M, Biesterfeld S, Vieth M, Galle PR, Neurath MF. In vivo diagnosis of collagenous colitis by confocal endomicroscopy. *Gut* 2006; **55**: 591-592
- 37 **Zambelli A**, Villanacci V, Buscarini E, Bassotti G, Albarello L. Collagenous colitis: a case series with confocal laser microscopy and histology correlation. *Endoscopy* 2008; **40**: 606-608
- 38 **Meining A**, Phillip V, Gaa J, Prinz C, Schmid RM. Pancreaticoscopy with miniprobe-based confocal laser-scanning microscopy of an intraductal papillary mucinous neoplasm (with video). *Gastrointest Endosc* 2009; **69**: 1178-1180
- 39 **Meining A**, Frimberger E, Becker V, Von Delius S, Von Weyhern CH, Schmid RM, Prinz C. Detection of cholangiocarcinoma in vivo using miniprobe-based confocal fluorescence microscopy. *Clin Gastroenterol Hepatol* 2008; **6**: 1057-1060

S-Editor Wang JL L-Editor Cant MR E-Editor Ma WH



REVIEW

Signal molecule-mediated hepatic cell communication during liver regeneration

Zhen-Yu Zheng, Shun-Yan Weng, Yan Yu

Zhen-Yu Zheng, Shun-Yan Weng, Yan Yu, School of Agriculture and Biology, Shanghai Jiao Tong University, Shanghai 200240, China

Author contributions: Zheng ZY, Weng SY and Yu Y equally contributed to this paper.

Correspondence to: Yan Yu, PhD, School of Agriculture and Biology, Shanghai Jiao Tong University, 800 Dongchuan Road, Min Hang District, Shanghai 200240, China. yanyu@sjtu.edu.cn

Telephone: +86-21-34205833 **Fax:** +86-21-34205833

Received: September 5, 2009 **Revised:** October 14, 2009

Accepted: October 21, 2009

Published online: December 14, 2009

Abstract

Liver regeneration is a complex and well-orchestrated process, during which hepatic cells are activated to produce large signal molecules in response to liver injury or mass reduction. These signal molecules, in turn, set up the connections and cross-talk among liver cells to promote hepatic recovery. In this review, we endeavor to summarize the network of signal molecules that mediates hepatic cell communication in the regulation of liver regeneration.

© 2009 The WJG Press and Baishideng. All rights reserved.

Key words: Signal molecule; Hepatic cells; Cellular cross-talk; Signal communication; Liver regeneration

Peer reviewers: Filip Braet, Associate Professor, Australian Key Centre for Microscopy and Microanalysis, Madsen Building (F09), The University of Sydney, Sydney NSW 2006, Australia; Sanaa M Kamal, Professor, Department of Gastroenterology and Liver Disease, Ain Shams Faculty of Medicine, 22, Al Ahram St, Roxy, Heliopolis, Cairo, Egypt

Zheng ZY, Weng SY, Yu Y. Signal molecule-mediated hepatic cell communication during liver regeneration. *World J Gastroenterol* 2009; 15(46): 5776-5783 Available from: URL: <http://www.wjgnet.com/1007-9327/15/5776.asp> DOI: <http://dx.doi.org/10.3748/wjg.15.5776>

INTRODUCTION

The liver is a vital organ. It has a wide range of functions, which include synthesis, metabolism, storage and

redistribution of amino acids, proteins (e.g. albumin and acute-phase proteins, enzymes and cofactors), carbohydrates, fats and vitamins. It also is involved in detoxification through: (1) removal of waste and xenobiotics, by breakdown of insulin and other hormones, hemoglobin, toxic substances, and medical products of drugs; (2) conversion of ammonia to urea; and (3) production and excretion of bile. The parenchymal cells (hepatocytes), which make up 70%-80% of hepatic cells, carry out most of these functions. The other 20% comprise the non-parenchymal cells, which include Kupffer cells, stellate cells, sinusoidal endothelial cells (SECs), biliary epithelial cells, lymphocytes, and oval cells^[1].

The liver is the only organ that can regenerate fully after injury in mammals^[2]. When the liver is subjected to surgery, toxic substances, or viral infection, it has an amazing regenerative ability to restore functional hepatic mass. Injury induces the priming of recovery mechanisms with large changes in hepatic composition, such as activation of non-parenchymal cells, production and activation of multiple factors. These factors further lead to proliferation of hepatocytes and non-parenchymal cells, recovery and re-establishment of tissue architecture. When the liver recovers its normal volume and function, the regenerative response is terminated. Liver regeneration is actually compensatory hyperplasia, which is mediated typically by the proliferation of surviving hepatocytes^[3]. When hepatocyte proliferation is inhibited, oval cell proliferation occurs^[4]. This review endeavors to summarize the roles of hepatocytes and non-parenchymal cells, as well as signal communication among the hepatic cells during liver regeneration.

FUNCTION OF VARIOUS TYPES OF LIVER CELL REGULATED BY DIFFERENT SIGNAL MOLECULES

Hepatocytes

Hepatocytes are organized into single-cell plates in mammals separated by vascular channels (sinusoids). Hepatocytes perform most liver functions such as synthesis, storage, metabolism and transformation of carbohydrates, amino acids, proteins, fats and vitamins, and detoxification, modification and excretion of exogenous and endogenous substances. The hepatocyte also initiates the formation and secretion of bile. During

liver regeneration, hepatocytes are primed to proliferate, maintain metabolic function, secrete interleukin (IL)-6, proteases and protease inhibitors, and hepatocyte growth factor (HGF)^[5].

Kupffer cells

Kupffer cells are liver-resident macrophages with a pronounced phagocytic and endocytic capacity mainly located within the sinusoids^[6]. Kupffer cells play an important role in the clearance of senescent and damaged erythrocytes. Kupffer cells also secrete potent mediators of the inflammatory response^[7]. During the priming phase of liver regeneration, Kupffer cells are activated and secrete pro-inflammatory cytokines, most prominently tumor necrosis factor (TNF)- α , IL-6, and IL-1 β , which can initiate the acute phase response in hepatocytes^[8]. Small-for-size orthotopic liver transplantation may often cause graft failure. In a mouse partial 30% liver transplantation model, interruption of TNF- α signaling by Kupffer cell inactivation through administration of pentoxifylline and GdCl₃, or the use of *Tnfr-1*^{-/-} mice improves animal survival and enhances liver regeneration. These results are partly due to the fact that inhibition of TNF- α reduces leukocyte adherence, and improves portal flow and microcirculation^[9].

Hepatic stellate cells (HSCs)

HSCs, also known as Ito cells, fat-storing cells or liver fibroblasts, are located in the space of Disse between the hepatocytes and the hepatic sinusoidal endothelial lining. In normal liver, HSCs sustain a quiescent state. Quiescent HSCs represent 5%-8% of liver cells, store 80% of total body retinol (vitamin A) as cytoplasmic lipid droplets, control turnover of extracellular matrix (ECM), and regulate the contractility of sinusoids^[5-7]. Following hepatic damage, HSCs trans-differentiate into ECM-secreting myofibroblasts (activated HSCs)^[10], with the loss of retinol-rich droplets^[11]. HSCs can secrete ECM proteins, including laminins, collagens and proteoglycans, growth factors such as HGF, fibroblast growth factor (FGF), transforming growth factor (TGF)- β and cytokines such as IL-6, and produce some matrix metalloproteinases and tissue inhibitors of metalloproteinases^[5]. The HSC is the major cell type involved in liver fibrosis. HSCs also behave as professional liver-resident antigen-presenting cells (APCs)^[6,11]. A recent study has suggested that quiescent HSCs of rats retained within the space of Disse express stem/progenitor cell markers (e.g. CD133 and Oct4) and possess a differentiation potential. The space of Disse acts as a HSC niche, which is similar to the stem cell niche. These characteristics of quiescent HSCs are determined by the special microenvironment in the space of Disse, which is composed of basal lamina proteins (laminin and collagen type IV), sympathetic innervation and the adjacent cells. The adjacent cells include SECs, which release stromal cell-derived factor-1 to attract HSCs via the cysteine-X-cysteine receptor 4, and hepatocytes, which synthesize β -catenin-dependent Wnt ligands and Jagged-1 to attract HSCs through Wnt receptor frizzled, and to have direct physical interactions with HSCs through

Jagged-1 receptor notch^[11-13].

Neurotropin receptor p75^{NTR} is a low-affinity pan-neurotropin receptor that belongs to the TNF receptor superfamily. In the diseased liver, p75^{NTR} is expressed in HSCs. When p75^{NTR} is activated, it activates the Rho/Rho kinase pathway, which enhances actin filament formation and phosphorylation of cofilin in a ligand-independent manner. This pathway contributes to the transition of quiescent stellate cells into myofibroblast-like cells that are important cellular sources of HGF. HGF drives healthy hepatocytes into proliferation. During perpetuation of trans-differentiation, secretion of pro-nerve growth factor (NGF) or NGF by neighboring regenerating hepatocytes leads to ligand-induced activation of apoptotic pathways, including the neurotrophin receptor interacting factor/TNF receptor-associated factor/Ras-related C3 botulinum toxin substrate/c-Jun N-terminal kinase/caspase pathway in stellate cells. In mice, depletion of p75^{NTR} exacerbates liver pathology and inhibits hepatocyte proliferation *in vivo*. p75^{NTR}^{-/-} HSCs fail to differentiate into myofibroblasts and do not support hepatocyte proliferation^[14,15].

SECs and biliary epithelial cells

Liver SECs constitute the wall of the hepatic sinusoid and separate hepatocytes from the sinusoidal blood. They perform an important filtration function due to the presence of open fenestrations, with an average diameter of 120 nm, which allow free diffusion of many substances, but not of particles of the size of chylomicrons, between the blood and the hepatocyte surface. SECs have large endocytic and metabolic capacity for many ligands including glycoproteins, lipoproteins, ECM components (e.g. hyaluronate, collagen fragments, fibronectin, or chondroitin sulfate proteoglycan), immune complexes, transferrin and ceruloplasmin. SECs may function as APCs in the context of both major histocompatibility complex (MHC)-I and MHC-II restriction, with the resulting development of antigen-specific T cell tolerance. They are also active in the secretion of cytokines (IL-6), HGF, TGF- β , eicosanoids (i.e. prostanooids and leukotrienes), endothelin-1, nitric oxide, and some ECM components^[5,7].

Biliary epithelial cells (cholangiocytes) constitute the bile ducts in hepatic portal triads. Cholangiocytes may transport water, ions and solutes; secrete growth factors and peptides that mediate cross-talk with other cells of the liver in a paracrine mode; secrete chemokines (e.g. monocyte chemotactic protein-1) and cytokines (e.g. IL-6) and express adhesion molecules that attract effector leukocytes and promote the clearance of infected cells; and promote fibrogenesis by attraction of HSCs^[5,16].

Notch-1 and Jagged-1 are expressed in bile duct cells and hepatocytes in normal rat liver. Moreover, Notch-1 is also expressed in endothelial cells of the sinusoids and small vessels. After partial hepatectomy (PH) in rats, both Notch-1 and Jagged-1 proteins are upregulated and mainly exist in periportal hepatocytes. Notch receptor expressed in endothelial cells may be stimulated by its ligand Jagged, which is highly expressed in proliferating hepatocytes. Such interactions between ligands/receptors cause a decrease in endothelial cell proliferation and

promote formation of mature sinusoids. The Jagged/Notch signal is required to maintain a differentiated phenotype of bile duct cells, but more functions of Jagged/Notch signaling in bile duct cell proliferation and duct assembly remain vague^[17].

Dendritic cells (DCs), natural killer (NK) cells and NKT cells

Interstitial liver DCs play important roles in innate and adaptive immunity. The outcome of liver DCs interacting with the antigen-specific T cells determines the balance between tolerance and immunity. Systemic and local environmental factors influence hepatic DC migration, maturation, and function^[18].

After 75% PH in male C57BL/6 mice, CD11c⁺ (DC marker) liver (L)DCs increased significantly within 6 h and maintained an inherent, immature phenotype in both PBS- and Flt3L (fms-like tyrosine-3 ligand, a hematopoietic growth factor that expands dramatically the number of DCs in lymphoid and non-lymphoid tissues, including the liver, without changing their maturation state)-pretreated mice^[19]. The increase was more notable in mice pretreated with Flt3L compared with PBS. The numbers of CD11c⁺ LDCs returned to pre-hepatectomy levels by 24 h. The expanded LDC population showed increased IL-10 and reduced interferon (IFN)- γ gene transcription 6 h after PH. The concomitant increase in expression of the anti-inflammatory cytokine IL-10 suggests that LDCs are involved actively in promoting a state of local immunosuppression. The decrease in IFN- γ is associated with inhibition of hepatic NK cell lytic activity. LDCs isolated from the liver 6 h after 75% PH exhibit enhanced estrogen receptor expression, concomitant with increased serum 17- β -estradiol levels. Flt3L-treated mice showed a significant increase in proliferating cell nuclear antigen labeling index compared with PBS-treated mice at 12, 24, 48 and 72 h after 40% PH, with a peak at 48 h. These results indicate that the increased numbers of estrogen-exposed DCs may play a key role in local immune suppression and promote progression of liver regeneration, by altering the balance toward a Th2-like microenvironment^[19].

NK cells are cytotoxic large granular lymphocytes derived from CD34⁺ hematopoietic stem cells. NKT cells have three categories: I type (classical, V α 14-J α 18⁺TCR/CD1-dependent); II type (non-classical, all other CD1d-dependent T cells); and NKT-like cells (CD1d-independent NK1.1⁺ T cells). NK and NKT cells are components of the innate immune system and participate in the inflammatory processes during hepatic injury. NK and NKT cells also contribute to adaptive immune responses by interacting with APCs^[20]. NK and NKT cells accelerate liver injury through production of pro-inflammatory cytokines and killing hepatocytes. NKs inhibit liver fibrosis *via* killing early-activated and senescent-activated stellate cells and producing IFN- γ . For the regulation of liver fibrosis, NKT cells appear to be less important than NK cells as a result of hepatic NKT cell tolerance^[21].

Treatment of mice with murine cytomegalovirus

(MCMV) infection and toll-like receptor (TLR)3 ligand poly I:C results in the activation of NK cells to produce IFN- γ and attenuates liver regeneration after PH. NKT cells may only play a minor role in the negative suppressive effects of MCMV and poly I:C on liver regeneration^[22]. However, in HBV transgenic (HBV-tg) mice, PH-induced liver regeneration is delayed. The impaired liver regeneration is related to the increased activation and number of NKT cells and their enhanced IFN- γ production. NKT cells usually are activated by antigen-loading CD1d on APCs and soluble cytokines, such as IL-12 that is produced by Kupffer cells. Elevated CD1d on hepatocytes contributes to NKT cell activation and subsequent impairment of liver regeneration in HBV-tg mice. The impairment of liver regeneration in HBV-tg mice is largely ameliorated by NKT cell depletion, but not by NK cell depletion^[23].

Pretreatment of V α 14 NKT/J α 281^{+/+} mice with IL-12 or α -galactosylceramide (α -GalCer) 5 d before PH induced activation of NKT cells. The activated NKT cells expressed increased mRNA levels for TNF- α and IFN- γ and enhanced liver injury at 24 h after PH. Hepatic NKT cells rather than Kupffer cells might produce TNF- α after the administration of IL-12 or α -GalCer. TNF- α produced by activated V α 14 NKT cells was more than sufficient to enhance liver damage during the early phase of liver regeneration. The regenerating hepatocytes were destroyed specifically through the TNF receptor 1 (TNFR1) mediated TNF- α /TNFR1 pathway, which led eventually to impaired liver regeneration^[24]. However, in another study, in mice injected with α -GalCer 36 h after 70% PH, the induced activation of NKT cells greatly enhanced hepatocyte mitosis 44 h after surgery, *via* the TNF- α /TNFR1 and Fas/FasL-mediated pathways, accompanied by increased expression of TNFR1 and FasL in liver NKT cells^[25].

Stem cells and progenitor cells

After injury, liver regeneration occurs typically through replication of existing hepatocytes, however, when hepatocyte proliferation is attenuated or blocked, the liver is repopulated by induction, proliferation, and differentiation of the progenitor cell compartment. Hepatic progenitor cells are rare quiescent cells that are thought to reside in the canals of Hering. The oval cells are a type of liver progenitor cells that express markers in common with cholangiocytes and embryonic hepatocytes in rodents^[4,26-28]. Oval cells are characterized by expressing phenotypic markers such as A6^[27,28] and thymus cell antigen 1, and α -fetoprotein (AFP)^[29].

Oval cells are much less sensitive to TGF- β -induced growth inhibition than hepatocytes *in vivo* and *in vitro*. These results are partly due to Mothers against decapentaplegic homolog (Smad)6 intervention. Smad6 is present in much higher amounts in oval cells (LE-2 and LE-6 cells) compared with hepatocytes (AML-12 cells or primary hepatocytes). The significant levels of Smad6 in oval cells inhibit TGF- β signaling by associating with the type I receptor, thereby interfering with Smad2 phosphorylation by the activated receptor complex, which

prevents translocation of Smad2 to the nucleus, and subsequent target gene transcription^[4]. The combination of IFN- γ with lipopolysaccharide (LPS) or TNF- α causes a reversible cell cycle arrest in cultured hepatocytes (AML-12 cells), but stimulates DNA replication in oval cells (LE-6 cells). Hepatocyte cell cycle arrest is caused, at least in part, through NO release produced by inducible NO synthase after IFN- γ /LPS or IFN- γ /TNF- α administration^[26].

The hepatic expression of *lymphotoxin- β* (*Lt- β* or *Tnf- β*) and *Ifn- γ* produced by oval cells is upregulated and promotes oval cell-mediated liver regeneration in a choline-deficient, ethionine-supplemented (CDE) diet/PH mouse model. In *Lt- β r* knock-out (KO), *Lt- β* KO, and *Ifn- γ* KO mice, oval cell-mediated liver regeneration is impaired, which confirms a role for LT- β /LT- β R and IFN- γ in oval cell-mediated liver regeneration^[27].

Gp130-mediated IL-6 signaling may play a role in oval cell proliferation *in vivo*. In livers of *IL-6*^{-/-} mice fed with a CDE diet, the numbers of oval cells were reduced compared with *IL-6*^{+/+} control mice. The hyperactive signal transducer and activator of transcription (STAT)3 signaling *Gp130*^{Y757F} mouse model was derived when the tyrosine 757 residue of gp130 was mutated to a phenylalanine that prevented suppressor of cytokine signaling proteins (SOCS)3 binding and Src homology 2 (SH2) domain-containing protein-tyrosine phosphatase (SHP)2/RAS/extracellular signal-regulated kinases (ERK) signaling upon gp130 activation. Hyperactive STAT3 signaling in *Gp130*^{Y757F} and *Socs3*^{-/-Ab} (*Socs3*^{-/-}) mice fed a CDE diet results in increased oval cell proliferation compared with wild-type and gp130-mediated hyperactive ERK1/2 signaling (*Gp130*^{STAT3T}) mice. However, SOCS3 overexpression or ERK1/2 activation inhibits oval cell proliferation in oval cell lines^[28]. Proliferation of oval cells is associated with activation of nuclear factor (NF)- κ B and STAT3 during oval cell-mediated liver regeneration in a 2-acetylaminofluorene (AAF)/PH rat model. Sustained NF- κ B signaling has a critical role in protecting oval cells against apoptosis during stem cell-mediated liver regeneration. STAT3 plays a important role in driving proliferation and regulating differentiation of the hepatic stem cell progenies^[30].

Connective tissue growth factor (CTGF or CCN2) is a secreted matricellular protein that belongs to the CCN family. This protein comprises four mosaic conserved modules. CTGF normally is expressed at a very low level in the liver. However, when the liver suffers from chronic or acute injury, CTGF level is upregulated in diverse repair processes^[29]. Recruitment and proliferation of Thy-1⁺ oval cells is a hallmark of liver regeneration in rats after 2-AAF/PH. Sorted Thy-1⁺ oval cells in rats after 2-AAF/PH express a high level of *Ctgf* gene accompanied by upregulated CTGF protein expression. Blocking CTGF induction by iloprost (a known inhibitor of CTGF synthesis) significantly decreased the oval cell proliferation and lowered the level of AFP expression as compared with control animals. These results suggest that CTGF induction is important for robust oval cell proliferation

after 2-AAF/PH treatment in rats^[31]. Yeast two hybrid experiments have identified that fibronectin (FN) is a CTGF-binding protein. FN that binds to modules I and IV of CTGF and co-localizes with CTGF on the provisional hepatic ECM around the periportal regions promotes oval cell adhesion and migration, thereby facilitating oval cell activation^[29].

In 2-AAF/PH-treated rats, hepatocytes strongly express multidrug resistance protein 1b, but oval cells express high levels of active multidrug resistance associated protein (Mrp)1 and Mrp3. Mrp1 functions mainly as a cellular efflux pump of cysteinyl-leukotrienes and glutathione-S-conjugates, and Mrp3 as a pump for glucuronides and mono- and divalent bile salts, thus Mrp1 and Mrp3 may have a role in removing exogenous and endogenous toxic drugs/metabolites from oval cells, and facilitate oval cell proliferation in conditions of severe hepatotoxicity^[32].

Sympathetic nervous system inhibition using prazosin (PRZ, an α -1 adrenoceptor antagonist) or 6-hydroxydopamine (6-OHDA, an agent that induces chemical sympathectomy) significantly enhanced hepatic accumulation of oval cells and reduced liver damage in mice fed antioxidant-depleted diets to induce liver injury. Neither PRZ nor 6-OHDA affects the expression of cytokines, growth factors, or growth factor receptors that are known to regulate progenitor cells^[33].

The plant lectin concanavalin A (Con A) may induce T cell-mediated hepatitis in mice. Following PH, ConA-treated mice show significantly impaired early regenerative responses, such as decreased cyclin D1 and E expression and STAT3 activation within hepatocytes, in conjunction with reduced IL-6 production, increased IFN- γ , TGF- β and p21^{waf} expression, and increased TGF- β -induced Smad2 phosphorylation. However, Con A may induce an increase in the number of NK cell-sensitive oval cells (CD117, AFP, albumin, and cytokeratin-positive cells) and hematopoietic-like cells (Sca-1⁺ cells) in these mice^[34]. Furthermore, much more accumulated lipid was seen in the liver of mice with Con A-induced hepatitis, by Oil Red O staining^[35].

The IL-6/gp80/gp130 signaling system contributed to rapid expansion of the progenitor cell populations including liver hematopoietic progenitor cells and liver epithelial progenitor cells in a Con A/PH-mediated mouse liver injury model^[36].

SIGNAL COMMUNICATION THAT OCCURS IN THE PROGRESSIVE PHASES OF LIVER REGENERATION

Liver injury causes significant changes in the expression and activity of a variety of signal mediators produced by hepatic cells, endocrine glands and platelets. These molecules include complement components C3 and C5; cytokines (TNF- α and ILs); growth factors [TGF, epidermal growth factor (EGF), platelet-derived growth factor, vascular endothelial growth factor (VEGF), FGF,

insulin-like growth factor (IGF)-I, and HGF]; hepatic ECM; extracellular proteases and protease inhibitors; hormones [insulin, growth hormone (GH), thyroid hormone, vasopressin, prostanoids, and endothelin-1] and neurotransmitters (serotonin); metabolites [bile acids, reactive oxygen species (ROS), NO, lipids, glutathione, S-adenosylmethionine, and sphingosine-1-phosphate]; and chemokines^[1,5,7,37-42]. Liver regeneration progression is highly coordinated by the signal communication between hepatocytes and non-parenchymal cells, and is also influenced by endocrine glands, sympathetic innervation, and blood circulation. The progression of liver regeneration is segmented into several phases. Here, we describe the mechanisms of liver regeneration in each phase.

Priming phase

In models of liver injury induced by toxins, such as CCl₄, or Fas ligand, the hepatocytes are damaged and undergo necrosis, for which, the growth factor- and cytokine-mediated pathways are similar to those in PH models^[1]. Liver injury causes the release of ROS and LPS, which trigger the activation of the complement system. After complement activation, cleavage of C3 or C5 leads to the generation of the potent anaphylatoxins C3a and C5a. LPS, C3a and C5a in turn activate the non-parenchymal cells such as Kupffer cells, through the cell surface receptor TLR4 and G protein-coupled receptors C3aR and C5aR, which causes activation of the NF-κB signaling pathway and the production of cytokines such as TNF-α and IL-6. TNF-α then interacts with TNFR on Kupffer cells, which stimulates intensive synthesis of TNF-α and IL-6. Furthermore, SECs, HSCs, biliary epithelial cells and hepatocytes may also produce IL-6^[5,43,44]. The cytokines TNF-α and IL-6 are responsible for priming the quiescent hepatocytes into the cell cycle (G0 to G1) through binding to their receptors TNFR1 and IL-6R; activating the NF-κB, JAK/STAT3 and MAPK signal pathway; initiating the transcription of immediate early genes; and sensitizing hepatocytes to the proliferative effects of growth factors^[37].

Proliferative phase

In rat liver PH models, the rate of DNA synthesis in hepatocytes begins to increase after about 12 h and peaks around 24 h. However, induction of DNA synthesis occurs later in the non-parenchymal cells (at about 48 h for Kupffer, biliary epithelial and stellate cells, and at about 96 h for endothelial cells). Subsequent levels of DNA synthesis in hepatocytes are lower, as complete restoration of liver mass requires an average of about 1.66 cycles of replication in all cells. By comparison, the peak in DNA synthesis in mice occurs later (36-40 h after PH) and varies between strains^[1,45]. Many growth factors and growth factor-binding proteins are produced to promote the progression of liver regeneration.

The bulk of IGF-I is synthesized by hepatocytes, but is also produced by other types of non-parenchymal liver cells. Hepatic IGF-I synthesis is not only regulated

by growth hormone, insulin, and IGF-I, but also by cytokines released from activated Kupffer (IL-1, TNF-α and TGF-β) or stellate (TGF-α and TGF-β) cells^[7]. The biological actions of IGF-I are mediated through its physiologic receptor IGF-1R and insulin receptor. The activity of IGFs is modulated by a family of high-affinity binding proteins (IGFBP-1-6) and IGFBP proteases^[46]. HGF is produced mainly by HSCs, but also by hepatocytes, SECs, and performs its functions through interacting with its receptor c-met^[5]. The EGF family consists of several members, including EGF, TGF-α, heparin-binding EGF-like growth factor (HB-EGF), amphiregulin (AR), β cellulin, and epiregulin^[47]. HB-EGF is expressed mainly in Kupffer and endothelial cells^[48]; TGF-α is synthesized mainly by hepatocytes^[49]; expression of AR is induced by hepatocytes, Kupffer cells and HSCs^[50,51]; and these factors transmit their signal through EGF receptor.

Most growth factors are usually formed in an inactive precursor bound with ECM or integral to membrane. During liver regeneration, extracellular protease activation and ECM degradation occur in the first few hours before hepatocyte DNA synthesis and division, and growth factors are released and activated from the bound ECM or cell membrane by the extracellular protease^[5]. These activated growth factors binding to their corresponding receptors drive hepatic cells into DNA replication and mitosis. Furthermore, factors such as insulin from the pancreas, EGF from the duodenum or salivary gland, norepinephrine from the adrenal gland, triiodothyronine from the thyroid gland, GH from the anterior pituitary gland, arginine vasopressin (AVP) from the posterior pituitary, serotonin from platelets, and prostaglandins (PGs) from Kupffer cells and hepatocytes are also involved in the process of liver regeneration^[1,38,52-54].

Remodeling phase

After cell division, hepatocytes are formed in clusters that no longer associate with sinusoids. The nascent endothelial cells travel among cell clusters to form sinusoids that will line hepatocyte plates. VEGF, angiopoietin and their receptors Flt-1 (VEGF-R1), Flk-1/KDR (VEGF-R2), Flt-4 (VEGF-R3), and Flt3/Flk2, as well as tyrosine kinase containing immunoglobulin and epidermal growth factor homology domain (Tie)-1 and Tie-2 might be involved in this process^[5,55]. Meanwhile, biliary epithelial cells rebuild the biliary tree in hepatic portal triads. Synthesis of new ECM, vasculature and biliary tree then reestablishes tissue architecture.

Terminating phase

TGF-β and activin A belong to the TGF-β superfamily of cytokines. TGF-β is produced mainly in HSCs, but is also expressed in SECs and Kupffer cells^[4,5]. In the liver, activin A is synthesized predominantly in hepatocytes, but is also expressed in non-parenchymal cells under pathological conditions. Activin A is an autocrine growth inhibitor that is produced in hepatocytes, and is involved in inhibiting the proliferation of hepatocytes,

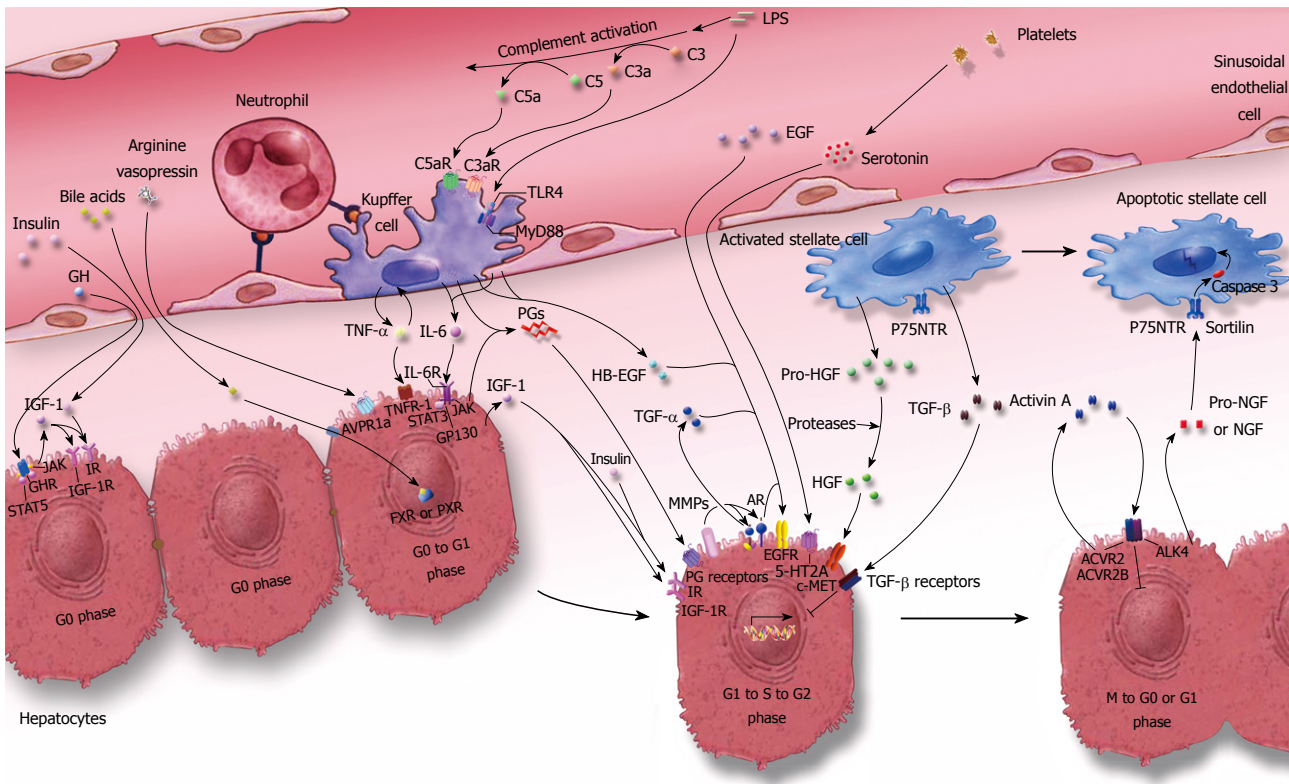


Figure 1 Scheme depicting the network of signaling among hepatic cells and blood during liver regeneration. After liver injury such as PH, gut-derived factors such as LPS reach the liver through the portal blood supply. LPS activate the complement system, which releases the anaphylatoxins C3a and C5a. LPS, C3a and C5a activate Kupffer cells through TLR4, C3aR and C5aR, and further lead to production of TNF- α and IL-6. These factors are involved in priming the hepatocytes from G0 to G1 phase. Insulin, GH, bile acids, AVP, platelet-derived serotonin, and EGF from the blood, cooperating with PGs, HB-EGF, HGF, as well as IGF-1, TGF- α and AR from different hepatic cells, promote hepatocyte transition from G1, through S and G2, to the M phase of the cell cycle. TGF- β produced mainly by HSCs inhibits G1 to S phase transition of hepatocytes, and TGF- β signalling is blocked during the proliferative phase. Pro-NGF or NGF produced by the neighboring regenerating hepatocytes promotes the termination of the activated state of HSCs by pro-NGF- or NGF-induced apoptotic pathways. When the liver mass is restored to its normal volume, the increased signaling by activin A, apoptosis and other factors may promote termination of liver regeneration. The prototype of this figure is originated from reference^[43].

inducing the differentiation of hepatocytes, augmenting the tubulogenesis of SECs, and stimulating collagen production in HSCs^[56].

TGF- β and activin A may bind to their high-affinity cell surface type II receptor TGFBR2/T β R II and ACVR2/ActR II or ACVR2B/ActR II b, respectively, either directly or *via* co-receptors, and recruit and activate their cell surface type I receptors TGFBR1/ALK5 (T β RI), ACVRL1/ALK1, ACVR1/ALK2 and ACVRL1/ALK1, ACVR1/ALK2, ACVR1B/ALK4, respectively, which leads to activation of their downstream Smad signal pathway^[57,58]. TGF- β inhibits G1 to S phase transition in hepatocytes, but TGF- β signaling is blocked during the proliferative phase; furthermore, intact TGF- β signaling is not required for the termination of liver regeneration^[1,59]. When the liver mass restores its normal volume, the increased signaling by activin A, apoptosis and other factors^[59], and the decreased expression and activation of promoting proliferation factors due to the restored ECM and tissue architecture may promote termination of liver regeneration. Figure 1 depicts the main signal communication network that occurs in the progression of liver regeneration.

Following liver injury, the expression and activity of signal molecules produced by activated hepatic cells

are controlled in a time- and micromilieu-dependent mode. The direct interactions among hepatic cells and the indirect interactions mediated by secreted signal molecules with hepatic cells constitute the dynamic recovery process of liver regeneration. Many more signal molecules and pathways are involved in the regulation of liver regeneration than those mentioned above. Further study will reveal more facts about the mechanisms of liver regeneration.

CONCLUSION

Liver regeneration is a very complex process, which is accompanied by a highly regulated intercellular and intracellular signal communication network. The extracellular signal molecules that regulate the progression of liver regeneration are produced by hepatic cells, endocrine glands and platelets in autocrine, paracrine, juxtacrine and endocrine modes. Most of these signal molecules are inactive precursors that need to be further processed into a mature form by activated proteases in ECM or on membrane of adjacent hepatic cells. The extracellular signaling interfaces with intracellular signals through their specific receptors. Liver regeneration is highly coordinated by the cross-talk between these signal

molecules and hepatic cells. Liver has a regenerative ability to restore functional hepatic mass after liver injury, but under some pathological conditions, the recovery of liver is not autonomous, so the study of the pathogeny of the diseased liver is more significant, to provide methods for treating patients with liver damage.

REFERENCES

- 1 **Taub R.** Liver regeneration: from myth to mechanism. *Nat Rev Mol Cell Biol* 2004; **5**: 836-847
- 2 **Beyer TA, Xu W, Teupser D, auf dem Keller U, Bugnon P, Hildt E, Thiery J, Kan YW, Werner S.** Impaired liver regeneration in Nrf2 knockout mice: role of ROS-mediated insulin/IGF-1 resistance. *EMBO J* 2008; **27**: 212-223
- 3 **Koniaris LG, McKillop IH, Schwartz SI, Zimmers TA.** Liver regeneration. *J Am Coll Surg* 2003; **197**: 634-659
- 4 **Nguyen LN, Furuya MH, Wolfraim LA, Nguyen AP, Holdren MS, Campbell JS, Knight B, Yeoh GC, Fausto N, Parks WT.** Transforming growth factor-beta differentially regulates oval cell and hepatocyte proliferation. *Hepatology* 2007; **45**: 31-41
- 5 **Mohammed FF, Khokha R.** Thinking outside the cell: proteases regulate hepatocyte division. *Trends Cell Biol* 2005; **15**: 555-563
- 6 **Winau F, Hegasy G, Weiskirchen R, Weber S, Cassan C, Sieling PA, Modlin RL, Liblau RS, Gressner AM, Kaufmann SH.** Ito cells are liver-resident antigen-presenting cells for activating T cell responses. *Immunity* 2007; **26**: 117-129
- 7 **Kmiec Z.** Cooperation of liver cells in health and disease. *Adv Anat Embryol Cell Biol* 2001; **161**: III-XIII, 1-151
- 8 **Malato Y, Sander LE, Liedtke C, Al-Masaoudi M, Tacke F, Trautwein C, Beraza N.** Hepatocyte-specific inhibitor-of-kappaB-kinase deletion triggers the innate immune response and promotes earlier cell proliferation during liver regeneration. *Hepatology* 2008; **47**: 2036-2050
- 9 **Tian Y, Jochum W, Georgiev P, Moritz W, Graf R, Clavien PA.** Kupffer cell-dependent TNF-alpha signaling mediates injury in the arterialized small-for-size liver transplantation in the mouse. *Proc Natl Acad Sci USA* 2006; **103**: 4598-4603
- 10 **Henderson NC, Forbes SJ.** Hepatic fibrogenesis: from within and without. *Toxicology* 2008; **254**: 130-135
- 11 **Atzori L, Poli G, Perra A.** Hepatic stellate cell: a star cell in the liver. *Int J Biochem Cell Biol* 2009; **41**: 1639-1642
- 12 **Sawitsa I, Kordes C, Reister S, Häussinger D.** The niche of stellate cells within rat liver. *Hepatology* 2009; **50**: 1617-1624
- 13 **Kordes C, Sawitsa I, Häussinger D.** Hepatic and pancreatic stellate cells in focus. *Biol Chem* 2009; **390**: 1003-1012
- 14 **Geerts A.** The simple truth is seldom true and never simple: dual role for p75(NTR) in transdifferentiation and cell death of hepatic stellate cells. *Hepatology* 2007; **46**: 600-601
- 15 **Passino MA, Adams RA, Sikorski SL, Akassoglou K.** Regulation of hepatic stellate cell differentiation by the neurotrophin receptor p75NTR. *Science* 2007; **315**: 1853-1856
- 16 **Tietz PS, Larusso NF.** Cholangiocyte biology. *Curr Opin Gastroenterol* 2006; **22**: 279-287
- 17 **Köhler C, Bell AW, Bowen WC, Monga SP, Fleig W, Michalopoulos GK.** Expression of Notch-1 and its ligand Jagged-1 in rat liver during liver regeneration. *Hepatology* 2004; **39**: 1056-1065
- 18 **Sumpter TL, Abe M, Tokita D, Thomson AW.** Dendritic cells, the liver, and transplantation. *Hepatology* 2007; **46**: 2021-2031
- 19 **Castellaneta A, Di Leo A, Francavilla R, Margiotta M, Barone M, Amoruso A, Troiani L, Thomson AW, Francavilla A.** Functional modification of CD11c+ liver dendritic cells during liver regeneration after partial hepatectomy in mice. *Hepatology* 2006; **43**: 807-816
- 20 **Notas G, Kissileva T, Brenner D.** NK and NKT cells in liver injury and fibrosis. *Clin Immunol* 2009; **130**: 16-26
- 21 **Gao B, Radaeva S, Park O.** Liver natural killer and natural killer T cells: immunobiology and emerging roles in liver diseases. *J Leukoc Biol* 2009; **86**: 513-528
- 22 **Sun R, Gao B.** Negative regulation of liver regeneration by innate immunity (natural killer cells/interferon-gamma). *Gastroenterology* 2004; **127**: 1525-1539
- 23 **Dong Z, Zhang J, Sun R, Wei H, Tian Z.** Impairment of liver regeneration correlates with activated hepatic NKT cells in HBV transgenic mice. *Hepatology* 2007; **45**: 1400-1412
- 24 **Ito H, Ando K, Nakayama T, Taniguchi M, Ezaki T, Saito K, Takemura M, Sekikawa K, Imawari M, Seishima M, Moriaki H.** Role of Valpha 14 NKT cells in the development of impaired liver regeneration in vivo. *Hepatology* 2003; **38**: 1116-1124
- 25 **Nakashima H, Inui T, Habu Y, Kinoshita M, Nagao S, Kawaguchi A, Miura S, Shinomiya N, Yagita H, Seki S.** Activation of mouse natural killer T cells accelerates liver regeneration after partial hepatectomy. *Gastroenterology* 2006; **131**: 1573-1583
- 26 **Brooling JT, Campbell JS, Mitchell C, Yeoh GC, Fausto N.** Differential regulation of rodent hepatocyte and oval cell proliferation by interferon gamma. *Hepatology* 2005; **41**: 906-915
- 27 **Akhurst B, Matthews V, Husk K, Smyth MJ, Abraham LJ, Yeoh GC.** Differential lymphotoxin-beta and interferon gamma signaling during mouse liver regeneration induced by chronic and acute injury. *Hepatology* 2005; **41**: 327-335
- 28 **Yeoh GC, Ernst M, Rose-John S, Akhurst B, Payne C, Long S, Alexander W, Croker B, Grail D, Matthews VB.** Opposing roles of gp130-mediated STAT-3 and ERK-1/2 signaling in liver progenitor cell migration and proliferation. *Hepatology* 2007; **45**: 486-494
- 29 **Pi L, Ding X, Jorgensen M, Pan JJ, Oh SH, Pintilie D, Brown A, Song WY, Petersen BE.** Connective tissue growth factor with a novel fibronectin binding site promotes cell adhesion and migration during rat oval cell activation. *Hepatology* 2008; **47**: 996-1004
- 30 **Sánchez A, Factor VM, Schroeder IS, Nagy P, Thorgeirsson SS.** Activation of NF-kappaB and STAT3 in rat oval cells during 2-acetylaminofluorene/partial hepatectomy-induced liver regeneration. *Hepatology* 2004; **39**: 376-385
- 31 **Pi L, Oh SH, Shupe T, Petersen BE.** Role of connective tissue growth factor in oval cell response during liver regeneration after 2-AAF/PHx in rats. *Gastroenterology* 2005; **128**: 2077-2088
- 32 **Ros JE, Roskams TA, Geukem M, Havinga R, Splinter PL, Petersen BE, LaRusso NF, van der Kolk DM, Kuipers F, Faber KN, Müller M, Jansen PL.** ATP binding cassette transporter gene expression in rat liver progenitor cells. *Gut* 2003; **52**: 1060-1067
- 33 **Oben JA, Roskams T, Yang S, Lin H, Sinelli N, Li Z, Torbenson M, Huang J, Guarino P, Kafrouni M, Diehl AM.** Sympathetic nervous system inhibition increases hepatic progenitors and reduces liver injury. *Hepatology* 2003; **38**: 664-673
- 34 **Hines IN, Kremer M, Isayama F, Perry AW, Milton RJ, Black AL, Byrd CL, Wheeler MD.** Impaired liver regeneration and increased oval cell numbers following T cell-mediated hepatitis. *Hepatology* 2007; **46**: 229-241
- 35 **Feng D, Xu L.** Lipid accumulation in concanavalin A-induced hepatitis: Another cause for impaired liver regeneration afterwards? *Hepatology* 2008; **47**: 765; author reply 765-766; author reply 766
- 36 **Sakamoto T, Ezure T, Lunz J, Murase N, Tsuji H, Fung JJ, Demetris AJ.** Concanavalin A simultaneously primes liver hematopoietic and epithelial progenitor cells for parallel expansion during liver regeneration after partial hepatectomy in mice. *Hepatology* 2000; **32**: 256-267
- 37 **Fausto N, Campbell JS, Riehle KJ.** Liver regeneration. *Hepatology* 2006; **43**: S45-S53
- 38 **Nicou A, Serrière V, Prigent S, Boucherie S, Combettes L, Guillou G, Alonso G, Tordjmann T.** Hypothalamic vasopressin release and hepatocyte Ca²⁺ signaling during liver regeneration: an interplay stimulating liver growth and bile flow. *FASEB J* 2003; **17**: 1901-1903

- 39 **Huang ZZ**, Chen C, Zeng Z, Yang H, Oh J, Chen L, Lu SC. Mechanism and significance of increased glutathione level in human hepatocellular carcinoma and liver regeneration. *FASEB J* 2001; **15**: 19-21
- 40 **Martínez-Chantar ML**, Vázquez-Chantada M, Garnacho M, Latasa MU, Varela-Rey M, Dotor J, Santamaría M, Martínez-Cruz LA, Parada LA, Lu SC, Mato JM. S-adenosylmethionine regulates cytoplasmic HuR via AMP-activated kinase. *Gastroenterology* 2006; **131**: 223-232
- 41 **Ikeda H**, Satoh H, Yanase M, Inoue Y, Tomiya T, Arai M, Tejima K, Nagashima K, Maekawa H, Yahagi N, Yatomi Y, Sakurada S, Takuwa Y, Ogata I, Kimura S, Fujiwara K. Antiproliferative property of sphingosine 1-phosphate in rat hepatocytes involves activation of Rho via Edg-5. *Gastroenterology* 2003; **124**: 459-469
- 42 **Michalopoulos GK**. Liver regeneration. *J Cell Physiol* 2007; **213**: 286-300
- 43 **Clavien PA**, Petrowsky H, DeOliveira ML, Graf R. Strategies for safer liver surgery and partial liver transplantation. *N Engl J Med* 2007; **356**: 1545-1559
- 44 **Strey CW**, Markiewski M, Mastellos D, Tudoran R, Spruce LA, Greenbaum LE, Lambris JD. The proinflammatory mediators C3a and C5a are essential for liver regeneration. *J Exp Med* 2003; **198**: 913-923
- 45 **Michalopoulos GK**, DeFrances MC. Liver regeneration. *Science* 1997; **276**: 60-66
- 46 **Guvakova MA**. Insulin-like growth factors control cell migration in health and disease. *Int J Biochem Cell Biol* 2007; **39**: 890-909
- 47 **Dreux AC**, Lamb DJ, Modjtahedi H, Ferns GA. The epidermal growth factor receptors and their family of ligands: their putative role in atherogenesis. *Atherosclerosis* 2006; **186**: 38-53
- 48 **Kiso S**, Kawata S, Tamura S, Higashiyama S, Ito N, Tsushima H, Taniguchi N, Matsuzawa Y. Role of heparin-binding epidermal growth factor-like growth factor as a hepatotrophic factor in rat liver regeneration after partial hepatectomy. *Hepatology* 1995; **22**: 1584-1590
- 49 **Mead JE**, Fausto N. Transforming growth factor alpha may be a physiological regulator of liver regeneration by means of an autocrine mechanism. *Proc Natl Acad Sci USA* 1989; **86**: 1558-1562
- 50 **Berasain C**, García-Trevijano ER, Castillo J, Erroba E, Lee DC, Prieto J, Avila MA. Amphiregulin: an early trigger of liver regeneration in mice. *Gastroenterology* 2005; **128**: 424-432
- 51 **Perugorria MJ**, Latasa MU, Nicou A, Cartagena-Lirola H, Castillo J, Goñi S, Vespasiani-Gentilucci U, Zagami MG, Lotersztajn S, Prieto J, Berasain C, Avila MA. The epidermal growth factor receptor ligand amphiregulin participates in the development of mouse liver fibrosis. *Hepatology* 2008; **48**: 1251-1261
- 52 **Conway-Campbell BL**, Wooh JW, Brooks AJ, Gordon D, Brown RJ, Lichanska AM, Chin HS, Barton CL, Boyle GM, Parsons PG, Jans DA, Waters MJ. Nuclear targeting of the growth hormone receptor results in dysregulation of cell proliferation and tumorigenesis. *Proc Natl Acad Sci USA* 2007; **104**: 13331-13336
- 53 **Lesurte M**, Graf R, Aleil B, Walther DJ, Tian Y, Jochum W, Gachet C, Bader M, Clavien PA. Platelet-derived serotonin mediates liver regeneration. *Science* 2006; **312**: 104-107
- 54 **Casado M**, Callejas NA, Rodrigo J, Zhao X, Dey SK, Boscá L, Martín-Sanz P. Contribution of cyclooxygenase 2 to liver regeneration after partial hepatectomy. *FASEB J* 2001; **15**: 2016-2018
- 55 **Ross MA**, Sander CM, Kleeb TB, Watkins SC, Stoltz DB. Spatiotemporal expression of angiogenesis growth factor receptors during the revascularization of regenerating rat liver. *Hepatology* 2001; **34**: 1135-1148
- 56 **Endo D**, Maku-Uchi M, Kojima I. Activin or follistatin: which is more beneficial to support liver regeneration after massive hepatectomy? *Endocr J* 2006; **53**: 73-78
- 57 **Gordon KJ**, Blobe GC. Role of transforming growth factor-beta superfamily signaling pathways in human disease. *Biochim Biophys Acta* 2008; **1782**: 197-228
- 58 **Rodgarkia-Dara C**, Vejda S, Erlach N, Losert A, Bursch W, Berger W, Schulte-Hermann R, Grusch M. The activin axis in liver biology and disease. *Mutat Res* 2006; **613**: 123-137
- 59 **Oe S**, Lemmer ER, Conner EA, Factor VM, Levéen P, Larsson J, Karlsson S, Thorgeirsson SS. Intact signaling by transforming growth factor beta is not required for termination of liver regeneration in mice. *Hepatology* 2004; **40**: 1098-1105

S- Editor Tian L L- Editor Kerr C E- Editor Zheng XM



REVIEW

Potential role of Th17 cells in the pathogenesis of inflammatory bowel disease

Zhan-Ju Liu, Praveen K Yadav, Jing-Ling Su, Jun-Shan Wang, Ke Fei

Zhan-Ju Liu, Praveen K Yadav, Jing-Ling Su, Jun-Shan Wang, Department of Gastroenterology, Shanghai Tenth People's Hospital, Tongji University, Shanghai 200072, China

Ke Fei, Department of Thoracic Surgery, Shanghai Tenth People's Hospital, Tongji University, Shanghai 200072, China

Author contributions: Liu ZJ and Fei K designed and supervised this work; Liu ZJ and Yadav PK wrote the manuscript; Su JL and Wang JS provided the collection of materials.

Supported by Grants From the National Natural Science Foundation of China, No. 30770988 and No. 30971358

Correspondence to: Dr. Zhan-Ju Liu, Professor, Department of Gastroenterology, Shanghai Tenth People's Hospital, Tongji University, Shanghai 200072, China. zhanjuli@yahoo.com

Telephone: +86-21-66301164 **Fax:** +86-21-66303893

Received: August 17, 2009 **Revised:** November 3, 2009

Accepted: November 10, 2009

Published online: December 14, 2009

Research Center for Liver diseases, Keck School of Medicine, University of Southern California, 2011 Zonal Avenue, HMR101, Los Angeles, CA 90033, United States

Liu ZJ, Yadav PK, Su JL, Wang JS, Fei K. Potential role of Th17 cells in the pathogenesis of inflammatory bowel disease. *World J Gastroenterol* 2009; 15(46): 5784-5788 Available from: URL: <http://www.wjgnet.com/1007-9327/15/5784.asp> DOI: <http://dx.doi.org/10.3748/wjg.15.5784>

Abstract

The etiopathology of inflammatory bowel disease (IBD) remains elusive. Accumulating evidence suggests that the abnormality of innate and adaptive immunity responses plays an important role in intestinal inflammation. IBD including Crohn's disease (CD) and ulcerative colitis (UC) is a chronic inflammatory disease of the gastrointestinal tract, which is implicated in an inappropriate and overactive mucosal immune response to luminal flora. Traditionally, CD is regarded as a Th1-mediated inflammatory disorder while UC is regarded as a Th2-like disease. Recently, Th17 cells were identified as a new subset of T helper cells unrelated to Th1 or Th2 cells, and several cytokines [e.g. interleukin (IL)-21, IL-23] are involved in regulating their activation and differentiation. They not only play an important role in host defense against extracellular pathogens, but are also associated with the development of autoimmunity and inflammatory response such as IBD. The identification of Th17 cells helps us to explain some of the anomalies seen in the Th1/Th2 axis and has broadened our understanding of the immunopathological effects of Th17 cells in the development of IBD.

© 2009 The WJG Press and Baishideng. All rights reserved.

Key words: Crohn's disease; Inflammatory bowel disease; Interleukin-17; Interleukin-23; Th17 cells; Ulcerative colitis

Peer reviewer: Zhang-Xu Liu, MD, PhD, Assistant Professor,

INTRODUCTION

Current evidence strongly suggests that inflammatory bowel disease (IBD) arises from a disruption of mucosal immune homeostasis in genetically susceptible individuals, resulting in altered processing of enteric antigens, pathogenic T cell activation, and chronic inflammation^[1-3]. Although the etiology of IBD remains unclear, accumulating evidence has indicated that dysfunction of the mucosal immune system plays an important role in the pathogenesis of IBD. Among a variety of inflammatory cells in the gut, mucosal CD4⁺ T cells are thought to play a central role in both the induction and persistence of chronic inflammation by producing proinflammatory cytokines. Studies have indicated that Th1-related cytokines [e.g. tumor necrosis factor (TNF), interferon (IFN)-γ, interleukin (IL)-12] as well as Th17-associated cytokines (e.g. IL-17A, IL-21, IL-23) are markedly increased in inflamed mucosa of CD, whereas the cytokine profiles in inflamed areas of UC seem to exhibit increased production of the Th2 cytokines such as IL-5 and IL-13^[1-3]. These proinflammatory cytokines are potent *in vitro* stimulators of intestinal mucosal effector functions including T cell and macrophage proliferation, adhesion molecule expression, chemokine expression, and secretion of other proinflammatory cytokines.

Th17 CELLS AND THE DIFFERENTIATION REGULATION

CD4⁺ T cells play an important role in the initiation of immune responses by providing help to other cells and by taking on a variety of effector functions during immune reactions. Upon antigenic stimulation, naive CD4⁺ T cells are activated, expand and differentiate into different effector subsets such as Th1 and Th2 cells

characteristic of the production of distinct cytokines and effector functions^[4,5]. Th1 cells produce IFN- γ and lymphotoxin and can mobilize the cellular arm of the immune system to combat intracellular pathogens. Th2 cells secrete IL-4, IL-13, and IL-25, which are essential for the generation of appropriate classes of antibodies and for the elimination of extracellular pathogens^[4,5].

The identification of the IL-17 family of cytokines as well as the IL-23-mediated expansion of IL-17-producing T cells uncovered a new subset of Th cells, designated as Th17 cells^[6,7]. Th17 cells require specific cytokines and transcription factors for their differentiation. Although the function of this cell subtype is not completely elucidated, emerging data suggest that Th17 cells may play an important role in host defense against extracellular pathogens, which are not efficiently cleared by Th1-type and Th2-type immunity. The first pathogen implicated in a Th17 response was observed in human Lyme arthritis caused by *Borrelia burgdorferi*, in which *B. burgdorferi*-derived lipopeptides could stimulate the production of IL-17A by T cells from synovial fluid, leading to a Th17 lineage differentiation^[8]. Previous work has demonstrated that Th17 cells with specificity for self-antigens lead to severe autoimmunity in various animal models. In the murine model of psoriasis, evidence has shown that Th17 cells along with their upstream cytokines (e.g. IL-23) and their downstream effector cytokines (e.g. IL-22) might play a critical role in the pathogenesis of psoriasis^[9,10]. Moreover, increased levels of IL-17 produced by Th17 cells have been observed in murine models of rheumatoid arthritis and correlate with more severe joint damage^[11].

The IL-17 cytokine family is a recently discovered group of cytokines, which includes six members, IL-17A, IL-17B, IL-17C, IL-17D, IL-17E (or IL-25) and IL-17F, and act *in vitro* and *in vivo* as potent proinflammatory cytokines^[6]. IL-17 can induce the expression of proinflammatory cytokines (such as IL-6 and TNF), chemokines (such as KC, MCP-1 and MIP-2) and matrix metalloproteases, which mediate tissue infiltration and tissue destruction^[12]. It is also involved in the proliferation, maturation and chemotaxis of neutrophils^[13]. In agreement with this point, mice deficient in the IL-17 receptor (IL-17R) are more sensitive to lung bacterial infection because of reduced recruitment of neutrophils to the lung^[14]. In contrast, overproduction of IL-17 in the lungs leads to chemokine expression and tissue inflammation infiltrated by large amounts of leukocytes^[15]. Moreover, IL-17 is able to costimulate T cells and enhance the maturation of dendritic cells^[16]. Taken together, these data indicate that IL-17 has pleiotropic activities, functions through the adaptive and innate immune system to promote immune response, and plays an important role in immune responses.

Several cytokines have been reported to be associated with the development and/or proliferation of Th17 cells. Neutralization of IFN- γ and IFN- α *in vitro* increases the number of IL-17-producing cells generated by IL-23 stimulation. The number of Th17 cells is further increased by the addition of an IL-4-neutralizing antibody, indicating that IL-4 and IFN- γ could inhibit the IL-23-driven

expansion of Th17 cells^[17]. IL-2, a cytokine important for growth and survival of Th1 and Th2 subsets, is also involved in the long-term expansion and survival of Th17 cells, since restimulation of differentiated Th17 cells with IL-2 could abolish IL-17 production and induce IFN- γ production^[18]. In addition, the differentiation of Th17 cells might also require costimulatory signals distinct from those involved in the differentiation of Th1 and Th2 cells. These studies of the costimulatory requirements of Th17 cells were undertaken to determine which costimulatory molecules are important for IL-6- and TGF- β -mediated differentiation of Th17 cells. However, recent work has also demonstrated that Th1-derived IFN- γ could trigger antigen-presenting cells to produce IL-23 and then induce memory Th17 cell expansion in a B7-H1-independent manner^[19]. These data indicate that this complex differentiation of Th17 cells may be dependent on various cytokine milieu.

IL-23 is a heterodimeric protein, which is a member of the IL-12 family of cytokines. It is composed of a p19 subunit in addition to a p40 subunit, which is also a component of IL-12^[20]. IL-23 functions through the receptor-signaling complex, which is composed of its distinct receptor (namely IL-23R) and IL-12R β 1^[21]. Because IL-23 and IL-12 share a common p40 subunit and IL-12R β 1, IL-23 may function like IL-12 to trigger Th1 response. However, p19-deficient mice could contribute to normal Th1 response but could not promote the production of IL-17 cells^[22]. Other work has demonstrated that Th17 cells are absent in IL-23^{-/-} mice, and could not be amplified and survive albeit in the presence of normal Th17 cells *in vivo*^[23]. Studies have shown that IL-23R is not expressed on naïve T cells, therefore IL-23 could not induce naïve T cells to differentiate into Th17 cells, but could promote Th17 cells amplification^[24]. These data imply that IL-23 could provide survival signaling to induce the differentiation of Th17 cells. Recently, increasing evidence has shown that IL-1 β and IL-23 are required for the generation of Th17 cells and differentiation^[23]. Naive T cells stimulated with TGF- β plus IL-6 could secrete large amounts of IL-17, whereas IL-23 could trigger the proliferation of Th17 cells from activated memory T cells, only the combination of IL-6 plus TGF- β is sufficient to induce differentiation of Th17 cells from naive T cells^[25]. Moreover, IL-1 β and TNF could increase the number of Th17 cells generated *in vitro* in the presence of IL-6 plus TGF- β ^[26]. These data suggest that an inflammatory milieu could regulate the expression of IL-23R on Th17 cells and thereby allow IL-23 to sustain and strengthen the Th17 phenotype.

IL-27 is another IL-12 family member and has been found to downregulate Th17 cell development^[27,28]. IL-27 is a heterodimeric cytokine composed of Epstein-Barr virus-induced gene 3 (*EBI-3*) and p28 chains. Activation of T cells in the presence of IL-27 induces T-bet, a transcription factor critical for the differentiation of naïve CD4 $^{+}$ T cells into Th1 cells. However, IL-27R-deficient mice develop severe immunopathology resulting from a general dysregulation of effector T cell responses not restricted to any particular Th cell subtype^[29,30]. The absence of IL-27-mediated signaling exacerbates

neuroinflammation, enhances the generation of Th17 cells and increases the number of IL-17-expressing T cells in inflamed tissue. The transcription of the two subunits of IL-27 is differentially regulated, leading to the immunosuppressive effects of IL-27. *EBI-3* is strongly induced by Toll-like receptors (TLRs) and the stimulation of TLR results in the binding of NF- κ B complexes to a promoter region of the *EBI-3* gene, while activation of TRIF downstream of TLR3 or TLR4 is critical in the induction of p28^[28]. IL-27, independently of IFN- γ R and IL-6R signaling, can inhibit the differentiation of Th17 cells triggered by IL-6 and TGF- β . Previous work has demonstrated that T-bet and the suppressor protein SOCS3 are not involved in the IL-27-mediated inhibition of Th17 cells, but that the transcription factor STAT1 seems to be required for the suppressive effect of IL-27 on the development of Th17 cells^[27,28].

ROR γ t, an orphan nuclear hormone receptor, is expressed by fetal lymphocyte tissue-inducer cells and participates in the formation of lymph nodes and Peyer's patches, intestinal lymphocyte tissue-inducer-like cells and immature thymocytes^[31]. Interestingly, ROR γ t is also found to be expressed by differentiated Th17 cells and IL-17-producing T cells present in the intestinal lamina propria (LP). Consistent with this, Th17 cells are observed to be absent in ROR γ t-deficient mice, whereas transduction of naive T cells with a ROR γ t-encoding retrovirus could induce IL-17 production. These data indicate the importance of ROR γ t in the differentiation of Th17 cells^[32]. In addition, a recent study has observed that ROR γ t-deficiency could not abolish Th17 cell generation and that Th17 cells also express high levels of another related nuclear receptor ROR α ^[33]. Importantly, ROR α deficiency results in reduced IL-17 expression, while coexpression of ROR α and ROR γ t synergistically leads to Th17 cell differentiation. Thus, these data indicate that Th17 differentiation is directed by two lineage-specific nuclear receptors, ROR α and ROR γ t^[33].

PATHOGENIC ROLE OF Th17 CELLS IN IBD

It was widely believed that the chronic intestinal inflammation characteristic of human IBD is the consequence of pathogenic Th1 CD4 $^{+}$ cell responses against the luminal flora, especially in CD, which in turn is driven by proinflammatory cytokines such as IL-12 and TNF^[1-3]. Animal models of IBD support this hypothesis as intestinal inflammation could be blocked by treatment with monoclonal antibodies specific for IL-12 or TNF^[34,35]. In recent years, studies on the Th17 cell subset has highlighted our understanding of the formation of human inflammatory diseases, which helps us to explain some of Th1/Th2 balance of abnormal phenomena, particularly in human IBD.

Evidence has shown that high numbers of CD4 $^{+}$ Th17 cells are found in the colonic LP of the ileum and colon but not the duodenum, jejunum, mesenteric lymph nodes or spleen in conventionally-raised mice, and that these cells are highly infiltrated in inflamed areas of colitic

mice^[36,37]. Further analysis confirmed that commensal gut flora contribute to the expansion of these CD4 $^{+}$ Th17 cells, leading to intestinal mucosal inflammation. In terms of mucosal immunity, the IL-23/IL-17 axis has been observed to play an important role in normal intestinal homeostasis, although the precise actions of these cytokines in the gut remain to be fully delineated. To date, IL-17 and other Th17-associated cytokines (e.g. IL-22, IL-23) have been found to have protective effects or pathogenic effects dependent on other effective factors in local tissue. Previous study has demonstrated that IL-23 is mainly expressed by LP dendritic cells in the terminal ileum of normal mice and the frequency of Th17 cells in the intestinal LP is markedly higher than their frequency in peripheral lymphoid tissues^[38]. Evidence has shown that IL-23 may have important immune protective effects in the gut and that IL-23 $^{-/-}$ mice exhibited enhanced susceptibility and mortality following infection with the intestinal bacterial pathogen *Citrobacter rodentium*^[38]. Interestingly, *C. rodentium*-infected IL-23 $^{-/-}$ mice still generate potent mucosal Th17 responses, suggesting that IL-23-mediated protective responses need not necessarily involve IL-17 production^[25]. Similarly, although studies in various murine colitis models have implied that IL-23-driven intestinal pathology is associated with increased IL-17 production, a plethora of other inflammatory cytokines have also been found to be elevated in the inflamed colon, including IL-1 β , IL-6, IFN- γ and TNF^[39]. In many of the T cell-dependent IBD murine models, Th1 cells clearly predominated in inflamed mucosa and inhibition of Th1 responses could attenuate disease^[1-3]. Moreover, the observations that IL-23 also drives chronic colitis mediated by cells of the innate immune system are also consistent with the hypothesis that IL-23-mediated intestinal inflammation need not necessarily involve Th17 cells^[39,40].

IL-17 mRNA has been found to be highly expressed in inflamed mucosa from both UC and CD patients, and immunohistochemistry revealed that CD68-positive cells express IL-17^[41]. Recent work^[42] has also demonstrated that most of the transcripts for Th17-related cytokines were increased in both UC and CD compared to normal controls, but more abundant in UC than in CD. In contrast, up-regulation of IFN- γ mRNA was marked in CD LP CD4 $^{+}$ T cells. Up-regulation of IL-23p19 mRNA was detected in colonic mucosa from both UC and CD patients. The significance of Th17 immunity in UC was further supported by the finding that recombinant IL-23 actually enhanced IL-17 production by LP CD4 $^{+}$ T cells in UC, but had a lesser effect on LP CD4 $^{+}$ T cells in CD. Since the Th1 pathway has been reported to antagonize the Th17 pathway via various mechanisms, IFN- γ or IL-12 could actually suppress IL-17 production by human LP CD4 $^{+}$ T cells. Therefore, we can hypothesize that excess IFN- γ production by Th1 cells in CD patients may negatively affect the IL-17 production by Th17 cells in CD, despite the fact that Th17 cells are present in CD mucosa.

A previous report has shown that IL-23 can enhance IFN- γ production by LPMCs from CD patients and that the mucosal IL-23p19 expression levels were correlated with IL-17 in UC and IFN- γ in CD^[43]. These results

suggest that IL-23 may enhance the production of distinct cytokines between UC and CD patients, thereby contributing to the local Th1/Th17 balance in IBD. Additionally, IL-21, belonging to the IL-2 family, has been described to play an important part in the differentiation and maintenance of Th17 cells^[44,45]. Comparing the Th1, Th2, and Th17 subsets, the largest amounts of IL-21 are produced by Th17 cells. IL-21 produced by differentiating Th17 cells may act in a positive feedback loop, which amplifies the precursor frequency of Th17 cells^[44,45]. Recently, our study found that IL-21 facilitated IBD CD4⁺ T cells to differentiate into Th17 cells, characterized by increased expression of IL-17A and RORyt. Thus, we proposed that IL-21 might be involved in the pathogenesis of IBD and blockage of IL-21R signaling may have therapeutic potential in IBD^[46].

The exact role of IL-17 and Th17 cells in intestinal pathology and homeostasis is currently not well understood. IL-17 may have some protective functions in the epithelial layer, as it has been shown to fortify tight junction formation between epithelial cells *in vitro*^[47], and treatment of mice with anti-IL-17 neutralizing antibody actually enhanced the severity of colitis induced by administration of dextran sodium sulphate^[48]. In contrast, a recent study comparing the ability of Th1 and Th17 cells to induce colitis in mice has proven that Th17 cells are significantly more pathogenic than their Th1 counterparts^[49].

So far, there have been few studies that have employed selective blockade of IL-17 during intestinal inflammation. However, in IL-10^{-/-} mice, treatment with anti-IL-17 specific antibody had little impact on colitis unless anti-IL-6 antibody was also co-administered^[48], suggesting that IL-17 may synergize with other inflammatory mediators in the gut. Recent studies have highlighted further potential heterogeneity within Th17 cell populations by demonstrating that some may even secrete IL-10^[50], a factor known to inhibit intestinal inflammation. Thus, it is possible that the actions of Th17 cells may differ dependently on other factors that may be present in the local environment. In the normal intestine, the primary function of Th17 cells may be like sentinels which contribute to maintaining epithelial barrier function, whereas in sites of chronic intestinal inflammation, high levels of IL-23 may activate their full pathogenic and anti-bacterial functions.

CONCLUSION

Through the potential role of Th17 cells in IBD animal models of chronic intestinal inflammation as well as in human IBD, target therapy directed against the Th17/IL-17 axis may have a therapeutic role in the treatment of intestinal mucosal inflammation. However, the precise mechanisms of the Th17/IL-17 axis in intestinal homeostasis should be further elucidated in murine models and human IBD patients.

REFERENCES

- 1 Sartor RB. Mechanisms of disease: pathogenesis of Crohn's

disease and ulcerative colitis. *Nat Clin Pract Gastroenterol Hepatol* 2006; **3**: 390-407

- 2 Shih DQ, Targan SR. Immunopathogenesis of inflammatory bowel disease. *World J Gastroenterol* 2008; **14**: 390-400
- 3 Yadav PK, Liu Z. Current strategies for the treatment of ulcerative colitis. *Recent Pat Inflamm Allergy Drug Discov* 2009; **3**: 65-72
- 4 Mosmann TR, Coffman RL. TH1 and TH2 cells: different patterns of lymphokine secretion lead to different functional properties. *Annu Rev Immunol* 1989; **7**: 145-173
- 5 Zhou L, Chong MM, Littman DR. Plasticity of CD4+ T cell lineage differentiation. *Immunity* 2009; **30**: 646-655
- 6 Kolls JK, Linden A. Interleukin-17 family members and inflammation. *Immunity* 2004; **21**: 467-476
- 7 Bettelli E, Oukka M, Kuchroo VK. T(H)-17 cells in the circle of immunity and autoimmunity. *Nat Immunol* 2007; **8**: 345-350
- 8 Codolo G, Amedei A, Steere AC, Papinutto E, Cappon A, Polenghi A, Benagiano M, Paccani SR, Sambri V, Del Prete G, Baldari CT, Zanotti G, Montecucco C, D'Elios MM, de Bernard M. *Borrelia burgdorferi NapA*-driven Th17 cell inflammation in lyme arthritis. *Arthritis Rheum* 2008; **58**: 3609-3617
- 9 Ma HL, Liang S, Li J, Napierata L, Brown T, Benoit S, Senices M, Gill D, Dunussi-Joannopoulos K, Collins M, Nickerson-Nutter C, Fouser LA, Young DA. IL-22 is required for Th17 cell-mediated pathology in a mouse model of psoriasis-like skin inflammation. *J Clin Invest* 2008; **118**: 597-607
- 10 Di Cesare A, Di Meglio P, Nestle FO. The IL-23/Th17 axis in the immunopathogenesis of psoriasis. *J Invest Dermatol* 2009; **129**: 1339-1350
- 11 Pernis AB. Th17 cells in rheumatoid arthritis and systemic lupus erythematosus. *J Intern Med* 2009; **265**: 644-652
- 12 Park H, Li Z, Yang XO, Chang SH, Nurieva R, Wang YH, Wang Y, Hood L, Zhu Z, Tian Q, Dong C. A distinct lineage of CD4 T cells regulates tissue inflammation by producing interleukin 17. *Nat Immunol* 2005; **6**: 1133-1141
- 13 Matsuzaki G, Umemura M. Interleukin-17 as an effector molecule of innate and acquired immunity against infections. *Microbiol Immunol* 2007; **51**: 1139-1147
- 14 Ye P, Rodriguez FH, Kanaly S, Stocking KL, Schurr J, Schwarzenberger P, Oliver P, Huang W, Zhang P, Zhang J, Shellito JE, Bagby GJ, Nelson S, Charrier K, Peschon JJ, Kolls JK. Requirement of interleukin 17 receptor signaling for lung CXC chemokine and granulocyte colony-stimulating factor expression, neutrophil recruitment, and host defense. *J Exp Med* 2001; **194**: 519-527
- 15 Hung LY, Velichko S, Huang F, Thai P, Wu R. Regulation of airway innate and adaptive immune responses: the IL-17 paradigm. *Crit Rev Immunol* 2008; **28**: 269-279
- 16 Zou GM, Tam YK. Cytokines in the generation and maturation of dendritic cells: recent advances. *Eur Cytokine Netw* 2002; **13**: 186-199
- 17 Mills KH. Induction, function and regulation of IL-17-producing T cells. *Eur J Immunol* 2008; **38**: 2636-2649
- 18 Hoyer KK, Dooms H, Barron L, Abbas AK. Interleukin-2 in the development and control of inflammatory disease. *Immunol Rev* 2008; **226**: 19-28
- 19 Kryczek L, Wei S, Gong W, Shu X, Szeliga W, Vatan L, Chen L, Wang G, Zou W. Cutting edge: IFN-gamma enables APC to promote memory Th17 and abate Th1 cell development. *J Immunol* 2008; **181**: 5842-5846
- 20 Langrish CL, McKenzie BS, Wilson NJ, de Waal Malefyt R, Kastelein RA, Cua DJ. IL-12 and IL-23: master regulators of innate and adaptive immunity. *Immunol Rev* 2004; **202**: 96-105
- 21 Parham C, Chirica M, Timans J, Vaisberg E, Travis M, Cheung J, Pflanz S, Zhang R, Singh KP, Vega F, To W, Wagner J, O'Farrell AM, McClanahan T, Zurawski S, Hannum C, Gorman D, Rennick DM, Kastelein RA, de Waal Malefyt R, Moore KW. A receptor for the heterodimeric cytokine IL-23 is composed of IL-12Rbeta1 and a novel cytokine receptor subunit, IL-23R.

- J Immunol* 2002; **168**: 5699-5708
- 22 **Cua DJ**, Sherlock J, Chen Y, Murphy CA, Joyce B, Seymour B, Lucian L, To W, Kwan S, Churakova T, Zurawski S, Wiekowski M, Lira SA, Gorman D, Kastelein RA, Sedgwick JD. Interleukin-23 rather than interleukin-12 is the critical cytokine for autoimmune inflammation of the brain. *Nature* 2003; **421**: 744-748
- 23 **Korn T**, Bettelli E, Oukka M, Kuchroo VK. IL-17 and Th17 Cells. *Annu Rev Immunol* 2009; **27**: 485-517
- 24 **Bettelli E**, Carrier Y, Gao W, Korn T, Strom TB, Oukka M, Weiner HL, Kuchroo VK. Reciprocal developmental pathways for the generation of pathogenic effector TH17 and regulatory T cells. *Nature* 2006; **441**: 235-238
- 25 **Mangan PR**, Harrington LE, O'Quinn DB, Helms WS, Bullard DC, Elson CO, Hatton RD, Wahl SM, Schoeb TR, Weaver CT. Transforming growth factor-beta induces development of the T(H)17 lineage. *Nature* 2006; **441**: 231-234
- 26 **Veldhoen M**, Hocking RJ, Atkins CJ, Locksley RM, Stockinger B. TGFbeta in the context of an inflammatory cytokine milieu supports de novo differentiation of IL-17-producing T cells. *Immunity* 2006; **24**: 179-189
- 27 **Kastelein RA**, Hunter CA, Cua DJ. Discovery and biology of IL-23 and IL-27: related but functionally distinct regulators of inflammation. *Annu Rev Immunol* 2007; **25**: 221-242
- 28 **Yoshida H**, Miyazaki Y. Regulation of immune responses by interleukin-27. *Immunol Rev* 2008; **226**: 234-247
- 29 **Batten M**, Li J, Yi S, Kljavin NM, Danilenko DM, Lucas S, Lee J, de Sauvage FJ, Ghilardi N. Interleukin 27 limits autoimmune encephalomyelitis by suppressing the development of interleukin 17-producing T cells. *Nat Immunol* 2006; **7**: 929-936
- 30 **Stumhofer JS**, Laurence A, Wilson EH, Huang E, Tato CM, Johnson LM, Villarino AV, Huang Q, Yoshimura A, Sehy D, Saris CJ, O'Shea JJ, Hennighausen L, Ernst M, Hunter CA. Interleukin 27 negatively regulates the development of interleukin 17-producing T helper cells during chronic inflammation of the central nervous system. *Nat Immunol* 2006; **7**: 937-945
- 31 **Eberl G**, Littman DR. Thymic origin of intestinal alphabeta T cells revealed by fate mapping of RORgamma τ cells. *Science* 2004; **305**: 248-251
- 32 **Ivanov II**, McKenzie BS, Zhou L, Tadokoro CE, Lepelley A, Lafaille JJ, Cua DJ, Littman DR. The orphan nuclear receptor RORgamma τ directs the differentiation program of proinflammatory IL-17 $^{+}$ T helper cells. *Cell* 2006; **126**: 1121-1133
- 33 **Yang XO**, Pappu BP, Nurieva R, Akimzhanov A, Kang HS, Chung Y, Ma L, Shah B, Panopoulos AD, Schluns KS, Watowich SS, Tian Q, Jetten AM, Dong C. T helper 17 lineage differentiation is programmed by orphan nuclear receptors ROR alpha and ROR gamma. *Immunity* 2008; **28**: 29-39
- 34 **Liu Z**, Geboes K, Heremans H, Overbergh L, Mathieu C, Rutgeerts P, Ceuppens JL. Role of interleukin-12 in the induction of mucosal inflammation and abrogation of regulatory T cell function in chronic experimental colitis. *Eur J Immunol* 2001; **31**: 1550-1560
- 35 **Liu Z**, Jiu J, Liu S, Fa X, Li F, Du Y. Blockage of tumor necrosis factor prevents intestinal mucosal inflammation through down-regulation of interleukin-23 secretion. *J Autoimmun* 2007; **29**: 187-194
- 36 **Niess JH**, Leithäuser F, Adler G, Reimann J. Commensal gut flora drives the expansion of proinflammatory CD4 T cells in the colonic lamina propria under normal and inflammatory conditions. *J Immunol* 2008; **180**: 559-568
- 37 **Ivanov II**, Atarashi K, Manel N, Brodie EL, Shima T, Karaoz U, Wei D, Goldfarb KC, Santee CA, Lynch SV, Tanoue T, Imaoka A, Itoh K, Takeda K, Umesaki Y, Honda K, Littman DR. Induction of intestinal Th17 cells by segmented filamentous bacteria. *Cell* 2009; **139**: 485-498
- 38 **Becker C**, Wirtz S, Blessing M, Pirhonen J, Strand D, Bechthold O, Frick J, Galle PR, Autenrieth I, Neurath MF. Constitutive p40 promoter activation and IL-23 production in the terminal ileum mediated by dendritic cells. *J Clin Invest* 2003; **112**: 693-706
- 39 **Kullberg MC**, Jankovic D, Feng CG, Hue S, Gorelick PL, McKenzie BS, Cua DJ, Powrie F, Cheever AW, Maloy KJ, Sher A. IL-23 plays a key role in Helicobacter hepaticus-induced T cell-dependent colitis. *J Exp Med* 2006; **203**: 2485-2494
- 40 **Yen D**, Cheung J, Scheerens H, Poulet F, McClanahan T, McKenzie B, Kleinschek MA, Owyang A, Mattson J, Blumenschein W, Murphy E, Sathe M, Cua DJ, Kastelein RA, Rennick D. IL-23 is essential for T cell-mediated colitis and promotes inflammation via IL-17 and IL-6. *J Clin Invest* 2006; **116**: 1310-1316
- 41 **Fujino S**, Andoh A, Bamba S, Ogawa A, Hata K, Araki Y, Bamba T, Fujiyama Y. Increased expression of interleukin 17 in inflammatory bowel disease. *Gut* 2003; **52**: 65-70
- 42 **Kobayashi T**, Okamoto S, Hisamatsu T, Kamada N, Chinen H, Saito R, Kitazume MT, Nakazawa A, Sugita A, Koganei K, Isobe K, Hibi T. IL23 differentially regulates the Th1/Th17 balance in ulcerative colitis and Crohn's disease. *Gut* 2008; **57**: 1682-1689
- 43 **Seiderer J**, Elben I, Diegelmann J, Glas J, Stallhofer J, Tillack C, Pfennig S, Jurgens M, Schmeichel S, Konrad A, Goke B, Ochsenkuhn T, Muller-Myhsok B, Lohse P, Brand S. Role of the novel Th17 cytokine IL-17F in inflammatory bowel disease (IBD): upregulated colonic IL-17F expression in active Crohn's disease and analysis of the IL17F p.His161Arg polymorphism in IBD. *Inflamm Bowel Dis* 2008; **14**: 437-445
- 44 **Korn T**, Bettelli E, Gao W, Awasthi A, Jager A, Strom TB, Oukka M, Kuchroo VK. IL-21 initiates an alternative pathway to induce proinflammatory T(H)17 cells. *Nature* 2007; **448**: 484-487
- 45 **Nurieva R**, Yang XO, Martinez G, Zhang Y, Panopoulos AD, Ma L, Schluns K, Tian Q, Watowich SS, Jetten AM, Dong C. Essential autocrine regulation by IL-21 in the generation of inflammatory T cells. *Nature* 2007; **448**: 480-483
- 46 **Liu Z**, Yang L, Cui Y, Wang X, Guo C, Huang Z, Kan Q, Liu Z, Liu Y. IL-21 enhances NK cell activation and cytolytic activity and induces Th17 cell differentiation in inflammatory bowel disease. *Inflamm Bowel Dis* 2009; **15**: 1133-1144
- 47 **Kinugasa T**, Sakaguchi T, Gu X, Reinecker HC. Claudins regulate the intestinal barrier in response to immune mediators. *Gastroenterology* 2000; **118**: 1001-1011
- 48 **Ogawa A**, Andoh A, Araki Y, Bamba T, Fujiyama Y. Neutralization of interleukin-17 aggravates dextran sulfate sodium-induced colitis in mice. *Clin Immunol* 2004; **110**: 55-62
- 49 **Elson CO**, Cong Y, Weaver CT, Schoeb TR, McClanahan TK, Fick RB, Kastelein RA. Monoclonal anti-interleukin 23 reverses active colitis in a T cell-mediated model in mice. *Gastroenterology* 2007; **132**: 2359-2370
- 50 **McGeachy MJ**, Bak-Jensen KS, Chen Y, Tato CM, Blumenschein W, McClanahan T, Cua DJ. TGF-beta and IL-6 drive the production of IL-17 and IL-10 by T cells and restrain T(H)-17 cell-mediated pathology. *Nat Immunol* 2007; **8**: 1390-1397



Role of the receptor for advanced glycation end products in hepatic fibrosis

Christina Lohwasser, Daniel Neureiter, Yury Popov, Michael Bauer, Detlef Schuppan

Christina Lohwasser, Yury Popov, Michael Bauer, Detlef Schuppan, Department of Medicine I, University of Erlangen-Nuremberg, Erlangen-Nürnberg, D-91054, Germany

Daniel Neureiter, Institute of Pathology, Paracelsus Private Medicine University, Salzburg, A-5020, Austria

Yury Popov, Detlef Schuppan, Division of Gastroenterology, Beth Israel Deaconess Medical Center, Harvard Medical School, Boston, MA 02215, United States

Author contributions: Lohwasser C, Bauer M, Popov Y and Neureiter D performed the experiments; Schuppan D designed the study; Lohwasser C, Neureiter D and Schuppan D wrote the manuscript.

Supported by Grants from the Interdisciplinary Center for Clinical Research (IZKF, Project B39) and the Johannes and Frieda Marohn Foundation of the University of Erlangen-Nuremberg, Germany

Correspondence to: Detlef Schuppan, MD, PhD, Division of Gastroenterology, Beth Israel-Deaconess Medical Center and Harvard Medical School, 330 Brookline Avenue, Dana 506, Boston, MA 02215, United States. dschuppa@bidmc.harvard.edu

Telephone: +1-617-6672371 **Fax:** +1-617-6672767

Received: July 25, 2009 **Revised:** October 1, 2009

Accepted: October 8, 2009

Published online: December 14, 2009

RAGE stimulation with AGE-BSA and CML-BSA did not alter HSC proliferation, apoptosis, fibrogenic signal transduction and fibrosis- or fibrolysis-related gene expression, except for marginal upregulation of procollagen α 1(I) mRNA by AGE-BSA.

CONCLUSION: Despite upregulation of RAGE in activated HSC, RAGE stimulation by AGE does not alter their fibrogenic activation. Therefore, RAGE does not contribute directly to hepatic fibrogenesis.

© 2009 The WJG Press and Baishideng. All rights reserved.

Key words: Advanced glycation end product; Extracellular matrix; Hepatic stellate cell; Matrix metalloproteinase; Myofibroblast; Receptor for advanced glycation end products; Transforming growth factor β ; Tissue inhibitor of metalloproteinase; Tumor necrosis factor α

Peer reviewers: Mark D Gorrell, PhD, Professor, Centenary Institute of Cancer Medicine and Cell Biology, Locked bag No. 6, Newtown, NSW 2042, Australia; Devanshi Seth, PhD, Senior Scientist, Centenary Institute & Drug Health Services, RPAH & Clinical Senior Lecturer, Clinical School of Medicine, University of Sydney, Camperdown, NSW 2050, Australia

Lohwasser C, Neureiter D, Popov Y, Bauer M, Schuppan D. Role of the receptor for advanced glycation end products in hepatic fibrosis. *World J Gastroenterol* 2009; 15(46): 5789-5798 Available from: URL: <http://www.wjgnet.com/1007-9327/15/5789.asp> DOI: <http://dx.doi.org/10.3748/wjg.15.5789>

Abstract

AIM: To study the role of advanced glycation end products (AGE) and their specific receptor (RAGE) in the pathogenesis of liver fibrogenesis.

METHODS: *In vitro* RAGE expression and extracellular matrix-related gene expression in both rat and human hepatic stellate cells (HSC) were measured after stimulation with the two RAGE ligands, advanced glycation end product-bovine serum albumin (AGE-BSA) and N^ε-(carboxymethyl) lysine (CML)-BSA, or with tumor necrosis factor- α (TNF- α). *In vivo* RAGE expression was examined in models of hepatic fibrosis induced by bile duct ligation or thioacetamide. The effects of AGE-BSA and CML-BSA on HSC proliferation, signal transduction and profibrogenic gene expression were studied *in vitro*.

RESULTS: In hepatic fibrosis, RAGE expression was enhanced in activated HSC, and also in endothelial cells, inflammatory cells and activated bile duct epithelia. HSC expressed RAGE which was upregulated after stimulation with AGE-BSA, CML-BSA, and TNF- α .

INTRODUCTION

Advanced glycation end products (AGE) are formed *in vitro* and *in vivo* from non-enzymatic glycation of the amino groups of proteins with reducing sugars such as glucose. Although serum levels of AGE are usually low due to constant turnover, they can be detected *in vivo* once levels of reducing sugars are elevated, as occurs in diabetes^[1]. Thus, glycated hemoglobin in the serum of diabetic patients was the first described physiologically relevant AGE^[2]. Interest in AGE has increased since several studies suggested that AGE may be responsible for pathological features associated with diabetes. For example, in endothelial cells, AGE were shown to increase the expression of pro-coagulant activity,

induce expression of vascular cell adhesion molecule-1, and promote nuclear translocation of nuclear factor- κ B (NF- κ B). In mononuclear phagocytes, AGE induce the production of platelet-derived growth factor, increase migration, and drive NF- κ B activation^[3,4].

AGE interact with several receptors, such as the receptor for advanced glycation end products (RAGE), 80K-H phosphoprotein, galectin-3, lactoferrin, scavenger receptors such as SRA or SRB I, and CD36^[5,6]. RAGE, a member of the immunoglobulin superfamily of cell surface receptors, is expressed in a variety of tissues and interacts with several AGE ligands, especially with N^ε-(carboxymethyl) lysine (CML)^[4].

However, while a role for RAGE in the progression of diabetic vasculopathy and kidney failure has been established^[7-9], its role in hepatic fibrosis is poorly understood. This is important due to the emerging epidemic of nonalcoholic steatohepatitis (NASH) related to obesity and the metabolic syndrome, conditions that are associated with increased AGE and RAGE and hepatic fibrosis^[10-12]. RAGE expression has been described in inflammatory cells^[13] and in activated hepatic stellate cells (HSCs)^[14], the major fibrogenic effector cells that can undergo activation to myofibroblasts producing the excess extracellular matrix in hepatic fibrosis^[15]. Many features of this activation process are mimicked by spontaneously occurring activation on tissue culture plastic *in vitro*^[16,17]. While certain cytokines, growth factors and culture conditions and, as recently demonstrated, AGE^[18], can modulate HSC activation and extracellular matrix (ECM) synthesis, the functional contribution of AGE and RAGE expression to fibrogenic activation of HSC and to hepatic fibrosis remains to be elucidated.

We have therefore studied whether physiological AGE concentrations occur in the serum of patients with diabetes^[1,19], and whether AGE-RAGE interactions are involved in the progression of liver fibrosis. To this end we investigated RAGE expression in HSC *in vitro*, and in normal and cirrhotic livers *in vivo*. Furthermore, the effects of AGE and the key proinflammatory cytokine tumor necrosis factor (TNF)- α on HSC RAGE expression and on the proliferation, kinase activation and profibrogenic and fibrolytic gene expression of HSC were determined.

MATERIALS AND METHODS

Synthesis of AGE and CML-modified BSA

For preparation of AGE-modified bovine serum albumin (BSA), 0.6 mmol/L BSA and 0.16 mmol/L D-glucose were dissolved in 20 mL PBS, sterile filtered, incubated for 60 d at 37°C and dialyzed against PBS under sterile conditions to remove unreacted D-glucose. Control BSA was incubated in parallel in the absence of D-glucose. Preparation of CML-modified BSA was carried out as previously described^[20].

Glycation of AGE-BSA and CML-BSA was determined using the 2,4,6-trinitrobenzenesulfonic acid (TNBS) assay^[21], resulting in a 45.6% and 36.5% glycation of lysines for AGE-BSA and CML-BSA, respectively.

After endotoxin removal with the Detoxi-Gel™ (Pierce, Rockford, IL), the final endotoxin concentration determined with the E-toxate® endotoxin detection kit (Sigma, Taufkirchen, Germany) was below 0.04 and 0.02 ng/mL for AGE-BSA and CML-BSA, respectively.

Cell lines

Cell lines were cultured as previously published^[20]. The fully activated rat HSC line HSC-T6 (kind donation of Dr. SL Friedman, NY)^[22], the moderately activated rat HSC line CFSC-2G (kindly provided by Dr. M Rojkind, Washington, D.C.)^[23] and human HSC of passage 3 to 5 (kind gift of Dr. M Pinzani, Florence, Italy)^[24] were maintained as previously described (references see below).

Cell culture and animal experimentation: Animals were treated according to the Council of International Organizations of Medical Sciences for the Care and Use of Laboratory Animals in Research. The experimental protocol was approved by the Animal Care Committee of the University of Erlangen-Nuremberg.

Isolation of rat primary hepatocytes: Hepatocytes were freshly isolated from male Wistar rats (190-200 g, Charles River, Sulzfeld, Germany) according to a modified two-step collagenase perfusion method^[25] as previously described in detail^[26]. Experiments were performed 6 h after plating with cell viabilities $\geq 85\%$ as determined by Trypan Blue exclusion.

Isolation of rat primary hepatic stellate cells: HSC were isolated from male Wistar rats (retired breeders, 400-500 g) as described^[27]. Cell viability was usually between 95%-98%. The purity of HSC was confirmed by their stellate shape, and autofluorescence of the cytoplasmic lipid-droplets at 390 nm. Freshly isolated HSC were activated by culture on plastic in the presence of 10% fetal calf serum (FCS) for 1, 5, and 10 d prior to lysis and RNA extraction. HSC plated for 1 d were designated as quiescent, those cultured for 5 and 10 d as partially and fully activated, respectively.

Experimental liver fibrosis: Experimental liver fibrosis was induced in groups of four adult male Wistar rats weighing about 400 g as follows: (1) bile duct ligation (BDL) for 6 wk, (2) thioacetamide (TAA) treatment, 200 mg/g body weight thrice weekly for 12 wk, as previously published^[27]. Sham-operated rats served as controls. After sacrifice of all animals, pieces of the right and left liver lobes were removed, fixed in 4% formalin and paraffin embedded, or snap frozen in liquid nitrogen for further analysis.

For RNA analysis 150-200 mg of tissue were homogenized in 1 mL RNAPure for 30 s and an aliquot representing 10 mg of tissue was mixed with 900 μ L fresh RNAPure. Morphology of connective tissue was evaluated with hematoxylin-eosin and Sirius Red staining.

Immunohistochemistry: For immunohistochemical analysis specimens from two different liver segments were

studied. Sequential deparaffinized sections were blocked with avidin and biotin. After antigen retrieval in a decloaking chamber for 30 s at 120°C in Target Retrieval Solution, pH 6.0 (Dako), sections were incubated overnight at room temperature with monoclonal antibodies to RAGE (1:30, kindly provided by Dr. B Weigle (Dresden, Germany), CD3 (1:10, Serotec MCA 772), CD45 (1:50, Serotec MCA 43R), CD68 (1:30, Serotec MCA 341R), and α -smooth muscle actin (SMA) (1:30, DAKO M 0851), followed by biotinylated horse anti-mouse IgG and streptavidin-biotin alkaline phosphatase^[28]. Sections were developed using Fast Red and nuclei counterstained with hematoxylin. RAGE was additionally detected with the catalyzed signal amplification system as previously described^[29,20]. For double staining, the slides were treated with a Double Staining Enhancer (Zytomed 50-056) for 30 min before application of the secondary antibody. RAGE antibody was first applied, followed by the other antibodies developed with Fast Red (RAGE) and with Fast Blue. The co-expressions of RAGE and of CD3, CD68 and of α -SMA inside the liver (portal and lobular areas) were counted in ten randomly selected high-power fields (400 \times magnification) using ImageAccess Enterprise 5 software (Imagic Bildverarbeitung, Glattbrugg, Switzerland). The number of immunohistochemically positive cells are given as the percentage of all cells (RAGE) and the respective cell population (CD3, CD68 and of α -SMA) in the studied areas.

SDS-PAGE and Western blotting

Preconfluent (80%) HSC lines, HSC-T6 and CFSC-2G, were seeded at 20 000 cells per well in 24-well plates, washed and incubated with 10–100 μ g/mL BSA, AGE-BSA, or CML-BSA, or with 0–10 ng/mL TNF- α (Sigma) in serum-free medium. Protein extraction and Western blotting were performed as previously described^[20].

Quantitative real time PCR

Total RNA was isolated using peqGOLD RNAPure reagent (PepLab Biotechnologie, Erlangen, Germany) and reverse transcribed, followed by real time RT-PCR using a LightCycler instrument (Roche, Mannheim, Germany), as described in detail elsewhere^[27,30,31], and the TaqMan principle^[32]. Results were normalized to glyceraldehyde-3-phosphate dehydrogenase (GAPDH) or β 2-microglobulin amplified in a parallel reaction. The specific sense and antisense oligonucleotide primers and probes have been published^[31,20].

Cell proliferation

Cell proliferation of CFSC-2G and HSC-T6 cells was determined using BrdU incorporation according to the manufacturer's protocol (Roche, Manheim, Germany) as recently described^[33].

Determination of p44/42 and p38 MAPK activity

These enzyme activities were determined as previously described^[27] using Western Blotting with antibodies to phosphorylated and total ERK1/2 MAPK (Thr202/Tyr204, 1:2000) and anti-phospho-p38 MAPK (Thr180/Tyr182, 1:1000) (from Cell Signaling Technology,

Frankfurt, Germany). Phospho-specific signals were normalized to unphosphorylated kinase signals.

Statistical analysis

Statistical analysis was performed with SPSS v. 16.0 (SPSS GmbH Software, Munich, Germany). Student's *t* test and univariate ANOVA (analysis of variance) was used to test for differences between two and more groups, respectively ($P < 0.05$ was significant). All graphs represent the mean \pm SD and were performed at least in triplicate.

RESULTS

Expression of RAGE by hepatic stellate cells

Freshly isolated rat HSC, and the rat HSC lines HSC-T6 and CFSC-2G, as well as human HSC, expressed significant RAGE transcripts and protein (Figure 1A and B). During culture, activation of freshly isolated rat HSC RAGE transcripts was upregulated 1.6- and 3.8-fold, respectively, on days 5 and 10 of primary culture (Figure 1C). Culture activation of HSC was associated with highly increased expression of procollagen- α 1(I) and α -SMA mRNA which were upregulated $>$ 100-fold and $>$ 50-fold after 5 and 10 d of activation (data not shown).

Upregulation of RAGE mRNA in rat models of cirrhosis

In cirrhotic livers of rats subjected to BDL, RAGE transcripts were upregulated 4-fold as compared to healthy controls ($P < 0.01$), whereas in thioacetamide (TAA)-induced cirrhosis RAGE mRNA expression remained unchanged. Fibrosis-related transcripts such as α -SMA, procollagen- α 1(I), matrix metalloproteinase (MMP)-13, and tissue inhibitor of metalloproteinase (TIMP)-1 mRNA were highly upregulated in both fibrosis models (Table 1).

Immunohistochemistry of normal livers showed a significantly lower expression of RAGE protein compared to the fibrotic/cirrhotic livers ($P < 0.001$, Table 2 and Figure 2A), with predominant expression in portal vein and arterial endothelial cells and sparse expression in lymphocytes and myofibroblasts in the hepatic lobule. Hepatocytes did not express RAGE. In BDL livers RAGE protein was highly expressed in bile duct proliferating epithelia, in periductular α -SMA positive myofibroblasts and in inflammatory cells that were identified as CD3-positive T-lymphocytes and CD68-positive macrophages by use of double staining immunohistochemistry (Table 2, Figure 2A and B). In TAA cirrhosis the number of RAGE-expressing cells was less pronounced than in biliary cirrhosis, in concert with lower RAGE gene expression and fewer inflammatory cell infiltrates, being primarily expressed by macrophages, as opposed to mostly T-lymphocytes and proliferating bile duct epithelia in BDL-cirrhosis (Table 2 and Figure 2B). Only a few α -SMA- and RAGE-positive myofibroblasts were detected in portal areas and septa of both models. The expression of RAGE by endothelial cells in the cirrhotic livers was slightly enhanced in areas of neo-capillarization compared to normal controls (Figure 2A).

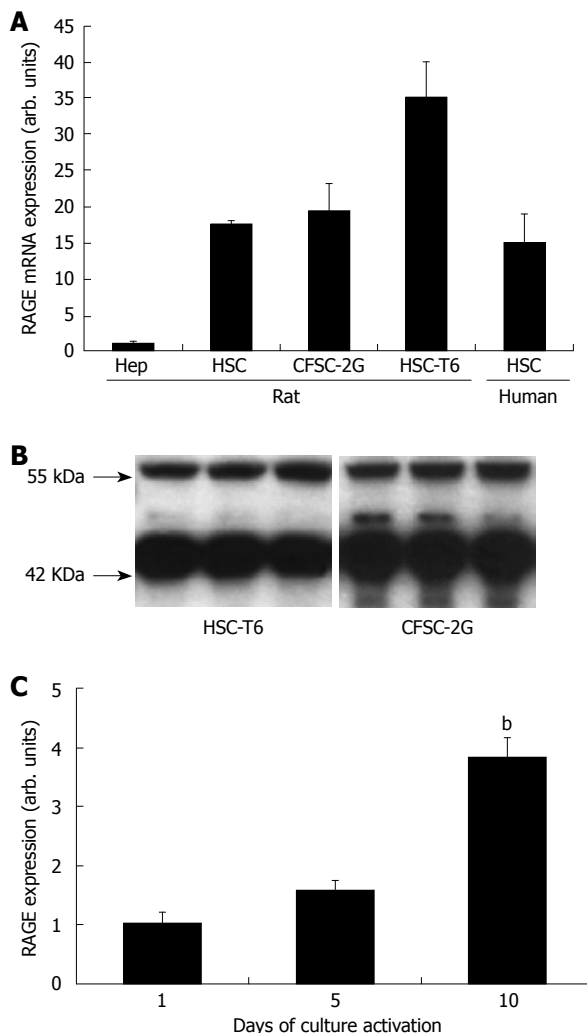


Figure 1 RAGE expression in hepatic stellate cells (A, B) and upregulation of RAGE expression during activation of HSC (C). A: Bars represent RAGE mRNA expression, as determined by real time quantitative PCR relative to GAPDH mRNA, by freshly isolated rat hepatocytes (Hep), 10 d culture-activated primary rat HSC, CFSC-2G and HSC-T6 HSC lines, and human HSC; B: RAGE protein is detected as a 57 kDa band after SDS-PAGE of cell lysates and Western blotting with a monoclonal anti-RAGE IgG. Experiments were repeated at least three times with similar results; C: Freshly isolated rat HSC were culture-activated for 1, 5, and 10 d and RAGE mRNA expression was quantified by real-time PCR. Bars represent mean RAGE expression \pm SD in arbitrary units relative to GAPDH from at least three individual experiments. Values were normalized to 50 ng of extracted RNA transcribed into cDNA. $^bP < 0.01$ vs 1 d activation. RAGE: Receptor for advanced glycation end products; HSC: Hepatic stellate cells; GAPDH: Glyceraldehyde-3-phosphate dehydrogenase.

Regulation of RAGE expression in HSC: induction by AGE and TNF- α

Incubation of CFSC-2G and HSC-T6 HSC with 50 μ g/mL AGE-BSA significantly ($P < 0.001$) upregulated RAGE protein expression by 2-3 fold (Figure 3A). While CFSC-2G cells were more sensitive to AGE-BSA, the highest concentration, 100 μ g/mL, was not effective in either cell line. Addition of 50 μ g/mL CML-BSA increased RAGE protein expression about 2 fold in both cell lines ($P < 0.05$) (Figure 3B).

Similarly, TNF- α upregulated RAGE protein expression significantly ($P < 0.01$) in both CFSC-2G and HSC-T6 HSC (Figure 3C). Again, a greater RAGE induction was

Table 1 Expression of RAGE and ECM-related genes in rats cirrhotic due to BDL and TAA treatment

	Control	BDL	TAA
RAGE	1.00 \pm 0.31	3.89 \pm 0.92 ^b	1.44 \pm 0.47
α -SMA	1.00 \pm 0.49	5.60 \pm 1.59 ^a	10.39 \pm 6.78
Procollagen- α 1(I)	1.00 \pm 0.99	26.45 \pm 3.37 ^d	21.92 \pm 8.48
MMP-13	1.00 \pm 0.38	3.68 \pm 2.50	52.88 \pm 25.34 ^a
TIMP-1	1.00 \pm 0.46	6.50 \pm 1.55 ^b	25.47 \pm 15.02

RAGE, α -SMA, procollagen- α 1(I), MMP-13, and TIMP-1 transcript levels relative to β 2-microglobulin \pm SD of four animals per group. Data are expressed as n-fold increase compared to sham-operated and normal rats, respectively. $^aP < 0.05$, $^bP < 0.01$, $^dP < 0.001$ vs normal controls. RAGE: Receptor for advanced glycation end products; ECM: Extracellular matrix; BDL: Bile duct ligation; TAA: Thioacetamide; SMA: Smooth muscle actin; MMP: Matrix metalloproteinase; TIMP: Tissue inhibitor of metalloproteinase.

Table 2 Cell-specific expression of RAGE as determined by immunohistochemistry

	RAGE	CD3	CD68	α -SMA
Normal liver				
P	2.8 \pm 0.7 ¹	3.3 \pm 0.7	0.3 \pm 0.5	0.8 \pm 0.7 ²
L	1.0 \pm 0.7	1.5 \pm 0.6	0.7 \pm 0.6	0.2 \pm 0.4
BDL				
P	11.1 \pm 1.5 ³	13.8 \pm 1.2	15.2 \pm 1.7	8.1 \pm 1.2 ⁴
L	8.1 \pm 1.7	13.2 \pm 1.9	13.8 \pm 1.6	4.8 \pm 1.0
TAA				
P	7.3 \pm 1.9	8.4 \pm 1.1	8.5 \pm 1.1	6.8 \pm 1.2 ⁵
L	5.7 \pm 1.0	6.6 \pm 1.1	6.0 \pm 1.1	1.9 \pm 0.7

Quantitative analysis of the immunohistochemical co-expression of RAGE with CD3, CD68 and α -SMA in normal controls and livers with cirrhosis due to BDL or TAA-intoxication using double staining immunohistochemistry and image analysis. Mean of cells [%] (\pm SD) per 10 high power fields. Quantitative assessment as described in material and methods. ¹Mainly endothelial cells in the portal areas; ²Vascular smooth muscle cells, subset of activated HSC; ³Focally highly expressed by proliferating bile duct epithelia; ⁴Mainly around proliferating bile ducts; ⁵Mainly at the portal interface and septa. P: Portal; L: Lobular.

observed in CFSC-2G cells, where 0.1 ng/mL TNF- α resulted in a nearly 3-fold ($P < 0.001$) upregulation of RAGE expression.

AGE do not modulate extracellular matrix-related gene expression in HSC

Incubation of CFSC-2G HSC with 50 g/mL AGE-BSA or CML-BSA did not significantly modify transcript levels of transforming growth factor (TGF)- β 1, α -SMA, and MMP-13, or RAGE itself, except for a marginal (23%, $P < 0.05$) but reproducible upregulation of procollagen- α 1(I) mRNA by AGE-BSA (Table 3). These results could be confirmed in HSC-T6 and human HSC (data not shown).

AGE do not modify hepatic stellate cell proliferation or p42/44 and p38 MAPK activation

CFSC-2G and HSC-T6 cells were exposed to 1-1000 μ g/mL AGE-BSA for 24 h, and DNA synthesis was assessed by BrdU incorporation. As opposed to the mitogen FCS, AGE-BSA did not induce DNA synthesis

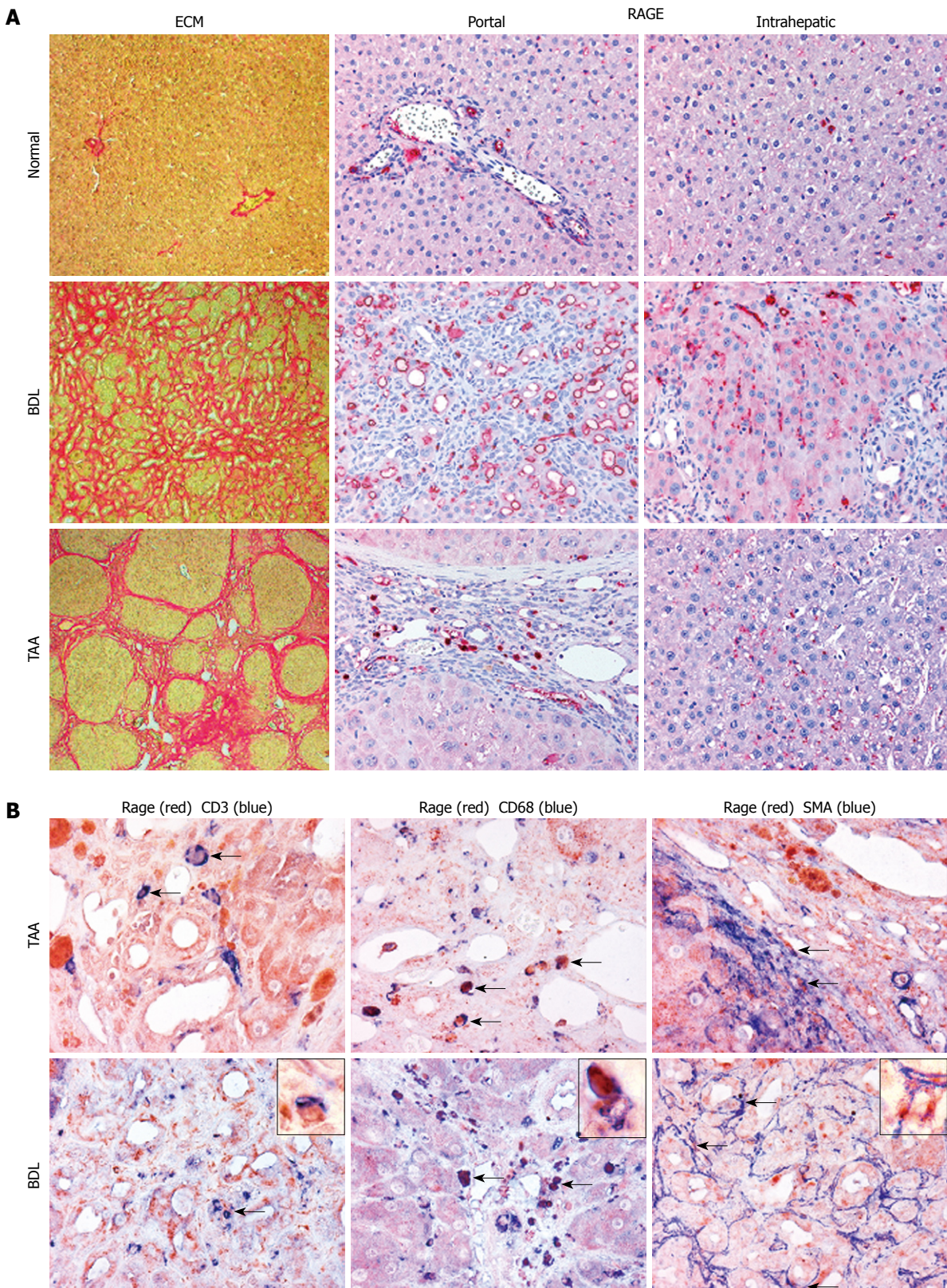


Figure 2 Cell-specific expression patterns of RAGE in normal and cirrhotic rat livers. A: Portal and lobular expression patterns of RAGE in normal liver and in livers of rats with cirrhosis due to BDL or TAA treatment (magnification, $\times 200$). Parallel sections were stained for collagen with picrosirius red. In normal liver, minor RAGE expression was found in endothelial cells of portal veins and arteries, in bile duct epithelia as well as in lymphocytes, macrophages and (myo-) fibroblasts in the hepatic lobular areas. No RAGE expression was found in hepatocytes. RAGE was clearly upregulated in cirrhosis induced by BDL and TAA, with higher numbers of RAGE-expressing cells in BDL, mainly attributable to a prominent contribution by proliferating bile duct epithelial cells. In areas of lobular fibrosis, perisinusoidal endothelia started to express RAGE, apparently in parallel with sinusoidal capillarization; B: Double labeling immunohistochemistry for RAGE (in red) in combination with CD3 (T-lymphocytes), CD68 (macrophages), and α -SMA (myofibroblasts) (in blue), magnification $\times 400$ being exemplarily highlighted with insets (magnification, $\times 1000$). In both cirrhosis models, mainly CD3-positive T-lymphocytes and CD68-positive macrophages expressed RAGE, independently of their microanatomic locations (portal, interface, septal or intrahepatic). Additionally, RAGE was more colocalized with macrophages than with T-lymphocytes independent of the cirrhosis model. RAGE expression was also found on α -SMA-positive myofibroblasts, either localized around periportal bile duct proliferations in BDL or in the interface and septal area in TAA-induced cirrhosis (co-localization indicated by arrows). BDL: Bile duct ligation; TAA: Thioacetamide; SMA: Smooth muscle actin; ECM: Extracellular matrix.

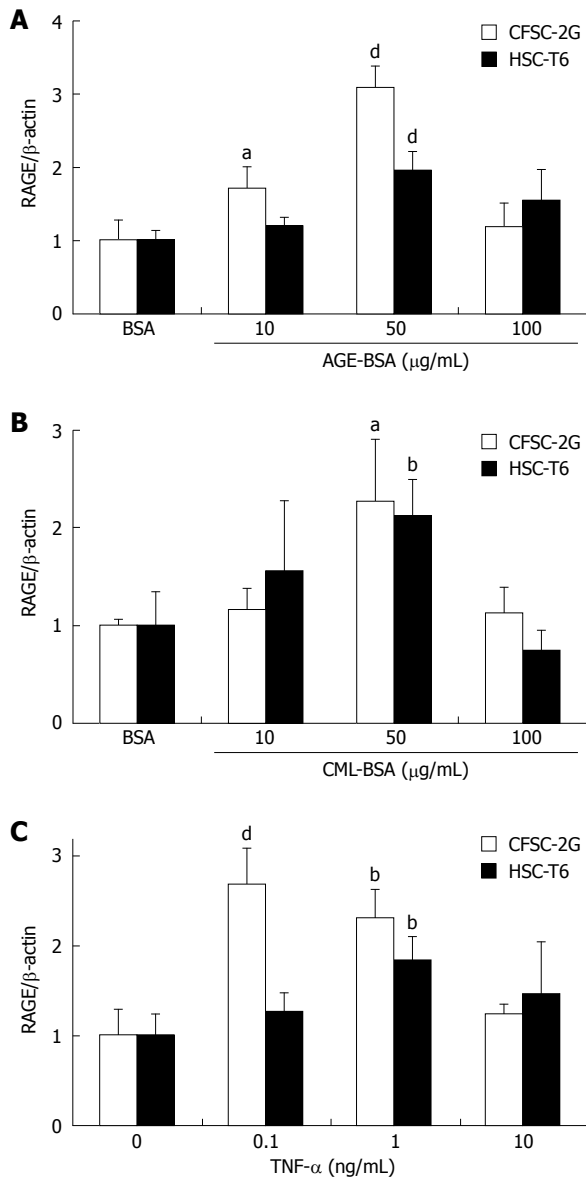


Figure 3 Advanced glycation end product-bovine serum albumin (AGE-BSA) (A), N^c(carboxymethyl) lysine (CML)-BSA (B) and tumor necrosis factor (TNF)- α (C) upregulate RAGE protein expression in hepatic stellate cells. Mean RAGE protein expression as determined by quantitative Western blotting from extracts of rat HSC lines relative to β -actin. Cells were incubated for 24 h and results are derived from at least three independent experiments and expressed as mean \pm SD. Data are shown as x-fold increase compared to cells incubated with BSA alone. ^a $P < 0.05$, ^b $P < 0.01$, ^d $P < 0.001$ vs BSA.

in these cells (Figure 4). In addition, cell numbers remained unchanged after addition of AGE-BSA (data not shown). In line with the proliferation data, AGE-BSA did not induce p44/42 (Figure 5A) or p38 (Figure 5B) MAPK activation when compared to 10% FCS as positive control.

DISCUSSION

Our findings show that RAGE, a prominent receptor for AGE, is expressed in hepatic stellate cells (HSC) derived from various species. Our data are in line with previous studies showing the RAGE upregulation in single culture-activated HSC either of rat or human origin^[14,18].

Table 3 Expression of RAGE and ECM-related genes after incubation of HSC with AGE

	BSA	AGE-BSA	CML-BSA
RAGE	1.00 \pm 0.14	1.20 \pm 0.11	1.26 \pm 0.07
TGF- β 1	1.00 \pm 0.06	1.12 \pm 0.21	0.99 \pm 0.07
Procollagen- α 1(I)	1.00 \pm 0.08	1.23 \pm 0.06 ^a	1.12 \pm 0.19
α -SMA	1.00 \pm 0.14	1.20 \pm 0.20	1.16 \pm 0.04
MMP-13	1.00 \pm 0.05	1.09 \pm 0.14	0.97 \pm 0.09

CFSC-2G HSC were incubated with 50 μ g/mL BSA, AGE-BSA, or CML-BSA for 24 h. RAGE, TGF- β 1, procollagen- α 1(I), α -SMA, and MMP-13 transcript levels are expressed relative to GAPDH and as n-fold increase compared to cells treated with BSA alone (means \pm SD of at least three individual experiments). ^a $P < 0.05$ vs BSA. ECM: Extracellular matrix; HSC: Hepatic stellate cells; AGE: Advanced glycation end product; BSA: Bovine serum albumin; CML: N^c-(carboxymethyl) lysine; TGF: Transforming growth factor.

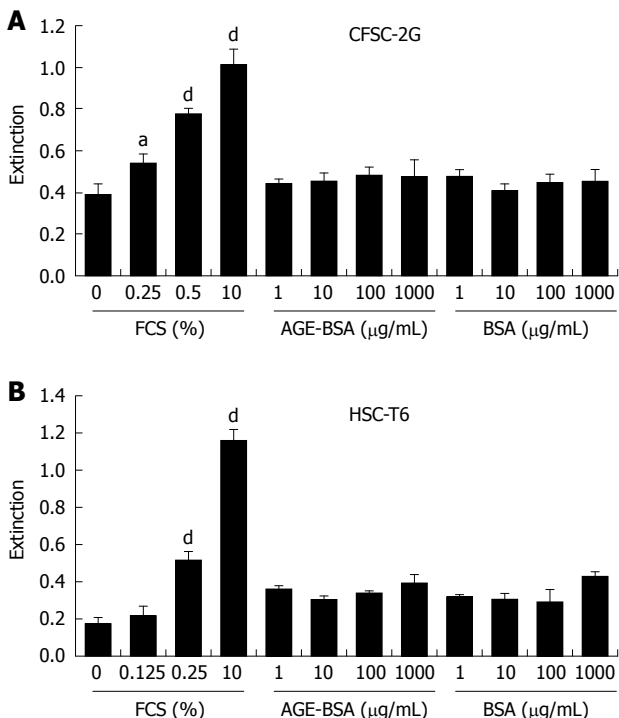


Figure 4 AGE do not stimulate DNA synthesis in hepatic stellate cells. DNA synthesis as a surrogate of proliferation was determined in CFSC-2G (A) and HSC-T6 (B) HSC after a 24 h incubation with increasing concentrations of FCS, AGE-BSA or CML-BSA in 0% FCS. Data are results of six independent experiments and expressed as mean \pm SD. ^a $P < 0.05$, ^d $P < 0.001$ vs 0% FCS.

Using different experimental hepatic fibrosis models in rats we found that transcript levels of RAGE correlate well with RAGE protein expression in agreement with our immunohistochemical co-localization studies. Compared with earlier studies of RAGE expression in other organs^[4], we could detect RAGE not only in myofibroblasts (HSC) and endothelial cells, but also in lymphocytes, macrophages/small Kupffer cells and proliferating bile duct epithelial cells. These results are in contrast to prior studies that either identified RAGE expression in bovine hepatocytes *in vivo*^[54], or exclusively in HSC and myofibroblasts, but not in hepatocytes, sinusoidal endothelial or Kupffer cells^[14]. The reasons for these discrepancies may be the use of different

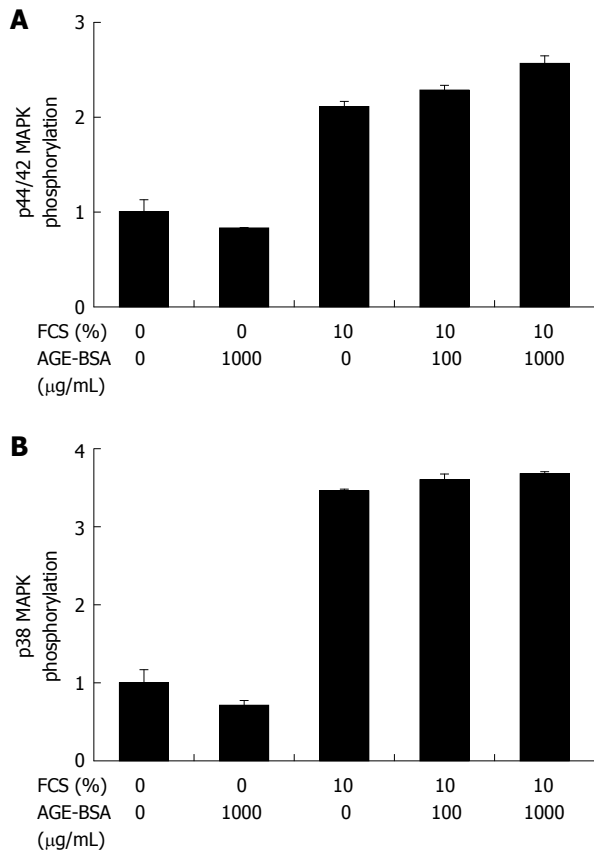


Figure 5 AGE-BSA does not activate p44/42 (A) and p38 (B) MAPK signaling in hepatic stellate cells. Kinase phosphorylation was determined in CFSC-2G and HSC-T6 HSC using quantitative western blotting with phosphospecific antibodies relative to total kinase antibodies after a 10 min incubation with increasing concentrations of AGE-BSA or CML-BSA in 0% to 10% FCS. Bars represent n-fold phosphorylation compared to controls with 0% FCS and results are derived from at least three individual experiments.

antibody reagents with different specificities. We used an antibody that has been characterized thoroughly and found to react specifically with cells on tissue sections^[28]. In addition, we could partly confirm our *in vivo* data with our *in vitro* studies using various types of HSC.

During culture-activation of HSC, RAGE expression was increased significantly. This increase was paralleled by the known upregulation of major transcripts related to fibrosis progression, i.e. TGF- β 1, the most prominent profibrogenic cytokine; procollagen α 1(I), a precursor of the major fibrillar collagen; TIMP-1, the central inhibitor of matrix metalloproteinases (MMP); and α -SMA, a marker for HSC activation^[16,17].

Enhanced RAGE expression in hepatic fibrogenesis was further shown in rats with cirrhosis induced by BDL and TAA treatment, which was in line with prior findings in CCl₄-induced hepatic fibrosis where RAGE transcript and protein levels were upregulated until 6 wk after the completion of CCl₄ treatment^[35]. Differences in RAGE expression may be due to the lack of inflammation in TAA-treated animals, since TAA treatment was stopped one week prior to tissue removal. Progressive injury, however, was still present in bile duct-ligated animals at the time of sacrifice, with enhanced numbers of CD68-positive macrophages/small Kupffer cells and CD3-

positive T-lymphocytes as compared to the TAA-cirrhosis model. Furthermore, we showed that α -SMA-positive HSC/myofibroblasts of the septal or portal interface, representing the prominent fibrogenic effectors, expressed RAGE in both fibrosis models.

In studies of diabetes-associated cardiovascular and renal disease, an upregulation of RAGE has been linked to enhanced levels of AGE^[7,9], in association with epithelial-myofibroblast transdifferentiation^[36] and induction of fibrogenesis^[37-39]. Additionally, inhibition of the interaction of AGE-RAGE with neutralizing monoclonal anti-RAGE antibodies or the AGE cross-link disrupting agent ALT-711 prevented pathological effects of hyperglycemia in blood vessels and kidneys^[8,40].

Our results show that AGE-BSA, as well as the specific RAGE ligand CML-BSA, upregulated the expression of the receptor itself in HSC. This phenomenon was reported previously in human vascular and umbilical vein endothelial cells^[41], where 50 μ g/mL AGE-BSA induced a 2- and 2.5-fold increased RAGE protein expression, respectively, compared to untreated cells. Other studies showed that certain vascular domains, renal glomeruli or intima media and adventitia of the aorta exhibit increased RAGE expression^[42] and that interactions of AGE with RAGE resulted in autoinduction of RAGE expression^[43]. Our observed reduction of response using higher concentrations of AGE-BSA could reflect receptor saturation, downregulation, or an antagonist effect on RAGE expression.

Addition of the proinflammatory cytokine TNF- α to HSC upregulated RAGE protein and mRNA expression up to 3-fold, in accordance with previous studies showing that RAGE is upregulated in inflamed tissues^[44]. Interestingly, the blockade of RAGE by murine-soluble RAGE as decoy could decrease acetaminophen-induced hepatotoxicity^[45] and liver injury in an ischemia and reperfusion model in mice^[46]. Furthermore, an approximately 2-fold increase of RAGE protein expression after incubation of human microvascular endothelial cells with up to 100 ng/mL TNF- α has been reported^[41]. In the present study, however, RAGE expression peaked at 0.1 and 1 ng/mL TNF- α and decreased to baseline levels at 10 ng/mL TNF- α , apparently due to receptor downregulation at high concentrations and this indicated a greater sensitivity of HSC than that of human microvascular endothelial cells to TNF- α . Increased RAGE expression under inflammatory conditions, such as those triggered by TNF- α , may result in enhanced binding of AGEs to RAGE, further increasing RAGE expression and expression of proinflammatory cytokines. This could be relevant for patients with insulin resistance, overt diabetes, and obesity, who frequently present with hepatic inflammation and fibrosis, i.e. patients with NASH.

The upregulated RAGE expression in HSC may lead to the conclusion that AGE-RAGE interactions play a role in hepatic fibrogenesis. However, in contrast to upregulation of RAGE by AGE/CML-AGE and TNF- α , we clearly showed that AGE-BSA and CML-BSA were unable to induce expression of fibrosis or

fibrolysis-related genes in CFSC-2G or HSC-T6 HSC. Using another experimental approach Xia *et al*^[35] showed that targeting of RAGE by specific siRNA downregulated fibrogenesis-related transcripts *in vitro* and *in vivo*. Of note, we took great care to synthesize AGE-BSA and CML-BSA in a sterile environment and to remove any remaining endotoxin contamination in the products. Possible discrepancies between previously published cellular effects of AGE and the present lack of induction may be explained by the presence of endotoxin in previously synthesized AGE preparations.

Another pathogenic feature of HSC activation, besides migration, apoptosis, ECM synthesis, or contractility, is increased proliferation^[47]. According to our experimental setup, we can conclude that AGE do not alter hepatic fibrogenesis through induction of HSC proliferation.

Previous studies of endothelial cells and monocytes, especially mononuclear phagocyte-derived dendritic cells of the liver after massive liver injury^[13], showed that interactions of AGE with RAGE induce, besides RAGE, the expression of proinflammatory cytokines, such as TNF- α and interleukin-1 and -6^[41]. These events are mediated by activation of redox-sensitive signaling pathways involving NADPH oxidase, or mitogenic pathways involving the small G-protein Ras that lead to activation of mitogen-activated protein kinases (MAPK), or involving nuclear factor- κ B (NF- κ B). Since no data on AGE-induced MAPK activation in HSCs exist, we aimed to investigate whether RAGE upregulation by AGE may be due to stimulation of MAPK signal transduction pathways. We could not find any stimulatory effect of endotoxin-free AGE-BSA or CML-BSA on activation of p44/42 MAPK, which mediates cellular growth and differentiation, and p38 MAPK, which regulates cytokine expression and controls cellular responses to cytokines and stress. Again, this contrasts with previous reports showing that interaction of AGE with RAGE induced intracellular signaling pathways involved in inflammatory responses including MAPK or NF- κ B activation^[48]. Moreover, downregulation of RAGE by specific siRNAs was associated with NF- κ B degradation supporting the linkage of RAGE to the NF- κ B pathway^[35]. Only a single study indicated that AGE may not uniformly play a role in cellular activation^[49].

In summary, the present data do not support a direct role of AGE and AGE-RAGE axis in the fibrogenic activation of HSC, such as profibrogenic ECM-related gene expression, signal transduction, or proliferation. However, the finding that RAGE in HSC is upregulated during their activation *in vitro* and in HSC/myofibroblasts, macrophages/small Kupffer cells, endothelia of neocapillarization and proliferating bile duct epithelia during fibrogenesis *in vivo* does not exclude the possibility that RAGE may drive fibrogenesis indirectly, e.g. *via* soluble factors that are released from these non-HSC cell types. This could still have relevance for patients with insulin resistance and NASH who display elevated serum and tissue levels of AGE^[1,50]. Whether the observed RAGE upregulation may contribute to fibrosis *via* these indirect pathways needs to be investigated in further studies using

either co-culture experiments, gene modified animals, or the administration of AGEs to animals with experimental liver fibrosis.

ACKNOWLEDGMENTS

We thank Christa Winkelmann, Gisela Weber, and Kunigunde Herbig (Department of Pathology, University of Erlangen-Nuremberg, Germany) for their expert technical assistance. The anti-RAGE IgG was kindly donated by Dr. B Weigle, Medical University of Graz, Austria, and the human hepatic stellate cells by Dr. M Pinzani, University of Florence, Italy. In addition, we thank Monika Pischetsrieder (Institute of Pharmacy and Food Chemistry, University of Erlangen-Nuremberg, Germany) for contributing to the concept of this study and fruitful discussion of the results.

COMMENTS

Background

Advanced glycation end products (AGE) and their specific receptor (RAGE) play an important role in the pathogenesis of inflammation and fibrosis in diabetes mellitus. While RAGE has been detected in numerous tissues, its role in organs such as the liver which are also exposed to (circulating) AGE remains largely unexplored.

Research frontiers

The study of liver fibrosis is a challenging research area due to the enormous socio-epidemiologic and medical-therapeutic impact of chronic liver diseases which frequently progress to cirrhosis. We have made tremendous progress in our understanding of the pathomechanisms underlying liver fibrosis progression, including the structural components of the hepatic scar tissue (extracellular matrix), the molecules that are central to its excess deposition and to its removal, and the direct and indirect effector cells that drive fibrosis progression, i.e. fibrogenesis (Friedman, Gastro 08; Schuppan and Afdhal, Lancet 08). Recent studies suggested an association of an activated AGE-RAGE-axis with fibrogenesis, but clear functional data were lacking.

Innovations and breakthroughs

The findings suggest a more indirect than direct effect of the AGE-RAGE-axis on liver fibrogenesis and rule out a direct effect of AGE on the fibrogenic effector cells, i.e. hepatic stellate cells.

Applications

Future applications depend on additional studies that would explore the putative indirect effects of RAGE on fibrogenesis, e.g. *via* cytokines produced by AGE-activated macrophages, biliary duct epithelia or endothelial cells. This could facilitate the development of specific AGE-RAGE-inhibitors that could generate a novel class of therapeutics, especially in conditions where AGE play a prominent role, such as non-alcoholic fatty liver disease.

Terminology

AGE are formed *in vitro* and *in vivo* from non-enzymatic glycation of the amino groups of proteins with reducing sugars such as glucose. AGE can be detected *in vivo* once levels of reducing sugars are elevated as occurs in diabetes. AGE interact with several receptors, most specifically with the receptor for advanced glycation end products (RAGE). RAGE is a member of the immunoglobulin superfamily of cell surface receptors which are expressed in a variety of tissues.

Peer review

The originality of this study resides in the broad and exhaustive study of RAGE expression in two well-defined and complementary rodent models of liver fibrosis, the use of different cells and cell lines, and extensive *in vitro* stimulation studies of hepatic stellate cells with AGE to assess their effect on the expression of extracellular matrix component and matrix dissolving metalloproteinases. This broad approach is novel and has for the first time provided clear results as to the effect of stimulation of the AGE-RAGE axis in hepatic stellate cells and the putative fibrogenic role it plays in fibrogenic activation of macrophages/Kupffer cells, endothelia or biliary duct epithelia.

REFERENCES

- 1 Schmidt AM, Yan SD, Stern DM. The dark side of glucose. *Nat Med* 1995; **1**: 1002-1004
- 2 Rahbar S, Blumenfeld O, Ranney HM. Studies of an unusual hemoglobin in patients with diabetes mellitus. *Biochem Biophys Res Commun* 1969; **36**: 838-843
- 3 Kirsstein M, Brett J, Radoff S, Ogawa S, Stern D, Vlassara H. Advanced protein glycosylation induces transendothelial human monocyte chemotaxis and secretion of platelet-derived growth factor: role in vascular disease of diabetes and aging. *Proc Natl Acad Sci USA* 1990; **87**: 9010-9014
- 4 Kislinger T, Fu C, Huber B, Qu W, Taguchi A, Du Yan S, Hofmann M, Yan SF, Pischetsrieder M, Stern D, Schmidt AM. N(epsilon)-(carboxymethyl)lysine adducts of proteins are ligands for receptor for advanced glycation end products that activate cell signaling pathways and modulate gene expression. *J Biol Chem* 1999; **274**: 31740-31749
- 5 Horiuchi S, Sakamoto Y, Sakai M. Scavenger receptors for oxidized and glycated proteins. *Amino Acids* 2003; **25**: 283-292
- 6 Iacobini C, Amadio L, Oddi G, Ricci C, Barsotti P, Missori S, Sorcini M, Di Mario U, Pricci F, Pugliese G. Role of galectin-3 in diabetic nephropathy. *J Am Soc Nephrol* 2003; **14**: S264-S270
- 7 Jerums G, Panagiotopoulos S, Forbes J, Osicka T, Cooper M. Evolving concepts in advanced glycation, diabetic nephropathy, and diabetic vascular disease. *Arch Biochem Biophys* 2003; **419**: 55-62
- 8 Forbes JM, Thallas V, Thomas MC, Founds HW, Burns WC, Jerums G, Cooper ME. The breakdown of preexisting advanced glycation end products is associated with reduced renal fibrosis in experimental diabetes. *FASEB J* 2003; **17**: 1762-1764
- 9 Bohlender JM, Franke S, Stein G, Wolf G. Advanced glycation end products and the kidney. *Am J Physiol Renal Physiol* 2005; **289**: F645-F659
- 10 Neuschwander-Tetri BA, Caldwell SH. Nonalcoholic steatohepatitis: summary of an AASLD Single Topic Conference. *Hepatology* 2003; **37**: 1202-1219
- 11 Wanless IR, Shiota K. The pathogenesis of nonalcoholic steatohepatitis and other fatty liver diseases: a four-step model including the role of lipid release and hepatic venular obstruction in the progression to cirrhosis. *Semin Liver Dis* 2004; **24**: 99-106
- 12 Sanyal AJ, Campbell-Sargent C, Mirshahi F, Rizzo WB, Contos MJ, Sterling RK, Luketic VA, Schiffman ML, Clore JN. Nonalcoholic steatohepatitis: association of insulin resistance and mitochondrial abnormalities. *Gastroenterology* 2001; **120**: 1183-1192
- 13 Cataldegirmen G, Zeng S, Feirt N, Ippagunta N, Dun H, Qu W, Lu Y, Rong LL, Hofmann MA, Kislinger T, Pachydaki SI, Jenkins DG, Weinberg A, Lefkowitch J, Rogiers X, Yan SF, Schmidt AM, Emond JC. RAGE limits regeneration after massive liver injury by coordinated suppression of TNF-alpha and NF-kappaB. *J Exp Med* 2005; **201**: 473-484
- 14 Fehrenbach H, Weiskirchen R, Kasper M, Gressner AM. Upregulated expression of the receptor for advanced glycation end products in cultured rat hepatic stellate cells during transdifferentiation to myofibroblasts. *Hepatology* 2001; **34**: 943-952
- 15 Bataller R, Brenner DA. Liver fibrosis. *J Clin Invest* 2005; **115**: 209-218
- 16 Friedman SL. Mechanisms of hepatic fibrogenesis. *Gastroenterology* 2008; **134**: 1655-1669
- 17 Schuppan D, Afdhal NH. Liver cirrhosis. *Lancet* 2008; **371**: 838-851
- 18 Iwamoto K, Kanno K, Hyogo H, Yamagishi S, Takeuchi M, Tazuma S, Chayama K. Advanced glycation end products enhance the proliferation and activation of hepatic stellate cells. *J Gastroenterol* 2008; **43**: 298-304
- 19 Jakus V, Rietbrock N. Advanced glycation end-products and the progress of diabetic vascular complications. *Physiol Res* 2004; **53**: 131-142
- 20 Lohwasser C, Neureiter D, Weigle B, Kirchner T, Schuppan D. The receptor for advanced glycation end products is highly expressed in the skin and upregulated by advanced glycation end products and tumor necrosis factor-alpha. *J Invest Dermatol* 2006; **126**: 291-299
- 21 Fields R. The rapid determination of amino groups with TNBS. *Methods in Enzymology* 1972; **25**: 464-468
- 22 Vogel S, Piantedosi R, Frank J, Lazar A, Rockey DC, Friedman SL, Blaner WS. An immortalized rat liver stellate cell line (HSC-T6): a new cell model for the study of retinoid metabolism in vitro. *J Lipid Res* 2000; **41**: 882-893
- 23 Rojkind M, Novikoff PM, Greenwel P, Rubin J, Rojas-Valencia L, de Carvalho AC, Stockert R, Spray D, Hertzberg EL, Wolkoff AW. Characterization and functional studies on rat liver fat-storing cell line and freshly isolated hepatocyte coculture system. *Am J Pathol* 1995; **146**: 1508-1520
- 24 Casini A, Pinzani M, Milani S, Grappone C, Galli G, Jezequel AM, Schuppan D, Rotella CM, Surrenti C. Regulation of extracellular matrix synthesis by transforming growth factor beta 1 in human fat-storing cells. *Gastroenterology* 1993; **105**: 245-253
- 25 Seglen PO. Hepatocyte suspensions and cultures as tools in experimental carcinogenesis. *J Toxicol Environ Health* 1979; **5**: 551-560
- 26 Dan Z, Popov Y, Patsenker E, Preimel D, Liu C, Wang XD, Seitz HK, Schuppan D, Stickel F. Hepatotoxicity of alcohol-induced polar retinol metabolites involves apoptosis via loss of mitochondrial membrane potential. *FASEB J* 2005; **19**: 845-847
- 27 Popov Y, Patsenker E, Bauer M, Niedobitek E, Schulze-Krebs A, Schuppan D. Halofuginone induces matrix metalloproteinases in rat hepatic stellate cells via activation of p38 and NF kappaB. *J Biol Chem* 2006; **281**: 15090-15098
- 28 Srikrishna G, Huttunen HJ, Johansson L, Weigle B, Yamaguchi Y, Rauvala H, Freeze HH. N-Glycans on the receptor for advanced glycation end products influence amphotericin binding and neurite outgrowth. *J Neurochem* 2002; **80**: 998-1008
- 29 van Gijlswijk RP, Wiegant J, Raap AK, Tanke HJ. Improved localization of fluorescent tyramides for fluorescence in situ hybridization using dextran sulfate and polyvinyl alcohol. *J Histochem Cytochem* 1996; **44**: 389-392
- 30 Benten D, Kumaran V, Joseph B, Schattenberg J, Popov Y, Schuppan D, Gupta S. Hepatocyte transplantation activates hepatic stellate cells with beneficial modulation of cell engraftment in the rat. *Hepatology* 2005; **42**: 1072-1081
- 31 Popov Y, Patsenker E, Fickert P, Trauner M, Schuppan D. Mdr2 (Abcb4)-/- mice spontaneously develop severe biliary fibrosis via massive dysregulation of pro- and antifibrogenic genes. *J Hepatol* 2005; **43**: 1045-1054
- 32 Dötsch J, Hogen N, Nyúl Z, Hänze J, Knerr I, Kirschbaum M, Rascher W. Increase of endothelial nitric oxide synthase and endothelin-1 mRNA expression in human placenta during gestation. *Eur J Obstet Gynecol Reprod Biol* 2001; **97**: 163-167
- 33 Patsenker E, Popov Y, Wiesner M, Goodman SL, Schuppan D. Pharmacological inhibition of the vitronectin receptor abrogates PDGF-BB-induced hepatic stellate cell migration and activation in vitro. *J Hepatol* 2007; **46**: 878-887
- 34 Brett J, Schmidt AM, Yan SD, Zou YS, Weidman E, Pinsky D, Nowyngrod R, Neper M, Przysiecki C, Shaw A. Survey of the distribution of a newly characterized receptor for advanced glycation end products in tissues. *Am J Pathol* 1993; **143**: 1699-1712
- 35 Xia JR, Liu NF, Zhu NX. Specific siRNA Targeting the Receptor for Advanced Glycation End Products Inhibits Experimental Hepatic Fibrosis in Rats. *Int J Mol Sci* 2008; **9**: 638-661
- 36 Oldfield MD, Bach LA, Forbes JM, Nikolic-Paterson D, McRobert A, Thallas V, Atkins RC, Osicka T, Jerums G, Cooper ME. Advanced glycation end products cause

- epithelial-myofibroblast transdifferentiation via the receptor for advanced glycation end products (RAGE). *J Clin Invest* 2001; **108**: 1853-1863
- 37 **Twigg SM**, Chen MM, Joly AH, Chakrapani SD, Tsubaki J, Kim HS, Oh Y, Rosenfeld RG. Advanced glycosylation end products up-regulate connective tissue growth factor (insulin-like growth factor-binding protein-related protein 2) in human fibroblasts: a potential mechanism for expansion of extracellular matrix in diabetes mellitus. *Endocrinology* 2001; **142**: 1760-1769
- 38 **Nakamura S**, Niwa T. Advanced glycation end-products and peritoneal sclerosis. *Semin Nephrol* 2004; **24**: 502-505
- 39 **Huang JS**, Guh JY, Chen HC, Hung WC, Lai YH, Chuang LY. Role of receptor for advanced glycation end-product (RAGE) and the JAK/STAT-signaling pathway in AGE-induced collagen production in NRK-49F cells. *J Cell Biochem* 2001; **81**: 102-113
- 40 **De Vriesse AS**, Flyvbjerg A, Mortier S, Tilton RG, Lameire NH. Inhibition of the interaction of AGE-RAGE prevents hyperglycemia-induced fibrosis of the peritoneal membrane. *J Am Soc Nephrol* 2003; **14**: 2109-2118
- 41 **Tanaka N**, Yonekura H, Yamagishi S, Fujimori H, Yamamoto Y, Yamamoto H. The receptor for advanced glycation end products is induced by the glycation products themselves and tumor necrosis factor-alpha through nuclear factor-kappa B, and by 17beta-estradiol through Sp-1 in human vascular endothelial cells. *J Biol Chem* 2000; **275**: 25781-25790
- 42 **Soulis T**, Thallas V, Youssef S, Gilbert RE, McWilliam BG, Murray-McIntosh RP, Cooper ME. Advanced glycation end products and their receptors co-localise in rat organs susceptible to diabetic microvascular injury. *Diabetologia* 1997; **40**: 619-628
- 43 **Schmidt AM**, Yan SD, Wautier JL, Stern D. Activation of receptor for advanced glycation end products: a mechanism for chronic vascular dysfunction in diabetic vasculopathy and atherosclerosis. *Circ Res* 1999; **84**: 489-497
- 44 **Cipollone F**, Iezzi A, Fazio M, Zucchelli M, Pini B, Cuccurullo C, De Cesare D, De Blasis G, Muraro R, Bei R, Chiarelli F, Schmidt AM, Cuccurullo F, Mezzetti A. The receptor RAGE as a progression factor amplifying arachidonate-dependent inflammatory and proteolytic response in human atherosclerotic plaques: role of glycemic control. *Circulation* 2003; **108**: 1070-1077
- 45 **Ekong U**, Zeng S, Dun H, Feirt N, Guo J, Ippagunta N, Guarnera JV, Lu Y, Weinberg A, Qu W, Ramasamy R, Schmidt AM, Emond JC. Blockade of the receptor for advanced glycation end products attenuates acetaminophen-induced hepatotoxicity in mice. *J Gastroenterol Hepatol* 2006; **21**: 682-688
- 46 **Zeng S**, Feirt N, Goldstein M, Guarnera J, Ippagunta N, Ekong U, Dun H, Lu Y, Qu W, Schmidt AM, Emond JC. Blockade of receptor for advanced glycation end product (RAGE) attenuates ischemia and reperfusion injury to the liver in mice. *Hepatology* 2004; **39**: 422-432
- 47 **Geerts A**. History, heterogeneity, developmental biology, and functions of quiescent hepatic stellate cells. *Semin Liver Dis* 2001; **21**: 311-335
- 48 **Hofmann MA**, Drury S, Fu C, Qu W, Taguchi A, Lu Y, Avila C, Kambham N, Bierhaus A, Nawroth P, Neurath MF, Slattery T, Beach D, McClary J, Nagashima M, Morser J, Stern D, Schmidt AM. RAGE mediates a novel proinflammatory axis: a central cell surface receptor for S100/calgranulin polypeptides. *Cell* 1999; **97**: 889-901
- 49 **Valencia JV**, Mone M, Zhang J, Weetall M, Buxton FP, Hughes TE. Divergent pathways of gene expression are activated by the RAGE ligands S100b and AGE-BSA. *Diabetes* 2004; **53**: 743-751
- 50 **Hyogo H**, Yamagishi S, Iwamoto K, Arihiro K, Takeuchi M, Sato T, Ochi H, Nonaka M, Nabeshima Y, Inoue M, Ishitobi T, Chayama K, Tazuma S. Elevated levels of serum advanced glycation end products in patients with non-alcoholic steatohepatitis. *J Gastroenterol Hepatol* 2007; **22**: 1112-1119

S- Editor Tian L **L- Editor** Logan S **E- Editor** Lin YP



Identification of TRPM7 channels in human intestinal interstitial cells of Cajal

Byung Joo Kim, Kyu Joo Park, Hyung Woo Kim, Seok Choi, Jae Yeoul Jun, In Youb Chang, Ju-Hong Jeon, Insuk So, Seon Jeong Kim

Byung Joo Kim, Hyung Woo Kim, School of Korean Medicine, Pusan National University, Yangsan 626-870, South Korea

Kyu Joo Park, Department of Surgery, College of Medicine, Seoul National University, Seoul 110-799, South Korea

Seok Choi, Jae Yeoul Jun, Department of Physiology, College of Medicine, Chosun University, Gwangju 501-759, South Korea

In Youb Chang, Department of Anatomy, College of Medicine, Chosun University, Gwangju 501-759, South Korea

Ju-Hong Jeon, Insuk So, Center for Bio-Artificial Muscle and Department of Physiology, College of Medicine, Seoul National University, Seoul 110-799, South Korea

Seon Jeong Kim, Center for Bio-Artificial Muscle and Department of Biomedical Engineering, Hanyang University, Seoul 133-791, South Korea

Author contributions: Kim BJ, Park KJ, Kim HW, Choi S, and Kim SJ designed the research; Kim BJ, Park KJ, Jun JY, and Chang IY performed the research; Jeon JH and So I contributed new reagents and analytic tools; Kim BJ, So I and Kim SJ analyzed the data; and Kim BJ, So I, and Kim SJ wrote the paper. **Supported by** The Creative Research Initiative Center for Bio-Artificial Muscle of the Ministry of Education, Science and Technology (MEST) in Korea

Correspondence to: Seon Jeong Kim, PhD, Center for Bio-Artificial Muscle and Department of Biomedical Engineering, Hanyang University, 17 Haengdang-Dong, Seongdong-gu, Seoul 133-791, South Korea. sjk@hanyang.ac.kr

Telephone: +82-2-22202321 **Fax:** +82-2-22912320

Received: August 6, 2009 **Revised:** September 24, 2009

Accepted: November 1, 2009

Published online: December 14, 2009

Abstract

AIM: To investigate the characteristics of slow electrical waves and the presence of transient receptor potential melastatin-type 7 (TRPM7) in the human gastrointestinal (GI) tract.

METHODS: Conventional microelectrode techniques were used to record intracellular electrical responses from human GI smooth muscle tissue. Immunohistochemistry was used to identify TRPM7 channels in interstitial cells of Cajal (ICCs).

RESULTS: The human GI tract generated slow electrical waves and had ICCs which functioned as pacemaker cells. Flufenamic acid, a nonselective cation channel blocker, and 2-APB (2-aminoethoxydiphenyl borate) and La³⁺, TRPM7 channel blockers, inhibited the slow

waves. Also, TRPM7 channels were expressed in ICCs in human tissue.

CONCLUSION: These results suggest that the human GI tract generates slow waves and that TRPM7 channels expressed in the ICCs may be involved in the generation of the slow waves.

© 2009 The WJG Press and Baishideng. All rights reserved.

Key words: Electrophysiology; Interstitial cells of Cajal; TRPM cation channels; Transient receptor potential melastatin-type 7 protein; Human; Gastrointestinal tract

Peer reviewer: Akio Inui, MD, PhD, Professor, Department of Behavioral Medicine, Kagoshima University Graduate School of Medical and Dental Sciences, 8-35-1 Sakuragaoka, Kagoshima 890-8520, Japan

Kim BJ, Park KJ, Kim HW, Choi S, Jun JY, Chang IY, Jeon JH, So I, Kim SJ. Identification of TRPM7 channels in human intestinal interstitial cells of Cajal. *World J Gastroenterol* 2009; 15(46): 5799-5804 Available from: URL: <http://www.wjgnet.com/1007-9327/15/5799.asp> DOI: <http://dx.doi.org/10.3748/wjg.15.5799>

INTRODUCTION

Smooth muscles in the gastrointestinal (GI) tract are spontaneously active with rhythmic generation of slow electrical waves^[1]. The slow waves determine the frequency and amplitude of the phasic contractions of GI muscles^[2]. Slow waves originate in specialized regions such as the border between the circular and longitudinal muscle layers in the stomach and small intestine and along the submucosal surface of the circular muscle layer in the colon^[3]. Each pacemaker region is populated by interstitial cells of Cajal (ICCs), and many studies have demonstrated the pacemaker role of these cells^[4-9]. ICCs generate spontaneous inward currents and slow wave-like depolarizations^[10,11]. Slow waves propagate within the ICC networks, conduct into smooth muscle cells via gap junctions, and initiate phasic contractions by activating Ca²⁺ entry through L-type Ca²⁺ channels. The pacemaker currents of the murine small intestine are due mainly to periodic activation of non-selective cation channels

(NSCCs)^[12].

In *Caenorhabditis elegans*, the melastatin-type transient receptor potential (TRPM) channel, particularly TRPM7, was suggested as being involved in the defecation process^[13]. Also recently, we suggested that TRPM7 was a good candidate for the NSCC in ICCs of the murine small intestine^[14]. TRP channels were first cloned from *Drosophila* species and constitute a superfamily of proteins that encode a diverse group of Ca^{2+} -permeable NSCCs^[15]. The TRP family is divided into 7 subfamilies: classical TRPs (TRPC), which display the greatest similarity to *Drosophila* TRP; vanilloid TRPs (TRPVs); TRPMs; mucolipin TRPs; polycystin TRPs; NOMPC (no mechanoreceptor potential C) TRP; ankyrin 1 TRPs. TRPC channels mediate cation entry in response to phospholipase C activation, whereas TRPV proteins respond to physical and chemical stimuli, such as changes in temperature, pH, and mechanical stress. The TRPM family members differ significantly from other TRP channels in terms of domain structure, cation selectivity, and activation mechanisms^[15].

The characteristics of the slow wave and the presence of TRPM7 in human GI tract have not yet been investigated. Therefore, we undertook to investigate the characteristics of the slow wave in the human GI tract and the involvement of TRPM7 in ICCs.

MATERIALS AND METHODS

Human tissue preparation

The segments of human colon or small intestine used in this study were obtained from cancer patients of either sex ranging in age from 46 to 59 years as discarded surgical tissue during operations. The protocol was approved by the human subjects research committees at Seoul National University College of Medicine. A segment of colon or jejunum was opened along the mesenteric border, and the mucosal layers, the serosal layers and a part of the longitudinal layers were carefully peeled away under a dissecting microscope. A tissue segment (about 0.5 mm wide and 0.5 mm long) was pinned out on a silicone rubber plate with the serosal side uppermost, and the plate was fixed at the bottom of an organ bath. The preparation was continuously perfused with CO_2 /bicarbonate-buffered Tyrode solution at 36–37°C and equilibrated for 2 h before the experiment, at a constant flow rate of about 2 mL/min.

Intracellular recording of electrical activity

Conventional microelectrode techniques were used to record intracellular electrical responses from smooth muscle tissues, and the glass capillary microelectrodes, filled with 3 mol/L KCl, had tip resistances of 40–80 M Ω . Electrical responses recorded via a high input impedance amplifier (Axoclamp-2B, Axon Instruments, USA) were displayed on a cathode ray oscilloscope (SS-7602, Iwatsu, Osaka, Japan) and also stored on a personal computer for later analysis.

Solutions and drugs

The ionic composition of the CO_2 /bicarbonate buffered-

Tyrode solution was as follows (mmol/L): NaCl 116, KCl 5.4, CaCl_2 1.5, MgCl_2 1, NaHCO_3 24, glucose 5. The solutions were aerated with O_2 containing 5% CO_2 , and the pH of the solutions was maintained at 7.3–7.4. Drugs used were flufenamic acid, 2-aminoethoxydiphenyl borate (2-APB), lanthanum ion (La^{3+}) and nifedipine (all from Sigma, USA). Drugs were dissolved in distilled water, and added to CO_2 /bicarbonate buffered-Tyrode solution to the desired concentrations, immediately prior to use. Addition of these chemicals to the Krebs solution did not alter the pH of the solution.

Immunohistochemistry

Whole-mount preparations from the colon or small intestine of human were used for immunohistochemistry. Experimental protocols approved by Seoul National University were followed. For whole-mount preparations, the mucosa was removed by sharp dissection, and the remaining muscle layer was stretched before fixation. Whole-mount preparations were fixed in cold acetone (4°C) for 5 min. After fixation, they were washed in phosphate-buffered saline (PBS; 0.01 mol/L; pH 7.4) and immersed in 0.3% Triton X-100 in PBS. After blocking with 1% bovine serum albumin (Sigma) in 0.01 mol/L PBS for 1 h at room temperature, they were incubated with a rat monoclonal antibody raised against c-kit (Ack2; eBioscience) at 0.5 $\mu\text{g}/\text{mL}$ or goat polyclonal antibody against TRPM7 (Abcam, Cambridgeshire, UK) in PBS for 24 h (4°C). After a rinse in PBS at 4°C, they were labeled with the fluorescein isothiocyanate-coupled donkey anti-goat immunoglobulin G secondary antibody (1:100; Jackson Immunoresearch Laboratories, Baltimore, MD, USA) or Texas red-conjugated donkey anti-rat immunoglobulin G (1:100; Jackson Immunoresearch Laboratories) for 1 h at room temperature. Control tissues and sections were prepared by omitting either the primary or secondary antibodies from the incubation solutions.

Statistics analysis

All data are expressed as mean \pm SE. The Student *t*-test for unpaired data was used to compare control and experimental groups. A *P*-value < 0.05 was considered statistically significant.

RESULTS

Spontaneous electrical activities recorded from intact tissue preparations of human colon and small intestine

In intact human colon preparations, most of the tissues generated slow electrical waves (Figure 1A). The membrane potential of cells generating slow waves with the most negative value (equal to the resting membrane potential) ranged between -54.7 mV and -68.7 mV (mean -61.9 ± 1.9 mV, $n = 6$; each n value represents the number of human tissues used). Slow waves had a frequency of $18.1 \pm 2.1/\text{min}$ ($n = 6$). In intact human small intestine preparations, most of the tissues generated slow waves (Figure 1B). The membrane potential of cells generating slow waves ranged between -51.2 mV and -63.5 mV (mean -57.3 ± 5.2 mV, $n = 5$). Slow waves had a frequency of 3.1

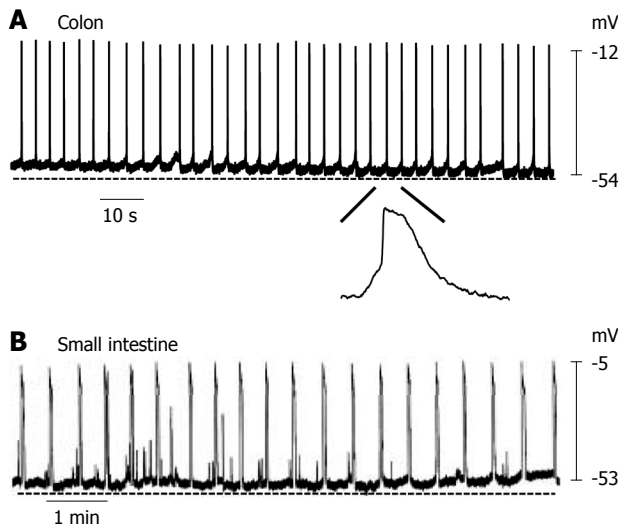


Figure 1 Spontaneous electrical activity of smooth muscle cells in human colon and small intestine. A: Colonic smooth muscle cells produced slow waves with a frequency of $18.1 \pm 2.1/\text{min}$; B: Small intestinal smooth muscle cells also produced slow waves with a frequency of $3.1 \pm 0.5/\text{min}$.

$\pm 0.5/\text{min}$ ($n = 5$). These results suggest that the GI tract in humans can generate slow waves and have ICCs which function as pacemaker cells.

Pharmacological properties of slow waves in human colon

We investigated the effect of a nonselective cation channel blocker and several TRPM7 channel blockers on the slow waves recorded from human colon tissue. First, we investigated the effects of flufenamic acid, a nonselective cation channel blocker. When flufenamic acid was applied in the bath solution, the slow waves were inhibited ($2.6 \pm 0.3/\text{min}$) (Figure 2A and D). As indicated previously, 2-APB is known to inhibit TRPM7 channels^[16]. When 2-APB was applied in the bath solution, the slow waves were inhibited in a concentration-dependent manner ($2.8 \pm 0.2/\text{min}$) (Figure 2B and D). Again, as described previously, TRPM7 has been shown to be blocked by trivalent ions such as La^{3+} ^[17]. When La^{3+} was applied in the bath solution, the slow waves were inhibited ($3.2 \pm 0.2/\text{min}$) (Figure 2C and D). These results indicate that NSCCs and TRPM7 in ICCs may be involved in the generation of the slow wave in the human GI tract.

Expression of TRPM7 protein in ICC of native tissues

To test this possibility more directly, we examined the expression of TRPM7 in ICCs in human tissues. Expression of TRPM7 proteins was investigated by immunohistochemistry. Double staining with anti-c-kit (a marker of ICCs) and anti-TRPM7 antibodies showed TRPM7 immunoreactivity in c-kit-immunopositive ICCs in the human colon (Figure 3), and human small intestine (Figure 4).

DISCUSSION

GI smooth muscles are spontaneously active, and

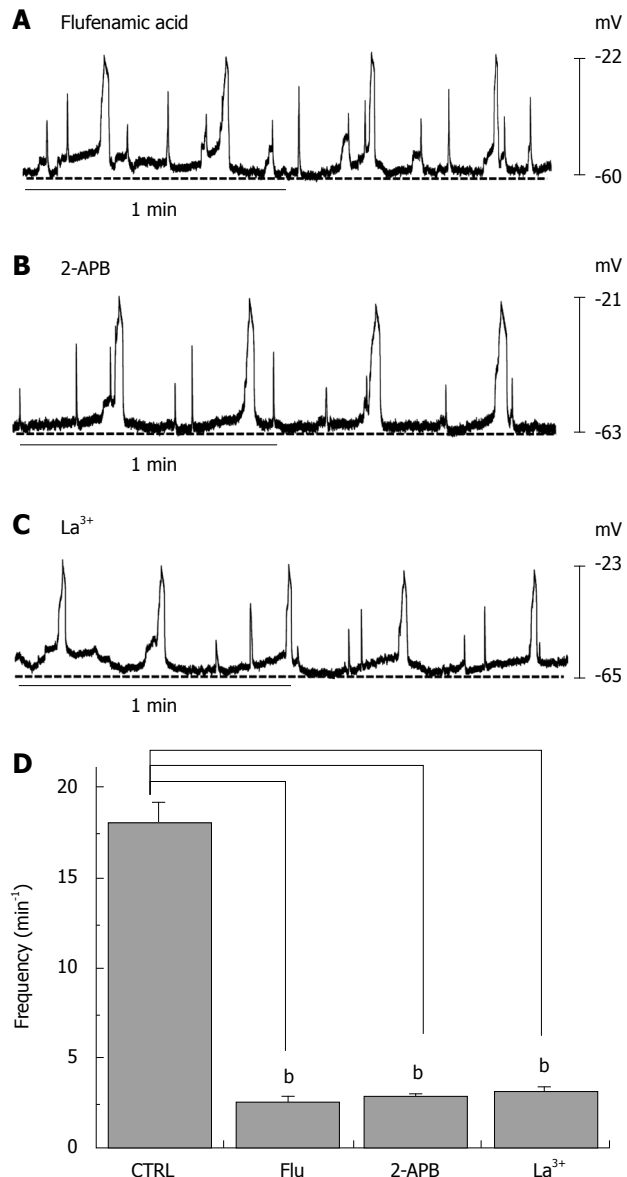


Figure 2 Effects of flufenamic acid, 2-aminoethoxydiphenyl borate (2-APB) and La^{3+} on electrical responses. Flufenamic acid ($50 \mu\text{M}$, A), 2-APB ($50 \mu\text{M}$, B) or La^{3+} ($50 \mu\text{M}$, C) were applied while recording electrical activity of isolated smooth muscles of the human colon. All drugs inhibited the spontaneous electrical activity; D: The histograms summarize the frequency of spontaneous electrical activities in human colon with flufenamic acid, 2-APB, and La^{3+} . ^b $P < 0.01$.

generate rhythmic slow electrical waves^[1]. The slow waves originate in the ICCs distributed in the GI tract^[4-9]. ICCs express c-kit immunoreactivity and form gap junctional connections with ICCs and with smooth muscle cells^[18-20]. Many types of ICC with different immunohistochemical and electrical properties, such as myenteric ICC (ICC-MY), intramuscular ICC, deep muscular plexus ICC and submucosal ICC, are distributed in the GI tract^[21]. In animal models lacking ICC-MY, the slow waves in the small intestine are strongly attenuated, indicating that these cells are indeed essential for pacemaking activity in the GI tract^[6,22].

Research into the distribution and function of ICCs was greatly stimulated by discovering that ICCs express

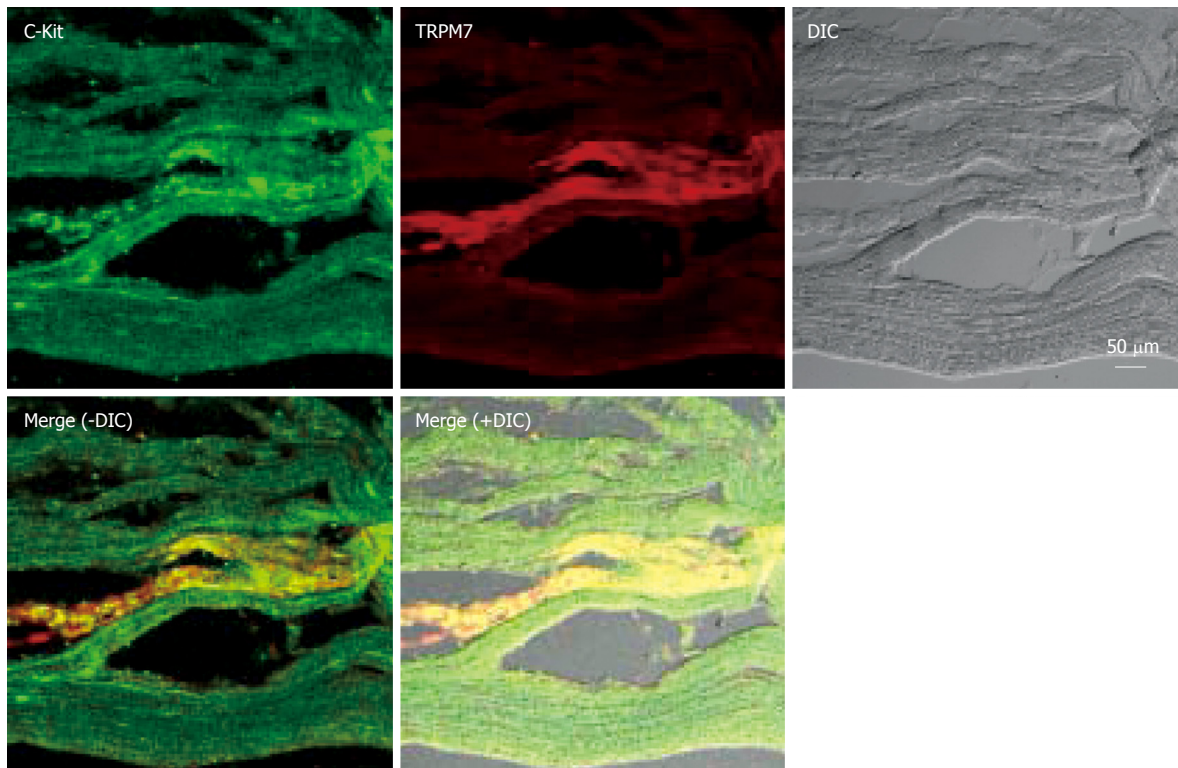


Figure 3 Expression of transient receptor potential melastatin-type 7 (TRPM7) protein in human colon. Double labeling of TRPM7-like immunoreactivity (red) and c-kit-like immunoreactivity (green) within smooth muscle layers of the human colon. The mixed color yellow indicates the colocalization of both TRPM7-like and c-kit-like immunoreactivity (bar = 50 μ m). DIC: differential interference contrast.

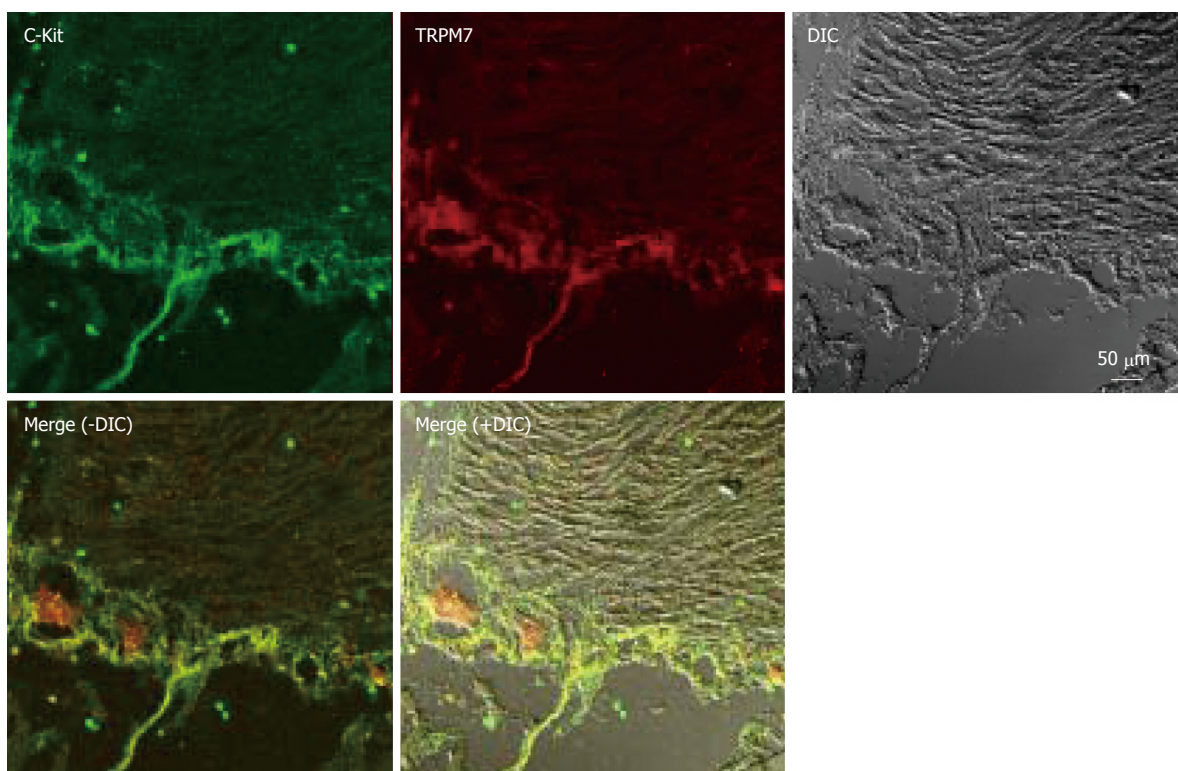


Figure 4 Expression of TRPM7 protein in human small intestine. Double labeling of TRPM7-like immunoreactivity (red) and c-kit-like immunoreactivity (green) within smooth muscle layers of human small intestine. The mixed color yellow indicates the colocalization of both TRPM7-like and c-kit-like immunoreactivity (bar = 50 μ m).

c-kit, and signaling *via* kit protein is necessary for development and maintenance of the ICC phenotype^[7,23]. ICCs are involved in physiological GI motility, therefore

have clinical importance in many bowel disorders, including inflammatory bowel disease, chronic idiopathic intestinal pseudo-obstruction, intestinal obstruction with

hypertrophy, achalasia, Hirschsprung disease, juvenile pyloric stenosis, juvenile intestinal obstruction, and anorectal malformation^[21].

Discovering the molecules involved in the generation of pacemaker activity in ICCs may lead to dramatic new therapies for chronic GI diseases that result in lifelong suffering.

Strege *et al*^[24] suggested that a mechanosensitive Na^+ channel current is present in human intestinal ICC and appears to play a role in the control of intestinal motor function. Also in human jejunum, each ICC-MY generates spontaneous pacemaker activity that actively propagates through the ICC network, and the pacemaker activity was dependent on inositol-1,4,5-triphosphate receptor-operated stores and mitochondrial function^[25]. Although some papers have identified the ion channels in ICCs^[10,11,26,27], there is little known about the ionic basis of its pacemaker activity. Recently, we used electrophysiological, molecular biological, and immunohistochemical techniques to establish the close relationship between NSCCs in ICCs and a mammalian TRP homologue, TRPM7 and found that TRPM7 is required for murine intestinal pacemaking^[14].

Little is known about the involvement of TRPM7 channels in ICCs in the human GI tract. In this study, we found that the human GI tract generated slow waves and various pharmacological properties of the slow waves were the same as those of TRPM7. Also, immunohistochemistry showed abundant and localized expression of TRPM7 protein in the human GI tract. TRPM7 has been suggested to have a central role in cellular Mg^{2+} homeostasis^[28], in central nervous system ischemic injury^[29], in skeletogenesis in zebrafish^[30], in the defecation rhythm in *C. elegans*^[13], in cholinergic vesicle fusion with the plasma membrane^[31], in phosphoinositide-3-kinase signaling in lymphocytes^[32], in cell death in gastric cancer^[33], in osteoblast proliferation^[34], and in breast cancer cell proliferation^[35].

The physiological role of TRPM7 channels in ICCs in human GI tract requires more investigation. As a primary molecular candidate for the NSCC responsible for pacemaking activity in ICCs, TRPM7 may be a new target for pharmacological treatment of GI motility disorders.

COMMENTS

Background

Previously, transient receptor potential melastatin-type 7 (TRPM7) was found to be required for intestinal pacemaking activity in mice. However, in the human gastrointestinal (GI) tract, the characteristics of slow electrical waves and the presence of TRPM7 has not been investigated.

Research frontiers

The human GI tract generates slow waves and TRPM7 channels are expressed in interstitial cells of Cajal (ICCs).

Innovations and breakthroughs

The human GI tract generates slow waves and has ICCs functioning as pacemaker cells. Flufenamic acid, a nonselective cation channel blocker, and 2-APB (2-aminoethoxydiphenyl borate) and La³⁺, TRPM7 channel blockers, inhibited the slow waves. Also, TRPM7 channels were expressed in ICCs in human tissues.

Applications

TRPM7 protein may be a new target for pharmacological treatment of GI motility disorders.

Peer review

The authors well demonstrated the involvement of TRPM7 in ICCs and characterized the pharmacological properties of slow waves in the human GI tract. The finding will form the basis for future treatments of GI motility disorders and is a useful addition to the literature.

REFERENCES

- Tomita T. Electrical activity (spikes and slow wave) in gastrointestinal smooth muscles. In: Bulbring E, Brading AF, Jones AW, Tomita T, editors. Smooth muscle. London: Edward Arnold, 1981: 127-156
- Szurszewski JH. Electrical basis for gastrointestinal motility. In: Physiology of the gastrointestinal tract. 2nd ed. New York: Raven, 1987: 383-422
- Sanders KM. A case for interstitial cells of Cajal as pacemakers and mediators of neurotransmission in the gastrointestinal tract. *Gastroenterology* 1996; **111**: 492-515
- Langton P, Ward SM, Carl A, Norell MA, Sanders KM. Spontaneous electrical activity of interstitial cells of Cajal isolated from canine proximal colon. *Proc Natl Acad Sci USA* 1989; **86**: 7280-7284
- Ward SM, Burns AJ, Torihashi S, Sanders KM. Mutation of the proto-oncogene c-kit blocks development of interstitial cells and electrical rhythmicity in murine intestine. *J Physiol* 1994; **480** (Pt 1): 91-97
- Huizinga JD, Thuneberg L, Kluppel M, Malysz J, Mikkelsen HB, Bernstein A. W/kit gene required for interstitial cells of Cajal and for intestinal pacemaker activity. *Nature* 1995; **373**: 347-349
- Torihashi S, Ward SM, Nishikawa S, Nishi K, Kobayashi S, Sanders KM. c-kit-dependent development of interstitial cells and electrical activity in the murine gastrointestinal tract. *Cell Tissue Res* 1995; **280**: 97-111
- Dickens EJ, Hirst GD, Tomita T. Identification of rhythmically active cells in guinea-pig stomach. *J Physiol* 1999; **514** (Pt 2): 515-531
- Ordog T, Ward SM, Sanders KM. Interstitial cells of cajal generate electrical slow waves in the murine stomach. *J Physiol* 1999; **518** (Pt 1): 257-269
- Koh SD, Sanders KM, Ward SM. Spontaneous electrical rhythmicity in cultured interstitial cells of cajal from the murine small intestine. *J Physiol* 1998; **513** (Pt 1): 203-213
- Thomsen L, Robinson TL, Lee JC, Farraway LA, Hughes MJ, Andrews DW, Huizinga JD. Interstitial cells of Cajal generate a rhythmic pacemaker current. *Nat Med* 1998; **4**: 848-851
- Koh SD, Jun JY, Kim TW, Sanders KM. A $\text{Ca}(2+)$ -inhibited non-selective cation conductance contributes to pacemaker currents in mouse interstitial cell of Cajal. *J Physiol* 2002; **540**: 803-814
- Vriens J, Owsianik G, Voets T, Droogmans G, Nilius B. Invertebrate TRP proteins as functional models for mammalian channels. *Pflugers Arch* 2004; **449**: 213-226
- Kim BJ, Lim HH, Yang DK, Jun JY, Chang IY, Park CS, So I, Stanfield PR, Kim KW. Melastatin-type transient receptor potential channel 7 is required for intestinal pacemaking activity. *Gastroenterology* 2005; **129**: 1504-1517
- Clapham DE. TRP channels as cellular sensors. *Nature* 2003; **426**: 517-524
- Prakriya M, Lewis RS. Separation and characterization of currents through store-operated CRAC channels and Mg^{2+} -inhibited cation (MIC) channels. *J Gen Physiol* 2002; **119**: 487-507
- Monteith-Zoller MK, Hermosura MC, Nadler MJ, Scharenberg AM, Penner R, Fleig A. TRPM7 provides an ion channel mechanism for cellular entry of trace metal ions. *J Gen Physiol* 2003; **121**: 49-60
- Komuro T, Seki K, Horiguchi K. Ultrastructural characterization of the interstitial cells of Cajal. *Arch Histol Cytol* 1999; **62**: 295-316
- Sanders KM. A case for interstitial cells of Cajal as pacemakers and mediators of neurotransmission in the gastro-

- intestinal tract. *Gastroenterology* 1996; **111**: 492-515
- 20 **Huizinga JD**, Thuneberg L, Vanderwinden JM, Rumessen JJ. Interstitial cells of Cajal as targets for pharmacological intervention in gastrointestinal motor disorders. *Trends Pharmacol Sci* 1997; **18**: 393-403
- 21 **Sanders KM**, Ordog T, Koh SD, Torihashi S, Ward SM. Development and plasticity of interstitial cells of Cajal. *Neurogastroenterol Motil* 1999; **11**: 311-338
- 22 **Maeda H**, Yamagata A, Nishikawa S, Yoshinaga K, Kobayashi S, Nishi K, Nishikawa S. Requirement of c-kit for development of intestinal pacemaker system. *Development* 1992; **116**: 369-375
- 23 **Torihashi S**, Ward SM, Sanders KM. Development of c-Kit-positive cells and the onset of electrical rhythmicity in murine small intestine. *Gastroenterology* 1997; **112**: 144-155
- 24 **Strege PR**, Ou Y, Sha L, Rich A, Gibbons SJ, Szurszewski JH, Sarr MG, Farrugia G. Sodium current in human intestinal interstitial cells of Cajal. *Am J Physiol Gastrointest Liver Physiol* 2003; **285**: G1111-G1121
- 25 **Lee HT**, Hennig GW, Fleming NW, Keef KD, Spencer NJ, Ward SM, Sanders KM, Smith TK. The mechanism and spread of pacemaker activity through myenteric interstitial cells of Cajal in human small intestine. *Gastroenterology* 2007; **132**: 1852-1865
- 26 **Farrugia G**. Ionic conductances in gastrointestinal smooth muscles and interstitial cells of Cajal. *Annu Rev Physiol* 1999; **61**: 45-84
- 27 **Huizinga JD**, Zhu Y, Ye J, Molleman A. High-conductance chloride channels generate pacemaker currents in interstitial cells of Cajal. *Gastroenterology* 2002; **123**: 1627-1636
- 28 **Schmitz C**, Perraud AL, Johnson CO, Inabe K, Smith MK, Penner R, Kurosaki T, Fleig A, Scharenberg AM. Regulation of vertebrate cellular Mg²⁺ homeostasis by TRPM7. *Cell* 2003; **114**: 191-200
- 29 **Aarts M**, Iihara K, Wei WL, Xiong ZG, Arundine M, Cerwinski W, MacDonald JF, Tymianski M. A key role for TRPM7 channels in anoxic neuronal death. *Cell* 2003; **115**: 863-877
- 30 **Elizondo MR**, Arduini BL, Paulsen J, MacDonald EL, Sabel JL, Henion PD, Cornell RA, Parichy DM. Defective skeletogenesis with kidney stone formation in dwarf zebrafish mutant for trpm7. *Curr Biol* 2005; **15**: 667-671
- 31 **Brauchi S**, Krapivinsky G, Krapivinsky L, Clapham DE. TRPM7 facilitates cholinergic vesicle fusion with the plasma membrane. *Proc Natl Acad Sci USA* 2008; **105**: 8304-8308
- 32 **Sahni J**, Scharenberg AM. TRPM7 ion channels are required for sustained phosphoinositide 3-kinase signaling in lymphocytes. *Cell Metab* 2008; **8**: 84-93
- 33 **Kim BJ**, Park EJ, Lee JH, Jeon JH, Kim SJ, So I. Suppression of transient receptor potential melastatin 7 channel induces cell death in gastric cancer. *Cancer Sci* 2008; **99**: 2502-2509
- 34 **Abed E**, Moreau R. Importance of melastatin-like transient receptor potential 7 and magnesium in the stimulation of osteoblast proliferation and migration by platelet-derived growth factor. *Am J Physiol Cell Physiol* 2009; **297**: C360-C368
- 35 **Guilbert A**, Gautier M, Dhennin-Duthille I, Haren N, Sevestre H, Ouadid-Ahidouch H. Evidence that TRPM7 is required for breast cancer cell proliferation. *Am J Physiol Cell Physiol* 2009; **297**: C493-C502

S- Editor Tian L **L- Editor** Cant MR **E- Editor** Ma WH



Role of diffusion-weighted magnetic resonance imaging in the differential diagnosis of focal hepatic lesions

Naoto Koike, Akihiro Cho, Katsuhiro Nasu, Kazuhiko Seto, Shigeyuki Nagaya, Yuji Ohshima, Nobuhiro Ohkohchi

Naoto Koike, Yuji Ohshima, Department of Surgery, Seirei Sakura Citizen Hospital, 2-36-2 Ebaradai, Sakura, Chiba 285-8765, Japan

Akihiro Cho, Department of Surgery, Chiba Cancer Center, 666-2 Nitona, Chuhohku, Chiba 260-8717, Japan

Katsuhiro Nasu, Department of Radiology, Institute of Clinical Medicine, University of Tsukuba, 1-1-1 Tennodai, Tsukuba, Ibaraki 305-8577, Japan

Kazuhiko Seto, Department of Radiology, Seirei Sakura Citizen Hospital, 2-36-2 Ebaradai, Sakura, Chiba 285-8765, Japan

Shigeyuki Nagaya, Department of Radiology, Seirei Mikatabara Hospital, 3453 Mikatabara, Kitaku, Hamamatsu, Shizuoka 433-8558, Japan

Nobuhiro Ohkohchi, Department of Surgery, Institute of Clinical Medicine, University of Tsukuba, 1-1-1 Tennodai, Tsukuba, Ibaraki 305-8577, Japan

Author contributions: Koike N wrote the paper; Cho A designed research; Koike N, Seto K, Nagaya S and Ohshima Y contributed to the imaging processing and analysis; Nasu K and Ohkohchi N critically revised the paper with an important conceptual and editorial input.

Correspondence to: Dr. Naoto Koike, Department of Surgery, Seirei Sakura Citizen Hospital, 2-36-2 Ebaradai, Sakura, Chiba 285-8765, Japan. naotk@sis.seirei.or.jp

Telephone: +81-43-4861151 **Fax:** +81-43-4868696

Received: August 15, 2009 **Revised:** October 26, 2009

Accepted: November 2, 2009

Published online: December 14, 2009

Abstract

AIM: To evaluate the utility of diffusion-weighted imaging (DWI) in screening and differential diagnosis of benign and malignant focal hepatic lesions.

METHODS: Magnetic resonance imaging (MRI) examinations were performed using the Signa Excite XI Twin Speed 1.5T system (GE Healthcare, Milwaukee, WI, USA). Seventy patients who had undergone MRI of the liver [29 hepatocellular carcinomas (HCC), four cholangiocarcinomas, 34 metastatic liver cancers, 10 hemangiomas, and eight cysts] between April 2004 and August 2008 were retrospectively evaluated. Visualization of lesions, relative contrast ratio (RCR), and apparent diffusion coefficient (ADC) were compared between benign and malignant lesions on DWI. Superparamagnetic iron oxide (SPIO) was administered to 59 patients, and RCR was compared pre- and post-administration.

RESULTS: DWI showed higher contrast between malignant lesions (especially in multiple small metastatic cancers) and surrounding liver parenchyma than did contrast-enhanced computed tomography. ADCs ($\text{mean} \pm \text{SD} \times 10^{-3} \text{ mm}^2/\text{s}$) were significantly lower ($P < 0.05$) in malignant lesions (HCC: 1.31 ± 0.28 and liver metastasis: 1.11 ± 0.22) and were significantly higher in benign lesions (hemangioma: 1.84 ± 0.37 and cyst: 2.61 ± 0.45) than in the surrounding hepatic tissues. RCR between malignant lesions and surrounding hepatic tissues significantly improved after SPIO administration, but RCRs in benign lesions were not improved.

CONCLUSION: DWI is a simple and sensitive method for screening focal hepatic lesions and is useful for differential diagnosis.

© 2009 The WJG Press and Baishideng. All rights reserved.

Key words: Hepatic tumor; Liver imaging; Magnetic resonance imaging; Diffusion-weighted imaging; Apparent diffusion coefficient

Peer reviewer: Dr. Serdar Karakose, Professor, Department of Radiology, Meram Medical Faculty, Selcuk University, Konya 42080, Turkey

Koike N, Cho A, Nasu K, Seto K, Nagaya S, Ohshima Y, Ohkohchi N. Role of diffusion-weighted magnetic resonance imaging in the differential diagnosis of focal hepatic lesions. *World J Gastroenterol* 2009; 15(46): 5805-5812 Available from: URL: <http://www.wjgnet.com/1007-9327/15/5805.asp> DOI: <http://dx.doi.org/10.3748/wjg.15.5805>

INTRODUCTION

Diffusion is the thermally induced motion of water molecules, which is also referred to as Brownian motion^[1]. Diffusion-weighted imaging (DWI) is a new magnetic resonance imaging (MRI) technique that provides imaging of diffusion in biological tissues.

DWI has been reported to be useful in evaluating the early stages of brain ischemia^[2-4]. Recent technical developments have reduced the image distortion associated with this technique and have increased the signal-to-noise ratio, thus making DWI of the body feasible^[5,6]. Screening, accurate detection, and characterization of focal hepatic lesions are important for planning

treatment of malignant hepatic lesions. The differential diagnosis of malignant and benign focal hepatic lesions remains a diagnostic challenge; however, to improve the diagnosis of such lesions, new methods for existing modalities, such as MRI, computed tomography (CT), angiography, and ultrasonography are being developed.

Recently, some studies have reported that the apparent diffusion coefficient (ADC), which is one of calculated parameters of DWI, might be useful for differential diagnosis of benign and malignant lesions in the liver^[7]. Superparamagnetic iron oxide (SPIO)-enhanced MRI was reported to be as useful as CT during arterioportography and CT during hepatic arteriography for diagnosing metastatic liver tumors^[8,9]. SPIO improves the contrast-to-noise ratio (CNR) between focal hepatic lesion and the surrounding liver parenchyma on T2-weighted imaging^[9]. SPIO has also been reported to further improve the performance of DWI of the liver because SPIO reduces the signal in normal liver parenchyma^[10].

The purpose of the present study was to retrospectively evaluate the utility of DWI in screening, accurate detection, and differential diagnosis of benign and malignant focal hepatic lesions.

MATERIALS AND METHODS

Patients

We retrospectively evaluated 70 patients (52 men and 18 women; age, 39–86 years; mean age, 65.3 years) with 85 lesions [29 hepatocellular carcinomas (HCC), four cholangiocarcinomas, 34 metastatic liver cancers, 10 hemangiomas, and eight cysts] who had been examined between April 2004 and August 2008. The locations of each focal hepatic lesion were: posterior segment in 32, anterior segment in 33, median segment in 15, and lateral segment in five patients. These lesions measured 1.0 to 10.0 cm (mean 3.1 cm) along their long axes on CT images.

The criteria for selecting patients to evaluate in the present study were as follows: (1) the diagnoses of HCC were pathology confirmed in 25 lesions and other lesions were confirmed by measurement of the serum α -fetal protein (AFP) level, clinical data, ultrasonography, angiography and CT or MRI or both; (2) hepatic metastasis of primary lesions was pathologically confirmed; (3) the diagnosis of cholangiocarcinomas was pathologically confirmed in three lesions and the other lesion was confirmed by clinical data, ultrasonography, CT and MRI; (4) the diagnosis of cavernous hemangioma and hepatic cysts was confirmed by clinical data, ultrasonography, CT or MRI or both, and follow-up observation.

Imaging protocol

MR examinations were performed using the Signa Excite XI Twin Speed 1.5T system (GE Healthcare, Milwaukee, WI, USA) with a four-channel torso-array coil. Diffusion weighted single-shot echo-planar imaging was performed

in individual patients using the following parameters: repetition time/echo time (TR/TE) = 6000/73.1 ms, 7–8 mm thickness, water selective excitation for fat suppression, matrix size = 128 × 128, field of view = 36 cm × 36 cm, number of excitations = 6.0, slice thickness/gap = 8 mm/0 mm, 20 axial slices, scan time = 2 min 24 s, *b* value = 0 and 1000 s/mm², under free breathing. A parallel imaging technique, array spatial sensitivity encoding technique (ASSET) was used. Motion-probing gradient pulses were placed along three orthogonal oblique directions. Additional post-contrast-enhanced DW images were obtained after intravenous administration of SPIO (Resovist; Bayer Schering Pharma AG, Berlin, Germany). The dose of SPIO was 0.016 mL/kg, corresponding to 0.45 mg/kg of Fe.

Contrast enhanced CT was conducted using the LightSpeed ultra 16-MDCT scanner (GE Healthcare, Milwaukee, WI, USA) with pre- and postcontrast triple-phase (arterial, portal venous, and equilibrium phase) scans after injection of 80 to 100 mL of Iopamidol (Iopamiro; Bayer Schering Pharma AG, Berlin, Germany) at an injection rate of 1.5 to 3.0 mL/s.

Visualization of lesions, relative contrast ratio between the lesion and surrounding liver parenchyma (RCR), and ADC values were compared between benign and malignant lesions on DWI. Analysis and measurements of DWI data was performed using the GE FUNTOOL software. All regions of interest (ROI) were created as large as possible in each lesion. In cases with multiple lesions, only the most conspicuous lesion was selected for quantitative measurements. If different types of lesions were mixed (for example, hepatocellular carcinomas and cysts), each lesion was measured.

Visualization of lesions

All but two lesions (CT examinations were not performed in one case of metastatic liver cancer and hemangioma.) were evaluated. Two diagnostic doctors performed a visual evaluation of each selected CT image (best phase for CT examinations in individual lesions) and DWI (only before SPIO administration) based on mutual agreement. They classified the visualization of lesions on CT and DWI into three categories according to the following criteria. Grade 1: no or slight visualization and unclear margin. Grade 2: moderate visualization and clear margin. Grade 3: marked visualization and very clear margin.

RCR measurements

SPIO was administered to 59 patients (18 HCC, 26 metastatic liver cancers, 10 hemangiomas, seven cysts) and the RCR was compared before and after SPIO administration to differentiate between benign and malignant lesions. The RCR was calculated by the following equation: $RCR = SI_{lesion}/SI_{liver}$, where SI is signal intensity of the lesion and SI_{liver} was evaluated from hepatic tissue surrounding the lesion. In this paper, the conventional contrast-to-noise ratio analysis was not employed because the standard deviation of the

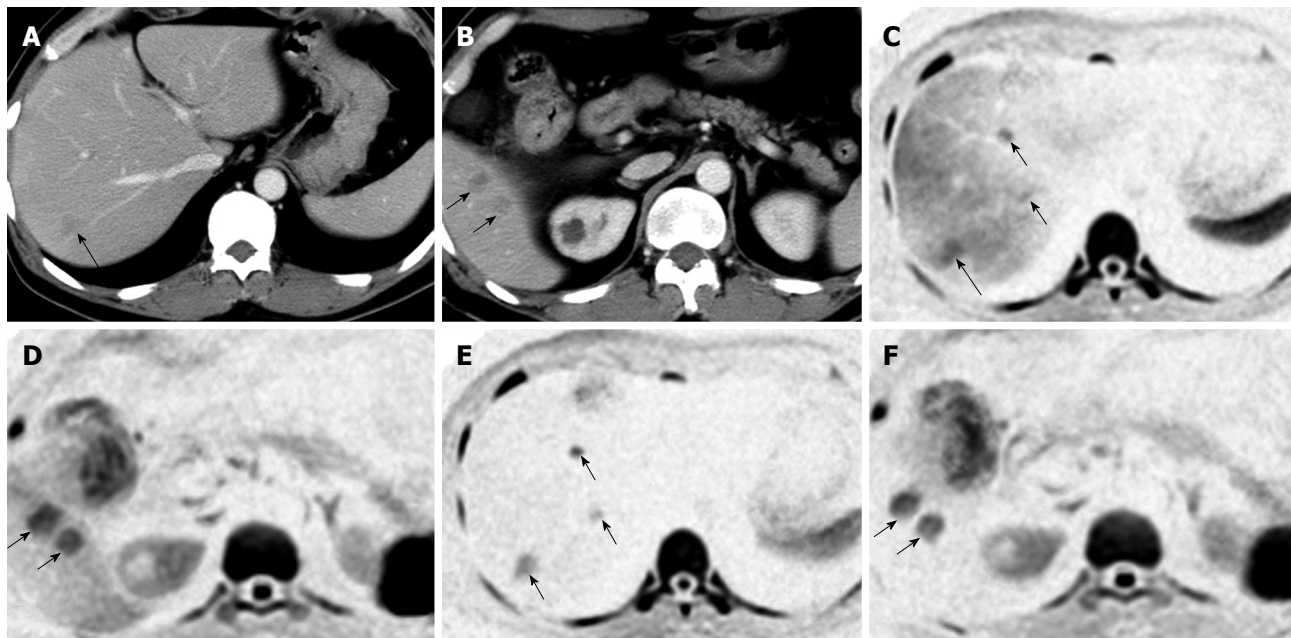


Figure 1 A case of hepatic metastases of colon cancer. A, B: Dynamic computed tomography of the liver in the portal phase showing multiple metastatic lesions, which are indicated as low-density masses (arrows); C, D: Diffusion-weighted imaging (DWI) of the same locations as in (A) and (B), clearly showing metastatic lesions as high signal intensities; E, F: After SPIO administration, the background signal intensity of the liver parenchyma was reduced and the signal intensities of the metastatic lesions were seen more clearly.

Table 1 Visual evaluation of focal hepatic lesions

Lesions	Modalities	Grade 1	Grade 2	Grade 3
Meta ^a (n = 33)	CT	9	17	7
	DWI	1	8	24
HCC ^a (n = 29)	CT	4	19	6
	DWI	6	11	12
Cholangiocarcinoma (n = 4)	CT	1	1	2
	DWI	0	0	4
Cyst ^a (n = 8)	CT	0	1	7
	DWI	8	0	0
Hemangioma ^a (n = 9)	CT	0	8	1
	DWI	5	2	2

Meta: Metastatic liver cancer; HCC: Hepatocellular carcinoma; DWI: Diffusion-weighted imaging; CT: Computed tomography. ^aP < 0.05.

background could not be measured easily in the images obtained using ASSET^[11].

ADC measurements

ADCs of both focal hepatic lesions and surrounding liver parenchymas (26 HCC, 32 metastatic liver cancers, four cholangiocarcinomas, 10 hemangiomas, eight cysts) were measured in 65 patients. Lesions in the lateral segments were excluded for ADC measurement because their ADC could not be correctly measured in the DWI sequences without simultaneous cardiac gating^[12].

Statistical analysis

ADC and SI were measured twice and averaged. All data are expressed as mean \pm SD. The visualization data was statistically analyzed by Wilcoxon's signed rank test, and RCR and ADC were analyzed by Student's *t* test using Prism 4.0 software (GraphPad Software, Inc., San Diego,

CA, USA). A *P* value of < 0.05 was considered statistically significant.

RESULTS

Visualization of lesions

Most malignant lesions were significantly more clearly visualized on DWI than on CT (Table 1). In particular, multiple small focal hepatic lesions were visualized clearly on DWI (Figure 1). Two malignant lesions were not detected on DWI, even though they could be easily detected on enhanced CT. These lesions were HCC just under the diaphragm of the lateral segment with liver cirrhosis. Benign lesions, by contrast, were significantly more poorly visualized on DWI than on CT. Similar to the results of several articles published previously^[13], cysts showed low or no signal intensities in six of eight cases on DWI (in these cases, no signal intensity means lower signal intensities than background signal intensities.). DWI visualized most hemangiomas; however, CT was better than DWI for the visualization of hemangiomas.

RCR measurements

The average RCR on DWI before and after SPIO administration is shown in Figure 2. RCR seemed to be significantly improved after SPIO administration in malignant lesions that were metastatic liver cancers (before: 2.39 ± 1.28 , after: 4.23 ± 1.34 , *n* = 26) and HCC (before: 1.85 ± 0.58 , after: 2.59 ± 1.28 , *n* = 18). On the other hand, the RCR was not significantly improved in benign lesions after SPIO administration. The RCR of cysts was 0.86 ± 0.30 (*n* = 7) before SPIO administration, because the SI of cysts was lower than background SI on DWI. Therefore, the RCR of cysts increased after SPIO

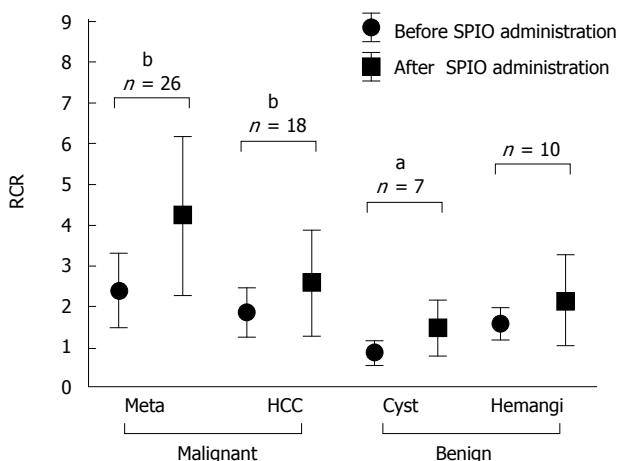


Figure 2 Relative contrast ratio (RCR) of focal hepatic lesions visualized by diffusion-weighted imaging (DWI) before and after the administration of superparamagnetic iron oxide (SPPIO). Meta: Metastatic liver cancer; HCC: Hepatocellular carcinoma; hemangi: Hepatic hemangioma. ^aP < 0.05, ^bP < 0.01.

administration (1.48 ± 0.65) as a result of a decrease in the SI of the liver. The RCR of hemangiomas was 1.58 ± 0.38 ($n = 10$) before and 2.15 ± 1.10 after SPPIO administration. This was not statistically significant. The RCRs of hemangiomas were reduced in three lesions after SPPIO administration. One example is shown in Figure 3.

Figure 4 is a case in which multiple small cysts and metastatic tumors of colon cancer were colocalized in the liver. Both cysts and cancers expressed high signal intensities in T2-weighted MR imaging. In contrast, only the metastatic nodules were expressed on DWI after SPPIO administration.

ADC measurements

Generally speaking, the lesions showing high signal intensity on DWI demonstrate low ADCs. The average ADCs in our study are shown in Figure 5. The ADCs (mean \pm SD $\times 10^{-3}$ mm 2 /s) of malignant lesions, both HCC (1.31 ± 0.28 , $n = 26$) and metastatic liver cancer (1.11 ± 0.22 , $n = 32$), were significantly lower than the ADCs of the surrounding hepatic tissues. The ADC of cholangiocarcinomas was 1.33 ± 0.23 ($n = 4$). Although this was lower than the ADC of the surrounding hepatic tissue, the difference was not significant.

In benign lesions, the ADCs of both cysts (2.61 ± 0.45 , $n = 8$) and hemangiomas (1.84 ± 0.37 , $n = 10$) were significantly higher than the ADC of the surrounding hepatic tissue. A representative hemangioma is shown in Figure 3, which expressed high signal intensity and high RCR on DWI. The ADC of the hemangioma was high even though their signal intensity was higher than the surrounding hepatic tissue on DWI. A representative hepatic cyst case is shown in Figure 6. The cyst expressed nearly no signal intensity on DWI after SPPIO administration. However, the cyst revealed a higher ADC value than the surrounding hepatic tissue on the ADC map.

DISCUSSION

Surgeons need new imaging modalities that can precisely

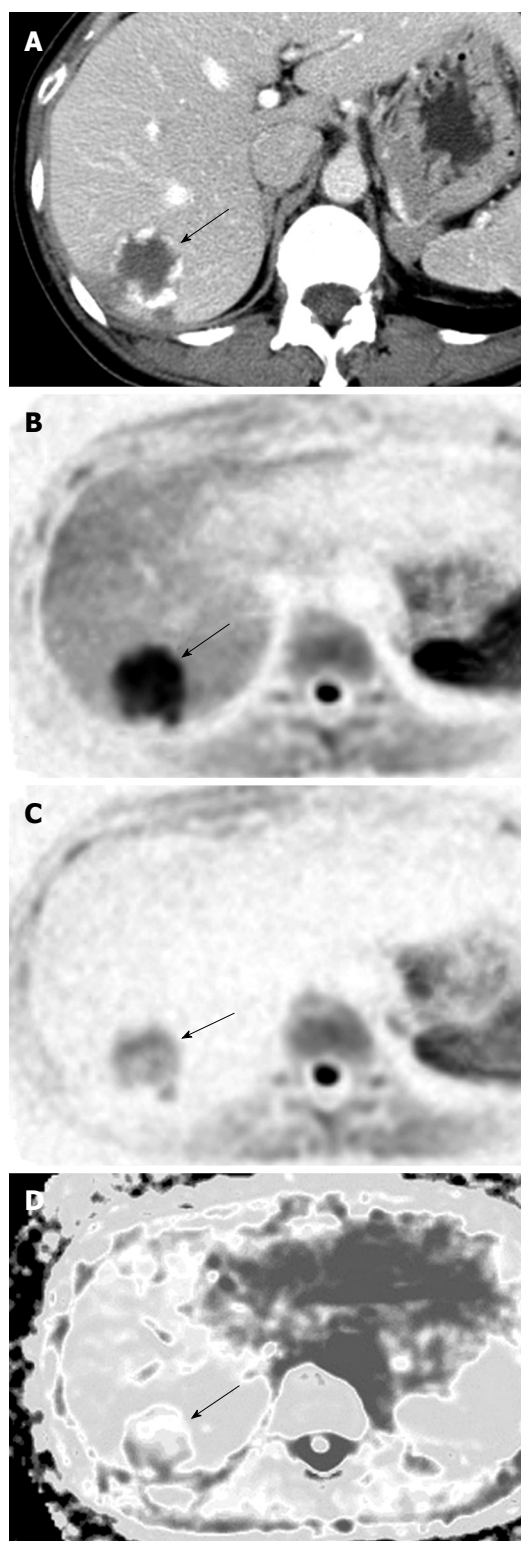


Figure 3 A case of hepatic hemangioma. A: Dynamic computed tomography in the portal phase showing a low-density mass with a marginal stain at the S7 lobe (arrow). This is a typical staining pattern for hemangiomas; B: The hemangioma (arrow) expressed high signal intensity on diffusion-weighted imaging; C: The intensity of this signal was reduced after administration of superparamagnetic iron oxide (arrow); D: The hemangioma showed a high apparent diffusion coefficient (ADC) value on the ADC map (arrow).

and concisely evaluate malignant lesions. DWI has recently emerged as a tool for detecting cancers in the abdominal organ field^[5,13,14]. Positron emission imaging is currently used as a powerful screening tool for malignancy^[15]. Some

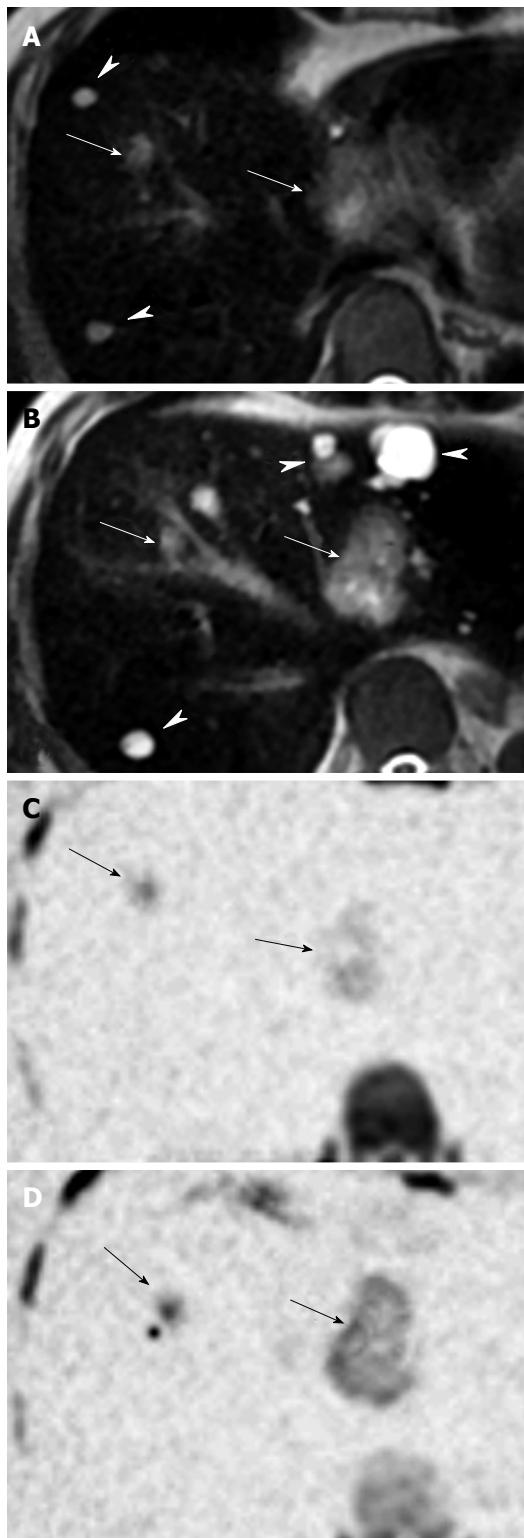


Figure 4 A case of multiple hepatic metastases of colon cancer with multiple hepatic cysts. A, B: T2-weighted magnetic resonance imaging showing high signal intensities on both metastatic lesions (arrows) and cysts (arrow heads); C, D: Diffusion-weighted imaging after administration of superparamagnetic iron oxide showing high signal intensities on metastatic lesions only (arrows).

articles have reported that SPIO-enhanced T2-weighted MR imaging and CT during arteriopertigraphy have the best ability to diagnose metastatic liver cancer^[8,9,16]. However, even with use of these modalities, differentiating

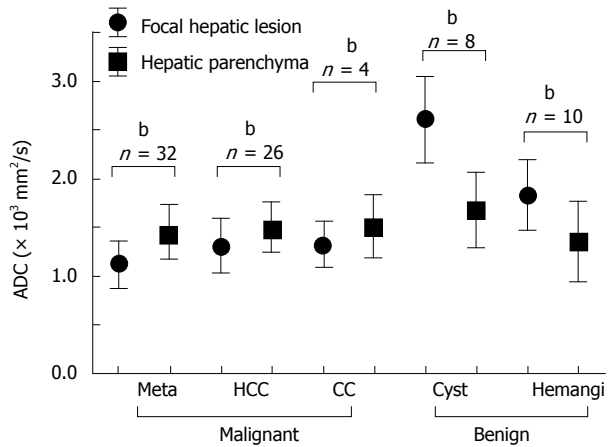


Figure 5 Comparison of apparent diffusion coefficient (ADC) between focal hepatic lesions and surrounding hepatic parenchyma. Meta: Metastatic liver cancer; HCC: Hepatocellular carcinoma; CC: Cholangiocarcinoma; Hemangi: Hepatic hemangioma. ^b $P < 0.01$.

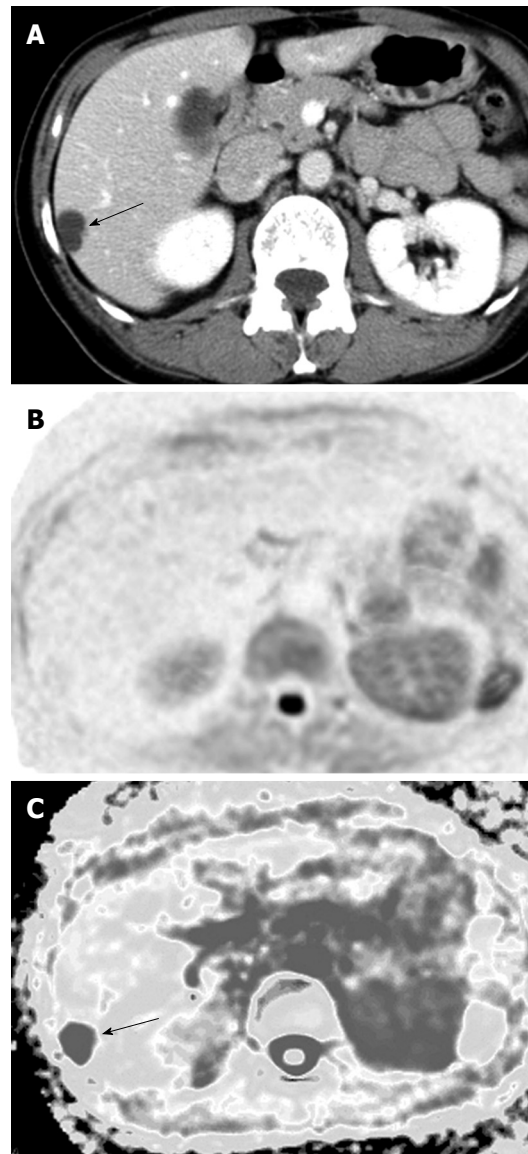


Figure 6 A case of hepatic cysts. A: Dynamic computed tomography in the portal phase showing the hepatic cyst as a low-density lesion (arrow); B: The lesion expressed no signal intensity on diffusion-weighted imaging; C: The lesion showed a high apparent diffusion coefficient (ADC) on the ADC map (arrow).

between malignant tumors and intrahepatic vascular structures (e.g. arterioportal shunts and thin vessels) or benign lesions (e.g. small cysts and hemangiomas) is sometimes difficult. One of the purposes of the current study was to evaluate the potential of DWI for differentiating malignant from benign lesions.

Nasu *et al*^[17] reported the sensitivity of DWI for detecting small metastases to be higher than that of SPIO-enhanced T2-weighted MR imaging because metastatic tumors tended to appear larger on DWI than on T2-weighted images, and intrahepatic vascular signals were suppressed on DWI. Parikh *et al*^[18] also reported that DWI was better than standard breath-hold T2-weighted imaging for the detection of focal hepatic lesions. In particular, they found much higher contrast between HCC and cirrhotic liver on DWI than on T2-weighted images. The contrasts between HCC and cirrhotic liver on DWI in the present study, however, were not higher than that between metastatic liver cancer and surrounding hepatic tissue. This finding might have been because the signal intensity of HCC was not so high as metastatic tumors and the signal intensity of the cirrhotic liver was irregularly increased in our study (data not shown), probably because of marked liver fibrosis, as previously noted^[19-21]. High signal intensities were found in most malignant focal hepatic lesions and DWI was useful for identifying them, as it was in previous studies^[17,18].

However, the findings of benign lesions differed from malignant lesions. Cysts and hemangiomas are most frequently found in the benign lesions of the liver. In the present study, the cysts had low or no signal intensities and hemangiomas had high or low signal intensities, similar to previous studies^[22]. Such lesions are usually diagnosed using major imaging modalities, such as ultrasonography and enhanced CT. However, because these lesions are small and multiple, differential diagnosis against malignant focal hepatic lesions is often difficult, even using these modalities. The characteristics of cysts on DWI, however, in which the cysts express low or no signal intensities, can enable differential diagnosis against malignant focal hepatic lesions, as shown in Figure 4.

Administration of SPIO in the present study reduced the signal intensity of liver parenchyma on DWI and increased the RCR of malignant focal hepatic lesions, but did not often increase the RCR of hepatic hemangiomas. Therefore, SPIO was quite useful for differential diagnosis, especially between small metastatic liver cancers and hepatic hemangiomas.

We used a high *b* value (1000 s/mm²) for DWI because a high *b* value allows delineation of malignant tumors with excellent conspicuity owing to the generally suppressed background noise. Furthermore, the differences in the RCR between malignant and benign lesions were increased with a high *b* value. However, this characteristic of DWI occasionally hinders defining the anatomical location of the abnormal signal on DWI. Therefore, the location of the signal must be correlated with ordinary T2 images by making the slice thickness, interslice gap, and fields of view uniform among these

images. Recent developments in fusion software can readily resolve this problem by anatomically overlapping DWI onto ordinary T2 images. Such fused images might allow improved detection of malignant tumors^[22].

ADC is a quantitative parameter calculated from DWI. ADC combines the effects of capillary perfusion and water diffusion in the extracellular and extravascular space^[1]. ADC is helpful for characterizing focal and diffuse diseases in the body. Several studies have reported that ADC can contribute to the differential diagnosis of benign and malignant focal lesions in the liver^[7,18,23].

Our results also revealed the contribution of ADC to the characterization of focal hepatic lesions. The ADC of malignant lesions was significantly lower than that of the surrounding hepatic tissue, whereas the ADC of benign lesions was higher than that of the surrounding hepatic tissue. Benign lesions, hemangiomas, and cysts in particular had high ADCs, even if they had high signal intensities on conventional DWI. The signal intensity of DWI includes both restricted diffusion and the effect of tissues with high T2 relaxation times, which is called the "T2 shine-through" effect. This might be why hemangiomas and cysts sometimes have high signal intensities on DWI. In any case, those results will be useful for differential diagnosis of malignant and benign focal hepatic lesions. For large lesions, however, the ADC was often markedly inhomogeneous on the locations and slices in the lesion. ADCs also seem to differ according to the machine used, the set-up conditions of the machine, and each human body^[24]. Thus, ADC must be carefully used in the evaluation of lesion characteristics.

A few malignant lesions could not be visualized by DWI in our study. These lesions were mainly located on the left lobe, just under the diaphragm. DWI is known to be extremely sensitive to motion. During clinical image interpretation of MRI, a signal drop is often encountered in the lateral segment of the liver, which is assumed to be due to cardiac pulsation. Not only the signal intensity of DWI, but also ADC, is thought to be incorrect for the lateral segment just under the diaphragm^[12,23,25]. Further studies need to be conducted to better understand the characteristics of DWI.

This study had some limitations. First, the subjects were a heterogeneous group, and the number of cases was relatively small. Second, histological proofs were not completely obtained, especially for the benign lesions. Therefore, the sensitivities and specificities of DWI cannot be reported here. Third, placement of the region of interest cursor might not be objective enough for measuring ADC and RCR. Additionally, inhomogeneity of hepatic lesions and motion may have affected the accuracy of the calculations, because the DWI was acquired with free breathing^[25].

Despite these limitations, we believe that DWI is a very useful imaging modality for identifying malignant focal lesions in the liver. Recently, a new MRI contrast medium, gadolinium-ethoxybenzyl-diethylenetriamine pentaacetic acid (Gd-EOB-DTPA), has been used for diagnosis of HCC. We plan to combine both Gd-EOB-

DTPA and DWI for diagnosing focal hepatic lesions.

In conclusion, DWI is a simple and sensitive method for screening focal hepatic lesions. SPIO administration can effectively improve the RCR of metastatic liver cancers. ADC measurement is occasionally helpful for differential diagnosis of malignant and benign small focal hepatic lesions.

COMMENTS

Background

Screening, accurate detection and characterization of focal hepatic lesions are important for planning treatment of malignant hepatic lesions. Recently, some studies have reported that the apparent diffusion coefficient (ADC), which is one of calculated parameters of diffusion-weighted imaging (DWI), might be useful for differential diagnosis of benign and malignant lesions in the liver. Superparamagnetic iron oxide (SPIO) has been reported to further improve the performance of DWI of the liver because SPIO reduces the signal in normal liver parenchyma. This study aimed to evaluate the usefulness of DWI in screening and differential diagnosis of benign and malignant focal hepatic lesions.

Research frontiers

In some previous studies, the ADC of benign lesions, such as hepatic cysts and hemangiomas, was reported to be higher than that of malignant lesions, such as hepatocellular carcinoma and metastasis. However, ADC seems differ according to the machine used, the set-up conditions of the machine, and each human body. In this study, the authors compared ADC of focal hepatic lesions with its surrounding hepatic parenchyma for this differential diagnosis. Only a few studies have statistically evaluated the contrast changes in focal hepatic lesions after SPIO administration.

Innovations and breakthroughs

This is the first report indicating that these simple ADC and RCR patterns are useful for the differential diagnosis of benign and malignant focal hepatic lesions.

Applications

DWI can be used for differential diagnosis of focal hepatic lesions using calculation of ADC or RCR after SPIO administration. This is a simple and concise method that is easily available, not only to the radiologist, but also the physician and surgeon. DWI also should become a good diagnostic tool for other intra-abdominal organs.

Terminology

Diffusion is the thermally induced motion of water molecules, which is also referred to as Brownian motion. DWI is a new magnetic resonance imaging (MRI) technique that provides images of the diffusion in biological tissues. The ADC is a quantitative parameter calculated from DWI and it combines the effects of capillary perfusion and water diffusion in the extracellular extravascular space. SPIO is a liver-specific particulate MRI contrast agent that is taken up by the reticuloendothelial system of the liver and improves the focal hepatic lesion-to-liver contrast-to-noise ratio and hepatic tumor detection.

Peer review

This is a retrospective study. The authors presented the results of their study and they reviewed the literature related with this subject. As a conclusion; the authors recommended that DWI by MR was a simple, sensitive and useful method for screening focal hepatic lesions and their differential diagnosis.

REFERENCES

- 1 Le Bihan D, Breton E, Lallemand D, Aubin ML, Vignaud J, Laval-Jeantet M. Separation of diffusion and perfusion in intravoxel incoherent motion MR imaging. *Radiology* 1988; **168**: 497-505
- 2 Sorenson AG, Buonanno FS, Gonzalez RG, Schwamm LH, Lev MH, Huang-Hellinger FR, Reese TG, Weisskoff RM, Davis TL, Suwanwela N, Can U, Moreira JA, Copen WA, Look RB, Finklestein SP, Rosen BR, Koroshetz WJ. Hyperacute stroke: evaluation with combined multislice diffusion-weighted and hemodynamically weighted echo-planar MR imaging. *Radiology* 1996; **199**: 391-401
- 3 Warach S, Chien D, Li W, Ronenthal M, Edelman RR. Fast magnetic resonance diffusion-weighted imaging of acute human stroke. *Neurology* 1992; **42**: 1717-1723
- 4 Moseley ME, Kucharczyk J, Mintorovitch J, Cohen Y, Kurhanewicz J, Derugin N, Asgari H, Norman D. Diffusion-weighted MR imaging of acute stroke: correlation with T2-weighted and magnetic susceptibility-enhanced MR imaging in cats. *AJNR Am J Neuroradiol* 1990; **11**: 423-429
- 5 Ichikawa T, Haradome H, Hachiya J, Nitatori T, Araki T. Diffusion-weighted MR imaging with single-shot echo-planar imaging in the upper abdomen: preliminary clinical experience in 61 patients. *Abdom Imaging* 1999; **24**: 456-461
- 6 Takahara T, Imai Y, Yamashita T, Yasuda S, Nasu S, Van Cauteren M. Diffusion weighted whole body imaging with background body signal suppression (DWIBS): technical improvement using free breathing, STIR and high resolution 3D display. *Radiat Med* 2004; **22**: 275-282
- 7 Gourtsoyianni S, Papanikolaou N, Yarmenitis S, Maris T, Karantanas A, Gourtsoyiannis N. Respiratory gated diffusion-weighted imaging of the liver: value of apparent diffusion coefficient measurements in the differentiation between most commonly encountered benign and malignant focal liver lesions. *Eur Radiol* 2008; **18**: 486-492
- 8 Strotzer M, Gmeinwieser J, Schmidt J, Fellner C, Seitz J, Albrich H, Zirngibl H, Feuerbach S. Diagnosis of liver metastases from colorectal adenocarcinoma. Comparison of spiral-CTAP combined with intravenous contrast-enhanced spiral-CT and SPIO-enhanced MR combined with plain MR imaging. *Acta Radiol* 1997; **38**: 986-992
- 9 Vogl TJ, Schwarz W, Blume S, Pietsch M, Shamsi K, Franz M, Lobeck H, Balzer T, del Tredici K, Neuhaus P, Felix R, Hammerstingl RM. Preoperative evaluation of malignant liver tumors: comparison of unenhanced and SPIO (Resovist)-enhanced MR imaging with biphasic CTAP and intraoperative US. *Eur Radiol* 2003; **13**: 262-272
- 10 Naganawa S, Sato C, Nakamura T, Kumada H, Ishigaki T, Miura S, Maruyama K, Takizawa O. Diffusion-weighted images of the liver: comparison of tumor detection before and after contrast enhancement with superparamagnetic iron oxide. *J Magn Reson Imaging* 2005; **21**: 836-840
- 11 Kwiat D, Einav S, Navon G. A decoupled coil detector array for fast image acquisition in magnetic resonance imaging. *Med Phys* 1991; **18**: 251-265
- 12 Nasu K, Kuroki Y, Sekiguchi R, Kazama T, Nakajima H. Measurement of the apparent diffusion coefficient in the liver: is it a reliable index for hepatic disease diagnosis? *Radiat Med* 2006; **24**: 438-444
- 13 Yamada I, Aung W, Himeno Y, Nakagawa T, Shibuya H. Diffusion coefficients in abdominal organs and hepatic lesions: evaluation with intravoxel incoherent motion echo-planar MR imaging. *Radiology* 1999; **210**: 617-623
- 14 Kim T, Murakami T, Takahashi S, Hori M, Tsuda K, Nakamura H. Diffusion-weighted single-shot echo-planar MR imaging for liver disease. *AJR Am J Roentgenol* 1999; **173**: 393-398
- 15 Rohren EM, Turkington TG, Coleman RE. Clinical applications of PET in oncology. *Radiology* 2004; **231**: 305-332
- 16 Kim YK, Kwak HS, Han YM, Kim CS. Usefulness of combining sequentially acquired gadobenate dimeglumine-enhanced magnetic resonance imaging and resovist-enhanced magnetic resonance imaging for the detection of hepatocellular carcinoma: comparison with computed tomography hepatic arteriography and computed tomography arteriopertigraphy using 16-slice multidetector computed tomography. *J Comput Assist Tomogr* 2007; **31**: 702-711
- 17 Nasu K, Kuroki Y, Nawano S, Kuroki S, Tsukamoto T, Yamamoto S, Motoori K, Ueda T. Hepatic metastases: diffusion-weighted sensitivity-encoding versus SPIO-enhanced MR imaging. *Radiology* 2006; **239**: 122-130
- 18 Parikh T, Drew SJ, Lee VS, Wong S, Hecht EM, Babb JS,

- Taouli B. Focal liver lesion detection and characterization with diffusion-weighted MR imaging: comparison with standard breath-hold T2-weighted imaging. *Radiology* 2008; **246**: 812-822
- 19 Lewin M, Poujol-Robert A, Boelle PY, Wendum D, Lasnier E, Viallon M, Guechot J, Hoeffel C, Arrive L, Tubiana JM, Poupon R. Diffusion-weighted magnetic resonance imaging for the assessment of fibrosis in chronic hepatitis C. *Hepatology* 2007; **46**: 658-665
- 20 Girometti R, Furlan A, Bazzocchi M, Soldano F, Isola M, Toniutto P, Bitetto D, Zuiani C. Diffusion-weighted MRI in evaluating liver fibrosis: a feasibility study in cirrhotic patients. *Radiol Med* 2007; **112**: 394-408
- 21 Taouli B, Tolia AJ, Losada M, Babb JS, Chan ES, Bannan MA, Tobias H. Diffusion-weighted MRI for quantification of liver fibrosis: preliminary experience. *AJR Am J Roentgenol* 2007; **189**: 799-806
- 22 Koyama T, Tamai K, Togashi K. Current status of body MR imaging: fast MR imaging and diffusion-weighted imaging. *Int J Clin Oncol* 2006; **11**: 278-285
- 23 Bruegel M, Holzapfel K, Gaa J, Woertler K, Waldt S, Kiefer B, Stemmer A, Ganter C, Rummeny EJ. Characterization of focal liver lesions by ADC measurements using a respiratory triggered diffusion-weighted single-shot echo-planar MR imaging technique. *Eur Radiol* 2008; **18**: 477-485
- 24 Kuroki Y, Nasu K, Nawano S, Sekiguchi R. Diffusion-weighted MR imaging of the liver. *Nichidoku-aho* 2007; **52**: 72-81
- 25 Nasu K, Kuroki Y, Sekiguchi R, Nawano S. The effect of simultaneous use of respiratory triggering in diffusion-weighted imaging of the liver. *Magn Reson Med Sci* 2006; **5**: 129-136

S- Editor Wang JL L- Editor Stewart GJ E- Editor Ma WH



NT4(Si)-p53(N15)-antennapedia induces cell death in a human hepatocellular carcinoma cell line

Li-Ping Song, Yue-Ping Li, Ning Wang, Wei-Wei Li, Juan Ren, Shu-Dong Qiu, Quan-Ying Wang, Guang-Xiao Yang

Li-Ping Song, Ning Wang, Wei-Wei Li, Juan Ren,
Department of Radiotherapy Oncology, First Hospital, Medical School of Xi'an Jiao Tong University, Xi'an 710061, Shaanxi Province, China

Yue-Ping Li, Center for Reproductive Medicine, Affiliated Hospital of Hainan Medical College, Haikou 570102, Hainan Province, China

Shu-Dong Qiu, Department of Anatomy and Histology & Embryology, Medical school of Xi'an Jiao Tong University, Xi'an 710061, Shaanxi Province, China

Quan-Ying Wang, Guang-Xiao Yang, Xi'an Huaguan Bioengineering Co, Xi'an 710061, Shaanxi Province, China

Author contributions: Song LP designed the research; Song LP, Li YP, Li WW and Wang N performed the research; Qiu SD, Wang QY and Yang GX provided the new reagents, analytical tools, and analyzed the data; Song LP, Li YP, Wang N, Li WW and Ren J wrote the paper.

Supported by The National Natural Science Foundation of China, No. 30471942 and the Key Science Research Project of Shaanxi Province, No. 2004k11-G3

Correspondence to: Li-Ping Song, MD, PhD, Department of Radiotherapy Oncology, First Hospital, Medical School of Xi'an Jiao Tong University, Xi'an 710061, Shaanxi Province, China. slpwn@126.com

Telephone: +86-29-85324029 Fax: +86-29-85323187

Received: September 20, 2009 Revised: November 5, 2009

Accepted: November 12, 2009

Published online: December 14, 2009

Abstract

AIM: To construct the recombinant lentivirus expression plasmid, pLenti6/V5-NT4 p53(N15)-antennapedia (Ant), and study its effect on HepG2 cells.

METHODS: Plasmid pLenti6/V5-NT4 p53(N15)-Ant was constructed incorporating the following functional regions, including signal peptide sequence and pro-region of neurotrophin 4, N-terminal residues 12-26 of p53 and 17 amino acid drosophila carrier protein, Ant. Hepatocellular carcinoma (HepG2) cells were used for transfection. 3-[4,5-dimethyl-thiazol-2yl]-2,5 diphenyl tetrazolium bromide (MTT) assay, lactate dehydrogenase (LDH) release assay, transmission electron microscopy (TEM) and flow cytometric analysis (FCM) were employed to investigate the effects of LV-NT4(Si)-p53(N15)-Ant *in vitro* on HepG2 cells. *In vivo* experiment was also performed to investigate the inhibitory effect of LV-NT4(Si)-p53(N15)-Ant on tumor growth in nude mice.

RESULTS: LV-NT4(Si)-p53(N15)-Ant significantly suppressed the growth of HepG2 cells. MTT assay showed that the growth of HepG2 cells was much more significantly inhibited by LV-NT4(Si)-p53(N15)-Ant than by LV-EGFP. The inhibition rate for HepG2 cell growth in the two groups was 46.9% and 94.5%, respectively, 48 h after infection with LV-NT4(Si)-p53(N15)-Ant, and was 33.9% and 95.8%, respectively, 72 h after infection with LV-NT4(Si)-p53(N15)-Ant ($P < 0.01$). Light microscopy and TEM showed morphological changes in HepG2 cells infected with LV-NT4(Si)-p53(N15)-Ant, but no significant changes in HepG2 cells infected with LV-EGFP. Changes were observed in ultra-structure of HepG2 cells infected with LV-NT4(Si)-p53(N15)-Ant, with degraded membranes, resulting in necrosis. LDH release from HepG2 cells was analyzed at 24, 48, 72 and 96 h after infection with LV-NT4(Si)-p53(N15)-Ant and LV-EGFP, which showed that LDH release was significantly higher in LV-NT4(Si)-p53(N15)-Ant treatment group (682 IU/L) than in control group (45 IU/L, $P < 0.01$). The longer the time was after infection, the bigger the difference was in LDH release. FCM analysis showed that LV-NT4(Si)-p53(N15)-Ant could induce two different kinds of cell death: necrosis and apoptosis, with apoptosis being the minor type and necrosis being the main type, suggesting that LV-NT4(Si)-p53(N15)-Ant exerts its anticancer effect on HepG2 cells by inducing necrosis. The *in vivo* study showed that LV-NT4(Si)-p53(N15)-Ant significantly inhibited tumor growth with an inhibition rate of 66.14% in terms of tumor size and weight.

CONCLUSION: LV-NT4(Si)-p53(N15)-Ant is a novel recombinant lentivirus expression plasmid and can be used in gene therapy for cancer.

© 2009 The WJG Press and Baishideng. All rights reserved.

Key words: Gene therapy; Lentivirus vector; Anticancer; Necrosis; LV-NT4(Si)-p53(N15)-Ant; Hepatocellular carcinoma cell line

Peer reviewers: Lin Zhang, PhD, Associate Professor, Department of Pharmacology & Chemical Biology, University of Pittsburgh Cancer Institute, University of Pittsburgh School of Medicine, UPCI Research Pavilion, Room 2.42d, Hillman Cancer Center, 5117 Centre Ave., Pittsburgh, PA 15213-1863, United States; Sung-Gil Chi, Professor, School of Life Sciences and Biotechnology, Korea University, #301, Nok-Ji Building, Seoul 136-701, Korea; Jian-Zhong Zhang, Professor, Department

of Pathology and Laboratory Medicine, Beijing 306 Hospital, 9 North Anxiang Road, PO Box 9720, Beijing 100101, China

Song LP, Li YP, Wang N, Li WW, Ren J, Qiu SD, Wang QY, Yang GX. NT4(Si)-p53(N15)-antennapedia induces cell death in a human hepatocellular carcinoma cell line. *World J Gastroenterol* 2009; 15(46): 5813-5820 Available from: URL: <http://www.wjgnet.com/1007-9327/15/5813.asp> DOI: <http://dx.doi.org/10.3748/wjg.15.5813>

INTRODUCTION

Hepatocellular carcinoma (HCC) is one of the most common causes of death worldwide, especially in Asian countries^[1]. To date, none of the conventional treatment modalities can completely eradicate HCC cells. In recent years, gene therapy has been evaluated as a novel treatment modality for HCC^[2-5], while conventional treatment modalities, including surgery, chemotherapy and liver transplantation, are still used^[6-8].

p53 is an important tumor suppressor gene which regulates many important cellular activities, including apoptosis. Mutations and deletions of the *p53* gene are common in HCC in a number of geographic regions. Since the mutation incidence ranges 5%-50%, *p53* has become an ideal target for gene therapy. Kanovsky *et al*^[9] and Do *et al*^[10] reported that a *p53* peptide, synthesized from residues 12-26 and fused with the Drosophila carrier protein antennapedia (Ant), can induce rapid tumor cell necrosis in all breast and pancreatic cancer cell lines irrespective of its status and exhibits a low cytotoxicity to normal cells, which is uncommonly observed in traditional cancer therapy. Human HCC cell line, HepG2, contains the wild-type *p53* gene and can thus be used in research of the relation between HCC and *p53* peptide gene therapy.

It is important to study the transfer of fusion gene and the secretion of expressed protein for the assessment of enhanced cancer-killing effects of a protein. In this study, NT4 signal peptide and its pro-region were used as the regions responsible for protein and peptide secretion from cells. Lentivirus gene expression plasmids were constructed for NT4(Si)-ADNF-9 and NT4(Si)-NAP fusion proteins containing the NT4 signal peptide and pro-region to enhance their expression. The restriction enzyme site *NaeI* at the NT4 signal peptidase fissure site and two restriction enzyme sites, *BamH I* and *Xho I*, in NT4(Si)-p53(N15)-Ant could ensure the correct construct. A novel recombinant lentivirus expression plasmid, pLenti6/V5-NT4 p53(N15)-Ant, was constructed, containing a signal peptide sequence and pro-region of neurotrophin 4 (NT4) fused to p53(N15)-Ant peptide. Its effect on HepG2 cells, both *in vitro* and *in vivo*, was investigated.

MATERIALS AND METHODS

Cells and cell culture

Human hepatoma HepG2 cells containing wild-type *p53* were cultured in RPMI 1640 containing 10% fetal bovine serum (FBS). 293T human kidney cells were

grown in Dulbecco's modified Eagle's medium (DMEM) supplemented with 10% FBS, 100 U/mL penicillin and 100 µg/mL streptomycin at 37°C in a humidified atmosphere containing 50 mL/L CO₂. All cell lines were supplied by Xi'an Huaguang Bioengineering Company (Xi'an, China).

Plasmid construction and virus titration

p53(N15)-Ant was synthesized by Beijing Sun Biotechnology Co, according to Kanovsky *et al*^[9] and Genbank. Two restriction enzyme sites (*Nae I* and *Xho I*) were introduced upstream and downstream of this sequence, respectively. p53(N15)-Ant was subcloned into pGEM-T-easy for sequencing, then into pBV220/NT4. Signal peptide sequence and pro-region of NT4 were cloned from human genomic DNA and subcloned into the *BamH I* / *Nae I* sites of pBV220. After digestion with restriction enzymes, the resulting NT4 p53(N15)-Ant gene with *BamH I* and *Xho I* sites from the pBV220/NT4-p53-(N15)-Ant plasmid was inserted into the multiple cloning site of the expression plasmid, pLenti6/V5-D-TOPO (Invitrogen) containing a cytomegalovirus (CMV) promoter, upstream of the inserted gene. The resulting plasmid was named pLenti6/V5-NT4 p53(N15)-Ant.

To generate a control plasmid containing green fluorescent protein, EGFP was amplified from EGFP-C2 by PCR. The sequences of sense and anti-sense primers are 5'CGGGATCCATGGTGAGCAAGGGCGAGG-3' and 5'CGCTCGAGTCAAGTCCGGCCGGACTTGTAC-3', respectively. The resultant PCR fragments were digested with *BamH I* and *Xho I* (underlined), subcloned into pLenti6/V5-D-TOPO, and verified by DNA sequencing.

The four-plasmid-based lentiviral expression system was purchased from Invitrogen. Briefly, four kinds of plasmid including 4.2 µg of pLP1, 2 µg of pLP2, 2.8 µg of pLP/VSVG and 3 µg of lentivector pLenti6/V5-NT4 p53(N15)-Ant or pLenti6/EGFP, were cotransfected into 293T cells using the calcium phosphate coprecipitation method. The conditioned medium was harvested 72 h after transfection and filtered through a 0.45 µm filter. Concentrated viral stocks were prepared by ultra-centrifugation of 3 mL conditioned medium at 50 000 g for 1.5 h at 4°C in a SW41 rotor (Beckman). The pellet was resuspended in 30 µL complete medium and stored at -80°C. The resulting recombinant lentivirus was named LV-NT4 p53(N15)-Ant and LV-EGFP, respectively.

Viral titer was measured by assessing the viral p24 antigen concentration using ELISA (Beckman Coulter, Fullerton, California, USA), showing that one microgram per milliliter of p24 corresponds to approximately 2×10^6 transducing units per milliliter of EGFP virus, as assessed by titration in 293 T cells.

Lentivirus-mediated gene transfer and expression in HepG2 cells

HepG2 cells were seeded into 6-well plates at a density of 1×10^6 cells/well, allowed to adhere for 24 h, and then infected with EGFP lentivirus at multiplicities of infection (MOI) of 4 transducing units (TU)/cell. EGFP-positive cells were observed and counted under a fluorescence microscope 48 h after infection.

Expression of the *NT4 p53(N15)-Ant* gene was detected by reverse transcription-polymerase chain reaction (RT-PCR). HepG2 cells were seeded in 100 mL culture flasks at a density of 1×10^6 cells/flask and infected with NT4-p53(N15)-Ant lentivirus at a MOI of 4 TU/cell. Forty-eight hours after infection, HepG2 cells were scraped from the flask surface with a brush (Paro-Isola, Thalwil, Switzerland). Total RNA was extracted using Trizol reagent (Gibco). A reverse transcription (RT) step was carried out for 60 min at 37°C using 1 µg total RNA treated with DNase and M-MLV reverse transcriptase (Invitrogen, USA) in the presence of random primers. PCR was performed in 50 µL reaction volume containing 10 µL (about 2.5 ng) cDNA, 1 µL of 10 mmol/L dNTP, 1 U of Taq DNA polymerase, 5 µL of 10 × Taq buffer, and 1 µL 50 pmol of forward primer (5'-CG GATCCATGCTCCCTCTCCCCTCATGC-3') and reverse primer (5'-CCTCGAGTCATCCCGCGCTGTACCTTACC-3') of the *NT4 p53(N15)-Ant* gene. Samples were subjected to RT-PCR at the following conditions: pre-denaturation for 5 min at 94°C, followed by 30 cycles of denaturation for 60 s at 94°C, annealing for 60 s at 60°C, extension for 90 s at 72°C, and a final extension for 5 min at 72°C. The RT-PCR products were separated by electrophoresis on 2% agarose gels (Qiagen, USA).

Immunohistochemical detection of p53(N15)-Ant expression in lung cancer H1299 cells

H1299 cells (null for p53) were seeded onto cover slips and infected with LV-NT4(Si)-p53(N15)-Ant at a MOI of 4 TU/well. Polybrene was added to a final concentration of 8 µg/mL. Twelve hours after infection, 2 mL of a new DMEM medium was added. Forty-eight hours after infection, H1299 cells were washed and fixed with cold acetone. Protein expression of p53(N15)-Ant in H1299 cells was determined by immunocytochemical staining with anti-p53 antibody (DO-1) (Santa Cruz Biotechnology, Santa Cruz, CA, USA) using the Vectastain Elite ABC kit following its manufacturer's instructions (Vector Laboratories, Burlingame, CA, USA).

MTT assay

To determine the effect of lentivirus-NT4(Si)-p53(N15)-Ant on HCC, HepG2 cells were seeded in 96-well plates at a concentration of 5×10^3 cells, grown for 24 h, infected with lentivirus-NT4(Si)-p53(N15)-Ant or lentivirus-EGFP at a MOI of 4 TU/cell with polybrene (8 µg/mL) for 12 h. The culture medium was then replaced with a fresh medium. MIT assay was performed at different time points (24, 48 and 72 h) after infection with lentivirus according to its manufacturer's instructions (Xi'an, China).

Examination of HepG2 cell morphology under light microscope

After infection with NT4(Si)-p53(N15)-Ant, morphology of HepG2 cells was observed under an inverted light microscope and recorded.

Examination of ultra-structure of HepG2 cells under electron microscope

Forty-eight hours after infection with NT4(Si)-p53(N15)-Ant, HepG2 cells were trypsinized, fixed with 2.5% glutar-

aldehyde for 2 h at 4°C, washed with 0.1 mol/L dimethyl arsenic trioxide buffer, fixed with 1% osmium acid for 2 h, dehydrated, and then embedded in 618 domestic epoxy resin, followed by polymerization for 24 h. The embedded block was cut into ultra-thin sections. The sections were double stained with uranyl acetate and lead citrate, and observed under a transmission electron microscope.

LDH release assay

To determine LDH leakage into the extra-cellular fluid, supernatant was collected at different time points (24, 48, 72, and 96 h) after infection with NT4(Si)-p53(N15)-Ant. LDH in the supernatant was detected with a RA-100 automatic biochemical analyzer.

Annexin V and PI double staining

When HepG2 cells were grown to 2×10^5 /mL, they were seeded into 9-well plates at a volume of 3 mL/well, and left to adhere for 24 h. The cells were then divided into control group and lentivirus treatment group. The cells in control group were grown in a serum-free medium. Forty-eight hours after infection with lentivirus, the cells were washed twice with PBS at 4°C, re-suspended in 250 µL of a combination buffer solution, and the cell concentration was adjusted to 1×10^5 /mL. Five microliter of Annexin V/FITC and 5 µL of 20 µg/mL propidium iodide were added to 100 µL of cell suspension. After incubation in the dark for 15 min, the cells were analyzed by flow cytometry (FCM).

Inhibition of HepG2 cells in nude mice by LV-NT4(Si)-p53(N15)-Ant

Twenty 6-8 wk old male and female BALB/c (nu/nu) mice, weighing 20.3 ± 2 g, were purchased from Laboratory Animal Center, Fourth Military Medical University (Xi'an, China).

HepG2 cells (2×10^5) were injected subcutaneously on the right side of each mouse's back to induce tumor formation. The animals were divided into three groups when the tumor volume reached 30 mm^3 with 0.1 mL LV-NT4(Si)-p53(N15)-Ant (2×10^6 TU/mL) injected into their tumor. Mice treated with PBS and LV-EGFP served as controls with 0.1 mL LV-EGFP (2×10^6 TU/mL) injected into their tumor (injection at different directions). Infection efficiency of lentivirus was observed under a confocal laser scanning microscope one week after infection.

The animals were sacrificed 3 wk after injection of lentivirus. Tumors were removed and weighed with their size measured using a vernier caliper and their volume calculated according to the following formula: $(3.14 \times L \times W \times H)/6$. Tumors were fixed in 4% formaldehyde and embedded in paraffin. Tumor tissue was cut into 5-µm thick sections which were stained with HE.

Tumor growth inhibition rate = $(A-B)/A * K$, where A is the average tumor weight of control group, B is the average tumor weight of treatment group, K represents 100%.

Statistical analysis

The data were expressed as mean \pm SD. LDH release and

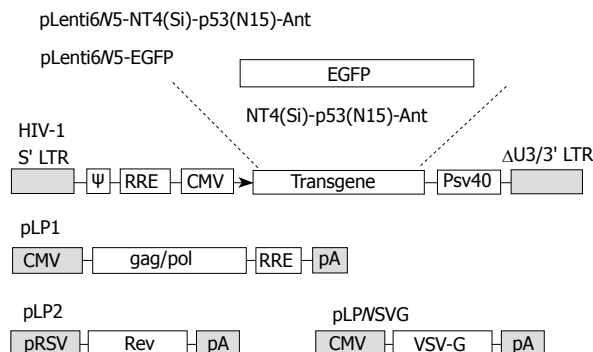


Figure 1 Packaging system of LV-NT4(Si)-p53(N15)-Ant and LV-EGFP. The packaging system: lentiviral vector, pLenti6/V5-D-TOPO, contains HIV-1 5'LTR, packaging signal (ψ), RRE sequence, CMV promoter and 3'LTR from which some regulatory sequences are deleted, resulting in "self-inactivation" of lentivirus after transduction of the target cells. pLP1, pLP2 and pLP/VSVG are three helper plasmids, which provide structural and replication proteins to produce lentivirus.

MIT were analyzed by *t*-test and χ^2 test, respectively. The data for animal experiment were processed by analysis of variance. Data analysis was performed using the SPSS 15.0. $P < 0.05$ was considered statistically significant.

RESULTS

Construction of lentivirus vector expressing NT4-p53(N15)-Ant or EGFP

The lentivirus expression vector, pLenti6 V5-D-TOPO we constructed, contains the elements required for virion packaging, such as 5' and 3' long terminal repeats and ψ packaging signal. The packaging system of LV-NT4(Si)-p53(N15)-Ant and LV-EGFP is shown in Figure 1.

The DNA sequence of the p53(N15)-Ant gene was identical to those of p53(N15) and 17 amino acid Ant^[9]. The length of NT4-p53(N15)-Ant was 349 bp, including a 247 bp fragment of the signal peptide sequence and pro-region of neurotrophin 4 with the two restriction sites (BamH I and Nae I). The DNA fragment of p53(N15)-Ant was 108 bp with Nae I and Xho I. Digestion of pLenti6/V5-NT4-p53(N15)-Ant with BamH I and Nae I followed by electrophoresis verified that the NT4-p53(N15)-Ant secretory expression cassette was correctly inserted into the multiple cloning site (MCS) of pLenti6/V5-D-TOPO, and pLenti6/V5-EGFP was confirmed in the same way as pLenti6/V5-NT4-p53(N15)-Ant.

Gene transfer and lentivirus expression in HepG2 cells

Fluorescent microscopic analysis showed that EGFP was expressed in over 60% of HepG2 cells 48 h after infection with pLenti6/V5-EGFP at a MOI of 4 TU/cell (Figure 2A and B).

Expression of NT4-p53(N15)-Ant in lentivirus-delivered H1299 cells

Since H1299 cells lack of the p53 gene (null-p53), H1299 lung cancer cells were used as target cells for the expression of p53(N15)-Ant. p53 protein could not be detected with immunohistochemical staining before or after infection with LV-EGFP (Figure 2C). However, 48 h

after infection with LV-NT4(Si)-p53(N15)-Ant, p53 protein was mainly expressed in cytoplasm of H1299 lung cancer cells (Figure 2D). Anti-DO-1 could identify and bind to amino acids 11-25 of p53, suggesting that LV-NT4(Si)-p53(N15)-Ant can effectively infect the target cells and express the p53 fusion peptide.

Killing effect of lentivirus-NT4 p53(N15)-Ant on HepG2 cells in vitro

HepG2 cells, infected with pLenti6/V5-NT4-p53(N15)-Ant in our study, were significantly killed, whereas pLenti6/V5-EGFP had no effect on cell viability, suggesting that growth of HepG2 cells can be inhibited by the transferred exogenous gene rather by viral toxicity (Figure 3).

Morphological changes in HepG2 cells observed under light microscope

Significant morphological changes were observed in HepG2 cells at different time points after infection with LV-NT4(Si)-p53(N15)-Ant but not after infection with LV-EGFP and LV-NT4(Si)-p53(N15)-Ant (Figure 4). However, the cells became swollen and their boundary was blurred 48 h after infection with LV-NT4(Si)-p53(N15)-Ant, while their viability was significantly declined with noticeable cell shrinkage, fragments and detachment 72 h after infection with LV-NT4(Si)-p53(N15)-Ant, but without significant morphological changes 72 h after infection with LV-EGFP infection.

Changes in ultra-structure of HepG2 cells observed under electron microscope

Forty-eight hours after infection with LV-EGFP, the membranes and nuclear membranes of HepG2 cells were intact with some crimples in the nuclear membranes, some microvilli on the surface of HepG2 cells, normal structure of mitochondria and ER (Figure 5A), and 2 completely divided HepG2 cells (Figure 5B), suggesting that LV-EGFP has no significant effect on cell growth and division. Forty-eight hours after infection with LV-NT4(Si)-p53(N15)-Ant, significant changes in ultra-structure of HepG2 cells, as well as in cell membranes and mitochondria, were observed under electron microscope. Cell membranes were incomplete with several fractures and the cells appeared to leak contents. Mitochondria were swollen with vacuolization. Vacuoles were also seen under the nuclear membrane with bare nuclei (Figure 5C and D). These findings suggest that NT4(Si)-p53(N15)-Ant may exert its anticancer effect mainly by inducing necrosis of cell membranes.

Determination of LDH release

LDH was significantly increased in LV-NT4(Si)-p53(N15)-Ant treatment group, but not in LV-EGFP treatment group, with no significant difference between the two groups. The longer the time was after the infection, the greater the difference was between the groups, suggesting that cell membranes are damaged.

Annexin V-PI double staining

Flow cytometry (FCM) was employed to detect the

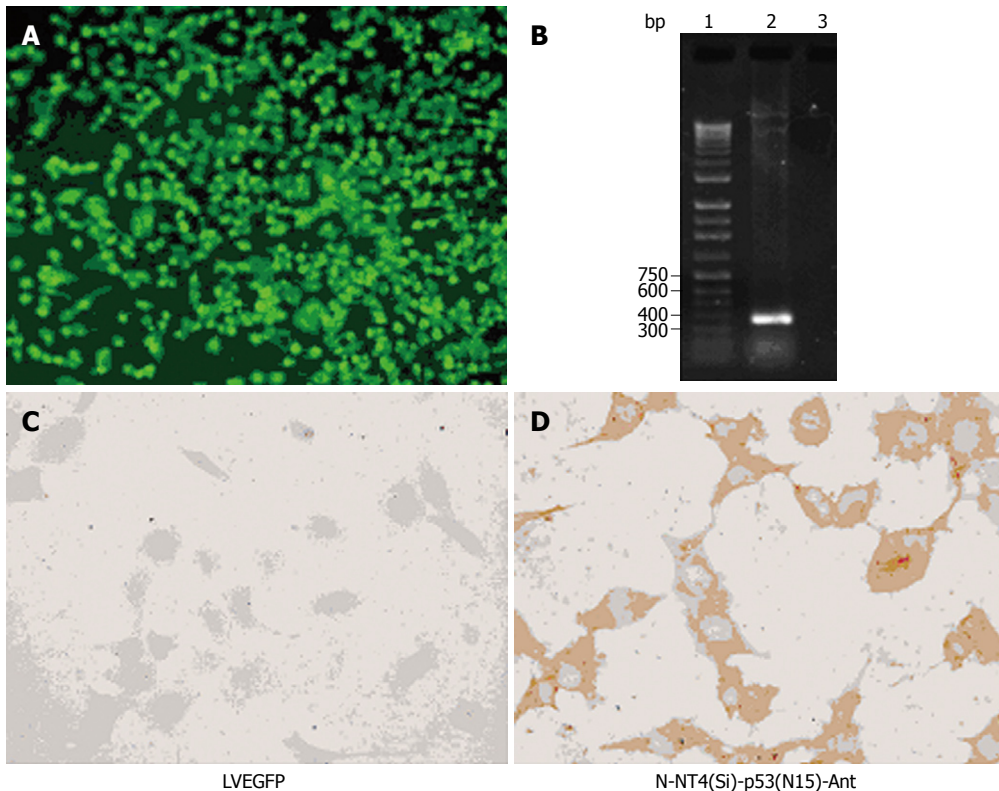


Figure 2 Fluorescent microscopic analysis and immunohistochemical staining. Fluorescence microscopy analysis showing EGFP expression in HepG2 cells (A), agarose gel electrophoresis of RT-PCR products from HepG2 cells (B) [lane 1: 1.0 kb DNA ladder; lane 2: RT-PCR products from cells infected with LV-NT4(Si)-p53(N15)-Ant; lane 3: negative controls infected with LV-EGFP], immunohistochemical staining showing no p53 protein (C), and p53 protein expression in cytoplasm of HepG2 cells (D) 48 h after infection with LV-NT4(Si)-p53(N15)-Ant.

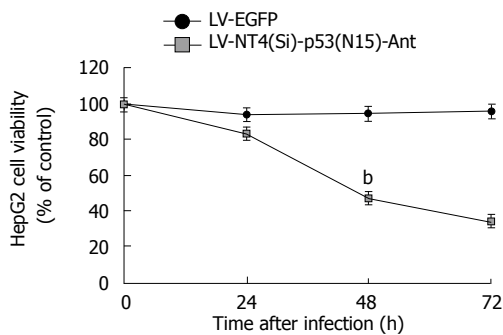


Figure 3 Cytotoxicity of LV-NT4(Si)-p53(N15)-Ant to HepG2 cells at different time points (24, 48 and 72 h) after infection with lentivirus. $^bP < 0.01$ vs LV-EGFP.

fluorescence intensity after HepG2 cells were double-stained with Annexin V and PI. A plot composed of 4 quadrants was detected by flow cytometry, which showed that the number of necrotic cells was significantly greater in LV-NT4(Si)-p53(N15)-Ant treatment group than in LV-EGFP treatment group 48 h after infection with lentivirus. The apoptosis level was also higher in cells expressing LV-p53(N15) than in controls. However, the number of necrotic cells was still much greater than that of apoptotic cells (Figure 6), suggesting that the NT4(Si)-p53(N15)-Ant gene kills tumor cells mainly by inducing necrosis of cell membrane.

Inhibition of HepG2 cell growth in nude mice by LV-NT4(Si)-p53(N15)-Ant

Nude mice developed tumor mass within 10 d after inoculation with HepG2 cells. Three weeks after infection with lentivirus, the size and weight of tumor mass were measured (Figure 7A and B). The inhibition

rate of tumor growth for LV-NT4(Si)-p53(N15)-Ant was 66.14%.

DISCUSSION

p53 protein plays an essential role in cell activities^[11,12]. Under various stress conditions, such as genotoxic damage, hypoxia, ribonucleotide depletion or oncogene activation, p53 molecule accumulates and is activated. Activated p53 acts as a transcription factor and activates or represses a variety of genes involved in cell-cycle regulation, induction of apoptosis or senescence. Therefore, the p53 gene represents an ideal target for cancer therapy. In non-stressed cells, p53 protein is present at a very low cellular concentration, because it interacts with the hdm2 protein, the human analogue of murine mdm2, which acts as a ligase of ubiquitin^[13,14] and promotes p53 degradation^[9,10]. Recent advances in regulation of p53 by hdm2 offer the possibility of generating new anticancer agents that activate wild-type p53 in tumors. Since hdm2 down-regulates p53, inhibition of this interaction would lead to an accumulation of p53 in tumor cells, eventually inducing their death^[10,15]. p53(N15)-Ant has been considered a novel cancer therapeutic peptide because it induces cancer cell death and does not seem to be cytotoxic to normal cells and may, therefore, prove useful as a general anticancer agent. In this study, we focused on how to improve the anticancer effect of peptide therapy by employing two strategies. The first was to enable the expressed therapeutic peptide to be secreted, and the second was to use the lentivirus gene transfer system. It is well-known that the signal peptide is located at the terminal of amino acid sequence of a secreted protein and plays an important role in protein targeting

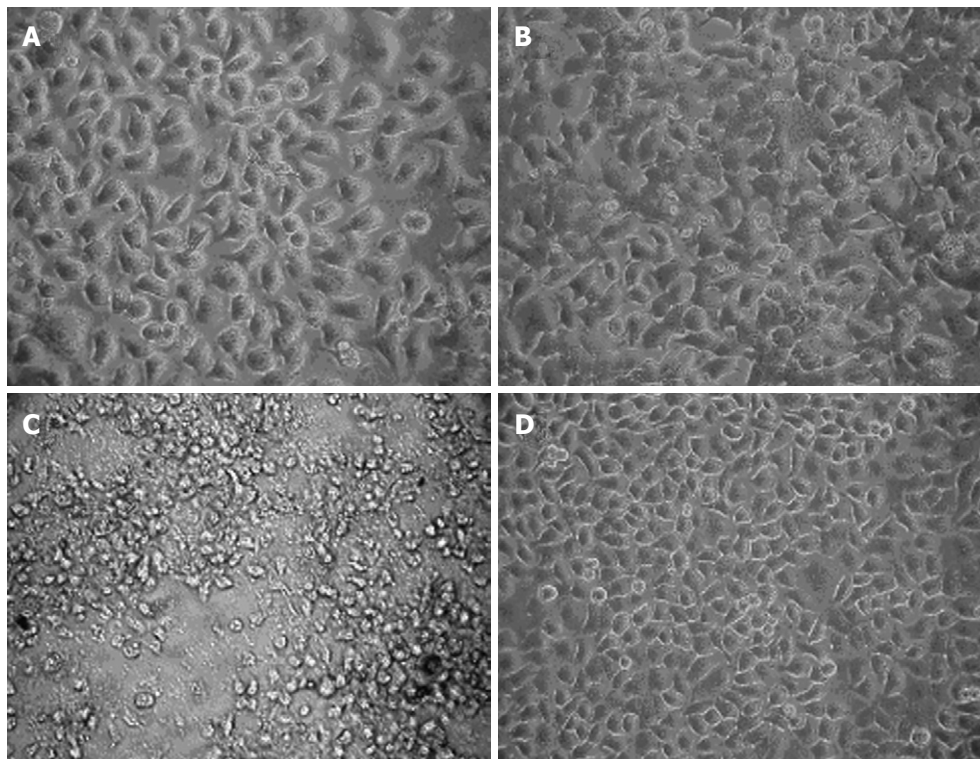


Figure 4 Morphological changes in HepG2 cells 24 h (A), 48 h (B), 72 h (C) after infection with LV-NT4(Si)-p53(N15)-Ant and 72 h (D) after infection with LV-EGFP ($\times 400$).

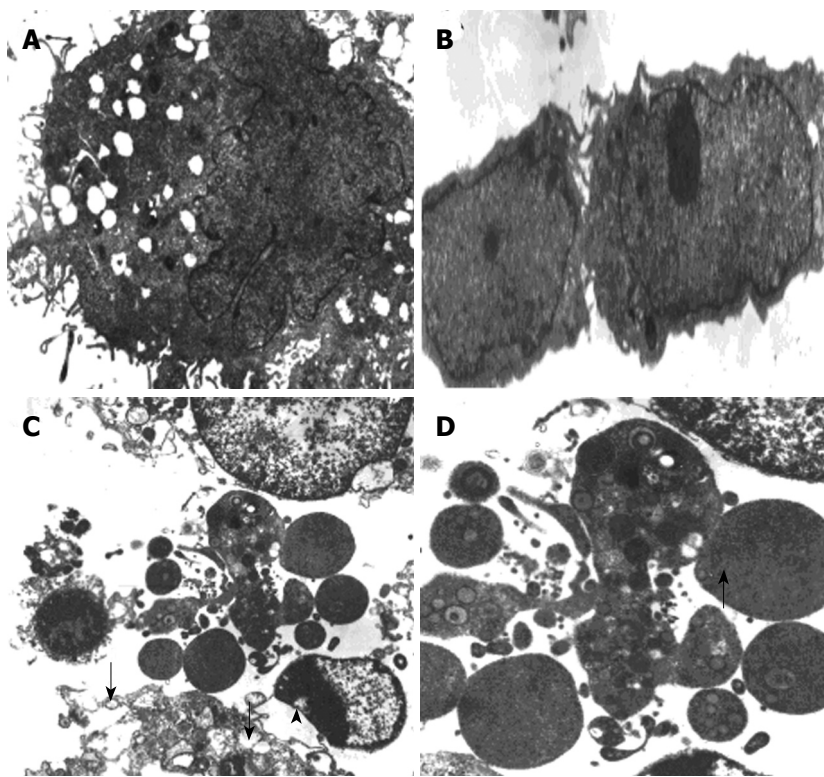


Figure 5 Ultra-structure of HepG2 cells 48 h after infection with LV-EGFP (A, B) and LV-NT4(Si)-p53(N15)-Ant (C, D) ($\times 5000$). A: Forty-eight hours after LV-EGFP infection, the cell membranes and nuclear membranes of HepG2 cells were intact; there were some crimples in the nuclear membranes and some microvilli on the surface of cells. The structure of mitochondria and ER was normal; B: Forty-eight hours after LV-EGFP infection, there were two HepG2 cells which had just completed division and this phenomenon suggested that LV-EGFP did not have a significant effect on cell growth and division; C: Forty-eight hours after LV-NT4(Si)-p53(N15)-Ant infection, it can be seen that cell membranes were incomplete and several fractures (arrows) were seen. Cell contents also appeared to be leaking. Mitochondria were swollen and showed vacuolization. Vacuoles were also seen under the nuclear membrane (arrowhead); D: Forty-eight hours after LV-NT4(Si)-p53(N15)-Ant infection, the remaining bare nuclei (arrow), after cytoplasm collapse can be seen.

and translocation in both prokaryotic and eukaryotic cells. NT4 is a member of the neurotrophin family, involved in controlling survival and differentiation of vertebrate neurons^[16]. Besides the common features of neurotrophins, NT4 has many unusual features. Unlike other neurotrophins, the expression of NT4 is ubiquitous and less influenced by environmental signals^[17]. In the present study, NT4 structure analysis showed that the human NT4 initiation codon was followed by a signal

peptide sequence, a pro-region and an apparent dibasic cleavage site, which was followed by the sequence of the mature NT4. The signal peptide sequence and pro-region of human NT4 are notably shorter (by = 243 bp) than those of other neurotrophins^[18]. In our previous study, the pre-protein NT4 could be cleaved into the signal peptide and the mature protein by *Escherichia coli* (*E. coli*) endopeptidase. There is a native Nael enzyme site in front of the site in the NT4 signal peptide,

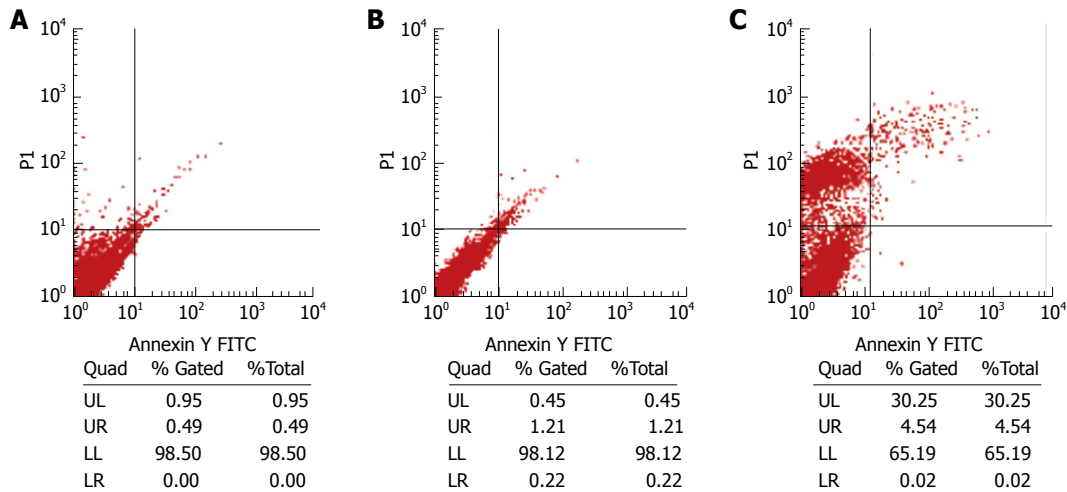


Figure 6 Flow cytometry analysis of HepG2 cells without treatment (A), 48 h after infection with LV-EGFP (B) and LV-NT4(Si)-p53(N15)-Ant (C) after stained with Annexin V and propidium iodide. The left lower quadrant represents normal cells (An-PI-), the right lower quadrant represents early apoptotic cells (An+ PI-), the right upper quadrant represents apoptotic cells and necrotic cells (An+ PI+), the upper left quadrant represents early necrotic cells (An-PI+).

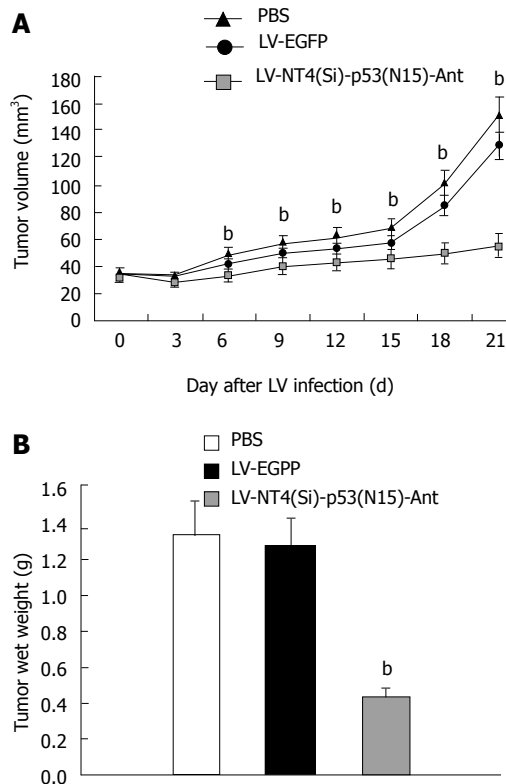


Figure 7 Tumor growth curve (A) and tumor wet weight (B) after treatment with LV-NT4(Si)-p53(N15)-Ant. A: Tumor growth curve after treatment with LV-NT4(Si)-p53(N15)-Ant. Tumors grew rapidly in the PBS and LV-EGFP groups, while the tumor growth was significantly inhibited in the LV-NT4(Si)-p53(N15)-Ant group 3 wk after infection. There was no statistical significance between the PBS group ($151.0 \pm 50.1 \text{ mm}^3$) and the LV-EGFP group ($128.5 \pm 45.3 \text{ mm}^3$) in terms of tumor volume ($P > 0.05$). But the tumor volume in the LV-NT4(Si)-p53(N15)-Ant group ($55.1 \pm 18.7 \text{ mm}^3$) was significantly less than that of the PBS and LV-EGFP groups (${}^bP < 0.01$). B: Tumor wet weight after treatment with LV-NT4(Si)-p53(N15)-Ant. There were no significant differences in the wet weight of tumors between the two control groups: PBS group $1.33 \pm 0.93 \text{ g}$ vs LV-EGFP group $1.27 \pm 1.04 \text{ g}$ ($P > 0.05$). But the wet weight of the LV-NT4(Si)-p53(N15)-Ant treatment group ($0.43 \pm 0.77 \text{ g}$) was significantly less than that of the two control groups (${}^bP < 0.01$).

thus ensuring the correct cleavage of therapeutic peptide, and making this signal peptide sequence highly

convenient for the expression of other exogenous peptides in a secretory manner. It has been shown that it is not only feasible, but also improves the therapeutic effect^[19]. In this study, we successfully constructed a LV containing the NT4(Si)-p53(N15) fusion gene with *in vitro* recombinant DNA technology.

To transfer the NT4(Si)-p53(N15)-Ant gene into the target cells and to achieve a consistent expression, selection of the gene transfer vector is a critical step. Lentiviruses, such as HIV and SIV, are a new generation of vectors and have many advantages over the traditional virus vectors, such as retroviral or adenovirus vector. These LVs can infect both dividing and non-dividing cells and efficiently integrate into the host DNA, thus providing stable transgene expression over several months^[20,21]. At the same time, LV is very safe because all lentivirus accessory genes have been removed, virus production components have been split into 3 or 4 separate parts, and self-inactivating deletions have been introduced into the vector^[21,22]. Since the aim of cancer gene therapy is to remove all cancer cells including those in a precancerous stage, only extensive gene transfer and long-term gene expression in cancer cells are appropriate. Thus, LV has a greater promise to become an ideal vector for gene delivery.

In this study, MTT assay showed that LV-NT4(Si)-p53(N15)-Ant could significantly induce HepG2 cell death 48 h after infection, LDH was significantly increased in the LV-NT4(Si)-p53(N15)-Ant treatment group but not in the LV-EGFP treatment group, suggesting that the cell membranes are damaged. Moreover, cytotoxicity occurred in a time-dependent manner. The ultra-structure of HepG2 cells, especially cell membranes and mitochondria, was significantly changed after infection with LV-NT4(Si)-p53(N15)-Ant, which was different from that during apoptosis and necrosis. In addition, FCM revealed that two cell death modes (apoptosis and necrosis) occurred 48 h after infection with LV-NT4(Si)-p53(N15)-Ant with necrosis being common and apoptosis being rare, revealing that LV-NT4(Si)-p53(N15)-Ant exerts its effect on HCC mainly by inducing necrosis of cell membranes.

This is probably related to the process of LV infection, integration of the therapeutic gene into the host genome and gene expression.

The *in vivo* study also showed that LV-NT4(Si)-p53(N15)-Ant significantly inhibited tumor growth. Since p53(N15) contains overlapping sequences from the p53 mdm-2 binding domain, p53(N15)-Ant peptide may block the interaction of mdm-2 with other proteins. Recently, a study investigating the secondary structure of the p53 fusion peptide has revealed that p53(N15)-Ant peptide plays an important role in membrane interaction^[15], showing that p53(N15)-Ant peptide forms distinctive S-shape helix-loop-helix structures, which can rapidly disrupt cancer cell membranes by forming a toroidal-like pore, resulting in necrosis. The two mechanisms exist simultaneously.

In conclusion, we have established a way to express lentivirus-introduced p53(N15)-Ant 32-peptide. The growth of HepG2 cells can be significantly inhibited by LV-NT4(Si)-p53(N15)-Ant. LV-NT4(Si)-p53(N15)-Ant gene therapy may be used as a novel anticancer strategy. Further study on the biological characteristics of the p53 peptide is needed by transfecting LV-NT4(Si)-p53(N15)-Ant into other cancer cell lines.

COMMENTS

Background

Peptide has emerged as a new anticancer agent in recent years. Numerous reports suggest that many low molecular weight peptides possess an anticancer effect but have almost no cytotoxic effect on normal cells. p53(N15)-Ant has been considered a novel cancer therapeutic peptide because it induces cancer cell death and does not seem to be cytotoxic to normal cells.

Research frontiers

It has been reported that p53 peptide, synthesized from residues 12-26 and fused with Drosophila carrier protein antennapedia (Ant), induces rapid tumor cell necrosis in all breast and pancreatic cancer cell lines tested, irrespective of the p53 status, whereas it shows a low cytotoxicity to normal cells. In this study, the authors constructed a novel recombinant lentivirus expression plasmid LV-NT4(Si)-p53(N15)-Ant and demonstrated its anticancer effect.

Innovations and breakthroughs

The signal peptide plays an important role in protein targeting and translocation in both prokaryotic and eukaryotic cells. In this experiment, the authors used the NT4 signal peptide to enable the therapeutic peptide to be secreted. Lentivirus vectors were also employed. LV-NT4(Si)-p53(N15)-Ant was constructed and successfully cultured at a high titer and verified to induce necrosis of cancer cells.

Applications

This work has established a way to express lentivirus-introduced p53(N15)-Ant 32-peptide. LV-NT4(Si)-p53(N15)-Ant dependent gene therapy may be a promising novel anticancer strategy. p53(N15)-Ant may represent a promising agent of gene therapy for hepatocellular carcinoma.

Terminology

NT4 signal peptide and its pro-region are protein sequences that can direct the secretion of proteins and peptides from cells. Such a mechanism is thought to be helpful in fusion peptide gene therapy as it can enhance the therapeutic effect.

Peer review

In this study, Song *et al* showed that the constructed lentivirus vector expressed in cancer cells could inhibit the growth of HepG2 cells. This vector can induce necrosis and apoptosis, and inhibit tumor growth *in vivo*. The study in general is significant and interesting.

REFERENCES

- 1 Di Bisceglie AM, Carithers RL Jr, Gores GJ. Hepatocellular

- carcinoma. *Hepatology* 1998; **28**: 1161-1165
- 2 Ruiz J, Qian C, Drozdzik M, Prieto J. Gene therapy of viral hepatitis and hepatocellular carcinoma. *J Viral Hepat* 1999; **6**: 17-34
- 3 Qian C, Drozdzik M, Caselmann WH, Prieto J. The potential of gene therapy in the treatment of hepatocellular carcinoma. *J Hepatol* 2000; **32**: 344-351
- 4 Mitry RR, Mansour MR, Havlik R, Habib NA. Gene therapy for liver tumours. *Adv Exp Med Biol* 2000; **465**: 193-205
- 5 Bálint EE, Vousden KH. Activation and activities of the p53 tumour suppressor protein. *Br J Cancer* 2001; **85**: 1813-1823
- 6 Boyd SD, Tsai KY, Jacks T. An intact HDM2 RING-finger domain is required for nuclear exclusion of p53. *Nat Cell Biol* 2000; **2**: 563-568
- 7 Courtois S, Verhaegh G, North S, Luciani MG, Lassus P, Hibner U, Oren M, Hainaut P. DeltaN-p53, a natural isoform of p53 lacking the first transactivation domain, counteracts growth suppression by wild-type p53. *Oncogene* 2002; **21**: 6722-6728
- 8 Donehower LA. The p53-deficient mouse: a model for basic and applied cancer studies. *Semin Cancer Biol* 1996; **7**: 269-278
- 9 Kanovsky M, Raffo A, Drew L, Rosal R, Do T, Friedman FK, Rubinstein P, Visser J, Robinson R, Brandt-Rauf PW, Michl J, Fine RL, Pincus MR. Peptides from the amino terminal mdm-2-binding domain of p53, designed from conformational analysis, are selectively cytotoxic to transformed cells. *Proc Natl Acad Sci USA* 2001; **98**: 12438-12443
- 10 Do TN, Rosal RV, Drew L, Raffo AJ, Michl J, Pincus MR, Friedman FK, Petrylak DP, Cassai N, Szmulewicz J, Sidhu G, Fine RL, Brandt-Rauf PW. Preferential induction of necrosis in human breast cancer cells by a p53 peptide derived from the MDM2 binding site. *Oncogene* 2003; **22**: 1431-1444
- 11 Haupt Y, Maya R, Kazaz A, Oren M. Mdm2 promotes the rapid degradation of p53. *Nature* 1997; **387**: 296-299
- 12 Kubbutat MH, Jones SN, Vousden KH. Regulation of p53 stability by Mdm2. *Nature* 1997; **387**: 299-303
- 13 Laín S. Protecting p53 from degradation. Protecting p53 from degradation. *Biochem Soc Trans* 2003; **31**: 482-485
- 14 Momand J, Jung D, Wilczynski S, Niland J. The MDM2 gene amplification database. *Nucleic Acids Res* 1998; **26**: 3453-3459
- 15 Rosal R, Brandt-Rauf P, Pincus MR, Wang H, Mao Y, Li Y, Fine RL. The role of alpha-helical structure in p53 peptides as a determinant for their mechanism of cell death: necrosis versus apoptosis. *Adv Drug Deliv Rev* 2005; **57**: 653-660
- 16 Smith DJ, Leil TA, Liu X. Neurotrophin-4 is required for tolerance to morphine in the mouse. *Neurosci Lett* 2003; **340**: 103-106
- 17 Timmus T, Belluardo N, Metsis M, Persson H. Widespread and developmentally regulated expression of neurotrophin-4 mRNA in rat brain and peripheral tissues. *Eur J Neurosci* 1993; **5**: 605-613
- 18 Ip NY, Ibáñez CF, Nye SH, McClain J, Jones PF, Gies DR, Belluscio L, Le Beau MM, Espinosa R 3rd, Squinto SP. Mammalian neurotrophin-4: structure, chromosomal localization, tissue distribution, and receptor specificity. *Proc Natl Acad Sci USA* 1992; **89**: 3060-3064
- 19 Fan G, Egles C, Sun Y, Minichiello L, Renger JJ, Klein R, Liu G, Jaenisch R. Knocking the NT4 gene into the BDNF locus rescues BDNF deficient mice and reveals distinct NT4 and BDNF activities. *Nat Neurosci* 2000; **3**: 350-357
- 20 Lever AM, Strappe PM, Zhao J. Lentiviral vectors. *J Biomed Sci* 2004; **11**: 439-449
- 21 Naldini L, Blömer U, Gallay P, Ory D, Mulligan R, Gage FH, Verma IM, Trono D. In vivo gene delivery and stable transduction of nondividing cells by a lentiviral vector. *Science* 1996; **272**: 263-267
- 22 Zufferey R, Nagy D, Mandel RJ, Naldini L, Trono D. Multiply attenuated lentiviral vector achieves efficient gene delivery in vivo. *Nat Biotechnol* 1997; **15**: 871-875

S-Editor Wang JL L-Editor Wang XL E-Editor Tian L



Separate basolateral and apical phosphatidylcholine secretion routes in intestinally differentiated tumor cells

Daniel Gotthardt, Annika Braun, Anke Tietje, Karl Heinz Weiss, Robert Ehehalt, Wolfgang R Stremmel

Daniel Gotthardt, Annika Braun, Anke Tietje, Karl Heinz Weiss, Robert Ehehalt, Wolfgang R Stremmel, Department of Gastroenterology, University Hospital Heidelberg, 69120 Heidelberg, Germany

Author contributions: Gotthardt D and Braun A contributed equally to this work, Gotthardt D, Ehehalt R and Stremmel WR designed the research; Gotthardt D, Braun A, Tietje A, Weiss KH performed the research; Gotthardt D, Braun A, Ehehalt R and Stremmel WR analyzed the data; Gotthardt D, Braun A and Stremmel WR wrote the manuscript.

Supported by A Grant From the Dietmar Hopp Foundation (Stremmel WR) and the Post-Doc programme of the Medical Faculty of the University of Heidelberg (Gotthardt D and Braun A)

Correspondence to: Wolfgang R Stremmel, Professor, Department of Gastroenterology, University Hospital Heidelberg, Im Neuenheimer Feld 410, 69120 Heidelberg,

Germany. wolfgang_stremmel@med.uni-heidelberg.de

Telephone: +49-6221-568705 **Fax:** +49-6221-564116

Received: August 4, 2009 **Revised:** September 14, 2009

Accepted: September 21, 2009

Published online: December 14, 2009

© 2009 The WJG Press and Baishideng. All rights reserved.

Key words: CaCo-2 cells; Epithelial cells; Mass spectrometry; Phosphatidylcholine; Secretion; Sphingomyelin

Peer reviewers: Akira Andoh, MD, Department of Internal Medicine, Shiga University of Medical Science, Seta Tukinowa, Otsu 520-2192, Japan; Elias A Kouroumalis, Professor, Department of Gastroenterology, University of Crete, Medical School, Department of Gastroenterology, University Hospital, PO Box 1352, Heraklion, Crete 71110, Greece

Gotthardt D, Braun A, Tietje A, Weiss KH, Ehehalt R, Stremmel WR. Separate basolateral and apical phosphatidylcholine secretion routes in intestinally differentiated tumor cells. *World J Gastroenterol* 2009; 15(46): 5821-5826 Available from: URL: <http://www.wjgnet.com/1007-9327/15/5821.asp> DOI: <http://dx.doi.org/10.3748/wjg.15.5821>

INTRODUCTION

The presence of phosphatidylcholine (PC) in intestinal mucus serves to protect the underlying mucosa from attack by the commensal bacterial flora which is of particular importance in the colon^[1]. Recently it was shown that the mucus PC content is markedly reduced (up to 70%) in patients with ulcerative colitis (UC), irrespective of whether acute inflammation of the colon is present - when compared to controls or patients with Crohn's disease^[2,3]. This suggests its significance in the pathogenesis of UC. Accordingly, therapeutic replacement of PC in UC was shown to be very effective^[4-6].

Furthermore, it was shown that apical PC secretion occurs mainly in the ileum, and is stimulated by bile acids^[7]. It is assumed that luminaly secreted PC -after absorption of bile acids in the terminal ileum- is attracted to the mucosal surface and moves along the colonic wall towards the rectum driven by colonic motility^[1]. The exposure of PC to phospholipases of commensal colonic bacteria thins the PC layer towards the rectum, the "last lawn" with least PC content^[1]. This could explain the continuous spread of inflammation starting from the rectum in UC where an intrinsic low PC content in the mucus is already present. Moreover, the fact that PC is mainly secreted in ileum^[7] and that it is significantly impaired in UC^[2,3] could explain the occurrence of pouchitis after colectomy due to the lack of protective

Abstract

AIM: To investigate whether the secretion of phosphatidylcholine (PC) in intestinal mucus occurs by apical secretion or *via* basolateral excretion and to determine its subsequent passage across the tight junctions to the apical mucus.

METHODS: We addressed this question using the polarized intestinally differentiated tumor cell line CaCo-2 grown on filters to confluence in Transwell culture chambers. The released PC and sphingomyelin (Sph) from apical and basolateral media were analyzed by mass spectrometry.

RESULTS: The secreted PC species were identical in both compartments indicating the same intracellular origin of PC. However, PC secretion into the basolateral compartment was more effective, and the PC:Sph ratio in the basolateral compartment was significantly higher than that in the apical compartment (8.18 ± 1.84 vs 4.31 ± 1.22 , $P = 0.01$). Both pathways were temperature sensitive and were unaltered in the presence of cyclosporine.

CONCLUSION: The data demonstrate the PC secretion capacity of CaCo-2 cells and indicate two separated apical and basolateral release mechanisms.

PC in mucus. In contrast, pouchitis is not observed after colectomy for familial adenomatous polyposis (FAP).

PC within mucus is arranged as lamellar structures facing the luminal and mucosal surface of the mucus as well as liposomal structures within the layer. Of all phospholipids within the mucus, 60%-90% are reported to represent PC species^[8,9]. This indicates a specific PC secretion mechanism. The conventional view of such a transport process would suggest apical secretion *via* vesicular excretion or by ABC-transporters similar to MDR 2/3 mediated translocation of PC at the apical pole of hepatocytes^[10,11]. However, Alpers *et al*^[12] claimed a predominant basolateral secretion mechanism with secondary back diffusion across the tight junctions and subsequent release into the mucus space.

To evaluate this secretion mechanism, we used the intestinally differentiated tumor cell line CaCo-2 which revealed a polarized growth in tissue culture. We addressed the following questions: (1) Is PC secretion detectable in CaCo-2 cells? (2) Does it occur apically, basolaterally or on both sides? (3) Are these secretion pathways identical? (4) What are the kinetic characteristics?

MATERIALS AND METHODS

Cell culture

Caco-2 cells were cultured routinely at 37°C, 5% CO₂ in DMEM (GIBCO Invitrogen, Karlsruhe, Germany), containing 10% fetal calf serum (FCS), 1% penicillin/streptomycin, 1% sodium pyruvate (Sigma-Aldrich, Munich, Germany) and 1% nonessential amino acids (Sigma-Aldrich, Munich, Germany). Cells were seeded in 6-well Corning® Transwell® polyester membrane inserts (pore size 3.0 µm, membrane diameter 24 mm) (Corning COSTAR, USA), at a density of 10⁵ cells/cm². Cells were cultured for up to 21 d after reaching confluence to allow complete apical/basolateral polarization. Transepithelial electric resistance was checked regularly to verify appropriate polarization (World Precision Instruments, Berlin, Germany).

Sampling for lipid measurement

For measurement of PC secretion, polarized Caco-2 cells on filters were washed with FCS-free medium three times to remove extracellular lipids. They were then incubated in FCS-free medium containing 1% bovine serum albumin (BSA) (Sigma-Aldrich, Munich, Germany) for 16 h unless otherwise stated. Apical and basolateral media were collected and detached cells removed by centrifugation at 300 g for 5 min. All samples were stored at -80°C until further processing.

For experiments at different temperatures, CO₂-independent medium (GIBCO Invitrogen, Karlsruhe, Germany) containing 1% w/v BSA was used. Where indicated, BSA was replaced by taurocholate (Sigma-Aldrich, Munich, Germany) at a concentration of 2.5 mmol/L. In addition, the following drugs were used at the following concentrations: (1) verapamil 500 µmol/L, (2) glibenclamide 50 µmol/L, (3) hydrocortisone

100 ng/mL, 500 ng/mL, and 1000 ng/mL, (4) cyclosporine 80 µmol/L (all Sigma-Aldrich, Munich, Germany). In experiments using hydrocortisone, cells were pre-incubated in regular medium containing the respective concentrations of hydrocortisone for 24 h to allow for changes in transcription. Experiments were performed in quadruplicate, except for the time-course experiments, which were performed in triplicate.

Differential centrifugation

To retrieve particles of different sizes, the following standard setup was used. Cells were incubated as described above. The supernatant (SN) of the 300 g/5 min centrifugation was centrifuged at 1200 g for 20 min (P2). To obtain the next pellet the resulting SN was centrifuged at 10 000 g for 30 min (P3). This SN was then centrifuged at 100 000 g for 1 h (P4). Resulting pellets (P2-4) and the final supernatant were then subjected to lipid analysis.

Lipid analysis

Lipids from the respective medium samples were extracted according to Folch^[13]. Before lipid extraction, non-physiologic 1,2-didodecanoyl-sn-glycero-3-PC, 1,2-tetradecanoyl-sn-glycero-3-PC, 1,2-dieicosanoyl-sn-glycero-3-PC, 1,2-dido-cosanoyl-sn-glycero-3-PC as well as 1-pentadecanoyl-2-hydroxy-sn-glycero-3-PC, 1-arachidonoyl-2-hydroxy-sn-glycero-3-PC and sphingomyelin (Sph) were added for internal standardization. The apical and basolateral media were dried with a speed vac. In brief 75 µL aqua dest and 50 µL of the lipid standard were added to each sample. 500 µL of methanol were added and the sample was vortexed for 5 min. 1000 µL chloroform was added and vortexed for 5 min. The supernatant of the 5 min/17 000 g centrifugation was transferred to a new reaction tube. 300 µm aqua dest was added and vortexed again for 5 min. Phase separation was achieved by centrifugation at 500 g for 5 min. The lower organic phases were transferred to a separate glass tube and dried before resuspension for mass spectrometry.

Nano-ESI tandem mass spectrometric analyses

Mass spectrometric analyses were performed with a triple quadrupole instrument [Finnigan MAT (San Jose, CA, USA) model TSQ 7000] equipped with a nano-electrospray source operating at a typical flow rate of 20 to 50 nL/min. The electrospray capillary was positioned at a distance of 0.5 to 1 mm away from the orifice of the heated transfer capillary which was maintained at 140°C. The instrument was used in the tandem MS mode. Argon was used as the collision gas at a nominal pressure of 2 mTorr. Crude lipid extracts, which had been dried completely, were resolved in 50 µL methanol/chloroform 2:1 (v/v), vortexed thoroughly, and infused into the capillary. The mass spectrometric resolution was set to about nominal mass resolution for the scan range of m/z 400 to 900. All specimens were analyzed in precursor ion scan mode for m/z 184. At least 150 consecutive scans, if possible more than 200 scans of 4-s duration, were averaged for each quantitative measurement.

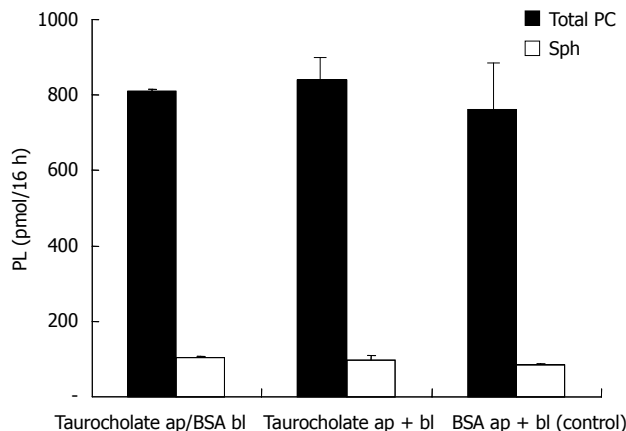


Figure 1 Release of phospholipids (PL) into the apical (ap) and basolateral (bl) media in the presence of BSA or taurocholate as solubilizing agents. The figure illustrates no differences in the amount of PC and Sph secreted regardless of whether taurocholate was applied only apically (left), both apically and basolaterally (middle) compared to control (right) ($P = \text{ns}$).

For quantification of the physiological PC and sphingomyelin species, regression curves were determined from the non physiological standards. Due to a general loss in sensitivity with increasing molecular weight, a set of four PC species was added as internal standards to bracket the profile of naturally occurring PCs. For the quantitative determination of Sph, we used a single internal standard. For correction of the measured values to the molar abundances, we used a calibration curve with the slope corresponding to that of PC.

The most abundant physiological PC and Sph species were determined after comparison of all spectra. The molecular weights were related to the number of carbon atoms and double bonds with the help of a lipid data bank.

Statistical analysis

SPSS 16.0 was used for statistical analysis of the data. A Mann-Whitney-U-test was performed to analyze the differences between different conditions. Differences were considered significant, if P was < 0.05 . In the time-course experiments a linear regression assuming a zero-crossing and applying the method of least squares was performed.

RESULTS

For polarization, CaCo-2 cells were grown on filters in Transwell culture dishes. Secretion of PC was examined in the apical and basolateral media containing, as lipid acceptors, taurocholate (2.5 mmol/L) or albumin (1% BSA). CaCo-2 cells showed PC secretion into both compartments. With regard to the acceptors of PC in both compartments (taurocholate or albumin), there was no difference recorded in the amount of PC or Sph released into the media (Figure 1). This indicated that under the experimental conditions employed, both acceptor molecules were present in excess and their capacity for PC and Sph solubilization was not

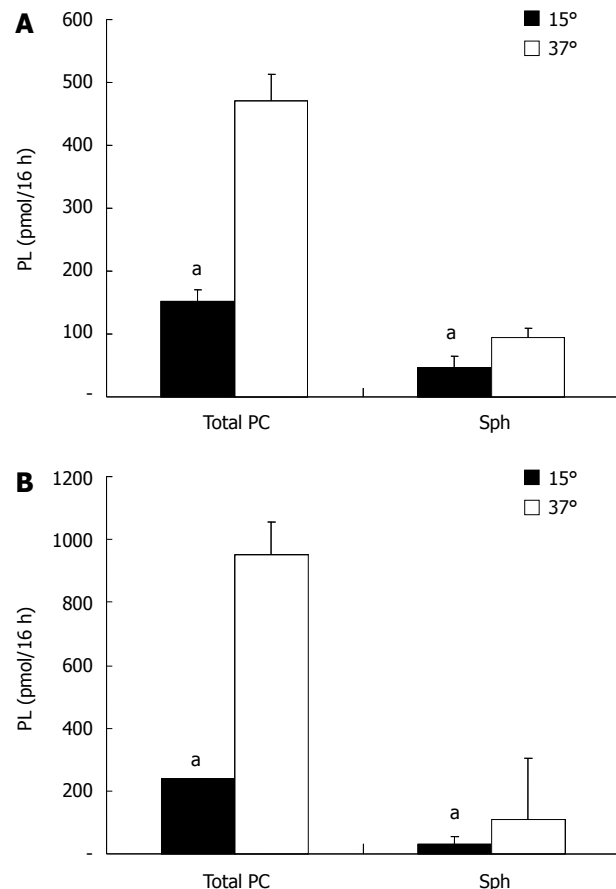


Figure 2 Temperature dependency of phospholipid (PL) secretion. Caco-2 cells were incubated either at 37°C or 15°C and secreted PC and Sph were measured. Both apical (A) and basolateral secretion (B) were drastically reduced at 15°C; apical PC by 68%, basolateral PC by 75%, apical Sph by 53% and basolateral Sph by 73% (* $P < 0.05$).

compromised. The secretion of PC and Sph in both compartments was temperature sensitive with a significant reduction in the secretion rate at 15°C. The degree of temperature-induced acceleration/deceleration of the transport rates was comparable for PC and Sph at each side. However, the total secretion rates towards the basolateral side were significantly more inhibited at 15°C than those at the apical side. This observed drop in secretion is typical for vesicular transport, because much lower transport rates in membrane carrier systems are expected at 15°C (Figure 2).

At 37°C the rate of secretion was significantly higher at the basolateral side compared to the apical side - also an indication of two different secretion capacities (Figure 3).

When the PC species and their secretion distribution on both sides were compared, they were virtually superimposable (Figure 4). This supports the concept that they originate from the same intracellular source. However, the relative fraction of Sph release compared to total PC release was significantly higher in the apical compartment. This corresponded to a higher level of Sph in the different pellets and the 100 000 g supernatant of the apical compartment vs the basolateral compartment (Figure 5). Sphingomyelins are typical phospholipids of vesicular membranes in the secretory pathway^[14]. A

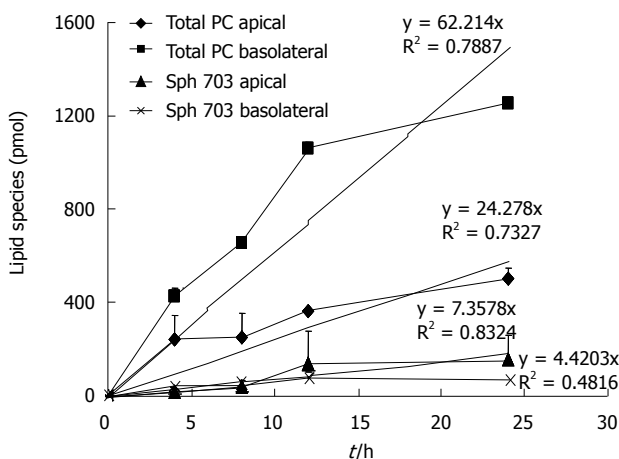


Figure 3 Time-course of phospholipid secretion. An almost linear secretion up to 12 h with some decline in secretion towards 24 h was registered. The average secretion rate of PC was 24.3 pmol/h on the apical side and 62.2 pmol/h on the basolateral side. Sph was secreted apically at 4.4 pmol/h and basolaterally at 7.4 pmol/h. The regression line for each setup was drawn.

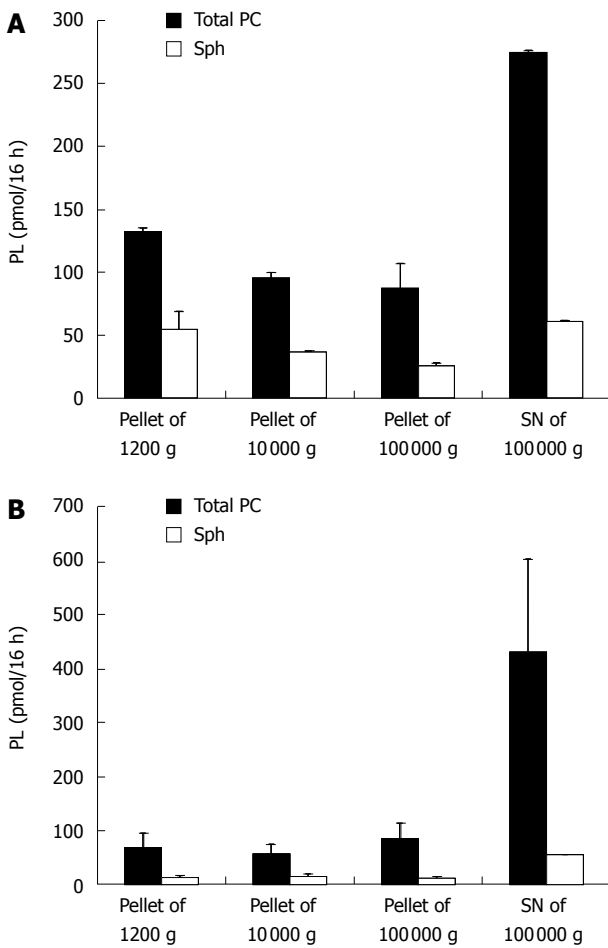


Figure 5 Distribution of secreted PL in pellets and supernatants obtained from the apical (A) and basolateral (B) compartments. The majority of the PL is retrieved in the 100 000 g supernatant resembling a rather soluble fraction. In the medium of the basolateral compartment a reduced amount of PC and Sph could be found in the pellets, but more PC was found in the 100 000 g supernatant.

higher proportion of Sph compared to the “cargo”-PC is suggestive of smaller sized secretory vesicles (“containers”).

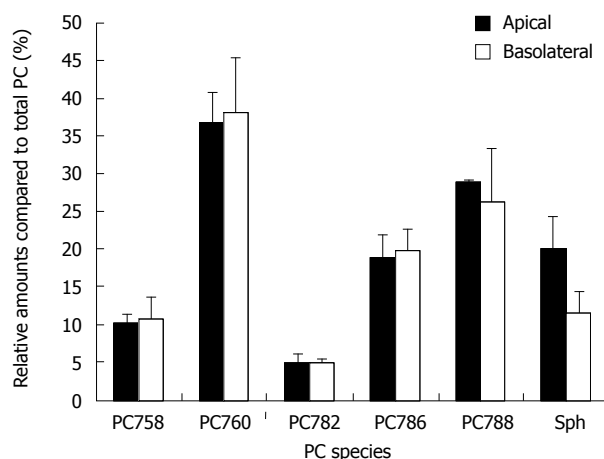


Figure 4 Typical distribution pattern of phospholipid species secreted. The PC species composition is similar in the apical and basolateral compartments. The relative amount of Sph 703 secreted is higher in the apical compartment ($P < 0.05$ when comparing the ratio of Sph 703 to total PC in the apical and basolateral compartments).

This is in line with the observation of a lower sensitivity towards temperature changes and a lower total apical PC secretion rate.

From a structural point of view, it would be easier for small sized vesicles to pass through the apical microvillous plasma membrane compared to large vesicles, which easily pass through the rather smooth basolateral side of the plasma membrane.

To further characterize the PC secretory pathway, we evaluated the effect of cyclosporine - a known inhibitor of ABC-transporters (Figure 6). No differences in transport rates were observed, underlying the hypothesis that PC secretion in intestinal mucosal cells more likely represents a vesicular excretion route. Similar results were obtained when other ABC-transport inhibitors (verapamil, glibenclamide and PSC833) were used (data not shown).

Since glucocorticoids are known to increase PC synthesis and excretion in the lung (surfactant), we evaluated their effects in CaCo-2 cells. Under the experimental conditions employed, no differences in secretion were detected (Figure 6). However, our experimental approach may have been too simple and unrefined to draw any further conclusions. It is possible that CaCo-2 cells do not express a glucocorticoid receptor.

DISCUSSION

The small intestine is an organ which is highly active in transport-mainly from the luminal to the basolateral side. It manages the complete absorption of all food constituents. The fact that the intestinal mucosa also has a secretory pathway towards the luminal site is a rather unrecognized feature. Thus, the high secretion rate at the basolateral side could be explained by the essential role of intestinal mucosal cells in the absorption process, in particular of lipids (high lipid throughput). After uptake of fatty acids, monoglycerides, lysophospholipids, and fat soluble vitamins into the mucosal cell, they are

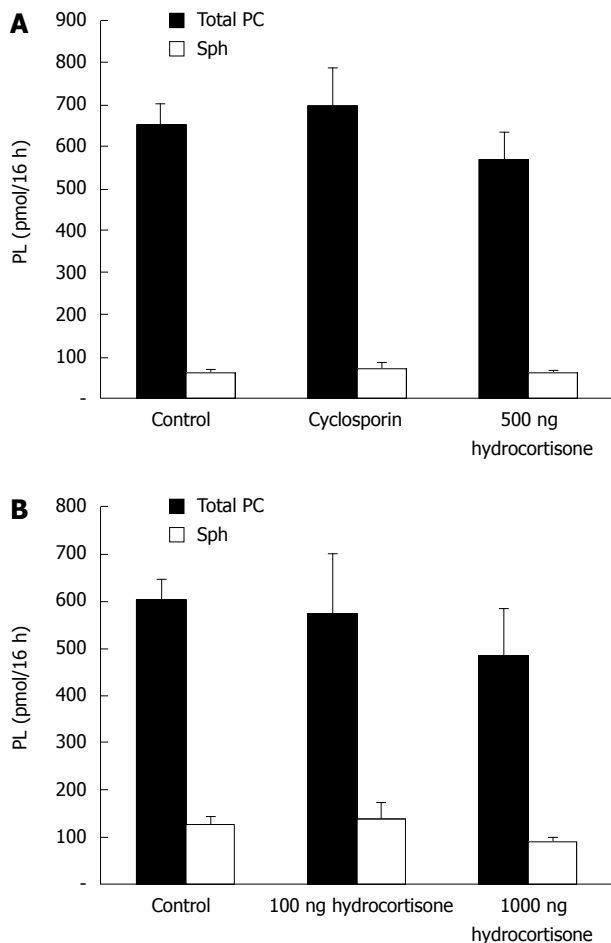


Figure 6 Effect of cyclosporine and hydrocortisone on PL secretion. Cyclosporine and hydrocortisone did not affect the amount or distribution of PL secretion at the apical (A) and basolateral side (B) ($P = \text{ns}$).

resynthesized to complex lipids (triglycerides, phospholipids), bound to apolipoproteins, and secreted at the basolateral side of mucosal cells *via* a vesicular pathway^[14,15]. In contrast, at the microvillous side of the plasma membrane, it is sufficient to utilize a low capacity PC secretory pathway because mucus resembles a low PC-turnover compartment. Our experiments support the notion, that there are two separate PC secretion pathways in intestinal epithelial cells: a high capacity basolateral and a low capacity apical vesicular excretion route. This now needs confirmation by cellular imaging techniques and the use of native intestinal mucosal cells. The fact that 60%-90% of the phospholipids in mucus represent PC^[8,9], indicates a specific PC secretion mechanism. The highly enriched PC arrangement within lamellar membranes establishes the protective hydrophobic surface layer of the mucus^[8,9]. In the case of ulcerative colitis, where a decrease in the mucus PC levels was detected, this may be due to impairment of PC synthesis, PC loading of secretory vesicles, apical membrane fusion and PC release into the mucus or adherence to mucus proteins. After verification of the data in native mucosal cell models, the experimental system can be used to examine whether the PC secretion mechanism can be modified for therapeutic purposes.

ACKNOWLEDGMENTS

We thank Professor Lehmann, Central Spectroscopy, German Cancer Research Center, Heidelberg, Germany, for providing equipment and assistance for mass spectrometry.

COMMENTS

Background

Intestinal mucus and the mucosal barrier are very important aspects of intestinal disease.

Research frontiers

Impaired mucosal barrier function, its pathophysiology and its impact on inflammatory bowel disease have become a very important focus of research.

Innovations and breakthroughs

The pathway by which phosphatidylcholine is secreted into the intestine to form mucus is not yet known. In this paper we provide evidence, that there are two separate secretion routes.

Applications

The used methodology and the acquired results might be the basis for future work, to confirm the data *in vivo* and to elucidate the role of phosphatidylcholine in pathophysiology.

Terminology

Phospholipids, mainly phosphatidylcholine are the constituents of intestinal mucus. Due to their hydrophobicity they are part of the intestinal barrier.

Peer review

The reviewers appreciated the innovative approach and techniques of this work. These data need to be confirmed in other experimental setups.

REFERENCES

- 1 Karner M, Ehehalt R, Stremmel W. Retarded release phosphatidylcholine: A new therapeutic option for ulcerative colitis. In: Dignass A, Rachmilewitz D, Stange EF, Weinstock JV, editors. Immunoregulation in inflammatory bowel diseases current understanding and innovation. Heidelberg, Dordrecht, New York: Springer, 2007: 161-170
- 2 Ehehalt R, Wagenblast J, Erben G, Lehmann WD, Hinz U, Merle U, Stremmel W. Phosphatidylcholine and lysophosphatidylcholine in intestinal mucus of ulcerative colitis patients. A quantitative approach by nanoElectrospray-tandem mass spectrometry. *Scand J Gastroenterol* 2004; **39**: 737-742
- 3 Braun A, Treede I, Gotthardt D, Tietje A, Zahn A, Ruhwald R, Schoenfeld U, Welsch T, Kienle P, Erben G, Lehmann WD, Fuellekrug J, Stremmel W, Ehehalt R. Alterations of phospholipid concentration and species composition of the intestinal mucus barrier in ulcerative colitis: a clue to pathogenesis. *Inflamm Bowel Dis* 2009; **15**: 1705-1720
- 4 Stremmel W, Merle U, Zahn A, Autschbach F, Hinz U, Ehehalt R. Retarded release phosphatidylcholine benefits patients with chronic active ulcerative colitis. *Gut* 2005; **54**: 966-971
- 5 Stremmel W, Ehehalt R, Autschbach F, Karner M. Phosphatidylcholine for steroid-refractory chronic ulcerative colitis: a randomized trial. *Ann Intern Med* 2007; **147**: 603-610
- 6 Croft NM. Phospholipid in UC: novel, safe and works--is it too good to be true? *Gastroenterology* 2006; **130**: 1003-1004; discussion 1004-1005
- 7 Ehehalt R, Jochims C, Lehmann WD, Erben G, Staffer S, Reininger C, Stremmel W. Evidence of luminal phosphatidylcholine secretion in rat ileum. *Biochim Biophys Acta* 2004; **1682**: 63-71
- 8 Lichtenberger LM. The hydrophobic barrier properties of gastrointestinal mucus. *Annu Rev Physiol* 1995; **57**: 565-583
- 9 Kao YC, Lichtenberger LM. A method to preserve extracellular surfactant-like phospholipids on the luminal surface

- of rodent gastric mucosa. *J Histochem Cytochem* 1990; **38**: 427-431
- 10 Rooney SA, Young SL, Mendelson CR. Molecular and cellular processing of lung surfactant. *FASEB J* 1994; **8**: 957-967
- 11 van Helvoort A, Smith AJ, Sprong H, Fritzsche I, Schinkel AH, Borst P, van Meer G. MDR1 P-glycoprotein is a lipid translocase of broad specificity, while MDR3 P-glycoprotein specifically translocates phosphatidylcholine. *Cell* 1996; **87**: 507-517
- 12 Alpers DH, Zhang Y, Ahnen DJ. Synthesis and parallel secretion of rat intestinal alkaline phosphatase and a surfactant-like particle protein. *Am J Physiol* 1995; **268**: E1205-E1214
- 13 Folch J, Lees M, Sloane Stanley GH. A simple method for the isolation and purification of total lipides from animal tissues. *J Biol Chem* 1957; **226**: 497-509
- 14 De Matteis MA, Di Campli A, D'Angelo G. Lipid-transfer proteins in membrane trafficking at the Golgi complex. *Biochim Biophys Acta* 2007; **1771**: 761-768
- 15 Stremmel W. Absorption of fat and fat-soluble vitamins. In: Caspary WF, editor. Structure and function of the small intestine. Amsterdam: Elsevier Science Publishers, 1987: 175-184

S-Editor Tian L L-Editor Webster JR E-Editor Ma WH



Value of three-dimensional reconstructions in pancreatic carcinoma using multidetector CT: Initial results

Miriam Klauß, Max Schöbinger, Ivo Wolf, Jens Werner, Hans-Peter Meinzer, Hans-Ulrich Kauczor, Lars Grenacher

Miriam Klauß, Hans-Ulrich Kauczor, Lars Grenacher, Department of Diagnostic and Interventional Radiology, University of Heidelberg, Heidelberg 69120, Germany
Max Schöbinger, Ivo Wolf, Hans-Peter Meinzer, Department of Medical and Biological Informatics, German Cancer Research Center (DKFZ), Heidelberg 69120, Germany
Jens Werner, Surgical Clinic, University of Heidelberg, Heidelberg 69120, Germany

Author contributions: Klauß M, Schöbinger M, Wolf I, Werner J, Meinzer HP, Kauczor HU and Grenacher L designed the research. Klauß M, Schöbinger M and Wolf I performed the research and analyzed the data; Klauß M, Schöbinger M and Wolf I mainly wrote the paper; Werner J, Meinzer HP, Kauczor HU and Grenacher L proof read the paper.

Correspondence to: Dr. Lars Grenacher, Professor, Department of Diagnostic and Interventional Radiology, University of Heidelberg, INF 110, Heidelberg 69120,

Germany. lars.grenacher@med.uni-heidelberg.de

Telephone: +49-6221-5639758 **Fax:** +49-6221-565730

Received: September 14, 2009 **Revised:** October 6, 2009

Accepted: October 13, 2009

Published online: December 14, 2009

(all pT3), and one patient had a serous cystadenoma. One tumor infiltrated the superior mesenteric vein. The infiltration was correctly evaluated. All carcinomas were resectable. In comparison to the CT image with axial and coronal reconstructions, the three-dimensional image was judged by the surgeons as better for operation planning and consistently described as useful.

CONCLUSION: A 3D-image of the pancreas represents an invaluable aid to the surgeon. However, the 3D-software must be further developed in order to be integrated into daily clinical routine.

© 2009 The WJG Press and Baishideng. All rights reserved.

Key words: Pancreatic carcinoma; 3D-reconstruction; Multidetector computed tomography; Pancreatic carcinoma invasion; Segmentation

Peer reviewers: Kiichi Tamada, MD, Department of Gastroenterology, Jichi Medical Shool, 3311-1 Yakushiji, Minamikawachi, Kawachigun, Tochigi 329-0498, Japan; Edward L Bradley III, MD, Professor of Surgery, Department of Clinical Science, Florida State University College of Medicine, 1600 Baywood Way, Sarasota, FL 34231, United States

Klauß M, Schöbinger M, Wolf I, Werner J, Meinzer HP, Kauczor HU, Grenacher L. Value of three-dimensional reconstructions in pancreatic carcinoma using multidetector CT: Initial results. *World J Gastroenterol* 2009; 15(46): 5827-5832 Available from: URL: <http://www.wjgnet.com/1007-9327/15/5827.asp> DOI: <http://dx.doi.org/10.3748/wjg.15.5827>

Abstract

AIM: To evaluate the use of three-dimensional imaging of pancreatic carcinoma using multidetector computed tomography (CT) in a prospective study.

METHODS: Ten patients with suspected pancreatic tumors were examined prospectively using multidetector CT (Somatom Sensation 16, Siemens, Erlangen, Germany). The images were evaluated for the presence of a pancreatic carcinoma and invasion of the peripancreatic vessels and surrounding organs. Using the isotropic CT data sets, a three-dimensional image was created with automatic vascular analysis and semi-automatic segmentation of the organs and pancreatic tumor by a radiologist. The CT examinations and the three-dimensional images were presented to the surgeon directly before and during the patient's operation using the Medical Imaging Interaction Toolkit-based software "ReLiver". Immediately after surgery, the value of the two images was judged by the surgeon. The operation and the histological results served as the gold standard.

RESULTS: Nine patients had a pancreatic carcinoma

INTRODUCTION

Pancreatic carcinomas are the fourth most frequent cause of death from cancer worldwide. The prognosis remains poor with a relative 5-year survival rate of about 5%. The only procedure resulting in significantly longer survival is R0 resection with adjuvant chemotherapy^[1].

Computed tomography (CT) is considered the method of choice for the detection and preoperative staging of pancreatic carcinomas^[1-6]. Currently, 16- and 64-row spiral CTs are increasingly becoming available, and these offer improved local resolution over older models. The high-resolution data sets gained from these also offer the option of three-dimensional image post-processing^[7,8].

In planning an operation, the location of the pancreatic tumor relative to the surroundings, surgically relevant vessels and adjacent organs is of utmost importance to the surgeon. The option of being able to assess the tumor volume in relation to the pancreatic tissue can also represent further valuable information.

In liver surgery, three-dimensional imaging is increasingly being used for the interactive planning of surgery in complex partial liver resections and living donors. Special procedures are used which - in addition to visualization - permit volumetric assessment of the primary data. Systems which can be used to gain additional information from the layer data include HepaVision2 (MeVis GmbH, Bremen, Germany)^[9], LiverLive (Navidez Ltd., Ljubljana, Slovenia), and Medical Imaging Interaction Toolkit (MITK) ReLiver (Deutsches Krebsforschungszentrum, Heidelberg, Germany).

The prerequisite for such procedures is the pre-processing step of segmentation, during which interesting regions of the image are marked on the section images. In a previous study, we have already shown that three-dimensional imaging of pancreatic tumors with semi-automatic segmentation is possible analogously to hepatic imaging^[10].

The aim of this study is to test in a prospective, clinically controlled study, whether the three-dimensional images of the pancreas and the surrounding structures gained using the CT data sets are useful to the surgeon in planning operations and for intraoperative orientation in patients with pancreatic carcinoma.

MATERIALS AND METHODS

Between March 2006 and August 2006, ten patients were included in the study with suspected operable pancreatic carcinoma. The criterion for inclusion in the study was urgent clinical suspicion of a pancreatic carcinoma. The study had the approval of the local ethics committee.

All patients underwent 16-row multislice CT (Somatom Sensation 16, Siemens, Erlangen, Germany), using the hydro technique with administration of Ultravist 370[®] (Schering, Berlin, Germany).

The operative findings and the histological results obtained during the operation served as the gold standard.

The evaluation was carried out by two experienced radiologists using a standardized evaluation form. This covered the location, size, and peripancreatic extent of the tumor. The resectability of the carcinoma was also assessed.

16-row spiral CT

Patients were examined using 16-row spiral CT (Somatom Sensation 16, Siemens, Erlangen, Germany) using the hydro technique. This involves distension of the stomach and duodenum using 1.5 L of still water, intestinal paralysis through intravenous administration of 40 mg N-butylscopolaminium bromide (Buscopan[®]) and positioning the patient on the right side at an angle of 30°^[4,11].

Firstly, a native spiral CT of the abdomen was carried out. Then an examination was carried out in the arterial

Table 1 Examination parameters

	Native CT	Arterial phase	Portal venous phase
Anode voltage (kV)	120	120	120
Anode current (mA)	140	170	185
Detector collimation	1.5 (slice: 6 mm)	0.75 (slice: 3 mm)	0.75 (slice: 3 mm)
Table feed (mm)	24	12	12
Reconstructed slice thickness (mm)	6	2/1	1.3/3; 2.1/0.5
Delay (s)		8	35

phase (delay 8 s) and in the portal venous phase (delay 35 s) using the Combined Application Reduced Exposure bolus technique with 120 mL contrast medium (Ultravist[®] 370, Schering AG, Berlin, 5 mL/s) (Table 1).

Three-dimensional imaging

The data sets obtained from CT were transmitted via an internal data connection (Chili, Heidelberg, Germany) to the Department of Medical and Biological Informatics at the German Cancer Research Center. There, the vascular structures were transferred to a semantic model in which the vascular branches could be individually colored, shown, or removed from view. All segmentations were carried out by a radiologist using the software program MITK ReLiver. During the process, the liver, kidneys, duodenum, stomach, pancreas, and pancreatic tumor were segmented using interactive segmenting tools in the section images. It was found to be particularly time-saving to use a combination of an interactive regional growth procedure and a form-based interpolation procedure^[12]. On this basis, it was possible to reduce the interaction time to a necessary minimum. Subsequently, the data from the vascular trees, the individually segmented organs and the tumor were fused into a three-dimensional scene.

These freely rotatable images were presented to the surgeon before and during the operation above the OP field, analogous to the three-dimensional image of the liver^[11]. The surgeon also saw the conventional CT images before the operation, which were also available to him in the operating theater on a monitor. After the operation, on a questionnaire, the surgeon assessed the value of the three-dimensional image compared with that of the conventional CT images (Table 2).

The questionnaire included comments about representation of the tumor, tumor location, tumor invasion of the vessels and surrounding organs, how well the imaging material matched the operative site, the manageability of the images, a score by which the surgeon could grade how secure he felt looking at the CT or three-dimensional images, and possible changes in the operative strategy.

The individual points on the questionnaire were graded with marks ranging from 1 for excellent to 5 for very bad.

Statistical analysis

Using the Wilcoxon test, we examined whether the

Table 2 Questionnaire put to the surgeon assessing the value of the three-dimensional image vs conventional CT images

Depiction of the tumor	
How well can the tumor localization be assessed?	1 = excellent; 2 = good; 3 = mediocre; 4 = bad; 5 = very bad
How well can vascular invasion be assessed?	
How well can organ invasion be assessed?	
How comfortable are you with the image?	Completely; partially; not at all
How well does the imaging material match the operative situation?	Less complicated; equally complicated; more complicated
How manageable was the 3D view in comparison with CT?	Yes; no
Was the operating strategy changed due to the images?	

Table 3 Three-dimensional reconstruction vs CT

Patients	Tumor image		Tumor localization		Vascular invasion		Organ invasion		Feel-good score	
	CT	3D	CT	3D	CT	3D	CT	3D	CT	3D
Φ	2.2	1.4	1.8	1.6	2.2	2.2	2.0	1.6	2.4	1.2
P-value		0.157		0.564		1.0		0.157		0.063

1 = excellent, 2 = good, 3 = mediocre, 4 = bad, 5 = very bad.

differences between the CT and three-dimensional images were statistically relevant. The *P* values were calculated using SPSS for Windows XP.

RESULTS

In nine patients, a pylorus-preserving Whipple procedure was carried out. In one patient, explorative laparotomy was performed with placement of a biliointestinal anastomosis and a gastrojejunostomy, since the patient's advanced age (80 years) made a portal vein resection seem too stressful.

Nine patients had adenocarcinomas of the pancreas and one had a serous cystadenoma. All carcinomas had grown beyond the margins of the organ and invaded the peripancreatic lipid tissue and the duodenum, and were thus staged histologically as T3. In one patient, invasion of the superior mesenteric vein was found intraoperatively.

Three dimensional imaging

The three-dimensional images of the pancreatic tumors, as evaluated on the questionnaire, were found to be graded more favorably with regard to assessment of tumor imaging, location, and invasion of the surrounding organs, and to the score indicating how secure the surgeon felt in assessing the images than the conventional CT examination. However, the differences were not statistically significant (*P* = 0.157, 0.564, 0.157, 0.063, respectively). In evaluating vascular invasion, the results were equally good for both procedures (*P* = 1.0) (Table 3).

The three-dimensional imaging correctly and completely matched the operative site in all cases.

The manageability of the three-dimensional image was deemed to be less complicated in four out of five cases and in one case to be equally good.

In one case the surgeon found that the three-dimensional image demonstrated much more clearly than the conventional CT image that there was no invasion of the portal vein (Figure 1). In a second case, extensive inva-



Figure 1 Lateral view of the three-dimensional model of a pancreatic carcinoma (pale green) in the processus uncinatus. There is contact between the tumor and the superior mesenteric vein but no invasion.

sion of the portal vein by the tumor could be established in both types of image, but the extent of the invasion was demonstrated to the surgeon better in the three-dimensional image, enabling the tumor to be classified as a resectable stage T3 and explorative laparotomy was performed. Intraoperatively, this long-distance invasion was confirmed but no tumor resection was carried out due to the patient's advanced age; vascular replacement of the portal vein was deemed too stressful (Figure 2).

DISCUSSION

Despite all the progress made in diagnosis and surgery, the prognosis for pancreatic carcinomas today is still poor. Surgical resection is the treatment of choice as a curative approach to pancreatic carcinomas. Thus, the main aim of diagnosis consists of correctly evaluating the surgically relevant vessels with regard to possible invasion in order to be able to safely distinguish between resectable and non-resectable pancreatic carcinomas.

Spiral CT is considered to be state of the art in the diagnosis of pancreatic carcinoma and in the evaluation of resectability in most centers^[6]. The sensitivity of spiral

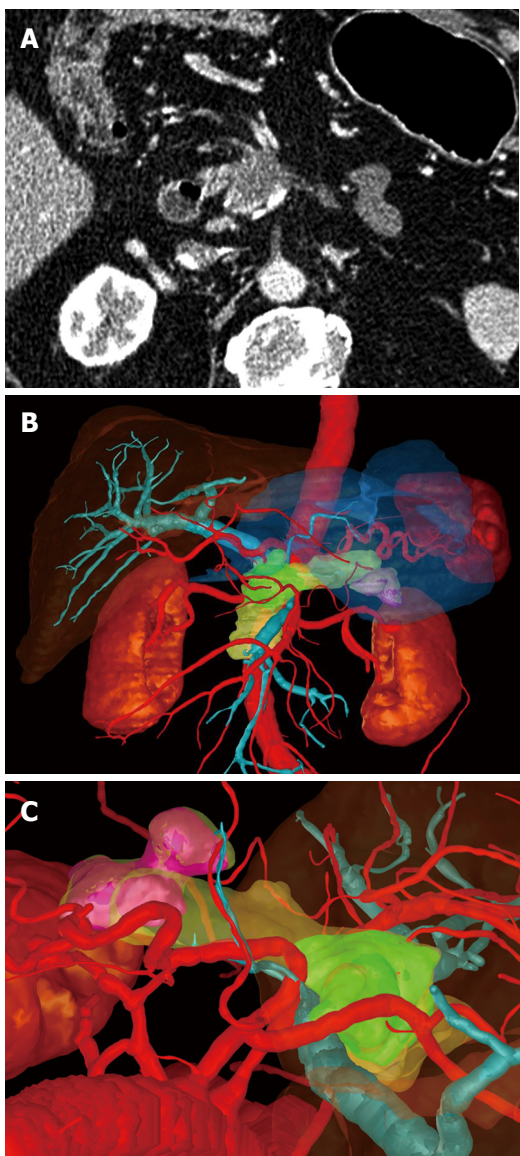


Figure 2 Patient with stage T3 pancreatic carcinoma with portal vein invasion; the preoperative assessment was correct. A: Axial slice through tumor; B: Three-dimensional reconstruction, frontal view (tumor = pale green); C: Three-dimensional reconstruction, cranial view (tumor = pale green).

CT, as cited in the literature, for evaluating resectability in pancreatic carcinoma is between 81% and 96.3%^[4,11,13-15].

Due to the particular anatomical relationship between the pancreas and the surrounding vessels, three-dimensional reconstructions are helpful in presenting additional information about this relationship^[16,17].

For the surgeon, it is valuable to be able to see the tumor, both by itself and in the context of its surrounding structures, in three dimensions from all sides whereby particular interest is obviously accorded to the presence and extent of contact to the relevant vessels or surrounding organs. In addition, the surgeon can more easily assess the tumor volume in relation to healthy pancreatic parenchyma. With the aid of a freely rotatable, three-dimensional image, he can picture the extent of venous invasion more clearly (even before the operation) than is possible with two-dimensional, axial, coronal and sagittal images.

Thus, the surgeon is provided with as detailed a picture as possible of the field of operation even before the operation takes place. As far as we know, there are no studies so far available assessing the clinical value of three-dimensional image processing of pancreatic tumors. To date, the Harvard Medical School has produced reconstructions of the pancreas and the neighboring vascular systems, but has not clinically evaluated them^[18].

Three-dimensional reconstruction already has a firm place in orthopedics and neurosurgery, where only unmoving and fixed anatomical structures are represented without any great range of variation.

The use of this method in visceral surgery is more difficult, since the organs can move and in some cases are shifted and reshaped during respiration and since the rate of anatomical variability is high^[10].

In the field of hepatic imaging and in the context of living liver donors and before complex partial liver resections, three-dimensional imaging of the liver, hepatic vessels, and bile ducts has managed to become established in some centers. In this case, in addition to visualization, the volumetry of various liver sections is of interest. Moreover, the three-dimensional reconstruction can be used preoperatively to consider various resection options and to evaluate their technical feasibility with regard to vascular and bile duct anatomy and to the expected liver volume after surgery.

The prerequisite for three-dimensional imaging of the primary data is semiautomatic segmentation of the structures of interest such as pancreas, tumor, stomach, liver, spleen, kidneys and any cysts that might be present. In pancreatic tumors, however, the segmentation process is particularly time-consuming and problematic, since the margins between organ tissue and inflammatory processes or of the tumor and surrounding structures are hard to recognize due to growth beyond the organ borders. In addition, the preparation of data includes all important organs and vascular structures in the abdominal cavity in order to provide the surgeon with a maximum amount of context information so that possible problems in exposure of the pancreas can be included in the surgical planning.

This means that the reconstruction procedure for visualizing pancreatic carcinomas today still requires a great amount of effort both technically and in terms of time required. In addition, an objective and precise localization of the tumor is not possible because segmentation is always conducted according to the subjective interpretation of the radiologist.

An automatic image processing procedure cannot be used for segmenting the tumor since the differences in thickness between organ tissue and tumor are sometimes very slight and cannot be recognized by a computer program. However, there are very promising approaches to segmenting the organs which make a largely automatic procedure seem tangible. Statistical form models learn the mean organ form with its variants from training data. Using even the current models, it can be shown that the work of segmentation can be significantly reduced for the liver^[19].

For vessels, no automatic segmentation program

exists that can independently mark vascular cross-sections by using the good contrast provided by the various contrast medium phases of the CT examination and the high contrast differences associated with it. Three-dimensional imaging of the vessels, moreover, only depicts the inside of the visualized vessel since the contrast medium that is used for processing the reconstruction only fills the vascular lumen.

Tumor invasion of the relevant vessel can thus only be indirectly visualized, just as with two-dimensional CT images, e.g. on the basis of a sudden difference in vessel caliber or complete vascular occlusion.

In the present study, three-dimensional post-processing of the data sets was highly acclaimed by the surgeons. Analysis of the questionnaire showed that the three-dimensional image was graded better in most points than conventional CT images. Only evaluation of the vessels was graded equally for both procedures.

The so-called "feelgood score" was better for the three-dimensional image than the two-dimensional image in all the cases.

This explains why in two cases the surgeon indicated that he found extensive portal vein invasion and exclusion of portal vein invasion to be much clearer for him on the three-dimensional image than on the conventional CT images.

The manageability of the three-dimensional image in comparison to the conventional CT images was deemed less complicated in four out of five cases. In all the cases the findings presented in the three-dimensional image material matched the intraoperative situation completely.

In complex liver surgery, three-dimensional visualization has already been shown to meet with high acclaim by surgeons. Its advantage consists in providing the surgeon with information about vascular anatomy that is indispensable for planning living liver transplantation or in providing additional information about the percentage of residual hepatic tissue following resection.

In their clinical study of the value of three-dimensional data sets before complex liver resections and before living liver donations, Fischer and Lamade found that although three-dimensional presentation did not lead to an improved segment allocation of hepatic tumors in comparison to axial sections, the three-dimensional presentation meant that the position of the tumor within the liver as marked on a liver model was significantly improved. It was shown that the three-dimensional presentation did indeed lead to improved OP representation. Overall, three-dimensional presentation led to approaching a 31% higher precision in tumor localization and improvement in resection recommendations^[20,21].

This study also illustrated the disadvantage of this method. The three-dimensional representation of the findings can only be as good as the primary data sets from CT in conjunction with the experience of the radiologist in evaluating CT data. If contact between the tumor and the encircling wall of a vessel can be visualized over a long distance on CT, this will also be visible in the three-dimensional image and can be interpreted in most cases, and in both procedures, as invasion of the relevant vessel.

The three-dimensional reconstruction cannot improve on the examination; it can only present the situation in a more plastic form.

A three-dimensional image will thus generally not improve the assessment of the resectability of pancreatic carcinomas. Overall, this new procedure, however, seems to provide a good aid in preoperative planning for the surgeon in surgical therapy of pancreatic carcinoma.

It remains to be seen whether the method, which still involves a great deal of effort, will stand the test of practical daily routine or if the time and technical input necessary for post-processing the image material is too high to be integrated practically into clinical routine or if these factors can be significantly reduced.

One restriction on the present study is the very small case number. The calculated *P* values showed no significant differences. Thus further studies should be conducted with a larger number of patients.

In summary, it can be said that three-dimensional imaging of pancreatic carcinomas with the surrounding vessels and organs is currently constrained by the great deal of effort involved, but it does primarily provide the surgeon with valuable additional information.

COMMENTS

Background

In planning a resection of a pancreatic carcinoma, the location of the pancreatic tumor relative to the surroundings, surgically relevant vessels and adjacent organs is of utmost importance to the surgeon.

Research frontiers

The aim is to provide better visualization of pancreatic carcinoma and peripancreatic vessels for the surgeon in the preoperative period.

Innovations and breakthroughs

In complex liver surgery, three-dimensional visualization has already been shown to meet with high acclaim by surgeons, but this study is the first which used this technique in pancreatic carcinoma patients. Its advantage consists in providing the surgeon with information about peripancreatic vascular anatomy that is helpful for planning the resection of a pancreatic carcinoma.

Applications

A three-dimensional image of the pancreas represents an additional, valuable aid to the surgeon. However, this method is still time-consuming. The software must be further developed to allow further automation of the segmentation to enable it to be integrated into daily clinical routine.

Terminology

Segmentation: To circumscribe a freehand region-of-interest on each single CT-slice, where, for example, the tumour or the pancreas is seen.

Peer review

This is a pilot study of 10 consecutive patients with suspected pancreatic carcinoma subjected to preoperative 3-D spiral CT reconstruction. This is the first such clinical study utilizing this technique.

REFERENCES

- Ishiguchi T, Ota T, Naganawa S, Fukatsu H, Itoh S, Ishigaki T. CT and MR imaging of pancreatic cancer. *Hepatogastroenterology* 2001; **48**: 923-927
- McNulty NJ, Francis IR, Platt JF, Cohan RH, Korobkin M, Gebremariam A. Multi-detector row helical CT of the pancreas: effect of contrast-enhanced multiphasic imaging on enhancement of the pancreas, peripancreatic vasculature, and pancreatic adenocarcinoma. *Radiology* 2001; **220**: 97-102
- Prokesch RW, Chow LC, Beaulieu CF, Bammer R, Jeffrey RB Jr. Isoattenuating pancreatic adenocarcinoma at multi-detector row CT: secondary signs. *Radiology* 2002; **224**: 764-768

- 4 Richter GM, Wunsch C, Schneider B, Düx M, Klar E, Seelos R, Kauffmann GW. [Hydro-CT in detection and staging of pancreatic carcinoma] *Radiologe* 1998; **38**: 279-286
- 5 Schima W, Ba-Ssalamah A. [Radiologic staging of liver and pancreatic malignancies] *Radiologe* 1999; **39**: 568-577
- 6 Schima W, Ba-Ssalamah A, Plank C, Kulinna-Cosentini C, Prokesch R, Tribl B, Sautner T, Niederle B. [Pancreas. Part II: Tumors] *Radiologe* 2006; **46**: 421-437; quiz 438
- 7 Baum U, Lell M, Nömayr A, Wolf H, Brunner T, Greess H, Bautz W. [Multiplanar spiral CT in the diagnosis of pancreatic tumors] *Radiologe* 1999; **39**: 958-964
- 8 Flohr T, Ohnesorge B, Stierstorfer K, Bruder H, Simon J, Süss C, Wildberger J, Baum U, Lell M, Küttner A, Heuschmid M, Wintersperger B, Becker C, Schaller S. [On the way to isotropic spatial resolution: technical principles and applications of 16-slice CT] *Radiologe* 2005; **45**: 608-617
- 9 Meier S, Schenk A, Mildenberger P, Bourquain H, Pitton M, Thelen M. [Evaluation of a new software tool for the automatic volume calculation of hepatic tumors. First results] *Rofo* 2004; **176**: 234-238
- 10 Grenacher L, Thorn M, Knaebel HP, Vetter M, Hassenpflug P, Kraus T, Meinzer HP, Büchler MW, Kauffmann GW, Richter GM. [The role of 3-D imaging and computer-based postprocessing for surgery of the liver and pancreas] *Rofo* 2005; **177**: 1219-1226
- 11 Richter GM, Simon C, Hoffmann V, DeBernardinis M, Seelos R, Senninger N, Kauffmann GW. [Hydrospiral CT of the pancreas in thin section technique] *Radiologe* 1996; **36**: 397-405
- 12 Kunert T, Heimann T, Schröter A, Schöbinger M, Böttger T, Thorn M, Wolf I, Engelmann U, Meinzer HP. An Interactive System for Volume Segmentation in Computer-Assisted Surgery. In: Galloway RL Jr, editor. Proc. SPIE Vol. 5367, Medical Imaging 2004: Visualization, Image-Guided Procedures, and Display. SPIE The International Society for Optical Engineering, Bellingham, 2004: 799-809
- 13 Bipat S, Phoa SS, van Delden OM, Bossuyt PM, Gouma DJ, Laméris JS, Stoker J. Ultrasonography, computed tomography and magnetic resonance imaging for diagnosis and determining resectability of pancreatic adenocarcinoma: a meta-analysis. *J Comput Assist Tomogr* 2005; **29**: 438-445
- 14 Klauss M, Mohr A, von Tengg-Kobligk H, Friess H, Singer R, Seidensticker P, Kauczor HU, Richter GM, Kauffmann GW, Grenacher L. A new invasion score for determining the resectability of pancreatic carcinomas with contrast-enhanced multidetector computed tomography. *Pancreatology* 2008; **8**: 204-210
- 15 Zeman RK, Cooper C, Zeiberg AS, Kladakis A, Silverman PM, Marshall JL, Evans SR, Stahl T, Buras R, Nauta RJ, Sitzmann JV, al-Kawas F. TNM staging of pancreatic carcinoma using helical CT. *AJR Am J Roentgenol* 1997; **169**: 459-464
- 16 Kalra MK, Maher MM, Mueller PR, Saini S. State-of-the-art imaging of pancreatic neoplasms. *Br J Radiol* 2003; **76**: 857-865
- 17 Smith SL, Rajan PS. Imaging of pancreatic adenocarcinoma with emphasis on multidetector CT. *Clin Radiol* 2004; **59**: 26-38
- 18 Nakagohri T, Jolesz FA, Okuda S, Asano T, Kenmochi T, Kainuma O, Tokoro Y, Aoyama H, Lorenzen WE, Kikinis R. Virtual panreatoscopy of mucin-producing pancreatic tumors. *Comput Aided Surg* 1998; **3**: 264-268
- 19 Heimann T, Wolf I, Meinzer HP. Active shape models for a fully automated 3D segmentation of the liver--an evaluation on clinical data. *Med Image Comput Comput Assist Interv Int Conf Med Image Comput Comput Assist Interv* 2006; **9**: 41-48
- 20 Lamadé W, Glombitska G, Fischer L, Chiu P, Cárdenas CE Sr, Thorn M, Meinzer HP, Grenacher L, Bauer H, Lehnert T, Herfarth C. The impact of 3-dimensional reconstructions on operation planning in liver surgery. *Arch Surg* 2000; **135**: 1256-1261
- 21 Fischer L, Thorn M, Chiu P, Grenacher L, Meinzer HP, Lamadé W. Virtuelle Operationsplanung in der Leberchirurgie. *Chir Praxis* 2003; **61**: 459-466

S-Editor Tian L L-Editor Logan S E-Editor Zheng XM



BRIEF ARTICLE

Iodized oil uptake assessment with cone-beam CT in chemoembolization of small hepatocellular carcinomas

Ung Bae Jeon, Jun Woo Lee, Ki Seok Choo, Chang Won Kim, Suk Kim, Tae Hong Lee, Yeon Joo Jeong, Dae Hwan Kang

Ung Bae Jeon, Jun Woo Lee, Ki Seok Choo, Department of Radiology, Pusan National University Yangsan Hospital, Yangsan 626-770, South Korea

Chang Won Kim, Suk Kim, Tae Hong Lee, Yeon Joo Jeong, Department of Radiology, Pusan National University Hospital, Pusan 602-739, South Korea

Dae Hwan Kang, Department of Internal Medicine, Pusan National University Yangsan Hospital, Yangsan 626-770, South Korea

Author contributions: Jeon UB performed TACE treatments, collected and analyzed the data, and wrote the manuscript; Kim CW performed TACE treatments, designed the study, collected and analyzed the data, and was involved in editing the manuscript; Lee JW, Choo KS, Kim S, Lee TH, Jeong YJ, Kang DH participated in the design and coordination of the work.

Supported by A Grant of the Korea Healthcare technology R&D Project, Ministry for Health, Welfare & Family Affairs, Republic of Korea, A091047

Correspondence to: Dr. Chang Won Kim, Department of Radiology, Pusan National University Hospital, 10, 1-Ga, Ami-Dong, Seo-Gu, Pusan 602-739, South Korea. radkim@hanafos.com

Telephone: +82-51-2407354 Fax: +82-51-2447354

Received: April 11, 2009 Revised: October 29, 2009

Accepted: November 5, 2009

Published online: December 14, 2009

iodized oil uptake in 22 of the lesions (sensitivity 85%). The degree of iodized oil uptake was overestimated (9%, 2/22) or underestimated (14%, 3/22) on spot image in five nodules compared with that of cone-beam CT.

CONCLUSION: Cone-beam CT is a useful and convenient tool for assessing the iodized oil uptake of small hepatic tumors (< 3 cm) directly after TACE.

© 2009 The WJG Press and Baishideng. All rights reserved.

Key words: Chemoembolization; Computed tomography; Hepatocellular carcinoma; Liver

Peer reviewer: Satoshi Mamori, MD, PhD, Department of Gastroenterology and Hepatology, Shinko Hospital, 1-4-47 Wakihama-cho, Chuo-ku, Kobe, Hyogo 651-0072, Japan

Jeon UB, Lee JW, Choo KS, Kim CW, Kim S, Lee TH, Jeong YJ, Kang DH. Iodized oil uptake assessment with cone-beam CT in chemoembolization of small hepatocellular carcinomas. *World J Gastroenterol* 2009; 15(46): 5833-5837 Available from: URL: <http://www.wjgnet.com/1007-9327/15/5833.asp> DOI: <http://dx.doi.org/10.3748/wjg.15.5833>

Abstract

AIM: To evaluate the utility of assessing iodized oil uptake with cone-beam computed tomography (CT) in transarterial chemoembolization (TACE) for small hepatocellular carcinoma (HCC).

METHODS: Cone-beam CT provided by a biplane flat-panel detector angiography suite was performed on eighteen patients (sixteen men and two women; 41-76 years; mean age, 58.9 years) directly after TACE for small HCC (26 nodules under 30 mm; mean diameter, 11.9 mm; range, 5-28 mm). The pre-procedural locations of the tumors were evaluated using triphasic multi-detector row helical computed tomography (MDCT). The tumor locations on MDCT and the iodized oil uptake by the tumors were analyzed on cone-beam CT and on spot image directly after the procedures.

RESULTS: All lesions on preprocedural MDCT were detected using iodized oil uptake in the lesions on cone-beam CT (sensitivity 100%, 26/26). Spot image depicted

INTRODUCTION

Transarterial chemoembolization (TACE) is a regional therapeutic modality that has become an accepted treatment for unresectable hepatocellular carcinoma (HCC). Triphasic multi-detector computed tomography (MDCT) is commonly used for the detection and preprocedural localization of hypervascular HCCs greater than 1 cm in diameter^[1-3].

Diagnostic angiography using digital subtraction angiography (DSA) is performed before TACE in order to detect hypervascular HCCs. Occasionally, the small neoplastic foci are uncertain, and difficult to detect. Some studies have reported that the detection rate of small HCCs, less than 3 cm, in DSA was about 70%^[4,5], and other studies showed higher sensitivity in nodule detection in helical biphasic CT than in DSA^[6]. This discrepancy can make it difficult to determine whether or not the same nodules exist on MDCT in cases of small tumor nodules.

Iodized oil retention pattern after TACE is a post-treatment prognostic marker and significant factors affect

local recurrence^[7,9], however, a method for evaluating this immediately after TACE, is to take a spot image. Follow-up unenhanced CT is usually performed within 1 mo after TACE, but it is sometimes difficult to determine whether there is washout of iodized oil uptake or initial failure of iodized oil uptake when there is partial iodized oil uptake in a lesion on the first follow-up CT. The exact method for comparing iodized oil retention in hypervascular nodules on preprocedural MDCT is to check the postprocedural CT directly after TACE and for this the patient must be transported from the angiography suite to the nearest CT scanner.

Cone-beam CT is a new technology provided by the combined angiography/CT suite that uses flat-panel detector (FD) technology. It provides images similar to those of CT and is able to obtain 3D reconstructions such as multiplanar reformat (MPR), maximum intensity projection (MIP), and 3D volume rendering (VR) with these data sets.

The purpose of this study was to evaluate the clinical value of cone-beam CT in the assessment of iodized oil uptake in TACE for small HCCs.

MATERIALS AND METHODS

Patients

From March 2006 to June 2006, eighteen patients (sixteen males and two females; 41–76 years; mean age, 58 years) with small HCCs (26 nodules; mean diameter 11.9 mm; range, 5–28 mm), underwent cone-beam CT and TACE consecutively. All patients had underlying liver cirrhosis. The diagnosis of HCC was made clinically in these patients by using typical imaging findings on MDCT and an elevated level of serum alpha fetoprotein. The size and location of the tumors were evaluated with triphasic MDCT before TACE (Figures 1 and 2). Eleven patients had previously undergone TACE for multiple nodules. The first TACE was performed in seven patients who were not candidates for surgery. According to our institutional guidelines, institutional review board approval was not required for this report.

TACE

Angiography was conducted using the AXIOM Artis FD Biplane Angio suite with cone-beam CT (DynaCT; Siemens Medical Solutions, Erlangen, Germany). For angiography, a 5-Fr catheter was inserted using the Seldinger technique from the right common femoral artery into the celiac trunk. After confirming the location of the tumor and its feeding artery, a 3-Fr 100-cm-long microcatheter (Progreat; Terumo, Tokyo, Japan) with a 0.016-inch, 150-cm long guidewire covered by hydrophilic polymer (Radiofocus; Terumo, Tokyo, Japan), was advanced through a 5-Fr catheter into the peripheral portion of the feeding artery as close to the lesion as possible (Figures 1 and 2). If tumor staining or feeders were uncertain, cone-beam CT hepatic arteriography (cone-beam CTHA) was performed (contrast media injection rate was 2 mL/s; X-ray delay used in 1.5 s). After these baseline studies, TACE using an emulsion of epirubicin hydrochloride (Pharmorubicin; Ildong, Seoul, Korea) dissolved in me-

Table 1 Degree of iodized oil uptake by the tumors

Degree	Spot image	Cone-beam CT
Excellent	11	16
Good	8	7
Poor	3	3
Total	22	26

Discordance between the two modalities-5 nodules [over-: 9% (2/22), underestimated: 14% (3/22) in spot image]. CT: Computed tomography.

glumine ioxitalamate (Telebrix; Guerbet, Aulnay-sous-Bois, France) mixed with iodized oil (Lipiodol Ultra Fluid; Guerbet, Aulnay-sous-Bois, France) was performed. The end point of TACE was when an “oily portogram” was achieved. Finally, spot image and cone-beam CT were performed to determine the deposition of iodized oil.

Cone-beam CT

Cone-beam CT acquisition was obtained using the following parameters: 10-s rotation; 0.4° increment; 1024 × 793 matrix in projections at zoom 0 after resampling; 217° total angle; and 11°/s, 27 frames/s, system dose 0.36 μGy/pulse, total 273 projections. The image reconstruction was performed on a commercially available dedicated workstation (X-Leonardo with DynaCT; Siemens Medical Solutions). The volume dataset was displayed on the monitor in the MPR.

Image analysis

The tumor locations, as shown on MDCT, iodized oil uptake by the tumor in the lesion on cone-beam CT and spot image, were determined directly after the procedures were analyzed. The enhancing tumor locations as shown on MDCT and iodized oil uptake by the tumors were compared. The degree of iodized oil uptake by the tumor (excellent, 100% deposition of iodized oil in the lesion; good, 51%–99%; poor, ≤ 50%) on cone-beam CT and spot image were also compared. The spot images were evaluated at the workstation, while cone-beam CT images were evaluated by images created by MPR, and MIP (maximum intensity projection). All images were graded by two radiologists, and decisions were reached by consensus.

RESULTS

Cone-beam CT was successfully completed in all study patients. It only took about 5 min to obtain MPR images. Cone-beam CT visualized the iodized oil uptake in all the nodules (26/26, sensitivity 100%), but spot image only visualized iodized oil uptake in 22 of the lesions (sensitivity 85%) (Figures 1 and 2).

Degree of iodized oil uptake in tumors

The degree of iodized oil uptake was somewhat different in the two modalities (Table 1). Cone-beam CT depicted iodized oil uptake in the nodules more clearly than spot image. Two nodules were not seen in spot image but were clearly evaluated with cone-beam CT. There was discordance between the two modalities in 5 nodules and

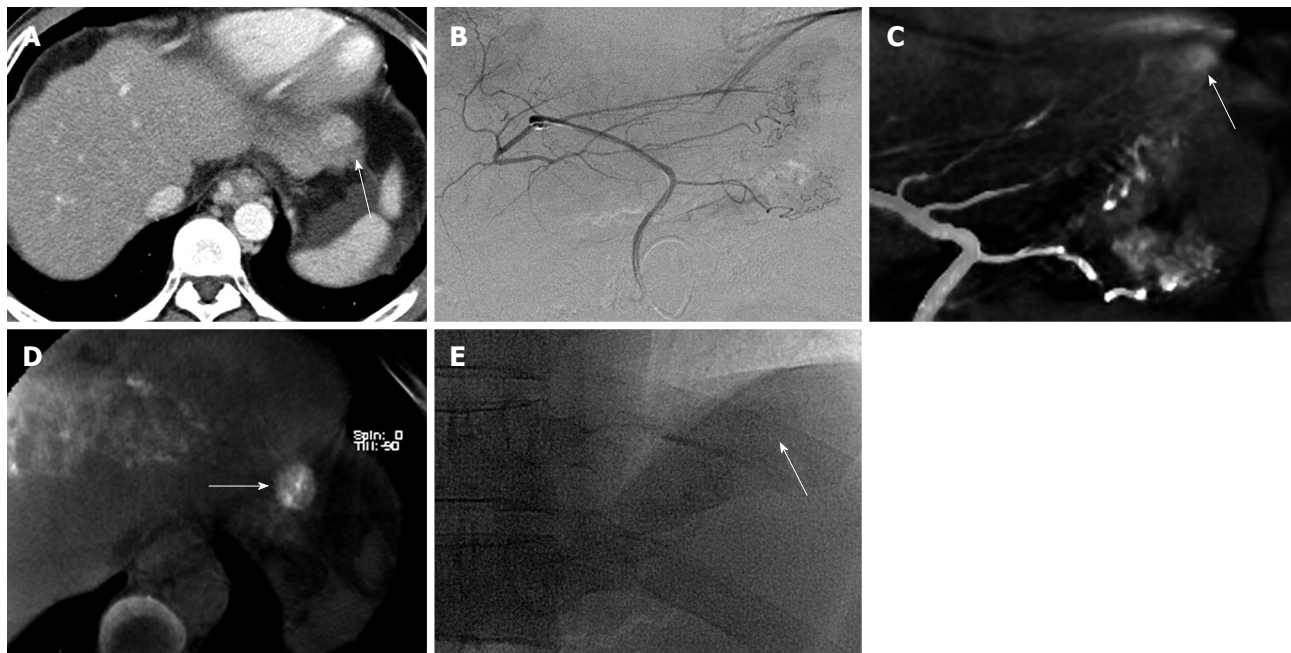


Figure 1 A 47-year-old man with hepatocellular carcinoma in S2 for 2nd TACE. A: Preprocedural late arterial phase MDCT scan reveals hypervascular HCC near the diaphragm (arrow); B: Left gastric angiogram shows aberrant left hepatic artery with no tumor staining in suspected area; C: Tumor staining (arrow) and feeder artery are found after acquiring MIP image from cone-beam CT hepatic arteriography (Cone-beam CTHA); D: Cone-beam CT directly after TACE shows good grade iodized oil uptake in S2 (arrow); E: Spot image shows subtle lipiodol uptake near the left hemidiaphragm (arrow), but nodular iodized oil uptake is not observed.

Table 2 Degree of iodized oil uptake by the tumors according to size

Size	Degree of iodized oil uptake in spot image			Degree of iodized oil uptake in cone-beam CT		
	Excellent	Good	Poor	Excellent	Good	Poor
≤ 1	5	3	1	7	4	
≤ 2	6	4	2	8	2	3
≤ 3		1		1	1	
Total	11	8	3	16	7	3

Discordance in degree of iodized oil uptake occurred in nodules less than 2 cm (3 nodules less than 1 cm).

iodized oil uptake was over-(9%, 2/22) or underestimated (14%, 3/22) in spot image compared with cone-beam CT.

The iodized oil uptake in 4 nodules was not seen in spot image, two nodules were less than 1 cm, one was between 1 cm and 2 cm, and one was over 2 cm. The discordance between the two modalities occurred in nodules less than 2 cm (Table 2).

Nodules with atypical enhancement patterns in MDCT

Three nodules showed atypical enhancement patterns in MDCT, and additional dynamic magnetic resonance imaging (MRI) was performed for one nodule (Figure 2). Their feeders were uncertain on selective right or left hepatic arteriography, but were detected with cone-beam CTHA. Enhancement patterns and iodized oil uptake in the nodules are shown in Table 3.

DISCUSSION

Several treatment options for small HCCs have been

Table 3 Enhancement patterns and iodized oil uptake in three nodules without typical enhancement patterns of HCCs on MDCT and MRI

Nodule	Modality	Phase		Degree of iodized oil uptake	
		EA	Delayed	Spot image	Cone-beam CT
1	CT	Subtle E	Washout	Poor	Poor
2 ¹	CT	No E	No E	Poor	Excellent
3	MRI	Subtle E	Washout	Invisible	Good

¹Same patient in Figure 2. EA: Early arterial phase; Delayed: Delayed phase; Subtle E: Subtle enhancement; No E: No enhancement. HCC: Hepatocellular carcinoma; MDCT: Multi-detector row helical computed tomography; MRI: Magnetic resonance imaging.

introduced for patients who are not surgical candidates. These options include TACE, percutaneous ethanol injection (PEI), radiofrequency ablation (RFA), microwave coagulation therapy (MCT), laser thermal ablation (LTA), and combination therapy^[10,11]. Among them, TACE is widely performed, because it is minimally invasive, repeatable, and more effective in combination with other treatments^[10-15].

TACE was found to be as effective as hepatic resection for early stage tumors when iodized oil was compactly retained within the tumor^[8]. Iodized oil uptake pattern can be a prognostic index^[7]. Various studies have suggested that iodized oil uptake in a tumor can correlate well with hepatic necrosis, and compact iodized oil uptake on unenhanced CT may represent necrosis^[16,17]. Takayasu *et al*^[16] reported that the highest degree of necrosis usually occurs immediately after TACE and the regrowth of viable cancer cells will occur later if complete necrosis of the tumor was not achieved. At this

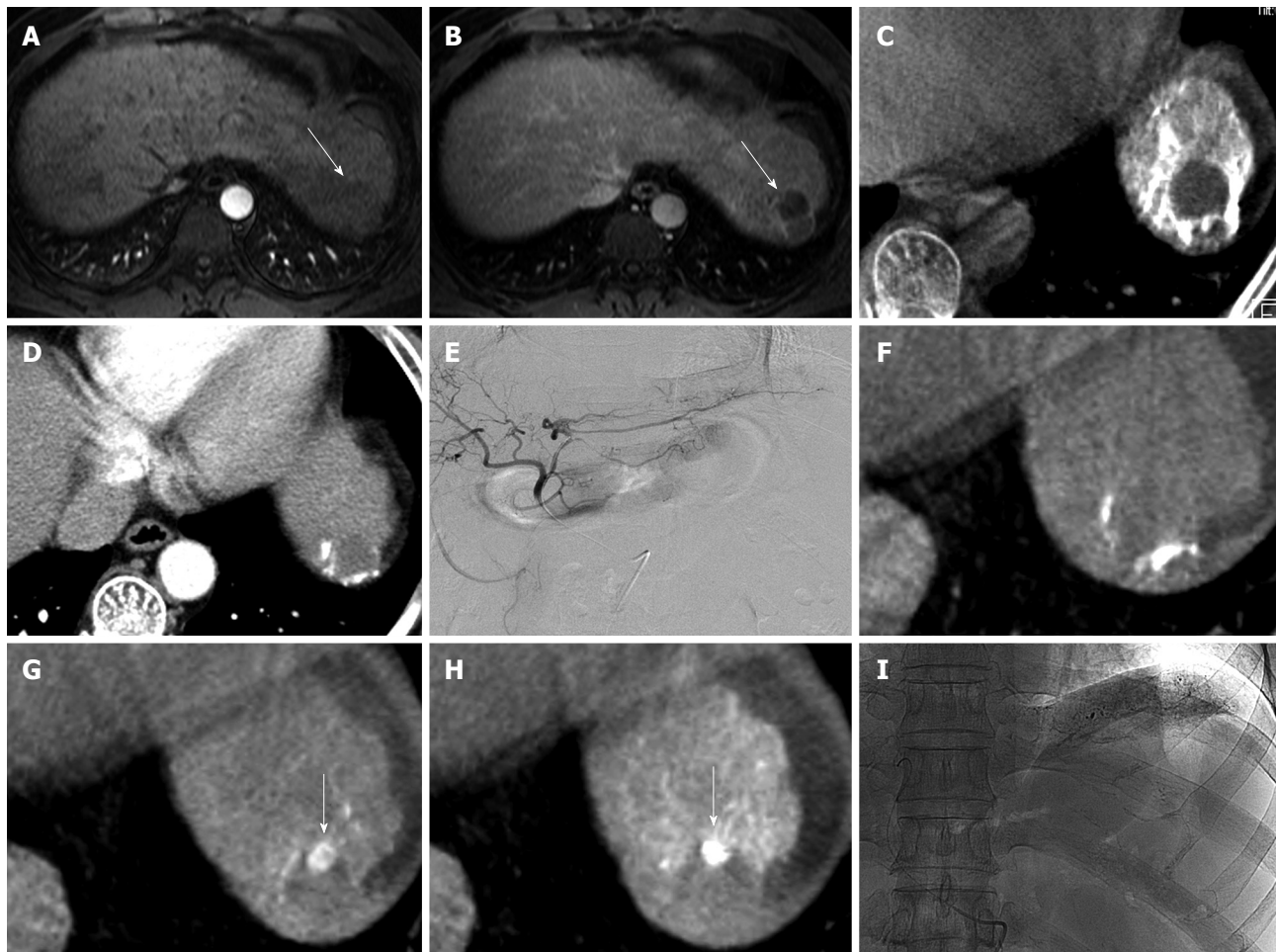


Figure 2 A 52-year-old man with HCC in S2 for 2nd TACE. A, B: Early arterial phase (A) and delayed phase (B) of MRI reveals nodule (arrow) in segment 2 with no enhancement (arrow); C: Cone-beam CT after TACE shows poor grade of iodized oil uptake by the tumor; D: Early arterial phase of MDCT shows washout of iodized oil uptake near nodule, but no enhancing portion within the nodule 3 mo later; E: Left hepatic angiogram during TACE reveals no tumor and feeding artery 1 mo later; F, G: Cone-beam CT with (F) and without (G) hepatic arteriography shows small enhancing nodule (arrow) in the nodule; H, I: Cone-beam CT after infusion of emulsion (H) shows excellent grade iodized oil uptake by the nodule (arrow). This case shows typical "nodule-in-nodule" appearance of HCC, but spot image (I) did not distinguish nodular uptake.

point, compact iodized oil uptake by the tumor directly after the procedure prevents regrowth of tumors, but to confirm this, only spot image is usually acquired. If the tumor is large enough to appear on spot images, it is easy to determine the degree of iodized oil uptake, but if the tumor is small, especially less than 2 cm, the degree of iodized oil uptake is incorrectly determined, which can cause tumor regrowth. It is also impossible to refuse chemotherapeutic agents directly if there is partial iodized oil uptake in a lesion on the first follow-up CT.

Cone-beam CT was first used in neuroendovascular procedures, and the image quality is sufficient to make a diagnosis when a complication is suspected^[18]. In the era of assessing the degree of iodized oil uptake, cone-beam CT is also a convenient tool during and after TACE and clearly correlates with MDCT. If cone-beam CT images shows non-compact iodized oil uptake, immediate re-intervention can be achieved. The disadvantages of this CT-like image are low temporal resolution and a small field of view, however, it is sufficient to locate lesions previously diagnosed on MDCT^[19].

Takayasu *et al*^[9] reported "targeted transarterial oily chemoembolization" which is a similar method to ours,

but these authors used a unified helical CT and angiography system. Our system is only a DSA machine without a helical CT system and has more simple structures.

The radiation dose from cone-beam CT was not measured, however, Hirota *et al*^[20] measured the radiation dose of cone-beam CT with a flat-panel-detector digital angiography system (similar system with ours) and single helical CT using a cylindrical phantom model of CT dose index with a dosimeter. They reported that the radiation dose by cone-beam CT was less than that of single helical CT. In addition, the radiation dose from cone-beam CT can be calculated *via* a pre-set radiation dose (0.36 µGy/pulse) and total fluoro time (7.5 pulse/s, 10 s). Compared with nonenhanced MDCT for TACE follow-up, the calculated radiation dose of cone-beam CT is low.

Cone-beam CTHA placing the microcatheter in the nearest arteries was performed in only three nodules in this study. Another study^[20] also reported this method, and this technique is very useful to confirm a perfusion area in the artery. Although a small number of cases were included in this study, this method is a very useful and time-saving technique in TACE and other interventional procedures, especially for small lesions.

In conclusion, cone-beam CT is a useful and convenient tool for assessing the iodized oil uptake by small hepatic tumors (< 3 cm) directly after TACE. In addition, in cases with suspected small HCC nodules without typical enhancement patterns on CT, cone-beam CTHA will be very useful, however, further study is required.

COMMENTS

Background

Iodized oil retention pattern after transarterial chemoembolization (TACE) is a posttreatment prognostic marker, and significant factors affect local recurrence, however, a method for evaluating this immediately after TACE is to take a spot image. Follow-up unenhanced computed tomography (CT) is usually performed within 1 mo after TACE, but it is sometimes difficult to determine whether there is washout of iodized oil uptake or initial failure of iodized oil uptake when there is partial iodized oil uptake in a lesion on the first follow-up CT.

Research frontiers

Comparing iodized oil retention in small hypervascular nodules on preprocedural multi-detector row helical computed tomography (MDCT) directly after TACE is possible without transporting patients from the angiography suite to the nearest CT scanner.

Innovations and breakthroughs

In the present study, the authors investigated the efficacy of cone-beam CT with regard to iodized oil uptake after TACE for small hepatocellular carcinoma (HCC)s.

Applications

The study showed that cone-beam CT is a useful and convenient tool for assessing the iodized oil uptake by small hepatic tumors directly after TACE.

Terminology

Cone-beam CT is a new technology provided by the combined angiography/CT suite that uses flat-panel detector technology. It provides images similar to those of CT and is able to make 3D reconstructions such as multiplanar reformat, maximum intensity projection, and 3D volume rendering with these data sets.

Peer review

This is an interesting study which shows the advantages of assessing iodized oil uptake after TACE for small HCC with cone-beam CT. It may provide useful information for us.

REFERENCES

- 1 **Murakami T**, Kim T, Takamura M, Hori M, Takahashi S, Federle MP, Tsuda K, Osuga K, Kawata S, Nakamura H, Kudo M. Hypervascular hepatocellular carcinoma: detection with double arterial phase multi-detector row helical CT. *Radiology* 2001; **218**: 763-767
- 2 **Zhao H**, Zhou KR, Yan FH. Role of multiphase scans by multirow-detector helical CT in detecting small hepatocellular carcinoma. *World J Gastroenterol* 2003; **9**: 2198-2201
- 3 **Kim SK**, Lim JH, Lee WJ, Kim SH, Choi D, Lee SJ, Lim HK, Kim H. Detection of hepatocellular carcinoma: comparison of dynamic three-phase computed tomography images and four-phase computed tomography images using multidetector row helical computed tomography. *J Comput Assist Tomogr* 2002; **26**: 691-698
- 4 **Bartolozzi C**, Lencioni R, Caramella D, Palla A, Bassi AM, Di Candio G. Small hepatocellular carcinoma. Detection with US, CT, MR imaging, DSA, and Lipiodol-CT. *Acta Radiol* 1996; **37**: 69-74
- 5 **De Santis M**, Romagnoli R, Cristani A, Cioni G, Casolo A, Vici FF, Ventura E. MRI of small hepatocellular carcinoma: comparison with US, CT, DSA, and Lipiodol-CT. *J Comput Assist Tomogr* 1992; **16**: 189-197
- 6 **Nakayama A**, Imamura H, Matsuyama Y, Kitamura H, Miwa S, Kobayashi A, Miyagawa S, Kawasaki S. Value of lipiodol computed tomography and digital subtraction angiography in the era of helical biphasic computed tomography as preoperative assessment of hepatocellular carcinoma. *Ann Surg* 2001; **234**: 56-62
- 7 **Mondazzi L**, Bottelli R, Brambilla G, Rampoldi A, Rezakovic I, Zavaglia C, Alberti A, Ideo G. Transarterial oily chemoembolization for the treatment of hepatocellular carcinoma: a multivariate analysis of prognostic factors. *Hepatology* 1994; **19**: 1115-1123
- 8 **Lee HS**, Kim KM, Yoon JH, Lee TR, Suh KS, Lee KU, Chung JW, Park JH, Kim CY. Therapeutic efficacy of transcatheter arterial chemoembolization as compared with hepatic resection in hepatocellular carcinoma patients with compensated liver function in a hepatitis B virus-endemic area: a prospective cohort study. *J Clin Oncol* 2002; **20**: 4459-4465
- 9 **Takayasu K**, Muramatsu Y, Maeda T, Iwata R, Furukawa H, Muramatsu Y, Moriyama N, Okusaka T, Okada S, Ueno H. Targeted transarterial oily chemoembolization for small foci of hepatocellular carcinoma using a unified helical CT and angiography system: analysis of factors affecting local recurrence and survival rates. *AJR Am J Roentgenol* 2001; **176**: 681-688
- 10 **Zheng XH**, Guan YS, Zhou XP, Huang J, Sun L, Li X, Liu Y. Detection of hypervascular hepatocellular carcinoma: Comparison of multi-detector CT with digital subtraction angiography and Lipiodol CT. *World J Gastroenterol* 2005; **11**: 200-203
- 11 **Ferrari FS**, Stella A, Pasquinucci P, Vigni F, Civel L, Pieraccini M, Magnolfi F. Treatment of small hepatocellular carcinoma: a comparison of techniques and long-term results. *Eur J Gastroenterol Hepatol* 2006; **18**: 659-672
- 12 **Bartolozzi C**, Lencioni R, Caramella D, Vignali C, Cioni R, Mazzeo S, Carrai M, Maltinti G, Capria A, Conte PF. Treatment of large HCC: transcatheter arterial chemoembolization combined with percutaneous ethanol injection versus repeated transcatheter arterial chemoembolization. *Radiology* 1995; **197**: 812-818
- 13 **Matsui O**, Kadoya M, Yoshikawa J, Gabata T, Arai K, Demachi H, Miyayama S, Takashima T, Unoura M, Kogayashi K. Small hepatocellular carcinoma: treatment with subsegmental transcatheter arterial embolization. *Radiology* 1993; **188**: 79-83
- 14 **Pacella CM**, Bizzarri G, Cecconi P, Caspani B, Magnolfi F, Bianchini A, Anelli V, Pacella S, Rossi Z. Hepatocellular carcinoma: long-term results of combined treatment with laser thermal ablation and transcatheter arterial chemoembolization. *Radiology* 2001; **219**: 669-678
- 15 **Qian J**, Feng GS, Vogl T. Combined interventional therapies of hepatocellular carcinoma. *World J Gastroenterol* 2003; **9**: 1885-1891
- 16 **Takayasu K**, Arii S, Matsuo N, Yoshikawa M, Ryu M, Takasaki K, Sato M, Yamanaka N, Shimamura Y, Ohto M. Comparison of CT findings with resected specimens after chemoembolization with iodized oil for hepatocellular carcinoma. *AJR Am J Roentgenol* 2000; **175**: 699-704
- 17 **Choi BI**, Kim HC, Han JK, Park JH, Kim YI, Kim ST, Lee HS, Kim CY, Han MC. Therapeutic effect of transcatheter oily chemoembolization therapy for encapsulated nodular hepatocellular carcinoma: CT and pathologic findings. *Radiology* 1992; **182**: 709-713
- 18 **Heran NS**, Song JK, Namba K, Smith W, Niimi Y, Berenstein A. The utility of DynaCT in neuroendovascular procedures. *AJNR Am J Neuroradiol* 2006; **27**: 330-332
- 19 **Akpek S**, Brunner T, Benndorf G, Strother C. Three-dimensional imaging and cone beam volume CT in C-arm angiography with flat panel detector. *Diagn Interv Radiol* 2005; **11**: 10-13
- 20 **Hirota S**, Nakao N, Yamamoto S, Kobayashi K, Maeda H, Ishikura R, Miura K, Sakamoto K, Ueda K, Baba R. Cone-beam CT with flat-panel-detector digital angiography system: early experience in abdominal interventional procedures. *Cardiovasc Interv Radiol* 2006; **29**: 1034-1038



BRIEF ARTICLE

Image-guided conservative management of right colonic diverticulitis

Sun Jin Park, Sung Il Choi, Suk Hwan Lee, Kil Yeon Lee

Sun Jin Park, Sung Il Choi, Suk Hwan Lee, Kil Yeon Lee,
Department of Surgery, Kyung Hee University School of Medicine,
Seoul 130-701, South Korea

Author contributions: Park SJ carried out acquisition of data, analysis of data and drafting the article; Choi SI revised the article critically for important intellectual content; Lee SH revised the article critically for important intellectual content; Lee KY conceived and designed the study, carried out acquisition of data, revised the article critically for important intellectual content and approved the final version prior to publication.

Supported by The research paper scholarship of the graduate school of Kyung Hee University in the second semester of 2007

Correspondence to: Kil Yeon Lee, MD, PhD, Department of Surgery, Kyung Hee University School of Medicine, Seoul 130-701, South Korea. isaac34@korea.com

Telephone: +82-2-9588241 **Fax:** +82-2-9669366

Received: October 11, 2009 **Revised:** October 29, 2009

Accepted: November 5, 2009

Published online: December 14, 2009

CONCLUSION: Our results indicate that right colonic diverticulitis is essentially benign and image-guided conservative treatment is primarily required.

© 2009 The WJG Press and Baishideng. All rights reserved.

Key words: Ascending colon; Cecum; Medical therapy; Colonic diverticulitis

Peer reviewer: Dr. Marco Scarpa, Department of Surgical & Gastroenterological Sciences (Gastroenterology section), University of Padova, Padova 35128, Italy

Park SJ, Choi SI, Lee SH, Lee KY. Image-guided conservative management of right colonic diverticulitis. *World J Gastroenterol* 2009; 15(46): 5838-5842 Available from: URL: <http://www.wjgnet.com/1007-9327/15/5838.asp> DOI: <http://dx.doi.org/10.3748/wjg.15.5838>

Abstract

AIM: To study the clinical outcomes of medical therapy in patients with right colonic diverticulitis.

METHODS: The records of 189 patients with right colonic diverticulitis which was finally diagnosed by computed tomography, ultrasonography, or operative findings were retrospectively reviewed.

RESULTS: Of the 189 patients hospitalized for right colonic diverticulitis, the stages of diverticulitis by a modified Hinchen classification were 26 patients (13.8%) in stage 0, 139 patients (73.5%) in stage I a, 23 patients (12.2%) in stage I b, and 1 patient (0.5%) in stage III. Medical therapy was undertaken in 185 of 189 patients (97.9%). One hundred and eighty three of 185 patients were successfully treated with bowel rest and antibiotics. Two patients in stage I b required a resection or surgical drainage because of an inadequate response to conservative treatment. Recurrent diverticulitis developed in 15 of 183 patients (8.2%) who responded to medical therapy. All 15 patients who suffered a second attack had uncomplicated diverticulitis, and were successfully treated with medical therapy.

INTRODUCTION

Interestingly, there is a unique predilection for diverticular disease of the colon in Western and Asian populations, and is predominant in the left colon in Caucasians^[1], while much more common in the right colon in Asians^[2]. Many studies have focused on left colonic diverticulitis and subsequently, therapeutic guidelines have been established, while that of right colonic diverticulitis still remains controversial^[2-8]. In the past, the majority of patients with right colonic diverticulitis were faced with an operation for presumed appendicitis^[3,4,9]. Thus, there is a lack of objective information for patients with right colonic diverticulitis compared with left colonic diverticulitis. Much of this information is based on case series data, which have relatively small sample sizes and the preoperative diagnosis was not made using imaging studies. Recent studies suggest that colonic diverticulitis can be correctly diagnosed by computed tomography (CT) scan^[6,7,10], or ultrasonography (US)^[11-14], and with the use of these imaging studies, right colonic diverticulitis is more common than has been previously assumed^[7]. The aim of this study was to evaluate the clinical course and results of medical therapy in patients with right colonic diverticulitis, of which the final diagnosis was based on radiographic evidence from CT or US, or operative findings.

MATERIALS AND METHODS

Patients

Using computerized patient databases, we searched for all patients who were hospitalized with the diagnosis of colonic diverticulitis from January 1998 to August 2007 at Kyung Hee University Hospital, Seoul, Korea. Excluded were patients who were clinically suspected of having colonic diverticulitis without operative findings or radiologic evidence from CT or US, patients whose colonic diverticulosis alone was present without any evidence of inflammation, and those whose follow-up records were unobtainable. A total of 189 patients were retrospectively reviewed and data were collected with regard to age and sex, clinical presentation, location of disease, diagnostic studies (CT, US, barium enema, and colonoscopy), laboratory findings, type of complication, treatment modality, preoperative diagnosis, operative findings, type of operation, and outcome. The final diagnosis was based on radiographic evidence from CT or US, or operative findings. CT was performed in 138 patients (73%) and US was performed in 114 patients (60.3%). Both CT and US were performed in 80 patients (42.3%) and 17 patients underwent surgery without CT or US. Recurrence of diverticulitis was defined as the presence of the same symptoms and signs leading to re-hospitalization. Recurrence was tracked either by interviewing the patient or by telephone contact.

A modification of the Hinckley classification system was used to define the patients^[15,16]. Patients were categorized into the six stages according to CT, US, or operative findings. Complicated diverticulitis is defined as diverticulitis associated with abscess, fistula, obstruction, or free perforation^[17]. Therefore, uncomplicated diverticulitis included stage 0 and I a, whereas complicated diverticulitis included stage I b, II III, and IV.

The data were analyzed using the chi-square test or Fisher's exact test. All *P* values of less than 0.05 were considered to be statistically significant.

RESULTS

Characteristics and presentation of patients

Of the 189 patients hospitalized for right colonic diverticulitis, 111 were men and 78 were women. The median age of the patients was 37 years (range, 14-88 years). The mean age of women (40.4 years) was not significantly different from that of men (36.7 years) (*P* = 0.088). One hundred and eight patients (57.1%) were under the age of 40 years. By a modified Hinckley classification, stages of diverticulitis present on admission were as follows: 26 patients (13.8%) in stage 0, 139 patients (73.5%) in stage I a, 23 patients (12.2%) in stage I b, and 0 (0%), 1 (0.5%), 0 (0%) patient in stage II, stage III and stage IV, respectively (Table 1). The majority of patients commonly presented with phlegmon. The majority of patients (87.3%) had mild diverticulitis (stage 0 or I a) on admission and only 24 patients (12.7%) had complicated diverticulitis. The average white blood cell count was 11417 ± 275 . Fever was seen in 20.6% of patients.

Table 1 Presentation of patients by a modified Hinckley classification^[15]

Modified Hinckley classification		Total (n = 189)
0	Direct visualization of the diverticulum with Sx or Sign ¹	26
I a	Confined pericolic inflammation (phlegmon)	139
I b	Confined pericolic abscess	23
II	Distant intraabdominal or retroperitoneal abscess	0
III	Generalized purulent peritonitis	1
IV	Fecal peritonitis	0

¹Right abdominal pain, leukocytosis, or fever with no radiologic evidence of appendicitis. Sx: Symptom.

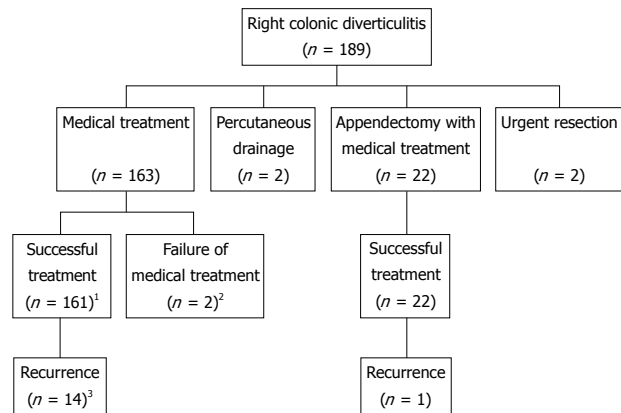


Figure 1 Treatment and outcome of 189 patients with right colonic diverticulitis. ¹After successful medical treatment, seven patients had elective surgery at the surgeon's request; ²One patient required a resection and another underwent surgical drainage; ³After successful medical treatment, five patients had elective surgery at the surgeon's request.

Treatment

Patients were initially managed with medical therapy alone, percutaneous drainage, or an urgent operation. Elective surgery was determined after a cooling-off period. Medical therapy was undertaken in 185 of 189 patients (97.9%), including 22 patients who incidentally underwent an appendectomy for presumed appendicitis (Figure 1). Two patients in stage I b underwent percutaneous drainage and two patients (one in stage I b and one in stage III) underwent urgent surgery (1 ileocecal resection, 1 right hemicolectomy). One hundred and eighty three of 185 patients were successfully treated with bowel rest and antibiotics. However, two patients in stage I b required a resection or surgical drainage because of an inadequate response to conservative treatment. Seven patients who were successfully treated with bowel rest and antibiotics had an elective operation at the surgeon's request.

Recurrence

Recurrent diverticulitis developed in 15 of 183 patients (8.2%) who responded to medical therapy. The median interval to the onset of recurrence was 11 mo (range, 0.5-96 mo). The median disease free period was 44 mo (range, 0.5-129 mo). All 15 patients who suffered a

second attack had uncomplicated diverticulitis, and were successfully treated with medical therapy. One patient, an 80-year-old woman, experienced five episodes of right colonic diverticulitis, which were uncomplicated and successfully treated with medical therapy. Five of these 15 patients had an elective operation at the surgeon's request after successful conservative treatment. There were no deaths in these patients with right colonic diverticulitis.

Pathology and follow-up study

A total of 15 patients underwent colonic resection. Nine of these 15 patients were reported to have multiple false diverticula. The pathologic reports of the other six patients contained no mention of the type of diverticulum.

During the original hospitalization, CT or US was supplemented by colonoscopy or double-contrast barium enema in 31 patients. In addition, 1 mo after recovery from an initial episode of diverticulitis, 60 patients agreed to re-evaluation by double-contrast barium enema (54 patients) or colonoscopy (six patients). In a total of 87 patients, including four patients duplicated, multiple diverticula were reported in 62 patients (71.3%) and a solitary diverticulum was reported in 13 patients (14.9%). The number of diverticulum could not be identified in 12 patients due to poor bowel preparation.

DISCUSSION

The Hinchey classification and its several modifications have been used to define the stages of acute diverticulitis although the systems were mostly applied to left colonic diverticulitis^[15,18]. In the present study, the diagnosis of right colonic diverticulitis was made in 167 of 172 (97%) patients using CT or US. The original Hinchey classification is not detailed enough to reflect right colonic diverticulitis with which the majority of patients have mild forms. We therefore used a modified system including subcategories in the early stage^[15,16]. The majority of patients (87.3%) had uncomplicated diverticulitis (stage 0 or I a) on admission and the other patients even those with complicated diverticulitis had a relatively early stage (stage I b) such as pericolic abscess with the exception of one patient (stage III).

To date, no therapeutic guidelines for patients with right colonic diverticulitis have been established^[3,6-9,19-21]. In contrast, practice parameters for the treatment of left colonic diverticulitis do exist^[17]. Conservative treatment is recommended for uncomplicated left colonic diverticulitis because it results in resolution of the problem in 70% to 100% of patients^[22-29]. In our study, all of the 165 patients with uncomplicated right colonic diverticulitis (stage 0 or I a) were successfully treated with bowel rest and antibiotics, including 22 patients who underwent an appendectomy for presumed appendicitis. We believe that patients with uncomplicated right colonic diverticulitis can be successfully treated with medical treatment in the same way as those with uncomplicated left colonic diverticulitis.

However, some authors advocate surgical resection for right colonic diverticulitis encountered during surgery

for presumed appendicitis^[3-5]. Lo *et al*^[3] reported their experience of 22 patients over an 11-year period. They performed preoperative US and CT in only one patient. At operation, an inflammatory phlegmon or indurated mass was found in 18 patients, however, colectomy with primary ileocolic anastomosis was performed in 21 patients including these 18 patients. Lane *et al*^[4] reported a series of 49 patients over a 22-year period. The authors stated that because the pathophysiology of cecal diverticula may be different in the Asian population and the recurrence of symptoms may be more common in the Western population, conservative management may not be applicable to the Western population. A correct radiologic diagnosis was preoperatively made in only three patients. Immediate right hemicolectomy was performed in 39 patients at the time of laparotomy, but operative findings or the severity of diverticulitis was not provided. Fang *et al*^[5] analyzed 85 patients during a 5-year period. Thirty four patients had right hemicolectomy, 9 patients had diverticulectomy, and 42 patients received conservative treatment (antibiotics or appendectomy plus antibiotics). In 34 patients receiving right hemicolectomy, the indications for surgery included repeated attack of symptoms in six and phlegmon, abscess, or perforation of the diverticulum in ten. In 42 patients receiving conservative treatment, ten patients developed recurrent diverticulitis and only three of these ten patients had complicated diverticulitis. However, the authors mentioned that the disease process of cecal diverticulitis might not be benign and recurrence of diverticulitis should be an indication for aggressive resection. In the above studies, we guess that all patients who underwent colonic resection would not essentially require surgery, and conservative treatment alone might have been sufficient in some patients. We believe that the correct pretreatment diagnosis for right colonic diverticulitis does not only avoid unnecessary surgery but also allows clinicians to determine optimal management according to the severity of the diverticulitis.

It is uncertain whether the pathophysiology of right colonic diverticulitis is really different between Asian and Western populations. Oudenhoven *et al*^[7] reviewed 44 patients with right colonic diverticulitis in a Western population (including one Asian patient). Forty one patients were successfully treated conservatively and three patients underwent diverticulectomy. They concluded that the natural history of right colonic diverticulitis is benign and surgical intervention can be avoided in the vast majority of patients. In a large post-mortem survey of diverticular disease, Hughes^[11] reported that the incidence of solitary cecal diverticula lies between 2.5% and 5%. Histologically all the diverticula were thin-walled, false diverticula and no case of cecal diverticulum had muscle in its wall. The author mentioned that congenital cecal diverticulum may largely be a pathological myth. Graham and Ballantyne^[9] reviewed the American experiences. Among 128 histologic cases compiled from the medical literature, they found that 52 (41%) were true diverticula while 76 (59%) were, in fact, false diverticula. In addition, among 288 cases gathered from the literature, 233 (81%) were solitary, while 55 (19%) were multiple. In the

present study, nine of 15 patients who underwent colonic resection were reported to have multiple false diverticula. Of 87 patients receiving double-contrast barium enema or colonoscopy, multiple diverticula were reported in 62 patients (71.3%) and solitary diverticulum was reported in 13 patients (14.9%). The incidence of true or false diverticula in the right colon is not well known, particularly between Western and Asian populations. This is because the pathologic differentiation between true and false diverticula may be difficult once inflammation occurs^[4], and to our knowledge, the type of diverticula in right colonic diverticulitis has not been pathologically described in the Asian literature.

Some authors who advocate aggressive resection for right colonic diverticulitis assert that leaving the diseased foci *in situ* with the possibility of developing some serious complications later seems to be impractical and recurrence of diverticulitis should be an indication for aggressive resection. If recurrence is high and complications frequent, surgical resection is essentially required. However, after successful conservative treatment, a recurrence rate of 3.6% to 23.8% has been reported in the literature^[5,7,8,20,21,30]. Ngai et al^[31] reported a recurrence rate of 1.5%, but 38% of their patients underwent diverticulectomy. It is interesting to note that in these studies, there was little complicated diverticulitis in recurrent cases: Fang et al^[5] reported three complicated cases in 10 recurrences in 42 patients receiving conservative treatments, and Harada et al^[30] reported one complicated case in four recurrences in 29 patients. The other authors reported that all of the recurrent cases were uncomplicated diverticulitis, which responded well to medical therapy. Komuta et al^[8] mentioned that recurrent uncomplicated right colonic diverticulitis responded well to medical therapy regardless of the number of recurrences. In our study, 15 of 183 patients (8.2%) who responded to medical therapy developed recurrent diverticulitis. All 15 patients had uncomplicated diverticulitis, and were successfully treated with medical therapy. Therefore, we believe that if the recurrence rate after conservative treatment is not high and if complications are not frequent even after recurrence occurs, recurrence of right colonic diverticulitis should initially be an indication for medical treatment and not for surgery.

In conclusion, our results indicate that right colonic diverticulitis is essentially benign and image-guided conservative treatment is primarily required. Although our study is limited by the retrospective design and relatively few recurrent patients, our results suggest that recurrence after conservative treatment of right colonic diverticulitis is low, and rarely associated with complicated diverticulitis. Thus, recurrence of right colonic diverticulitis should initially be an indication for medical treatment, while surgical resection should be selectively considered for patients with complicated diverticulitis.

COMMENTS

Background

Right colonic diverticulitis is a rare condition in Western populations, while it

is much more common in Asian populations. There is a lack of information available on the clinical course and results of medical therapy for patients with right colonic diverticulitis compared with left colonic diverticulitis.

Research frontiers

The final diagnosis of all patients with right colonic diverticulitis was based on radiographic evidence from computed tomography or ultrasonography, or operative findings. The majority of patients with right colonic diverticulitis had a mild form on admission and initially required medical therapy. Recurrent diverticulitis developed in 8.2%, but all recurrent patients had uncomplicated diverticulitis, and were successfully treated with medical therapy.

Innovations and breakthroughs

Right colonic diverticulitis is essentially benign and image-guided conservative treatment is primarily required. The correct pretreatment diagnosis for right colonic diverticulitis does not only avoid unnecessary surgery but also allows clinicians to determine optimal management according to the severity of the diverticulitis. Even recurrence of right colonic diverticulitis should initially be an indication for medical treatment, while surgical resection should be selectively considered for patients with complicated diverticulitis.

Terminology

Complicated diverticulitis is defined as diverticulitis associated with abscess, fistula, obstruction, or free perforation.

Peer review

This is an interesting study about right colonic diverticulitis management that has been quite rarely discussed.

REFERENCES

- Hughes LE. Postmortem survey of diverticular disease of the colon. I. Diverticulosis and diverticulitis. *Gut* 1969; **10**: 336-344
- Sugihara K, Muto T, Morioka Y, Asano A, Yamamoto T. Diverticular disease of the colon in Japan. A review of 615 cases. *Dis Colon Rectum* 1984; **27**: 531-537
- Lo CY, Chu KW. Acute diverticulitis of the right colon. *Am J Surg* 1996; **171**: 244-246
- Lane JS, Sarkar R, Schmit PJ, Chandler CF, Thompson JE Jr. Surgical approach to cecal diverticulitis. *J Am Coll Surg* 1999; **188**: 629-634; discussion 634-635
- Fang JF, Chen RJ, Lin BC, Hsu YB, Kao JL, Chen MF. Aggressive resection is indicated for cecal diverticulitis. *Am J Surg* 2003; **185**: 135-140
- Katz DS, Lane MJ, Ross BA, Gold BM, Jeffrey RB Jr, Mindelzun RE. Diverticulitis of the right colon revisited. *AJR Am J Roentgenol* 1998; **171**: 151-156
- Oudenhoven LF, Koumans RK, Puylaert JB. Right colonic diverticulitis: US and CT findings--new insights about frequency and natural history. *Radiology* 1998; **208**: 611-618
- Komuta K, Yamanaka S, Okada K, Kamohara Y, Ueda T, Makimoto N, Shiogama T, Furui J, Kanematsu T. Toward therapeutic guidelines for patients with acute right colonic diverticulitis. *Am J Surg* 2004; **187**: 233-237
- Graham SM, Ballantyne GH. Cecal diverticulitis. A review of the American experience. *Dis Colon Rectum* 1987; **30**: 821-826
- Jang HJ, Lim HK, Lee SJ, Lee WJ, Kim EY, Kim SH. Acute diverticulitis of the cecum and ascending colon: the value of thin-section helical CT findings in excluding colonic carcinoma. *AJR Am J Roentgenol* 2000; **174**: 1397-1402
- Liljegren G, Chabok A, Wickbom M, Smedh K, Nilsson K. Acute colonic diverticulitis: a systematic review of diagnostic accuracy. *Colorectal Dis* 2007; **9**: 480-488
- Pradel JA, Adell JF, Taourel P, Djafari M, Monnin-Delhom E, Bruel JM. Acute colonic diverticulitis: prospective comparative evaluation with US and CT. *Radiology* 1997; **205**: 503-512
- Chou YH, Chiou HJ, Tiu CM, Chen JD, Hsu CC, Lee CH, Lui WY, Hung GS, Yu C. Sonography of acute right side colonic diverticulitis. *Am J Surg* 2001; **181**: 122-127
- Hollerweger A, Macheiner P, Rettenbacher T, Brunner W, Gritzmann N. Colonic diverticulitis: diagnostic value and appearance of inflamed diverticula-sonographic evaluation. *Eur Radiol* 2001; **11**: 1956-1963

- 15 **Wasvary H**, Turfah F, Kadro O, Beauregard W. Same hospitalization resection for acute diverticulitis. *Am Surg* 1999; **65**: 632-635; discussion 636
- 16 **Kaiser AM**, Jiang JK, Lake JP, Ault G, Artinyan A, Gonzalez-Ruiz C, Essani R, Beart RW Jr. The management of complicated diverticulitis and the role of computed tomography. *Am J Gastroenterol* 2005; **100**: 910-917
- 17 **Wong WD**, Wexner SD, Lowry A, Vernava A 3rd, Burnstein M, Denstman F, Fazio V, Kerner B, Moore R, Oliver G, Peters W, Ross T, Senatore P, Simmang C. Practice parameters for the treatment of sigmoid diverticulitis--supporting documentation. The Standards Task Force. The American Society of Colon and Rectal Surgeons. *Dis Colon Rectum* 2000; **43**: 290-297
- 18 **Hinchey EJ**, Schaal PG, Richards GK. Treatment of perforated diverticular disease of the colon. *Adv Surg* 1978; **12**: 85-109
- 19 **Markham NI**, Li AK. Diverticulitis of the right colon--experience from Hong Kong. *Gut* 1992; **33**: 547-549
- 20 **Yang HR**, Huang HH, Wang YC, Hsieh CH, Chung PK, Jeng LB, Chen RJ. Management of right colon diverticulitis: a 10-year experience. *World J Surg* 2006; **30**: 1929-1934
- 21 **Moon HJ**, Park JK, Lee JI, Lee JH, Shin HJ, Kim WS, Kim MS, Jeong JH. Conservative treatment for patients with acute right colonic diverticulitis. *Am Surg* 2007; **73**: 1237-1241
- 22 **Parks TG**, Connell AM. The outcome in 455 patients admitted for treatment of diverticular disease of the colon. *Br J Surg* 1970; **57**: 775-778
- 23 **Larson DM**, Masters SS, Spiro HM. Medical and surgical therapy in diverticular disease: a comparative study. *Gastroenterology* 1976; **71**: 734-737
- 24 **Haglund U**, Hellberg R, Johnsén C, Hultén L. Complicated diverticular disease of the sigmoid colon. An analysis of short and long term outcome in 392 patients. *Ann Chir Gynaecol* 1979; **68**: 41-46
- 25 **Thompson WG**, Patel DG. Clinical picture of diverticular disease of the colon. *Clin Gastroenterol* 1986; **15**: 903-916
- 26 **Cheskin LJ**, Bohlman M, Schuster MM. Diverticular disease in the elderly. *Gastroenterol Clin North Am* 1990; **19**: 391-403
- 27 **Detry R**, Jamez J, Kartheuser A, Zech F, Vanheuverzwijn R, Hoang P, Kestens PJ. Acute localized diverticulitis: optimum management requires accurate staging. *Int J Colorectal Dis* 1992; **7**: 38-42
- 28 **Hachigian MP**, Honickman S, Eisenstat TE, Rubin RJ, Salvati EP. Computed tomography in the initial management of acute left-sided diverticulitis. *Dis Colon Rectum* 1992; **35**: 1123-1129
- 29 **Kellum JM**, Sugerman HJ, Coppa GF, Way LR, Fine R, Herz B, Speck EL, Jackson D, Duma RJ. Randomized, prospective comparison of cefoxitin and gentamicin-clindamycin in the treatment of acute colonic diverticulitis. *Clin Ther* 1992; **14**: 376-384
- 30 **Harada RN**, Whelan TJ Jr. Surgical management of cecal diverticulitis. *Am J Surg* 1993; **166**: 666-669; discussion 669-671
- 31 **Ngoi SS**, Chia J, Goh MY, Sim E, Rauff A. Surgical management of right colon diverticulitis. *Dis Colon Rectum* 1992; **35**: 799-802

S-Editor Wang YR L-Editor Webster JR E-Editor Zheng XM



BRIEF ARTICLE

Changes in intestinal mucosal immune barrier in rats with endotoxemia

Chong Liu, Ang Li, Yi-Bing Weng, Mei-Li Duan, Bao-En Wang, Shu-Wen Zhang

Chong Liu, Ang Li, Yi-Bing Weng, Mei-Li Duan, Department of Critical Care Medicine, Beijing Friendship Hospital Affiliated to Capital Medical University, Beijing 100050, China

Bao-En Wang, Liver Research Center, Beijing Friendship Hospital Affiliated to Capital Medical University, Beijing 100050, China

Shu-Wen Zhang, Department of Infectious Disease and Critical Care Medicine, Beijing Friendship Hospital Affiliated to Capital Medical University, Beijing 100050, China

Author contributions: Zhang SW and Liu C designed the research; Liu C performed the majority of experiments and analyzed data; Li A, Weng YB, Duan ML and Wang BE were involved in editing the manuscript; Liu C and Zhang SW wrote the manuscript.

Supported by Beijing Municipal Science & Technology Commission Major Sci-tech Program, No. H020920050130

Correspondence to: Shu-Wen Zhang, MD, Professor, Department of Infectious Disease and Critical Care Medicine, Beijing Friendship Hospital Affiliated to Capital Medical University, No. 95 Yongan Road, Xuanwu District, Beijing 100050, China. zsw401106@sina.com

Telephone: +86-10-63138749 **Fax:** +86-10-63138011

Received: June 26, 2009 **Revised:** October 29, 2009

Accepted: November 5, 2009

Published online: December 14, 2009

induced endotoxemia results in small intestinal mucosa injury. The number of M-cells, DCs, CD8⁺ T cells, and IgA⁺ B cells were decreased while Tr cell and apoptotic lymphocyte numbers were increased significantly. The number of CD4⁺ T cells increased in the early stages and then slightly decreased by 24 h. The level of IL-4 significantly increased in the early stages and then reversed by the end of the study period. The level of IFN- γ increased slightly in the early stages and then decreased markedly by the 24 h time point. Level of Foxp3 increased whereas sIgA level decreased.

CONCLUSION: Mucosal immune dysfunction forms part of the intestinal barrier injury during endotoxemia. The increased number and function of Tr cells as well as lymphocyte apoptosis result in mucosal immunodeficiency.

© 2009 The WJG Press and Baishideng. All rights reserved.

Key words: Endotoxemia; Rats; Intestinal mucosa; Immunity

Peer reviewer: Dr. Adrian G Cummins, Department of Gastroenterology and Hepatology, (DX 465384), 28 Woodville Road, Woodville South, 5011, South Australia, Australia

Liu C, Li A, Weng YB, Duan ML, Wang BE, Zhang SW. Changes in intestinal mucosal immune barrier in rats with endotoxemia. *World J Gastroenterol* 2009; 15(46): 5843-5850 Available from: URL: <http://www.wjgnet.com/1007-9327/15/5843.asp> DOI: <http://dx.doi.org/10.3748/wjg.15.5843>

Abstract

AIM: To investigate the dysfunction of the immunological barrier of the intestinal mucosa during endotoxemia and to elucidate the potential mechanism of this dysfunction.

METHODS: Male Wistar rats were randomly distributed into two groups: control group and lipopolysaccharide (LPS) group. Endotoxemia was induced by a single caudal venous injection of LPS. Animals were sacrificed in batches 2, 6, 12 and 24 h after LPS infusion. The number of microfold (M)-cells, dendritic cells (DCs), CD4⁺ T cells, CD8⁺ T cells, regulatory T (Tr) cells and IgA⁺ B cells in the intestinal mucosa were counted after immunohistochemical staining. Apoptotic lymphocytes were counted after TUNEL staining. The levels of interleukin (IL)-4, interferon (IFN)- γ and forkhead box P3 (Foxp3) in mucosal homogenates were measured by ELISA. The secretory IgA (sIgA) content in the total protein of one milligram of small intestinal mucus was detected using a radioimmunological assay.

RESULTS: This research demonstrated that LPS-

INTRODUCTION

Endotoxemia can induce sepsis which is among the leading causes of death in noncardiac intensive care units (ICUs) in the US, with approximately 750 000 cases and up to 200 000 deaths per year^[1]. An epidemiological investigation in 3665 ICUs in China showed that the overall hospital mortality of severe sepsis is 48.7%; the mean hospital cost is \$11 390 per patient at a mean cost of \$502 per patient per day^[2]. Despite hospital mortality of 20% for simple sepsis and 40% or higher for severe sepsis or septic shock, there has nonetheless been improvement over the past decade^[3].

Lipopolysaccharide (LPS) is a component of the outer cell wall of gram-negative bacteria, which gives rise to

various manifestations of gram-negative endotoxemia and septic shock^[4]. Endotoxemia-induced sepsis has been associated with deleterious functional and structural changes in many organs, such as the gastrointestinal tract^[5], lungs, and other organs. During sepsis, the most frequent complications within the gastrointestinal tract are mucosal barrier dysfunction and ileus^[6]. One of the most important functions of the gastrointestinal tract is the ability to act as a mucosal barrier to infections. Mucosal barrier dysfunction plays an important role in the pathophysiology of sepsis by promoting bacterial stasis, bacterial overgrowth, and bacterial translocation, which can lead to the development of secondary infections and multiple organ failure^[7]. Intestinal mucosal barriers consist of a mechanical barrier, a chemical barrier, an immunological barrier, and a biological barrier^[8]. Damage to any one of these components causes mucosal barrier dysfunction. The immunological barrier is considered as the first line of defense of the intestinal mucosa from bacterial invasion^[9] and plays an important role in the overall defense. It consists of Peyer's patches, which are the induction sites of the immune response, and diffused lymphoid tissue which are the effector sites. Intestinal mucosa immune responses rely largely on humoral immunity. The primary functions of the immunological barrier include^[10-12] inhibiting bacterial adhesion to the mucosa so that they can be eliminated, neutralizing viruses and toxins, enclosing some antigens of acquired extraneous material to prevent systemic reactions, activating the complement 3 (C3) pathway, participating in the anti-infection effect, and protecting probiotics. Therefore, damage to the intestinal immune barrier will result in bacterial translocation and gut-derived endotoxemia.

Previous studies have discussed the changes to immunity during sepsis, but what happens to immunity, specifically the gut immunity, during endotoxemia before sepsis is not clear. Thus in the present study, changes to the number and function of intestinal mucosal immune cells in rats with endotoxemia were observed to investigate whether dysfunction of immunological barrier occurred during endotoxemia and to elucidate the potential mechanism of this dysfunction.

MATERIALS AND METHODS

Animals

Male Wistar rats weighing 200.5 ± 12.3 g were purchased from Vital River Laboratories (Beijing, China). The rats were fed a standard laboratory chow diet (Vital River Laboratories) for 72 h before the experiment and maintained at $24 \pm 1^\circ\text{C}$, at a relative humidity of $50\% \pm 1\%$ with a 12/12-h light/dark cycle. The animals were fasted for 12 h before the experiment, allowing free access to water. All animals were handled according to the institutional criteria for the care and use of laboratory animals in research.

Methods

Establishment of animal model: A total of 80 animals were included and randomly distributed into the control

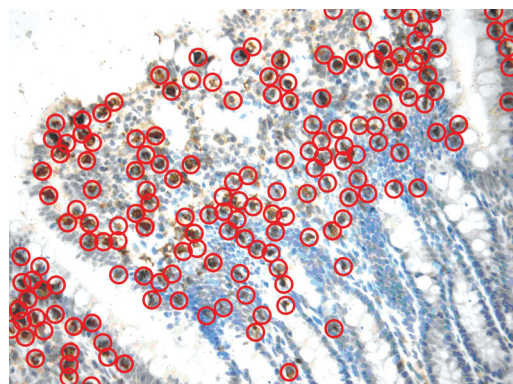


Figure 1 A sample image of immunohistochemical staining and TUNEL staining. Some sample cells are circled to illustrate the positive cells that were counted (400 \times).

group (40 rats) and LPS (*Escherichia coli*, O55: B5, Sigma, St Louis, MO, USA) group (40 rats). In accordance with the study of Cheng *et al*^[13], endotoxemia was induced by a single caudal venous injection of LPS at 10 mg/kg, while control animals received caudal venous injections of saline. Ten animals were sacrificed in each group at each time point (2, 6, 12 and 24 h) after LPS infusion.

Histological testing: Small intestinal tissue was obtained from the middle part of the ileum. Samples were fixed in 4% paraformaldehyde and then observed by hematoxylin and eosin (HE) staining to explore the histopathological changes in the intestinal mucosa.

Cytological testing: A 5-cm-long tissue section with Peyer's patches cut off was obtained from the ileum near the cecum and observed by immunohistochemical staining after fixation in 4% paraformaldehyde to investigate immune cell changes in the mucosa. The fixed tissue was transferred to phosphate buffer solution (PBS) overnight at 4°C and then transferred to 30% sucrose for 2 h at 4°C . Then the tissue was mounted in optimum cutting temperature (OCT) embedding medium and placed on dry ice until frozen before cryosectioning of 4 μm thick continuous slides. The slides were washed 3 \times 5' (3 times, 5 min each) with PBT (Phosphate Buffer Saline with 0.02% Tween 20). Next, 500 μL of diluted primary antibody in blocking buffer (containing 40 mL PBT, 400 μL heat-inactivated goat serum, 400 μL heat-inactivated donkey serum, 400 μL 10% Triton X-100) was added to each slide before they were covered and stored at 4°C overnight. The slides were then washed 6 \times 5' with PBT before the addition of 500 μL of diluted secondary antibody in blocking buffer to each slide. The slides were then covered and incubated at room temperature for 90 min before being washed 6 \times 5' with PBT. The slides were then mounted with Vectashield. After staining, six clear-viewed slides were selected from each group and two viewing fields for each slide at high magnification (400 \times) were randomly selected for counting immune cells. Brownish-yellow stained lymphocytes were an indication of positive cells (Figure 1). Rabbit anti-rat cytokeratin 8^[14], integrin α E2^[15], cluster of differentiation (CD) 4, CD8,

neuropilin-1 (NRP-1)^[16] and immunoglobulin A (IgA) polyclonal antibodies were purchased from Biosynthesis Biotechnology (Beijing, China) to indicate microfold cells (M-cells), dendritic cells (DC), CD4⁺ thymus dependent lymphocytes (T cells), CD8⁺ T cells, CD4⁺CD25⁺ T cells (regulatory T cell, Tr) and IgA⁺ bursa dependent lymphocytes (B cells), respectively.

The terminal deoxynucleotidyl transferase mediated dUTP-biotin nick end labeling (TUNEL) assay was used to observe apoptotic lymphocytes in the small intestinal mucosa. The TUNEL kit was obtained from Roche Diagnostics (Indianapolis, IN, USA) to label apoptotic lymphocytes. The slides were deparaffinized in two changes of xylene for 5 min each, hydrated with two changes of 100% ethanol for 3 min each and 95% ethanol for 1 min, and then rinsed in distilled water. Slides were then incubated in TdT reaction buffer for 10 min before incubation in TdT reaction mixture for 1-2 h at 37-40°C in a humidified chamber. The reaction was stopped by rinsing the slides in stop wash buffer for 10 min. The slides were then rinsed 3 × 2' in PBT before incubation with FITC-Avidin D in PBS for 30 min at room temperature. Slides were then rinsed 3 × 2' in PBT, counterstained with PI or DAPI for 20 min and rinsed in PBS for 5 min. Slides were then mounted with Vectashield. Brownish-yellow stained lymphocytes were an indication of positive cells. The intraepithelial apoptotic lymphocytes were identified and counted.

Detection of IL-4, IFN-γ and Foxp3: The small intestinal mucosa was stripped off by circumferentially pushing the muscularis with a moist cotton applicator, as described previously^[17] and then weighed to prepare a 10% homogenate by adding an appropriate amount of normal saline. The homogenate was then centrifuged at 3000 × g for 10 min at 0°C. The supernatant was harvested and diluted with normal saline to make a 1% homogenate. The levels of interferon-γ (IFN-γ), interleukin-4 (IL-4) and forkhead box P3 (Foxp3) in the homogenate were measured by enzyme-linked immunosorbent assays (ELISA) to evaluate the function of Helper T-cell (TH) 1, TH2 and Tr cells. The IFN-γ and IL-4 ELISA kits were obtained from R&D Systems (Minneapolis, MN, USA). The Foxp3 ELISA kit was obtained from Adlitteram Diagnostic Laboratories (San Diego, CA, USA). The ELISA assays were performed according to the manufacturer's instructions.

Detection of sIgA: Secretory IgA (sIgA) was detected using a radioimmunological assay (RIA). A 10-cm-long tissue section was obtained from the small intestine, dissected and carefully washed with normal saline. Small intestinal mucus was collected into an Eppendorf tube, and 1 mL of 0.01 mol/L PBS was added into the Eppendorf tube. The solution was then centrifuged at 3000 × g for 10 min at 0°C. The supernatant was then harvested and the level of sIgA was measured by a double antibody sandwich RIA purchased from Beijing Nuclear Research Center (Beijing, China). The total protein level

of the intestinal mucus was assayed by the Bradford brilliant blue method simultaneously. The sIgA content in 1 mg of total protein from small intestinal mucus was detected.

Statistical analysis

All statistical analyses were performed using the SPSS 15.0 software package. All data were expressed as the mean ± SD. Group comparisons were carried out using a one-factor analysis of variance. P < 0.05 was considered statistically significant.

RESULTS

Mortality of rats in different groups

During the course of the study there were no rats that died in the control group. A total of 5 rats died in the LPS group; 3 at 12 h and 2 at 24 h after LPS injection.

Histological changes

As shown in Figure 2, the intestinal mucosa of saline-treated rats was complete and the villi were presented in an orderly fashion. Samples displayed no abnormal epithelial cell morphology and there was no evidence of congestion, edema or infiltration of inflammatory cells (Figure 2A). In contrast, the intestinal mucosal villi of rats with endotoxemia were loosened and atrophic where the epithelial cells were necrotic. The mucosa was edematous and infiltrated with inflammatory cells (Figure 2B-E). These abnormal changes to the intestinal mucosa were most obvious 12 h after LPS injection (Figure 2D).

Numbers of immune cells and apoptotic lymphocytes in the intestinal mucosa

The effects on the immune system induced by LPS were assessed in the rat intestinal mucosa (Figure 3). We found that M-cell and CD8⁺ T cell numbers in the small intestinal mucosa were significantly decreased 6 and 12 h after LPS challenge compared to controls. Furthermore, the number of DCs was significantly decreased after 2, 6 and 12 h. In contrast, the number of CD4⁺ T cells was significantly increased after 6 and 12 h, before decreasing slightly by 24 h, although this decrease was not statistically significant. The number of Tr cells was significantly increased at 2, 6 and 12 h. The number of IgA⁺ B cells and apoptotic lymphocytes were significantly increased at all time points.

Levels of IL-4, IFN-γ and Foxp3 in the small intestinal mucosa

As shown in Figure 4, the level of IL-4 was significantly increased in the small intestinal mucosa after 2 h before significantly decreasing after 6 and 12 h in LPS-treated animals compared with controls. The level of IFN-γ was increased slightly after 2, 6 and 12 h before decreasing markedly by 24 h. The level of Foxp3 was significantly increased after 12 and 24 h.

Level of intestinal mucus sIgA

As shown in Figure 5, LPS induced a significant decrease

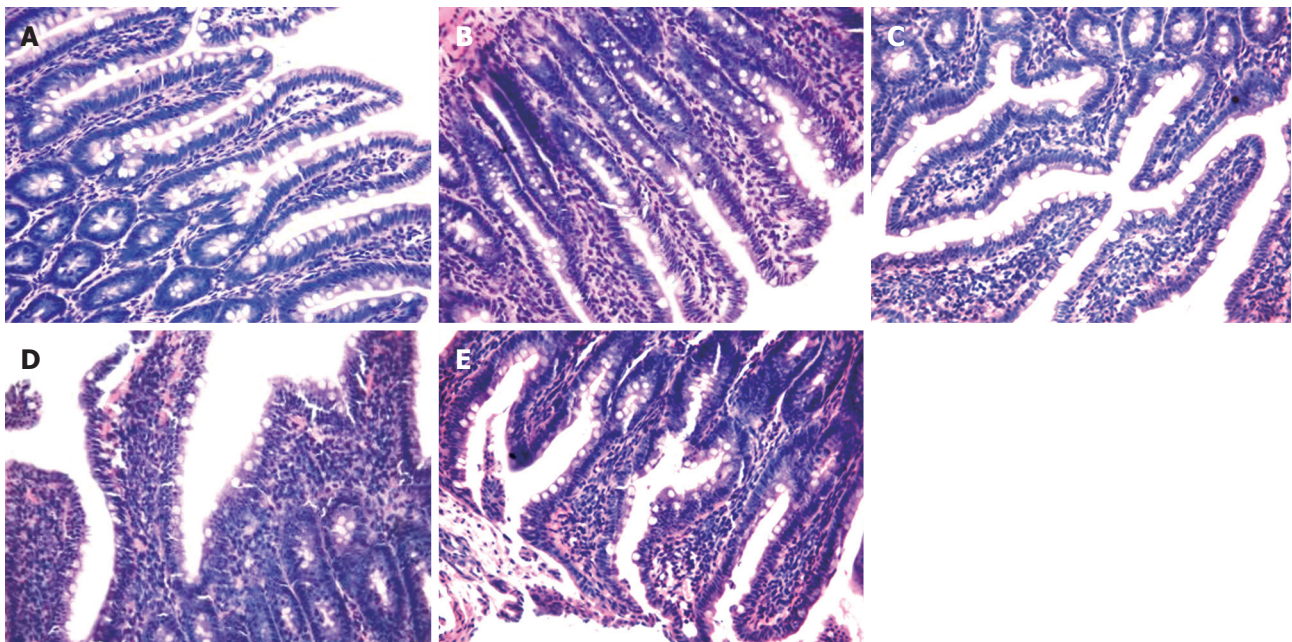


Figure 2 Representative images of the histological changes in the small intestinal mucosa of rats after LPS injection. A: The intestinal mucosa of normal rats was complete and the villi were in an orderly fashion with no abnormal morphology present in the epithelial cells, as well as no manifestation of congestion, edema or infiltration of inflammatory cells; B-E: Representative of the changes 2, 6, 12 and 24 h after LPS treatment. The intestinal mucosal villi of rats with endotoxemia were loosened and atrophic while the epithelial cells were necrotic and the mucosa was edematous and infiltrated with inflammatory cells. The LPS-induced changes to the intestinal mucosa were most obvious in the rats after 12 h.

in sIgA levels in rat intestinal mucus after 2, 12 and 24 h compared with controls.

DISCUSSION

This study has demonstrated that LPS-induced endotoxemia results in small intestinal mucosa injury. The number of M-cells, DCs, CD8⁺ T cells and IgA⁺ B cells were decreased and the number of Tr cells and apoptotic lymphocytes were increased significantly. The number of CD4⁺ T cells was increased in the early stages before slightly decreasing by the end of the study period. Similarly, the level of IL-4 was significantly increased at early time points and then reversed by the 24 h time point, while IFN- γ levels were also increased slightly at early time points before decreasing markedly by the end of the study. The level of Foxp3 was increased whereas the level of sIgA decreased.

Many researchers have demonstrated that the digestive tract is the largest immune organ in the body^[18]. The immune response of the digestive tract mucosa primarily relies on humoral immunity. The induction site of mucosal immune responses is at the Peyer's patches and the effector site is at the mucosa^[19]. The mucosal immune response involves a number of processes: the M-cells of the Peyer's patches collect granular antigens and pass them to DCs and macrophages which can then activate the T cells. The activated T cells will further activate B cells and the latter will produce antigen-specific sIgA after homing to the effector site.

During endotoxemia, oxidative stress causes direct damage to cells and tissues and is involved in inflammatory cytokine production. The response of the immune

system to LPS is an inflammatory reaction in the early phase and anti-inflammatory reaction in the later period^[20].

LPS can activate phagocytes, stimulating them to release large amounts of cytokines and inflammatory factors which can further induce microcirculatory disturbances and intestinal epithelium injury, resulting in intestinal barrier damage^[21]. In this study, it was observed that the small intestinal mucosa was injured in rats with endotoxemia, suggesting that the intestinal barrier was damaged and that the most severe damage occurred 12 h after LPS injection. This study also demonstrated that the immune function of the small intestinal mucosa changed most significantly after 12 h, indicating that the immune barrier dysfunction was a part of intestinal mucosal barrier injury.

To investigate the changes to local immune induction during endotoxemia we observed the numbers of M-cells and DCs in the intestinal mucosa. M-cells are a special kind of intestinal epithelium mucosa cell that can play a role by delivering antigen to antigen presenting cells (APCs). It is believed that the M-cell is the first step in intestinal immunity^[22]. It has been observed that the number of M-cells decreased and the intestinal barrier was damaged during chronic intestinal inflammation and bacterial invasion^[23]. In this study, we found the same change in M-cells during acute LPS stimulation, suggesting that endotoxemia could impair the first step of intestinal immunity. DCs are a kind of APC and a previous study by Hotchkiss *et al*^[24] demonstrated DC depletion in patients with sepsis. In this study, a decrease in DC number was observed in the intestinal mucosa, suggesting the same change in rats with endotoxemia. The decreases in M-cell and DC numbers in the small intestinal mucosa in

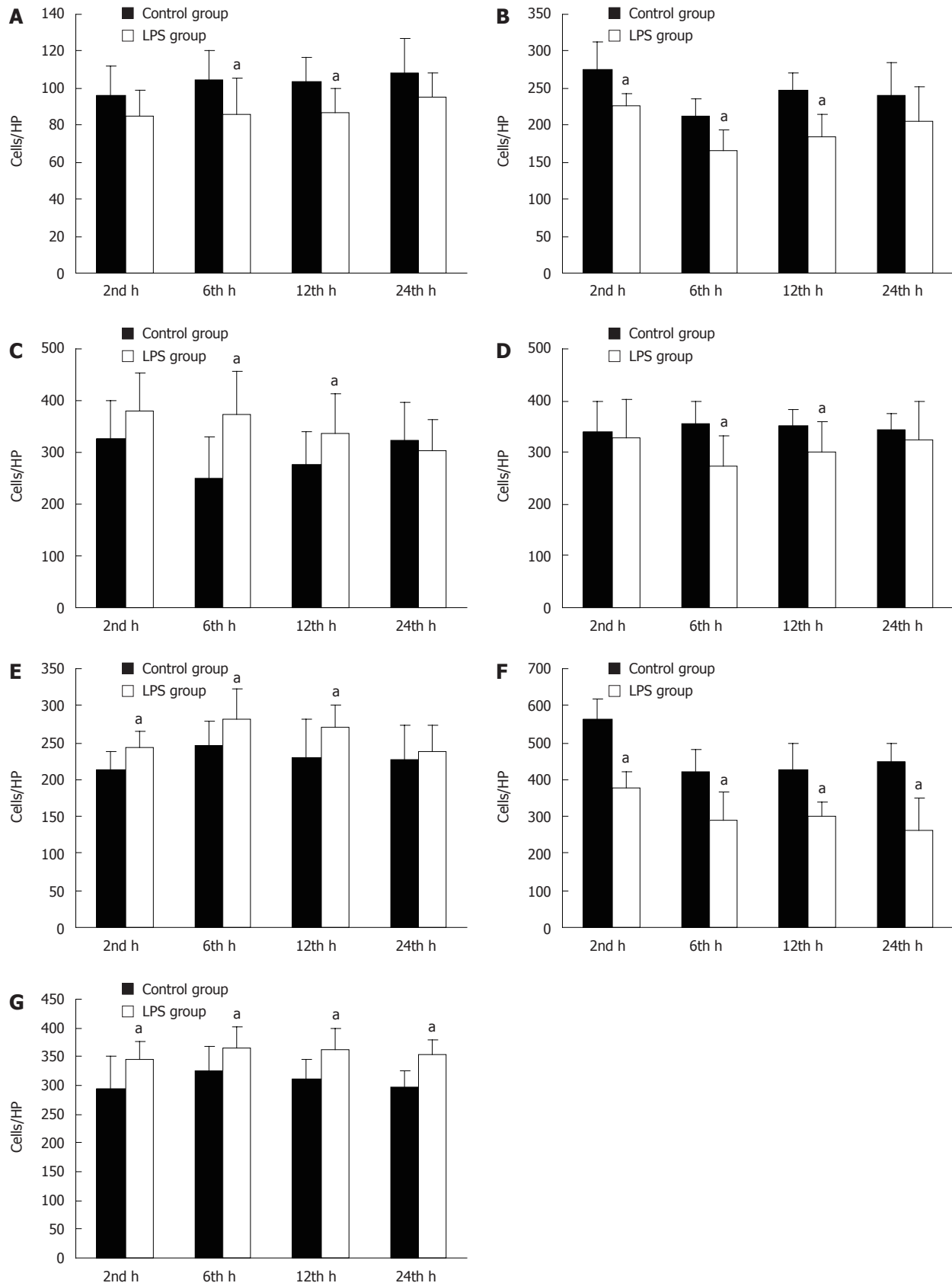


Figure 3 The number of immune cells and apoptotic lymphocytes in the intestinal mucosa. A: The number of M-cells was significantly decreased after 6 and 12 h in the LPS group; B: The number of DCs was significantly decreased after 2, 6 and 12 h in the LPS group; C: The number of CD4⁺ T cells was significantly increased after 6 and 12 h before slightly decreasing by 24 h in the LPS group; D: The number of CD8⁺ T cells was significantly decreased after 6 and 12 h in the LPS group; E: The number of Tr cells was significantly increased after 2, 6 and 12 h in the LPS group; F: The number of IgA⁺ B cells was significantly increased at all time points in the LPS group; G: The number of apoptotic lymphocytes was significantly increased at all time points in the LPS group. ^aP < 0.05.

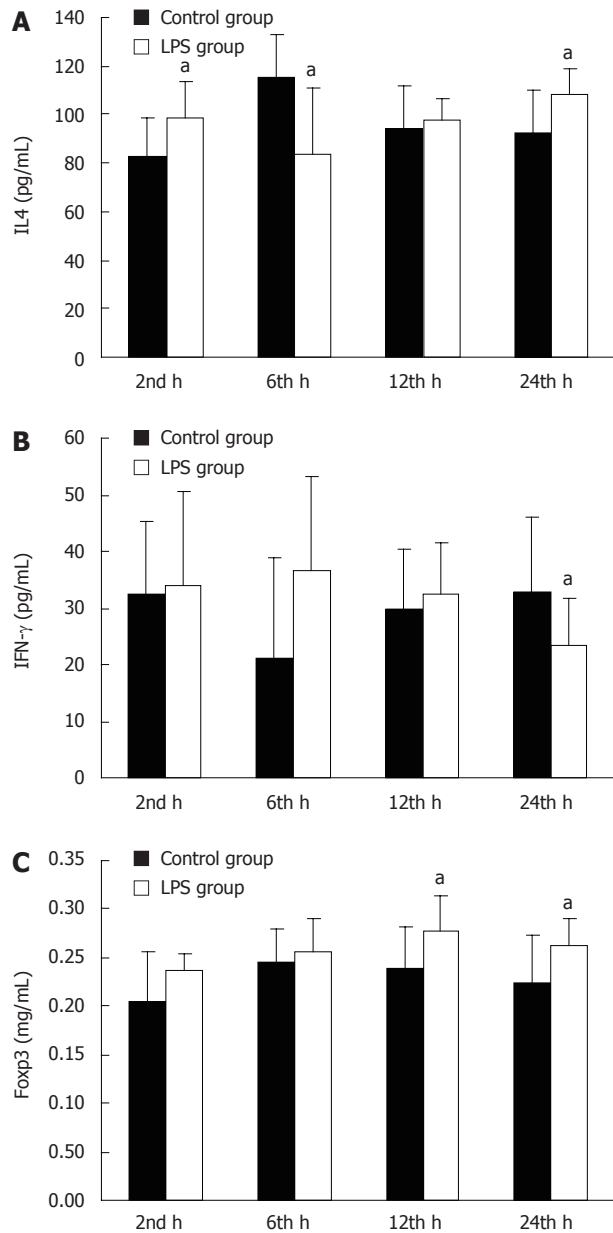


Figure 4 Levels of IL-4, IFN- γ and Foxp3 in small intestinal mucosa. A: The level of IL-4 was significantly increased after 2 h and significantly decreased by 6 and 12 h in the LPS group; B: The level of IFN- γ was increased slightly after 2, 6 and 12 h and decreased markedly by 24 h in the LPS group; C: The level of Foxp3 was significantly increased after 12 and 24 h in the LPS group. $^aP < 0.05$.

rats with endotoxemia implied that the induction of local immune responses was impaired.

T lymphocytes, especially the Tr cells, play a major regulatory role in mucosal immunity. T cells can be classified into CD4 $^{+}$ T cells and CD8 $^{+}$ T cells according to the different protein markers on their cell surface. TH cells and Tr cells belong to the CD4 $^{+}$ T cell family. TH cells can be further divided into TH1 and TH2, where TH1 secretes inflammatory factors such as IFN- γ to mediate the protective immune response while TH2 secretes anti-inflammatory factors such as IL-4 to mediate the non-specific immune response $^{[25]}$. A previous study demonstrated a TH1/TH2 drift $^{[26]}$, suggesting that the immune response progressed from being active to a suppressed state during sepsis, while a further study demonstrated that it was Tr cells that mediated this drift $^{[27]}$. In addition, other studies have demonstrated that Tr cells could selectively kill and directly suppress B cells $^{[28,29]}$. It was reported that circulating Tr numbers were markedly elevated and induced immunoparalysis in sepsis $^{[30]}$. The development and function of Tr cells can be investigated by the expression level of Foxp3 $^{[31]}$. CD8 $^{+}$ T cells include cytotoxic T (Tc) cells and suppressor T (Ts) cells, which are the effector cells of cell immunity and suppressors of TH cells, respectively. In accordance with Bruder *et al* $^{[16]}$ study, we inferred Tr cell numbers from a single marker of NRP-1 positive cells in our study. We only observed the intraepithelial NRP-1 positive cells to exclude interference since NRP-1 can be expressed by other cells such as DCs. Our study showed that CD4 $^{+}$ T cells increased in the early stages of endotoxemia before sepsis and then slightly decreased in the later phase, while CD8 $^{+}$ T cells decreased and Tr cells increased in the small intestinal mucosa in rats with endotoxemia. It should also be noted that in this study the level of IL-4 increased at the beginning and then decreased by the end of the study whereas the level of IFN- γ demonstrated the opposite change and the level of Foxp3 increased. Though a lot of activated immunological cells can secrete IL-4 and IFN- γ , the effects of IL-4 and IFN- γ remained unchanged. Similarly, Foxp3 is not exclusively expressed by Tr cells but also by activated effector T cells. The combination of an increase in NRP-1 cells and intestinal Foxp3 levels could suggest that Tr cells are increased. These results suggest a trend of immune changes whereby cellular immunity progressed from an active to a suppressed state during endotoxemia before sepsis. It can be concluded from this study that the rise in the number and function of Tr cells is one of the major reasons for immunosuppression in the small intestinal mucosa of rats with endotoxemia before sepsis.

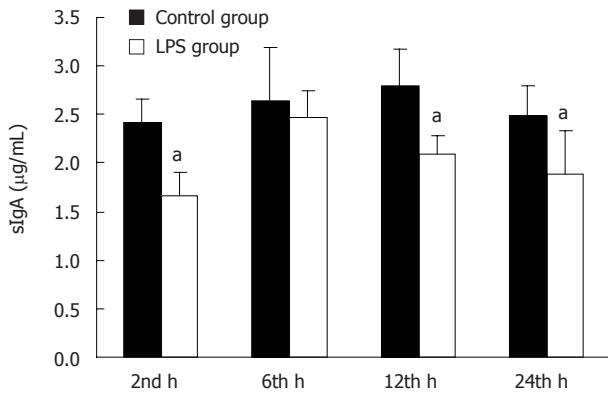


Figure 5 Small intestinal mucosa sIgA levels. The level of intestinal mucus sIgA was significantly decreased after 2, 12 and 24 h in the LPS group. $^aP < 0.05$.

IgA+ B cells are identified by positive IgA staining, because only B cells produce IgA or have surface IgA. A previous study showing decreases in the level of sIgA, the number of IgA+ B cells and the number of Gram-negative bacteria enclosed by sIgA in the intestinal tract during stress suggested that humoral immune function

was inhibited dramatically^[32]. Our study demonstrated that the level of sIgA and the number of IgA⁺ B cells diminished during endotoxemia, suggesting that LPS-induced endotoxemia inhibited humoral immune function of the digestive tract in accordance with the previous report. One explanation for this could be due to the rise in the number and function of Tr cells, as demonstrated in our study, which could lead to the suppression of B cell function.

Mongini *et al*^[33] reported that relocation of endotoxin after injury can increase the number of apoptotic lymphocytes. Our research demonstrated a similar change, with an increase in the number of apoptotic lymphocytes in the intestinal mucosa of rats with endotoxemia. This could contribute to the immunosuppression of the small intestine in rats with endotoxemia.

In conclusion, our study showed that mucosal immune barrier dysfunction was a part of intestinal mucosal barrier injury. Cellular immunity was active in the early phase of endotoxemia and suppressed in later periods, humoral immunity was abnormal and lymphocyte apoptosis was increased. Our study suggests that the increased number and function of Tr cells and the increase in lymphocyte apoptosis are the reasons for intestinal mucosal immunodeficiency. Based on these findings, an earlier protective or immunoregulatory treatment aimed at gastrointestinal immune function may be of benefit to severely infected patients. We suggest future studies could be designed to test this hypothesis.

COMMENTS

Background

Immune dysfunction is one of the most frequent complications within the gastrointestinal mucosal barrier during sepsis. Mucosal barrier dysfunction plays an important role in the pathophysiology of sepsis by promoting bacterial stasis, bacterial overgrowth, and bacterial translocation, which can lead to the development of secondary infections and multiple organ failure. The changes of gastrointestinal immune function may appear at the beginning or even before sepsis.

Research frontiers

Intestinal mucosal barriers consist of a mechanical barrier, a chemical barrier, an immunological barrier, and a biological barrier. The immunological barrier is considered as the first line of defense of the intestinal mucosa from bacterial invasion and plays an important role in the overall defense. This study observed the changes in the gastrointestinal immunological barrier during endotoxemia.

Innovations and breakthroughs

Previous studies have discussed the changes to immunity during sepsis, but what happens to immunity, specifically the gut immunity, during endotoxemia before sepsis is not clear. In this study, changes to the number and function of intestinal mucosal immune cells in rats with endotoxemia were observed to investigate whether dysfunction of the immunological barrier occurred during endotoxemia and to elucidate the potential mechanism of this dysfunction.

Applications

By observing the changes of gastrointestinal immune function, the study shows that the gastrointestinal immune dysfunction occurs during endotoxemia before sepsis. Thus, a protective or an immunoregulatory treatment of gastrointestinal immune function should be used earlier in severely infected patients.

Terminology

Lipopolysaccharides (LPS) are large molecules consisting of a lipid and a polysaccharide joined by a covalent bond; they are found in the outer membrane of Gram-negative bacteria, act as endotoxins and elicit strong immune responses in animals. Endotoxemia is the immune responses to LPS in animals. Cytokines: non-antibody proteins secreted by inflammatory leukocytes

and some non-leukocytic cells, which act as intercellular mediators. Sepsis is defined as infection plus systemic manifestations of infection.

Peer review

This is a descriptive study of the effect of intravenous LPS on intestinal immune cells and cytokine levels in the rat. Straightforward and generally well written paper.

REFERENCES

- Angus DC, Linde-Zwirble WT, Lidicker J, Clermont G, Carcillo J, Pinsky MR. Epidemiology of severe sepsis in the United States: analysis of incidence, outcome, and associated costs of care. *Crit Care Med* 2001; **29**: 1303-1310
- Cheng B, Xie G, Yao S, Wu X, Guo Q, Gu M, Fang Q, Xu Q, Wang D, Jin Y, Yuan S, Wang J, Du Z, Sun Y, Fang X. Epidemiology of severe sepsis in critically ill surgical patients in ten university hospitals in China. *Crit Care Med* 2007; **35**: 2538-2546
- Brun-Buisson C. [Epidemiology of severe sepsis] *Presse Med* 2006; **35**: 513-520
- Opal SM, Scannon PJ, Vincent JL, White M, Carroll SF, Palardy JE, Parejo NA, Pribble JP, Lemke JH. Relationship between plasma levels of lipopolysaccharide (LPS) and LPS-binding protein in patients with severe sepsis and septic shock. *J Infect Dis* 1999; **180**: 1584-1589
- Garrison RN, Spain DA, Wilson MA, Keelen PA, Harris PD. Microvascular changes explain the "two-hit" theory of multiple organ failure. *Ann Surg* 1998; **227**: 851-860
- Carrico CJ, Meakins JL, Marshall JC, Fry D, Maier RV. Multiple-organ-failure syndrome. *Arch Surg* 1986; **121**: 196-208
- MacFie J, O'Boyle C, Mitchell CJ, Buckley PM, Johnstone D, Sudworth P. Gut origin of sepsis: a prospective study investigating associations between bacterial translocation, gastric microflora, and septic morbidity. *Gut* 1999; **45**: 223-228
- Baumgart DC, Dignass AU. Intestinal barrier function. *Curr Opin Clin Nutr Metab Care* 2002; **5**: 685-694
- Reilly PM, Wilkins KB, Fuh KC, Haglund U, Bulkley GB. The mesenteric hemodynamic response to circulatory shock: an overview. *Shock* 2001; **15**: 329-343
- Ellen JM, Lammel CJ, Shafer MA, Teitle E, Schachter J, Stephens RS. Cervical secretory immunoglobulin A in adolescent girls. *J Adolesc Health* 1999; **25**: 150-154
- Tyler BM, Cole MF. Effect of IgA1 protease on the ability of secretory IgA1 antibodies to inhibit the adherence of *Streptococcus mutans*. *Microbiol Immunol* 1998; **42**: 503-508
- Cebra JJ, Periwal SB, Lee G, Lee F, Shroff KE. Development and maintenance of the gut-associated lymphoid tissue (GALT): the roles of enteric bacteria and viruses. *Dev Immunol* 1998; **6**: 13-18
- Cheng PY, Lee YM, Wu YS, Chang TW, Jin JS, Yen MH. Protective effect of baicalein against endotoxic shock in rats *in vivo* and *in vitro*. *Biochem Pharmacol* 2007; **73**: 793-804
- Rautenberg K, Cichon C, Heyer G, Demel M, Schmidt MA. Immunocytochemical characterization of the follicle-associated epithelium of Peyer's patches: anti-cytokeratin 8 antibody (clone 4.1.18) as a molecular marker for rat M cells. *Eur J Cell Biol* 1996; **71**: 363-370
- Chen-Woan M, Delaney CP, Fournier V, Wakizaka Y, Murase N, Fung J, Starzl TE, Demetris AJ. A new protocol for the propagation of dendritic cells from rat bone marrow using recombinant GM-CSF, and their quantification using the mAb OX-62. *J Immunol Methods* 1995; **178**: 157-171
- Bruder D, Probst-Kerper M, Westendorf AM, Geffers R, Beissert S, Loser K, von Boehmer H, Buer J, Hansen W. Neuropilin-1: a surface marker of regulatory T cells. *Eur J Immunol* 2004; **34**: 623-630
- Su GL, Walgenbach KJ, Heeckt PH, Wang Q, Halfter W, Whiteside TL, Bauer AJ. Increased expression of interferon-gamma in a rat model of chronic intestinal allograft

- rejection. *Transplantation* 1996; **62**: 242-248
- 18 **Takahashi I**, Kiyono H. Gut as the largest immunologic tissue. *JPEN J Parenter Enteral Nutr* 1999; **23**: S7-S12
- 19 **Kraehenbuhl JP**, Neutra MR. Molecular and cellular basis of immune protection of mucosal surfaces. *Physiol Rev* 1992; **72**: 853-879
- 20 **Jones-Carson J**, Fantuzzi G, Siegmund B, Dinarello C, Tracey KJ, Wang H, Fang FC, Vazquez-Torres A. Suppressor alphabeta T lymphocytes control innate resistance to endotoxic shock. *J Infect Dis* 2005; **192**: 1039-1046
- 21 **Aranow JS**, Fink MP. Determinants of intestinal barrier failure in critical illness. *Br J Anaesth* 1996; **77**: 71-81
- 22 **Meynell HM**, Thomas NW, James PS, Holland J, Taussig MJ, Nicoletti C. Up-regulation of microsphere transport across the follicle-associated epithelium of Peyer's patch by exposure to *Streptococcus pneumoniae* R36a. *FASEB J* 1999; **13**: 611-619
- 23 **Kucharzik T**, Lugering N, Rautenberg K, Lugering A, Schmidt MA, Stoll R, Domschke W. Role of M cells in intestinal barrier function. *Ann N Y Acad Sci* 2000; **915**: 171-183
- 24 **Hotchkiss RS**, Tinsley KW, Swanson PE, Grayson MH, Osborne DF, Wagner TH, Cobb JP, Coopersmith C, Karl IE. Depletion of dendritic cells, but not macrophages, in patients with sepsis. *J Immunol* 2002; **168**: 2493-2500
- 25 **Hauer AC**, Breese EJ, Walker-Smith JA, MacDonald TT. The frequency of cells secreting interferon-gamma and interleukin-4, -5, and -10 in the blood and duodenal mucosa of children with cow's milk hypersensitivity. *Pediatr Res* 1997; **42**: 629-638
- 26 **Liu JH**, Zhang YQ, Huang B, Fang Q, Huo X, Hu H. [The effects of endotoxin on the Th1/Th2 cells and immune modulation of Astragalus membranaceus] *Zhonghua Er Ke Za Zhi* 2003; **41**: 613-614
- 27 **Purcell EM**, Dolan SM, Kriylovich S, Mannick JA, Lederer JA. Burn injury induces an early activation response by lymph node CD4+ T cells. *Shock* 2006; **25**: 135-140
- 28 **Zhao DM**, Thornton AM, DiPaolo RJ, Shevach EM. Activated CD4+CD25+ T cells selectively kill B lymphocytes. *Blood* 2006; **107**: 3925-3932
- 29 **Lim HW**, Hillsamer P, Banham AH, Kim CH. Cutting edge: direct suppression of B cells by CD4+ CD25+ regulatory T cells. *J Immunol* 2005; **175**: 4180-4183
- 30 **Monneret G**, Debard AL, Venet F, Bohe J, Hequet O, Bienvenu J, Lepape A. Marked elevation of human circulating CD4+CD25+ regulatory T cells in sepsis-induced immunoparalysis. *Crit Care Med* 2003; **31**: 2068-2071
- 31 **Fontenot JD**, Rudensky AY. A well adapted regulatory contrivance: regulatory T cell development and the forkhead family transcription factor Foxp3. *Nat Immunol* 2005; **6**: 331-337
- 32 **Van Leeuwen PA**, Boermeester MA, Houdijk AP, Meyer S, Cuesta MA, Wesdorp RI, Rodrick ML, Wilmore DW. Pretreatment with enteral cholestyramine prevents suppression of the cellular immune system after partial hepatectomy. *Ann Surg* 1995; **221**: 282-290
- 33 **Mongini C**, Ruybal P, Garcia Rivello H, Mocetti E, Escalada A, Christiansen S, Argibay P. Apoptosis in gut-associated lymphoid tissue: a response to injury or a physiologic mechanism? *Transplant Proc* 1998; **30**: 2673-2676

S- Editor Wang JL L- Editor Logan S E- Editor Ma WH



Effect of implanting fibrin sealant with ropivacaine on pain after laparoscopic cholecystectomy

Jian-Zhu Fu, Jie Li, Ze-Li Yu

Jian-Zhu Fu, Jie Li, Ze-Li Yu, Department of General Surgery, Beijing Tongren Hospital, Capital Medical University, Beijing 100730, China

Author contributions: Fu JZ performed most of the study; Li J and Yu ZL were also involved in designing the study and editing the manuscript.

Correspondence to: Jie Li, Associate Professor, Department of General Surgery, Beijing Tongren Hospital, Capital Medical University, Beijing 100730, China. kingknife@gmail.com

Telephone: +86-10-58268538 **Fax:** +86-10-58268509

Received: August 25, 2009 **Revised:** October 9, 2009

Accepted: October 16, 2009

Published online: December 14, 2009

Peer reviewer: Ian C Roberts-Thomson, Professor, Department of Gastroenterology and Hepatology, The Queen Elizabeth Hospital, 28 Woodville Road, Woodville South 5011, Australia

Fu JZ, Li J, Yu ZL. Effect of implanting fibrin sealant with ropivacaine on pain after laparoscopic cholecystectomy. *World J Gastroenterol* 2009; 15(46): 5851-5854 Available from: URL: <http://www.wjgnet.com/1007-9327/15/5851.asp> DOI: <http://dx.doi.org/10.3748/wjg.15.5851>

Abstract

AIM: To investigate the safety and efficacy of implanting fibrin sealant with sustained-release ropivacaine in the gallbladder bed for pain after laparoscopic cholecystectomy (LC).

METHODS: Sixty patients (American Society of Anesthesiologists physical status was I or II and underwent LC) were randomly divided into three equal groups: group A (implantation of fibrin sealant in the gallbladder bed), group B (implantation of fibrin sealant carrying ropivacaine in the gallbladder bed), and group C (normal saline in the gallbladder bed). Postoperative pain was evaluated, and pain relief was assessed by visual analog scale (VAS) scoring.

RESULTS: The findings showed that 81.7% of patients had visceral pain, 50% experienced parietal, and 26.7% reported shoulder pain after LC. Visceral pain was significantly less in group B patients than in the other groups ($P < 0.05$), and only one patient in this group experienced shoulder pain. The mean VAS score in group B patients was lower than that in the other groups.

CONCLUSION: Visceral pain is prominent after LC and can be effectively controlled by implanting fibrin sealant combined with ropivacaine in the gallbladder bed.

© 2009 The WJG Press and Baishideng. All rights reserved.

Key words: Analgesia; Fibrin sealant; Laparoscopic cholecystectomy; Pain; Ropivacaine

INTRODUCTION

Since the widespread adoption of laparoscopic cholecystectomy (LC) in the late 1980s, LC has become the gold standard for chronic cholecystitis^[1]. Postoperative pain after LC is generally less than that after open cholecystectomy, however, the postoperative pain experienced by patients still causes preventable distress. Treating postoperative pain is an important and primary objective, because it affects patients' comfort, postoperative morbidity, and, inevitably, social costs due to prolonged hospitalization and work inactivity. Pain after LC can be divided into three components, namely, visceral, parietal, and shoulder pain, with different intensities and time courses^[2]. LC is mainly associated with visceral pain^[3] which may refer to the shoulder in 35% to 60% of cases^[4,5]. Various treatments have been proposed to make this surgery as pain-free as possible^[6-8]. The main objective of this study was to assess the effectiveness of implanting fibrin sealant combined with ropivacaine in the gallbladder bed for pain control after LC.

MATERIALS AND METHODS

The study was designed as a single-center, randomized trial. Of the 78 patients who underwent LC from October 2008 to August 2009, 60 patients (42 women, 18 men) were enrolled in this study, which was performed after approval was received from the Ethics Committee of Beijing Tongren Hospital, Capital Medical University. All patients whose American Society of Anesthesiologists (ASA) physical status were I or II underwent diagnostic abdominal ultrasound, liver function tests, and coagulation profile along with hematologic and biochemical investigations. Patients with previous major upper abdominal surgeries, choledocholithiasis, acute

cholecystitis, or conversion to open cholecystectomy were excluded from the study. Patients with a body mass index higher than 35, and those with diminished liver and kidney functions were not evaluated in this study. The visual analog pain evaluation scale (VAS) was introduced to the patients before surgery and the details of the study were explained to the patients. All patients stated that they understood the VAS. Patients who were unable to comprehend the scale were not included in the study. Only patients who were suitable and compatible with the study design were included. The patients were randomly divided into 3 equal groups with the help of computer-generated randomization numbers.

All patients underwent LC under a standard general anesthetic technique for premedication and during the intraoperative period. The anesthetist performed intraoperative, noninvasive monitoring. Ventilation was adjusted to maintain an end-tidal CO₂ pressure below 38 mmHg. Second-generation cephalosporin (cefoxitin) 1 g was injected intravenously before the induction of anesthesia. LC was carried out using the standard three-port technique, and CO₂ pneumoperitoneum pressure was maintained at 14 mmHg throughout the procedure. The procedures were performed by the same experienced surgeon. After complete hemostasis and the gallbladder bed washed with normal saline, the different treatments were performed according to the different groups. Group A: Fibrin sealant (5 mL) (Guangzhou Bioseal Biotech, Guangzhou, China) was implanted in the gallbladder bed. Group B: Fibrin sealant (5 mL) combined with ropivacaine (1 mg/kg body weight) was implanted in the gallbladder bed. Group C: The gallbladder bed was doused with normal saline only.

Following LC, carbon dioxide was evacuated through the ports by applying gentle pressure all over the abdomen. Gallbladders were taken out of the peritoneal cavity via the umbilical incision. Rescue analgesia (intramuscular dolantin 50 mg) or rescue antiemetic (intramuscular ondansetron 8 mg) was administered if the VAS was higher than 10 or the patient complained of vomiting. The amount of dolantin used was noted.

The degree of postoperative pain was assessed every 4 h in the first 12 h after surgery and then every 12 to 48 h, using a VAS (0 = no pain, 10 = worst possible pain), by nursing staff who were unaware of the perioperative intervention. The character of the pain was also assessed simultaneously. Visceral pain was defined as deep-seated pain located in the right hypochondrium or referred to the shoulder. Parietal pain was defined as incisional pain located at the trocar sites.

Statistical analysis

Data were expressed as the mean \pm SE. All data were prepared and compiled using SPSS 16.0 software. Statistical differences were determined by ANOVA using the Dunnet procedure in non-repeated measures obtained by the mean postoperative VAS scores for the various groups. Categorical variables were recorded as numbers (percentages) and compared by using the χ^2 test with

Table 1 Patient characteristic data (mean \pm SE)

Variables	Group A	Group B	Group C
Age (yr)	41.6 \pm 16.1	42.2 \pm 14.7	40.8 \pm 17.6
Weight (kg)	62.6 \pm 18.3	65.3 \pm 16.8	64.7 \pm 19.1
Sex (M/F)	14/6	14/6	14/6
Duration of anesthesia (min)	106.7 \pm 21.4	98.2 \pm 24.3	103.7 \pm 25.7
Duration of surgery (min)	66.4 \pm 20.1	62.8 \pm 19.5	68.5 \pm 18.3

Table 2 Multiple comparisons of visual analog scale (VAS) scores for various groups vs group C (the control) (mean \pm SE)

Time (h)	Group	n	VAS	P value
4	G1	20	7.2 \pm 2.8	0.547
	G2	20	4.3 \pm 1.2	0.007
	G3	20	8.3 \pm 3.5	
8	G1	20	6.5 \pm 3.7	0.435
	G2	20	3.4 \pm 1.6	0.008
	G3	20	7.0 \pm 3.1	
12	G1	20	5.1 \pm 1.9	0.327
	G2	20	2.5 \pm 0.8	0.001
	G3	20	5.9 \pm 2.0	
24	G1	20	3.5 \pm 1.3	0.264
	G2	20	1.8 \pm 0.9	0.001
	G3	20	4.0 \pm 1.8	
36	G1	20	2.7 \pm 1.2	0.362
	G2	20	1.2 \pm 0.6	0.001
	G3	20	2.9 \pm 1.0	
48	G1	20	2.0 \pm 0.8	0.538
	G2	20	0.8 \pm 0.3	0.001
	G3	20	2.2 \pm 0.8	

Yates correction. The threshold for statistical significance was considered $P < 0.05$.

RESULTS

The 60 study patients (42 women and 18 men) varied in age from 25 to 63 years (median, 41.2 years). The three groups did not differ in mean age, body weight, or ASA status. None of the patients had a history of jaundice or gallstone pancreatitis. Eleven patients (18.3%) had previously undergone lower abdominal surgery. There was no significant difference in the duration of surgery among the three groups ($P = 0.587$): 66.4 \pm 20.1 min for group A, 62.8 \pm 19.5 min for group B, 68.5 \pm 18.3 min for group C (Table 1).

The VAS score decreased after surgery in all patients. Analysis of variance followed by multiple comparisons using the Dunnet procedure, with group C used as a control, suggested that the mean VAS score for group B was significantly less than that for group A and C. The mean VAS scores for group A were lower than Group C, but the difference was not significant (Table 2).

The overall incidence of visceral, parietal, and shoulder pain in our study were 81.7%, 50.0%, and 26.7%, respectively. However, the incidence of visceral pain in group B was less than that in the other groups ($P < 0.05$) (Table 3). The number of patients in group B experiencing visceral pain after surgery was also significantly lower

Table 3 Character of pain after laparoscopic cholecystectomy n (%)

Group	n	Visceral	Parietal	Shoulder
A	20	18 (90.0)	10 (50.0)	7 (35.0)
B	20	12 (60.0)	9 (45.0)	1 (5.0)
C	20	19 (95.0)	11 (55.0)	8 (40.0)
Total	60	49 (81.7)	30 (50.0)	16 (26.7)

than that in the other groups ($P < 0.05$). The overall incidence of parietal pain was 50.0% in group A, 45.0% in group B and 55.0% in group C ($P > 0.05$). There was no difference in the incidence of parietal pain between the three groups. Only one patient in group B reported shoulder pain, as compared with 16 (26.7%) of the 40 patients in groups A and C ($P < 0.01$).

Rescue analgesia (intramuscular pethidine hydrochloride 50 mg once) was administered if the VAS was higher than 10. The amount of pethidine hydrochloride used per capita in group B (2.5 ± 11.2 mg) was significantly lower than that in group A (30.0 ± 25.1 mg) and group C (25.0 ± 25.6 mg).

DISCUSSION

Even though postoperative pain after LC is markedly less than that after open cholecystectomy, pain is still the patient's first complaint after LC^[9]. Although postoperative pain is reduced compared to laparotomic surgery^[10], effective analgesic treatment still remains crucial for early patient discharge^[11]. Usually, postoperative pain following LC peaks immediately after surgery, and decreases within 24 h, and then increases to a second or even a third peak later^[12].

The incidence of pain after laparoscopy may be attributed to the carbon dioxide gas (CO₂) used to induce pneumoperitoneum^[13,14]. CO₂ remains in the peritoneal cavity for several days after surgery and causes stretching of the phrenic nerve endings^[15], local hypothermia, and diaphragmatic irritation via carbonic acid^[16]. The benefit of using intraperitoneal local anesthetics for shoulder and abdominal pain control has been proven^[7,17-19], however, several other studies did not confirm these findings^[20-23].

Pain after LC includes three components, visceral, parietal, and shoulder pain^[3]. In the early postoperative period, many studies report that visceral pain is predominant, especially during the first hours after surgery^[3]. At the same time, parietal pain is less intense because of the small incisions and limited damage to the abdominal wall. Shoulder pain may occur later with visceral pain. The most common location of postoperative pain is in the right upper quadrant, followed by the trocar site and the shoulder^[24].

In this study, all operations were progressed according to the line of least tissue damage. We took the gallbladder out of the peritoneal cavity via the umbilical incision which was less sensitive than the other incisions. Thus, we observed that parietal pain was mild in this study and did not contribute substantially to the VAS score.

Fibrin sealant has been an extremely effective and

widely used adjunct to surgical procedures for the control of diffuse slow bleeding over large surfaces. In addition, fibrin sealant has been used as a carrier for other compounds. Thus, it has been used to release medicines slowly at a fixed site which are therefore effective for a long time.

We observed a significant reduction in pain after gallbladder bed implantation of fibrin sealant combined with ropivacaine. This effect was indirectly reflected in the progressive reduction in both the VAS score and visceral pain in this group of patients. This suggests that the progressive reduction in the VAS score in this group of patients was primarily attributable to the effective control of visceral pain.

The VAS score for the patients with fibrin sealant alone implanted in the gallbladder bed was less than that of the control group, although the differences were not statistically significant. This suggests that the gallbladder bed with implanted fibrin sealant alone may lead to a slight relief in postoperative pain.

Verma *et al*^[19] reported that visceral pain is prominent after LC and can be effectively controlled by 0.5% bupivacaine-soaked Surgicel in the gallbladder bed alone. They used bupivacaine 0.5% (2 mg/kg) instilled over the oxidized regenerated cellulose strips (Surgicel) in the gallbladder bed, and found that the postoperative pain was significantly less in these patients than in the control groups (bupivacaine infiltrated at the trocar sites and normal saline in the gallbladder bed and at the trocar sites).

These findings are in accordance with the anatomical characteristics of the phrenic nerve which supplies the gallbladder, porta hepatis, and liver, while sharing the root of nerves to the shoulder^[25]. We used fibrin sealant carrying ropivacaine adhered to the gallbladder bed. Using this method, ropivacaine was released slowly and the stickiness of the fibrin sealant ensured that the drug remained in contact with the wound for a longer period of time. In our study, implanting fibrin sealant combined with ropivacaine in the gallbladder bed was effective in controlling shoulder pain, and only one of the patients in this treatment group experienced shoulder pain.

In conclusion, we conclude that implanting fibrin sealant combined with ropivacaine in the gallbladder bed is effective in controlling both visceral and shoulder pain after LC.

COMMENTS

Background

Even though postoperative pain after laparoscopic cholecystectomy (LC) is markedly less than that after open cholecystectomy, pain is still the patient's first complaint after LC.

Research frontiers

According to the anatomical characteristics of the nerve which supplies the gallbladder, the use of fibrin sealant carrying ropivacaine adhered to the gallbladder bed can relieve postoperative pain.

Innovations and breakthroughs

This study determined that implantation of fibrin sealant with sustained-release ropivacaine in the gallbladder bed could relieve the pain after LC.

Applications

The implantation of 5 mL fibrin sealant combined with ropivacaine (1 mg/kg

body weight) in the gallbladder bed provided significant postoperative pain relief compared with the implantation of fibrin sealant alone.

Terminology

Fibrin sealant can be used as a carrier for ropivacaine. With fibrin sealant, ropivacaine could be released slowly, and the stickiness of the fibrin sealant ensured that the drug remained in contact with the wound for a longer period of time.

Peer review

The authors have assessed the use of a fibrin sealant with local anaesthetic in the gallbladder bed on post-operative pain after LC. Fibrin sealant with local anaesthetic was associated with lower post-operative pain scores.

REFERENCES

- 1 Soper NJ, Stockmann PT, Dunnegan DL, Ashley SW. Laparoscopic cholecystectomy. The new 'gold standard'? *Arch Surg* 1992; **127**: 917-921; discussion 921-923
- 2 Bisgaard T, Klarskov B, Rosenberg J, Kehlet H. Characteristics and prediction of early pain after laparoscopic cholecystectomy. *Pain* 2001; **90**: 261-269
- 3 Joris J, Thiry E, Paris P, Weerts J, Lamy M. Pain after laparoscopic cholecystectomy: characteristics and effect of intraperitoneal bupivacaine. *Anesth Analg* 1995; **81**: 379-384
- 4 Lau H, Brooks DC. Predictive factors for unanticipated admissions after ambulatory laparoscopic cholecystectomy. *Arch Surg* 2001; **136**: 1150-1153
- 5 Edwards ND, Barclay K, Catling SJ, Martin DG, Morgan RH. Day case laparoscopy: a survey of postoperative pain and an assessment of the value of diclofenac. *Anesthesia* 1991; **46**: 1077-1080
- 6 Akaraviputh T, Leelouhapong C, Lohsiriwat V, Aroonpruksakul S. Efficacy of perioperative parecoxib injection on postoperative pain relief after laparoscopic cholecystectomy: a prospective, randomized study. *World J Gastroenterol* 2009; **15**: 2005-2008
- 7 Feroci F, Kröning KC, Scatizzi M. Effectiveness for pain after laparoscopic cholecystectomy of 0.5% bupivacaine-soaked Tabotamp placed in the gallbladder bed: a prospective, randomized, clinical trial. *Surg Endosc* 2009; **23**: 2214-2220
- 8 Mentes O, Harlak A, Yigit T, Balkan A, Balkan M, Cosar A, Savaser A, Kozak O, Tufan T. Effect of intraoperative magnesium sulphate infusion on pain relief after laparoscopic cholecystectomy. *Acta Anaesthesiol Scand* 2008; **52**: 1353-1359
- 9 Bisgaard T. [Treatment of pain after laparoscopic cholecystectomy] *Ugeskr Laeger* 2005; **167**: 2629-2632
- 10 Black NA, Downs SH. The effectiveness of surgery for stress incontinence in women: a systematic review. *Br J Urol* 1996; **78**: 497-510
- 11 Salihoglu Z, Yildirim M, Demirok S, Kaya G, Karatas A, Ertem M, Aytac E. Evaluation of intravenous paracetamol administration on postoperative pain and recovery characteristics in patients undergoing laparoscopic cholecystectomy. *Surg Laparosc Endosc Percutan Tech* 2009; **19**: 321-323
- 12 Reuben SS, Steinberg RB, Maciolek H, Joshi W. Preoperative administration of controlled-release oxycodone for the management of pain after ambulatory laparoscopic tubal ligation surgery. *J Clin Anesth* 2002; **14**: 223-227
- 13 Dobbs FF, Kumar V, Alexander JI, Hull MG. Pain after laparoscopy related to posture and ring versus clip sterilization. *Br J Obstet Gynaecol* 1987; **94**: 262-266
- 14 Shantha TR, Harden J. Laparoscopic cholecystectomy: anesthesia-related complications and guidelines. *Surg Laparosc Endosc* 1991; **1**: 173-178
- 15 Korell M, Schmaus F, Strowitzki T, Schneeweiss SG, Hepp H. Pain intensity following laparoscopy. *Surg Laparosc Endosc* 1996; **6**: 375-379
- 16 Semm K, Arp WD, Trappe M, Kube D. [Pain reduction after pelvi-/laparoscopic interventions by insufflation of CO₂ gas at body temperature (Flow-Therme)] *Geburtshilfe Frauenheilkd* 1994; **54**: 300-304
- 17 Elhakim M, Amine H, Kamel S, Saad F. Effects of intraperitoneal lidocaine combined with intravenous or intraperitoneal tenoxicam on pain relief and bowel recovery after laparoscopic cholecystectomy. *Acta Anaesthesiol Scand* 2000; **44**: 929-933
- 18 Tobias JD. Postoperative analgesia and intraoperative inhalational anesthetic requirements during umbilical herniorrhaphy in children: postincisional local infiltration versus preincisional caudal epidural block. *J Clin Anesth* 1996; **8**: 634-638
- 19 Verma GR, Lyngdoh TS, Kaman L, Bala I. Placement of 0.5% bupivacaine-soaked Surgicel in the gallbladder bed is effective for pain after laparoscopic cholecystectomy. *Surg Endosc* 2006; **20**: 1560-1564
- 20 Rademaker BM, Kalkman CJ, Odoom JA, de Wit L, Ringers J. Intraperitoneal local anaesthetics after laparoscopic cholecystectomy: effects on postoperative pain, metabolic responses and lung function. *Br J Anaesth* 1994; **72**: 263-266
- 21 Scheinin B, Kellokumpu I, Lindgren L, Haglund C, Rosenberg PH. Effect of intraperitoneal bupivacaine on pain after laparoscopic cholecystectomy. *Acta Anaesthesiol Scand* 1995; **39**: 195-198
- 22 Paulson J, Mellinger J, Baguley W. The use of intraperitoneal bupivacaine to decrease the length of stay in elective laparoscopic cholecystectomy patients. *Am Surg* 2003; **69**: 275-278; discussion 278-279
- 23 Papaziogas B, Argiriadou H, Papagiannopoulou P, Pavlidis T, Georgiou M, Syfri E, Papaziogas T. Preincisional intravenous low-dose ketamine and local infiltration with ropivacaine reduces postoperative pain after laparoscopic cholecystectomy. *Surg Endosc* 2001; **15**: 1030-1033
- 24 Mraović B, Jurisić T, Kogler-Majeric V, Sustic A. Intraperitoneal bupivacaine for analgesia after laparoscopic cholecystectomy. *Acta Anaesthesiol Scand* 1997; **41**: 193-196
- 25 Peter LW, Roger W, Mary D, Lawrence HB. Biliary duct and gallbladder. In: Gray's anatomy. 37th ed. London: Churchill Livingstone, 1989: 1394-1395

S-Editor Wang YR L-Editor Webster JR E-Editor Zheng XM



Multidrug resistance protein 3 R652G may reduce susceptibility to idiopathic infant cholestasis

Xiu-Qi Chen, Lin-Lin Wang, Qing-Wen Shan, Qing Tang, Shu-Jun Lian

Xiu-Qi Chen, Lin-Lin Wang, Qing-Wen Shan, Qing Tang, Shu-Jun Lian, Department of Pediatrics, First Affiliated Hospital, Guangxi Medical University, Nanning 530021, Guangxi Zhuang Autonomous Region, China

Author contributions: Chen XQ performed the experiments and wrote the paper; Wang LL contributed the conception and design of study and revised the paper; Shan QW and Tang Q analyzed the data and were also involved in editing the manuscript; Lian SJ collected the specimens and performed a small number of the experiments.

Supported by Guangxi Scientific Research and Technological Development Projects Funding (Ministry Science & Technology of Guangxi, No. 0816004-6)

Correspondence to: Lin-Lin Wang, Professor, Department of Pediatrics, First Affiliated Hospital, Guangxi Medical University, Nanning 530021, Guangxi Zhuang Autonomous Region, China. wll276@yahoo.com.cn

Telephone: +86-771-5356505 Fax: +86-771-5356781

Received: September 23, 2009 Revised: October 20, 2009

Accepted: October 27, 2009

Published online: December 14, 2009

© 2009 The WJG Press and Baishideng. All rights reserved.

Key words: Multidrug resistance protein 3; Single nucleotide polymorphisms; R652G; Infant; Cholestasis

Peer reviewer: Tamara Alempijevic, MD, PhD, Assistant Professor, Clinic for Gastroenterology and Hepatology, Clinical Centre of Serbia, 2 Dr Koste Todorovica St., Belgrade 11000, Serbia

Chen XQ, Wang LL, Shan QW, Tang Q, Lian SJ. Multidrug resistance protein 3 R652G may reduce susceptibility to idiopathic infant cholestasis. *World J Gastroenterol* 2009; 15(46): 5855-5858 Available from: URL: <http://www.wjgnet.com/1007-9327/15/5855.asp> DOI: <http://dx.doi.org/10.3748/wjg.15.5855>

Abstract

AIM: To evaluate the role of genetic factors in the pathogenesis of idiopathic infant cholestasis.

METHODS: We performed a case-control study, including 78 infants with idiopathic infant cholestasis and 113 healthy infants as controls. Genomic DNA was extracted from peripheral venous blood leukocytes using phenol chloroform methodology. Polymerase chain reaction was used to amplify the multidrug resistance protein 3 (MDR3) R652G fragment, and products were sequenced using the ABI 3100 Sequencer.

RESULTS: The R652G single nucleotide polymorphism (SNP) was significantly more frequent in healthy infants (allele frequency 8.0%) than in patients (allele frequency 2.60%) ($P < 0.05$), odds ratio, 0.29; 95% confidence interval, 0.12-0.84. The conjugated bilirubin in patients with the AG genotype was significantly lower than in those with the AA genotype ($44.70 \pm 6.15 \mu\text{mol/L}$ vs $95.52 \pm 5.93 \mu\text{mol/L}$, $P < 0.05$).

CONCLUSION: MDR3 R652G is negatively correlated with idiopathic infant cholestasis. Children with the R652G SNP in Guangxi of China may have reduced susceptibility to infant intrahepatic cholestasis.

INTRODUCTION

Idiopathic infant cholestasis is of unknown etiology and can occur in either a sporadic or a familial form. Most affected infants have a good prognosis. Approximately 5%-10% have persistent inflammation or fibrosis, and a few develop more severe liver disease, such as cirrhosis. Although the cause of idiopathic infant cholestasis is unknown, genetic factors have been suggested by the existence of some other entities with cholestasis, such as familial intrahepatic cholestasis-1 mutation in progressive familial intrahepatic cholestasis type 1 (PFIC-1), bile salt export pump deficiency in PFIC-2^[1-3], multidrug resistance protein 3 (MDR3) deficiency in PFIC-3^[4-6].

Studies have investigated the involvement of MDR3 variants in the development of disease, and we were interested to note that the MDR3 R652G single nucleotide polymorphism (SNP) has a high allele frequency in generally healthy people^[7]. Our aim was to study the MDR3 R652G SNP distribution frequency in idiopathic infant cholestasis and healthy infants and to determine whether there were any differences between them and, if so, their relevance.

MATERIALS AND METHODS

Patients

Seventy eight infants were diagnosed with idiopathic infant cholestasis in the case group and there were 113 healthy infants in the control group. The patients were included in the study on the basis of the following crite-

ria: (1) a history of chronic cholestasis onset in the neonatal/infant period with unknown origin; (2) presence of hepatomegaly or hepatosplenomegaly; (3) persistent marked serum alanine aminotransferase (ALT) activity; (4) elevated total bile acid concentration and total bilirubin (TB), mainly marked conjugated bilirubin (CB); (5) absence of viral infections (such as hepatitis A virus, hepatitis B virus, hepatitis C virus, cytomegalovirus).

For patients and healthy infants, the following biochemical parameters were recorded: serum ALT and aspartate aminotransferase (AST); γ -glutamyltransferase (γ -GT) and serum TB and CB.

We received informed consent from all the subjects' guardians to take part in the study, and the protocol was approved by the local ethical committee of the Hospital.

Polymerase chain reaction (PCR) amplified the MDR3 R652G and sequence analysis

Genomic DNA was extracted from peripheral venous blood leukocytes using standard phenol chloroform procedures. The DNA concentration was quantified by spectrophotometry. Primers for MDR3 R652G were forward (5'-CATCCATTGGAGACACACACAC-3') and reverse (5'-GTAGCAGTCATCTGTGCCTGAA A-3')^[7]. The primary PCR product fragments were 348 bp. PCRs for generating the R652G fragments were generally performed in a reaction volume of 50 μ L with 100 ng of genomic DNA, 1.5 U of *Taq* polymerase (Fermentas), 10 \times PCR buffer (Fermentas), 1.5 mmol/L of MgCl₂ (Fermentas), 200 μ mol/L deoxynucleoside-5-triphosphate (Takara) and 20 μ mol of each primer. PCR conditions included an initial denaturation step at 95°C for 5 min, followed by 30 cycles of denaturation at 94°C for 30 s, annealing at 65°C for 30 s and extension at 72°C for 1 min. The PCR reaction was terminated after an extension step at 72°C for 10 min. The PCR products were analyzed by 2% agarose gel with 0.5 μ g/mL ethidium bromide and quantitated approximately with a DNA marker (Takara, DaLiang). The PCR products sequence analysis was run in the ABI 3100 automated DNA sequencer. Sequences were compared with the sequence of the MDR3 in GenBank (NG_007118.1, GI: 169234676).

Statistical analysis

Data are given as mean \pm SD. Comparison of the frequency of the R652G SNP was made between patients and controls, and the analysis of association with the phenotype was performed by χ^2 test or Fisher's exact test when appropriate. A *P*-value < 0.05 was considered statistically significant. The data was analyzed using SPSS 13.0. The odds ratio (OR) was calculated with the corresponding 95% confidence intervals (95% CI). Allele frequency was tested for the Hardy-Weinberg equilibrium.

RESULTS

The study comprised 78 infants with idiopathic infant cholestasis and 113 controls. Details of the study groups are shown in Table 1. The mean total bilirubin was

Table 1 Clinical characteristics of the 78 idiopathic infant cholestasis patients (mean \pm SD)

	Patients	Controls
Age (mo)	1.8 \pm 0.31	1.2 \pm 0.25
TB (μ mol/L)	194.43 \pm 13.33 ^a	12.94 \pm 5.15
ALT (U/L)	123.80 \pm 11.63 ^a	29.09 \pm 2.62
AST (U/L)	273.86 \pm 27.90 ^a	34.43 \pm 2.43
γ -GT (U/L)	308.60 \pm 46.30 ^a	30.22 \pm 9.90

^a*P* < 0.05 vs control. TB: Total bilirubin; AST: Aspartate aminotransferase; ALT: Alanine aminotransferase; γ -GT: γ -glutamyltransferase.

Table 2 MDR3 R652G genotypes and allele frequencies in patients and controls *n* (%)

Groups	<i>n</i>	Genotypes			Allele frequency (%)	<i>P</i> -value
		A/A	A/G	G/G		
Patients	78	74 (94.9)	4 (5.1)	0	2.6	< 0.05 ¹
Controls	113	95 (84.1)	18 (15.9)	0	8.0	

¹Fisher's exact test between patients and controls for genotype frequency. *P* = 0.022; OR, 0.29; 95% CI, 0.12-0.84.

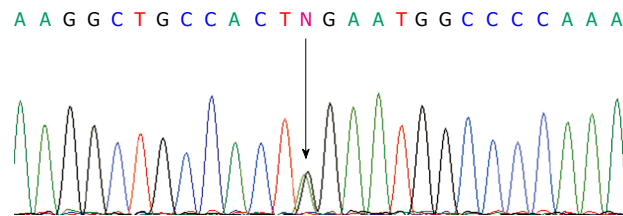


Figure 1 Sequence of the multidrug resistance protein-3 (MDR3) single nucleotide polymorphism R652G (A>G).

194.43 \pm 13.33 μ mol/L (normal \leq 20 μ mol/L). The mean CB was 105.75 \pm 6.44 μ mol/L. The mean serum transaminase levels were 273.86 \pm 27.90 and 123.80 \pm 11.63 U/L for AST and ALT, respectively (normal \leq 40 U/L), and mean serum γ -GT was 308.60 \pm 46.30 U/L (normal \leq 50 U/L). The levels were all normal in the control group. All the patients had hepatomegaly, and 62 of the 78 cases had splenomegaly.

PCR products sequence analysis showed a heterozygous substitution A>G (Figure 1) in codon 652 which creates an amino acid substitution in codon R652G in exon 16. Distribution of the genetic polymorphisms in patients and controls is shown in Table 2. Test results showed that the R652G genotype distribution in the 2 groups was in line with the Hardy-Weinberg equilibrium, indicating that the selected sample was representative of the population. The patient AG genotype frequency was significantly lower than in the control group (*P* < 0.05). The AG genotype was negatively correlated with idiopathic infant cholestasis (OR, 0.29, 95% CI: 0.12-0.84) showing that the AG genotype has a protective effect in the normal population (Table 2).

Biochemical markers comparison in patients with different genotypes

The patient group was divided into 2 sub-groups ac-

Table 3 Comparison of clinical characteristics in patient sub-groups according to genotype (mean \pm SD)

	Patients A/A	Patients A/G
TB ($\mu\text{mol/L}$)	198.94 \pm 14.85	91.65 \pm 15.70
CB ($\mu\text{mol/L}$)	95.52 \pm 5.93	44.70 \pm 6.15 ^a
ALT (U/L)	131.54 \pm 11.91	92.50 \pm 10.01
AST (U/L)	281.29 \pm 28.26	129.25 \pm 12.43
γ -GT (U/L)	317.68 \pm 47.64	77.00 \pm 18.78

CB: Conjugated bilirubin. ^aP < 0.05.

cording to genotype and serum biochemical parameters were compared. The CB of the AG genotype (44.70 \pm 6.15 $\mu\text{mol/L}$) was significantly lower compared with that of the AA genotype (95.52 \pm 5.93 $\mu\text{mol/L}$) (P < 0.05). Other serum markers in the sub-groups with the 2 genotypes were not significantly different (P > 0.05) (Table 3).

DISCUSSION

Our study is the first report of the MDR3 R652G SNP in children in China. Our data showed that the R652G SNP had a significantly higher proportional distribution in normal infants than in idiopathic infant cholestasis patients. Moreover, in the cholestasis group, the CB of AG genotype patients had a lower mean value than in the AA genotype patients. It is known that CB is a very important index that can reflect the extent of intrahepatic cholestasis. For this reason, we can infer that the R652G variant has a specific protective effect in the normal population.

In previous studies, in the analysis of MDR3 gene sequence variants in different countries, the R652G SNP was the only protein-altering variant with high allele frequency in all groups. It was 7.3% in Caucasians, 1.4% in Japanese and 2.3% in Koreans^[7]. In another study, the variant was 7.3% in healthy Caucasians, 8.6% in primary biliary cirrhosis patients and 12.8% primary sclerosing cholangitis patients^[8]. R652G is a MDR3 gene mutation that results in non-synonymous amino acid substitutions but is not associated with disease. In Switzerland, a study showed that the MDR3 R652G variant was 7% in healthy Caucasians, 9% in drug-induced cholestatic patients and 4% in hepatocellular/mixed liver injury^[9]. Pauli-Magnus *et al*^[10] reported the R652G variant in 10% of intrahepatic cholestasis pregnancy cases and 16.3% in healthy controls.

The previous studies indicated that the R652G variant was prevalent in the general population. Furthermore, studies of MDR3 R652G in a variety of diseases showed no evidence that the R652G variant was related to disease. In our study, the R652G variant was 15.9% in healthy children, with a higher frequency than in infant cholestasis patients. Therefore, we believe that the AG genotype has a protective effect in infant cholestasis, and the AG genotype is likely to reduce the risk of children suffering from cholestasis. In this study, the proportion of the AG gene type in the normal population was higher than in

previous reports from other regions, possibly because of the existence of racial and geographic differences.

There is also another phenomenon whereby R652G may have a protective effect and reduce the risk of suffering from disease. Jacquemin *et al*^[11] reported one patient with intrahepatic cholestasis of pregnancy carrying a R652G substitution, and whose biliary phospholipids were lower than other patients. Another study showed the A/G allele frequency was 6% in intrahepatic cholestasis of pregnancy patients and 17% in healthy controls in Sweden. The AA genotype subjects were more likely to suffer from cholestasis^[12]. Our result also confirmed this conclusion.

A recent study of gallstones in sibling pairs and controls showed that R652G variant frequency was 18% in patients and 25% in controls. In the control sub-groups, subjects with the GG genotype had significantly lower cholesterol compared with those with the AA genotype. It is known that cholesterol is the raw material for synthesis of bile acids^[13]. This gives an indication of the direction of future research.

It is worth noting that this is an interesting new result. Most of the MDR3 gene variants have reported an association with disease causation, such as PFIC and intrahepatic cholestasis of pregnancy^[14,15]. In contrast, the R652G variant seems to have a protective effect. It has been assumed that the missense mutation R652G is a neutral polymorphism. Sequence comparisons of MDR3 genes identified that the glycine residue is conserved in other species such as rat and hamster. More research will be required to confirm that in the future.

In conclusion, the MDR3 R652G SNP is negatively correlated with cholestasis (OR, 0.29, 95% CI, 0.12-0.84). Children in Guangxi of China with the R652G variant may have reduced susceptibility to infant intrahepatic cholestasis.

COMMENTS

Background

Idiopathic infant intrahepatic cholestasis is a common clinical disease that can occur in either a sporadic or a familial form. The incidence of idiopathic infant intrahepatic cholestasis is very high in China. If not treated early, approximately 5%-10% of patients can have persistent inflammation or fibrosis, and a few develop more severe liver disease, such as cirrhosis.

Research frontiers

All studies in recent years on the multidrug resistance protein 3 (MDR3) variants have involved the development of disease. However, an interesting phenomenon is that there was no positive evidence for the MDR3 R652G variant being involved in the pathogenesis of intrahepatic cholestasis. This study investigated the MDR3 R652G distributed allele frequency in idiopathic infant cholestasis and healthy infants to determine whether there were any difference and, if so, their relevance.

Innovations and breakthroughs

Most studies have concentrated on MDR3 mutations in the pathogenesis of progressive familial intrahepatic cholestasis type 3, intrahepatic cholestasis of pregnancy and cholelithiasis. There have been few studies investigating MDR3 and idiopathic infant intrahepatic cholestasis. In order to evaluate the role of the MDR3 R652G variant in the pathogenesis of idiopathic infant cholestasis, the authors analyzed the MDR3 R652G polymorphism in a case-control study in Guangxi Chinese infants. The authors found that the R652G variant was significantly more frequent in healthy infants than in patients. The results showed that the R652G variant has a protective effect in healthy infants and reduces the possibility of suffering from idiopathic infant cholestasis. The result

was not the same as a previous study. The reason may be a result of ethnic population differences and the variability in geographical location.

Applications

The study results suggest that the MDR3 R652G variant has a protective effect in healthy infants. This will give further information for comparing geographical regions, and it is very important to establish particular characteristics of MDR3 R652G that can be useful in the differential diagnosis of idiopathic infant cholestasis, and furthermore, may establish the influence of such an single nucleotide polymorphism (SNP) in prognosis.

Terminology

MDR3 R652G: MDR3 R652G is a SNP of the MDR3 in the 652 coding site. The MDR3 is encoded by the ABCB4 gene, and the 652 coding site is located in ABCB4 exon 16. The R652G is a gene mutation where the adenine (A) mutates into guanine (G) which causes AGA>GGA resulting in arginine substitution by glycine (R652G).

Peer review

The paper gives a significant contribution to basic science knowledge, as well as clinical practice. Publishing this manuscript will allow further comparison with data from other regions and help to clarify the pathogenesis of idiopathic infant cholestasis.

REFERENCES

- 1 **Strautnieks SS**, Kagalwalla AF, Tanner MS, Knisely AS, Bull L, Freimer N, Kocoshis SA, Gardiner RM, Thompson RJ. Identification of a locus for progressive familial intrahepatic cholestasis PFIC2 on chromosome 2q24. *Am J Hum Genet* 1997; **61**: 630-633
- 2 **Strautnieks SS**, Bull LN, Knisely AS, Kocoshis SA, Dahl N, Arnell H, Sokal E, Dahan K, Childs S, Ling V, Tanner MS, Kagalwalla AF, Németh A, Pawlowska J, Baker A, Mieli-Vergani G, Freimer NB, Gardiner RM, Thompson RJ. A gene encoding a liver-specific ABC transporter is mutated in progressive familial intrahepatic cholestasis. *Nat Genet* 1998; **20**: 233-238
- 3 **Treepongkaruna S**, Gaensan A, Pienvichit P, Luksan O, Knisely AS, Sornmayura P, Jirsa M. Novel ABCB11 mutations in a Thai infant with progressive familial intrahepatic cholestasis. *World J Gastroenterol* 2009; **15**: 4339-4342
- 4 **Jacquemin E**, Hadchouel M. Genetic basis of progressive familial intrahepatic cholestasis. *J Hepatol* 1999; **31**: 377-381
- 5 **Arnell H**, Nemeth A, Annerén G, Dahl N. Progressive familial intrahepatic cholestasis (PFIC): evidence for genetic heterogeneity by exclusion of linkage to chromosome 18q21-q22. *Hum Genet* 1997; **100**: 378-381
- 6 **de Vree JM**, Jacquemin E, Sturm E, Cresteil D, Bosma PJ, Aten J, Deleuze JF, Desrochers M, Burdelski M, Bernard O, Oude Elferink RP, Hadchouel M. Mutations in the MDR3 gene cause progressive familial intrahepatic cholestasis. *Proc Natl Acad Sci USA* 1998; **95**: 282-287
- 7 **Lang T**, Haberl M, Jung D, Drescher A, Schlagenhauf R, Keil A, Mornhinweg E, Stieger B, Kullak-Ublick GA, Kerb R. Genetic variability, haplotype structures, and ethnic diversity of hepatic transporters MDR3 (ABCB4) and bile salt export pump (ABCB11). *Drug Metab Dispos* 2006; **34**: 1582-1599
- 8 **Pauli-Magnus C**, Kerb R, Fattinger K, Lang T, Anwald B, Kullak-Ublick GA, Beuers U, Meier PJ. BSEP and MDR3 haplotype structure in healthy Caucasians, primary biliary cirrhosis and primary sclerosing cholangitis. *Hepatology* 2004; **39**: 779-791
- 9 **Lang C**, Meier Y, Stieger B, Beuers U, Lang T, Kerb R, Kullak-Ublick GA, Meier PJ, Pauli-Magnus C. Mutations and polymorphisms in the bile salt export pump and the multidrug resistance protein 3 associated with drug-induced liver injury. *Pharmacogenet Genomics* 2007; **17**: 47-60
- 10 **Pauli-Magnus C**, Lang T, Meier Y, Zodan-Marin T, Jung D, Breymann C, Zimmermann R, Kenngott S, Beuers U, Reichel C, Kerb R, Penger A, Meier PJ, Kullak-Ublick GA. Sequence analysis of bile salt export pump (ABCB11) and multidrug resistance p-glycoprotein 3 (ABCB4, MDR3) in patients with intrahepatic cholestasis of pregnancy. *Pharmacogenetics* 2004; **14**: 91-102
- 11 **Jacquemin E**, De Vree JM, Cresteil D, Sokal EM, Sturm E, Dumont M, Scheffer GL, Paul M, Burdelski M, Bosma PJ, Bernard O, Hadchouel M, Elferink RP. The wide spectrum of multidrug resistance 3 deficiency: from neonatal cholestasis to cirrhosis of adulthood. *Gastroenterology* 2001; **120**: 1448-1458
- 12 **Wasmuth HE**, Glantz A, Keppeler H, Simon E, Bartz C, Rath W, Mattsson LA, Marschall HU, Lammert F. Intrahepatic cholestasis of pregnancy: the severe form is associated with common variants of the hepatobiliary phospholipid transporter ABCB4 gene. *Gut* 2007; **56**: 265-270
- 13 **Acalovschi M**, Tirziu S, Chioorean E, Krawczyk M, Grünhage F, Lammert F. Common variants of ABCB4 and ABCB11 and plasma lipid levels: a study in sib pairs with gallstones, and controls. *Lipids* 2009; **44**: 521-526
- 14 **Floreani A**, Carderi I, Paternoster D, Soardo G, Azzaroli F, Esposito W, Montagnani M, Marchesoni D, Variola A, Rosa Rizzotto E, Braghin C, Mazzella G. Hepatobiliary phospholipid transporter ABCB4, MDR3 gene variants in a large cohort of Italian women with intrahepatic cholestasis of pregnancy. *Dig Liver Dis* 2008; **40**: 366-370
- 15 **Espinosa Fernández MG**, Navas López VM, Blasco Alonso J, Sierra Salinas C, Barco Gálvez A. [Progressive familial intrahepatic cholestasis type 3. An MDR3 defect] *An Pediatr (Barc)* 2008; **69**: 182-184

S- Editor Wang JL L- Editor Cant MR E- Editor Zheng XM



CASE REPORT

Two synchronous somatostatinomas of the duodenum and pancreatic head in one patient

Radoje B Čolović, Slavko V Matić, Marjan T Micev, Nikica M Grubor, Henry Dushan Atkinson, Stojan M Latinčić

Radoje B Čolović, Slavko V Matić, Marjan T Micev, Nikica M Grubor, Stojan M Latinčić, The First Surgical Clinic, Clinical Center of Serbia, Koste Todorovića 6, Belgrade 11000, Serbia
Henry Dushan Atkinson, Surgical Directorate, Imperial College School of Medicine, St Mary's Hospital, Praed St, London W2 1NY, United Kingdom

Author contributions: Čolović RB and Latinčić SM operated on the patient, Čolović RB and Matić SV wrote the paper, Matić SV and Grubor NM performed the literature research and analysis, Micev MT did all the pathological and immunohistochemical examinations, Atkinson HD revised the English translation of the article.

Correspondence to: Slavko V Matić, MD, PhD, Associate Professor of Surgery, Clinical Center of Serbia, Institute for Digestive diseases, K. Todorovića 6 street, Belgrade 11000, Serbia. slavko.matic@med.bg.ac.rs

Telephone: +381-64-2181949 **Fax:** +381-11-3031830

Received: October 23, 2009 **Revised:** November 12, 2009

Accepted: November 19, 2009

Published online: December 14, 2009

Peer reviewer: Wei Tang, MD, EngD, Assistant Professor, H-B-P Surgery Division, Artificial Organ and Transplantation Division, Department of surgery, Graduate School of Medicine, The University of Tokyo, Tokyo 113-8655, Japan

Čolović RB, Matić SV, Micev MT, Grubor NM, Atkinson HD, Latinčić SM. Two synchronous somatostatinomas of the duodenum and pancreatic head in one patient. *World J Gastroenterol* 2009; 15(46): 5859-5863 Available from: URL: <http://www.wjgnet.com/1007-9327/15/5859.asp> DOI: <http://dx.doi.org/10.3748/wjg.15.5859>

Abstract

Somatostatinomas are extremely rare neuroendocrine tumors of the gastrointestinal tract, first described in the pancreas in 1977 and in the duodenum in 1979. They may be functional and cause somatostatinoma or inhibitory syndrome, but more frequently are non-functioning pancreatic endocrine tumors that produce somatostatin alone. They are usually single, malignant, large lesions, frequently associated with metastases, and generally with poor prognosis. We present the unique case of a 57-year-old woman with two synchronous non-functioning somatostatinomas, one solid duodenal lesion and one cystic lesion within the head of the pancreas, that were successfully resected with a pylorus-preserving Whipple's procedure. No secondaries were found in the liver, or in any of the removed regional lymph nodes. The patient had an uneventful recovery, and remains well and symptom-free at 18 mo postoperatively. This is an extremely rare case of a patient with two synchronous somatostatinomas of the duodenum and the pancreas. The condition is discussed with reference to the literature.

© 2009 The WJG Press and Baishideng. All rights reserved.

Key words: Somatostatinoma; Duodenal neoplasms; Pancreatic neoplasms

INTRODUCTION

Somatostatinomas are extremely rare and account for < 1% of functional APUD (amine precursor uptake and decarboxylation) cell neuroendocrine tumors of the gastrointestinal tract^[1,2], with an annual incidence of 1 case per 40 million people^[3]. Somatostatinomas usually occur within the pancreas but can also manifest in the duodenum, and less frequently in the jejunum and cystic duct^[4-6]. Since the first description of somatostatinoma of the pancreas in 1977^[7], and duodenum in 1979^[8], 100-200 cases^[1,2,9] have been described in the world literature, each occurring as a single lesion. A PubMed search resulted in a single case report of two somatostatinomas in the same patient, associated with type I neurofibromatosis^[10].

We present an extremely rare case with two synchronous non-functioning somatostatinomas, one solid duodenal lesion and one cystic lesion within the head of the pancreas, without other disorders such as von Recklinghausen's disease.

CASE REPORT

A 57-year-old woman presented with moderate epigastric pain in January 2007. Clinically, she was found to have only mild tenderness in the epigastrium, and all laboratory data were within normal limits. Ultrasound (US) and computed tomography (CT) revealed a 3 cm × 3 cm tumor in the duodenum, which was causing narrowing of its lumen to 1 cm, as well as a mass with a gas-filled cyst within the head of the pancreas (Figure 1). A cyst was also found within the head of the pancreas. A barium meal confirmed the duodenal luminal narrowing, and the tumor position above the ampulla of Vater, and



Figure 1 Computed tomography (CT) showing well-vascularized mass within the duodenum and in the head of the pancreas. There is also a cystic lesion containing gas within the pancreatic mass.

upper gastrointestinal endoscopy provided a histological specimen that indicated a neuroendocrine tumor.

At laparotomy, two separate masses were found, one within the medial wall of the descending duodenum, and the second within the head of the pancreas. There were no visible or palpable secondaries within the liver or the peritoneal cavity. As both tumors appeared resectable, we proceeded with a pylorus-preserving Whipple's procedure, as well as regional lymph node dissection. The postoperative recovery was uneventful and the patient remains well at 18 mo.

Macroscopically, the first lesion was a well-demarcated solid nodular suprapapillary tumor of the duodenum, 42 mm in its greatest diameter, 25 mm from the pylorus, and penetrating 15 mm through the duodenal wall to reach the superior margin of the head of the pancreas. There was no obvious intrapancreatic or choledochal infiltration of the tumor. A transverse section showed the tumor to be composed of soft grey/yellow granular and light brown nodular tissues (Figure 2A-D).

The second was a distinctive cystic and hemorrhagic lesion, with a tiny fistula with the duodenum, within the enlarged head of the pancreas. The lesion measured 36 mm in its greatest diameter, contained necrotic and hemorrhagic coagula, and was surrounded by a thin fibrotic pseudocapsule zone. The inner surface of the cyst contained a layer of spongy tan/light brown tissue. There were no other notable micromorphological findings in the remainder of the resected pancreatic specimen.

Histopathology of the duodenal tumor revealed a dominant micronodular and insular growth of epithelioid cells, with rare trabecular or solid microorganization, and without necrotic areas (Figure 3A). The tumor cells were packed tightly with a high degree of uniformity and ill-defined ovoid/polygonal shapes. Their round nuclei were situated centrally, with low nuclear anaplasia and two mitotic figures per 10 high-power fields. However, despite expansive growth and a clearly demarcated border, peritumoral venous infiltration and microinfiltration of the periduodenal fatty tissue was found frequently.

The pseudocystic lesion of the pancreas showed an

obvious neoplastic proliferation with similar histology seen within the thin neoplastic peripheral rim. This narrow peripheral zone was surrounded by a pseudocapsule, and the vast majority of cells contained within the cyst showed hemorrhagic and necrotic changes (Figure 3B). No extrapancreatic spread or involvement of the regional lymph nodes was found, although focal venous infiltration was observed.

Immunohistochemistry confirmed that both tumors were derived from a similar cell origin. There was a significant cytoplasmic immunoexpression of pan-neuroendocrine markers: chromogranin A occurred more intensely and frequently than synaptophysin (Figure 4A). There was strong somatostatin immunoreactivity in over half of the duodenal tumor cells (Figure 4B) and 70% of the pancreatic tumor cells (Figure 5A), where a small percentage of cells that coexpressed glucagon and pancreatic polypeptide immunoreactivity were also found. Proliferative activity measured using Ki-67 protein labeling indices was approximately 3.5% in both tumors (Figure 5B). The final histopathological diagnosis of somatostatinoma of the duodenum and the pancreas was made in tumor stages pTNP: 2T (T3+T2) N0 Mx LOVI. It was concluded that despite the absence of regional and distant metastases, neither tumor could be categorized as benign, given their histopathological features, size, mitotic counts and proliferative activities.

One and a half years after surgery, the patient is symptom-free, with normal US and scintigraphy of the liver.

DISCUSSION

Somatostatinomas are extremely rare gastrointestinal tumors with an annual incidence of 1 case per 40 million adults^[3]. Two-thirds of somatostatinomas occur within the pancreas, with the duodenum being the next most common site^[9]; although some authors have found equal frequencies^[11]. They can occur at any age (range: 21-91 years)^[1,9], and pancreatic somatostatinomas show a slight female predominance (67%), with extrapancreatic sites being more often present in men^[1]. Forty-five percent of cases exist as part of multiple endocrine neoplasia type I syndrome or von Hippel-Lindau disease^[1] and it is vital to confirm or refute these associated conditions. Duodenal somatostatinomas may be associated with von Recklinghausen's neurofibromatosis^[1,12,13].

Differences exist between the pancreatic and extra-pancreatic types. Duodenal somatostatinomas usually are located in the second part of the duodenum, and most frequently in the ampullary or periampullary regions. Approximately 30% have lymph node or liver secondaries at the time of diagnosis, although these are less frequent when tumors are < 2 cm^[9]. About two-thirds of these tumors contain psammoma bodies within the lumina of their glandular structures, and their biological behavior is similar to that of carcinoid tumors. As a result of their location, patients often present earlier with bile duct obstruction and jaundice, hence the reason for their earlier discovery, earlier surgery, smaller

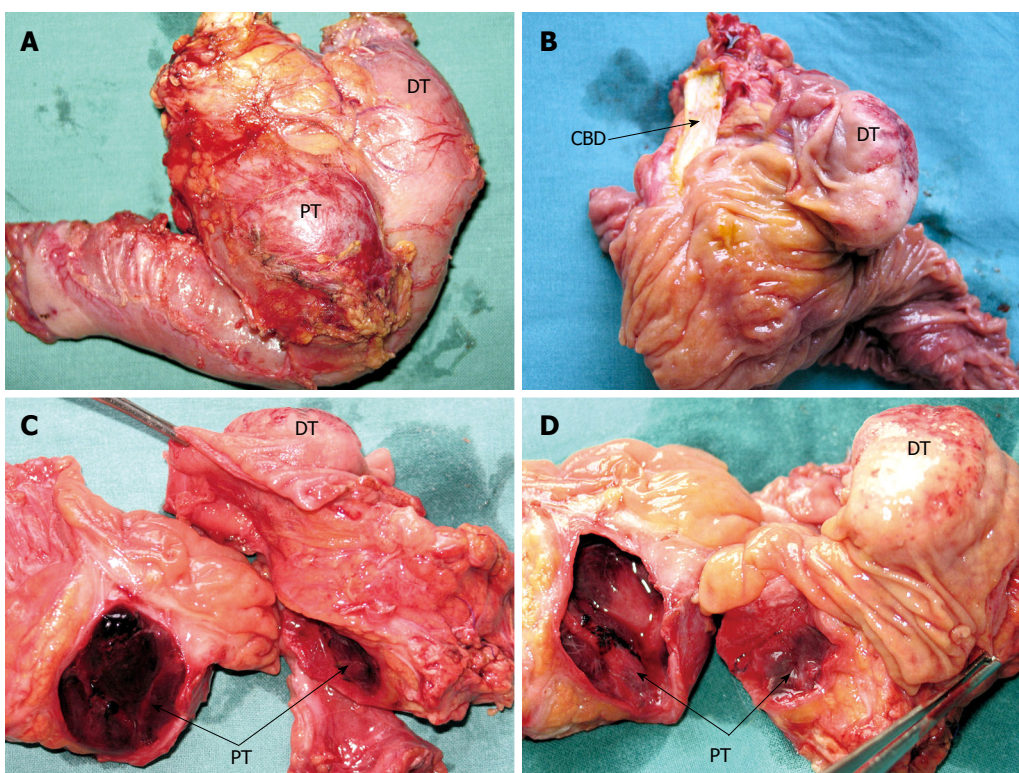


Figure 2 Resected duodenum and pancreatic head specimen containing both tumors. A: Posterior aspect; B: Resected duodenum highlighting the duodenal tumor and common bile duct; C, D: Transected head of the pancreas showing the cystic pancreatic and duodenal tumors. DT: Duodenal tumor; PT: Pancreatic tumor; CBD: Common bile duct.

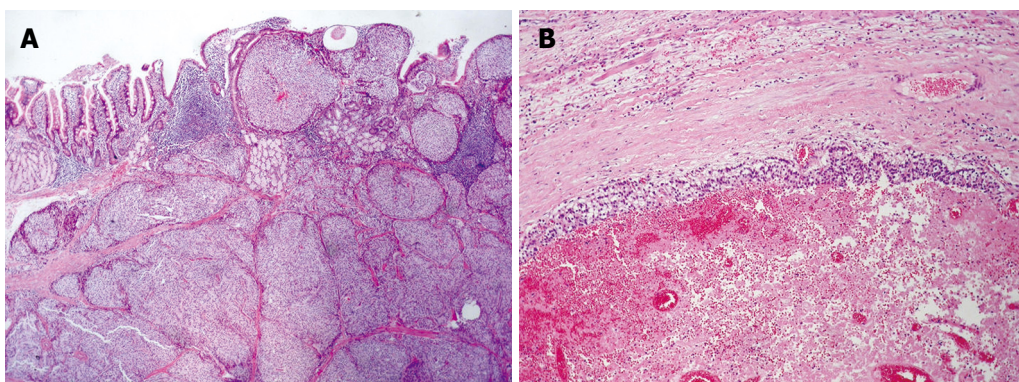


Figure 3 Histopathology. A: Mucosal and submucosal tumor infiltration of the duodenum, revealing an insular growth of rather uniform epithelioid cells (HE, $\times 25$). B: The pancreatic tumor presenting as a hemorrhagic pseudocyst, with a thin peripheral layer of neoplastic proliferation (HE, $\times 56$).

sizes and lower rates of metastasis^[1,2,9].

Almost 60% of pancreatic somatostatinomas are located in the head of the pancreas, and about 30% in the tail^[1]. They usually are larger (mean size: 5-6 cm), and are considered more malignant with a 70% incidence of metastases^[9]. Often the mass effect of the tumor itself leads to its diagnosis^[11].

Although somatostatin is the main secretory product, at least 10% of somatostatinomas produce other hormones, including glucagon, gastrin, vasoactive intestinal peptide (VIP), insulin, calcitonin, and adrenocorticotrophic hormones^[14-16], and the clinical picture may be dominated by the effects of these secreted hormones^[4]. Duodenal somatostatinomas more frequently secrete gastrin, VIP

and calcitonin^[9], while pancreatic somatostatinomas are also more likely to be multihormonal^[11].

Regardless of their plasma somatostatin levels, most patients present with indolent, nonspecific symptoms including vague abdominal pain, weight loss and a change in bowel habits^[1,2]. The classical somatostatinoma or inhibitory syndrome, which includes cholelithiasis, mild diabetes mellitus and steatorrhea with diarrhea, is present in only a small number of patients^[1,4]. The syndrome is the result of the inhibitory effects of somatostatin on endocrine and exocrine secretion, as well as its suppression of stomach and gallbladder motility^[9]. It occurs far less with duodenal than other extrapancreatic somatostatinomas^[1], and this may be due to their earlier

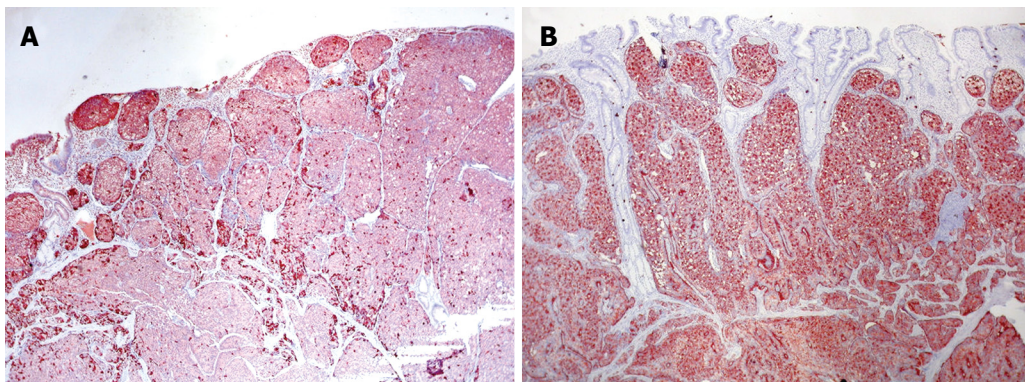


Figure 4 Duodenal tumor cells showing a non-homogeneous immunoreactivity against anti-chromogranin A antibody, but clear diffuse cytoplasmic immunohistochemical reactivity with anti-somatostatin antibody. A: Chromogranin A immunoreactivity, $\times 56$; B: Somatostatin immunoexpression, labeled streptavidin biotin (LSAB) method, aminoethylcarbazole (AEC) visualization, $\times 56$.

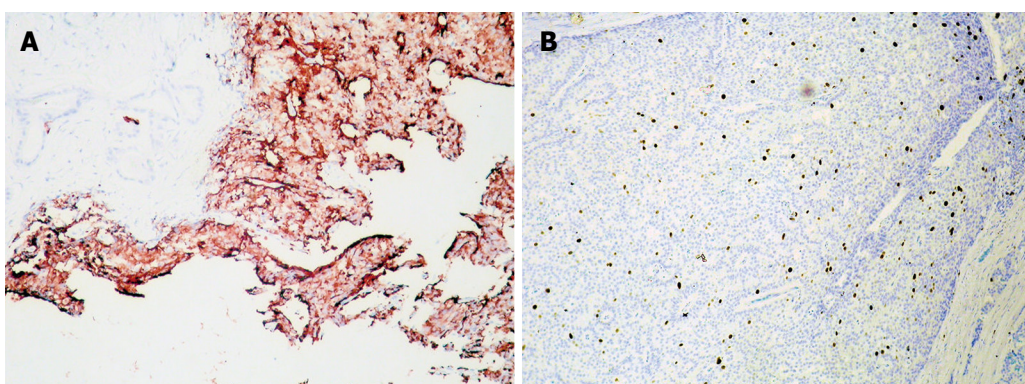


Figure 5 Pancreatic tumor cells showing strong immunoreactivity with anti-somatostatin antibody. A: Somatostatin immunoreactivity, $\times 100$; B: Ki-67 protein immunoexpression, LSAB+ method, AEC visualization, $\times 100$.

diagnosis, release of inactive peptides, or lower secretory activity of the smaller duodenal tumors^[2].

The preoperative diagnosis of somatostatinoma is extremely difficult to establish unless there is a high clinical suspicion based on the patient's symptomatology^[1], although elevated fasting serum levels of somatostatin that cause the somatostatinoma syndrome can be diagnostic, particularly if associated with tumors larger than 4 cm^[1]. CT and magnetic resonance imaging often fail to identify small tumors of the duodenum^[13], and these are often discovered during upper gastrointestinal endoscopy. The diagnosis is then made based upon histological assessment of biopsy specimens during upper gastrointestinal endoscopy^[1,13] or endoscopic US^[17]; with the exact histopathological diagnosis ultimately based on the resected specimen^[1,2]. Once the preoperative diagnosis is established, somatostatin receptor scintigraphy and positron emission tomography can localize accurately the disease^[18], and are particularly useful in identifying occult metastatic spread and recurrent disease^[19]. Scintigraphy positive for metastatic spread can obviate unnecessary surgery^[2]; similarly a negative scan can indicate that curative resection is a possibility^[19].

Surgical resection is the only form of curative treatment^[1] smaller lesions (< 2 cm) by enucleation larger lesions with extensive Whipple's type resections^[20] (due to

their common localization in the head of the pancreas and duodenum), or other similar anastomoses. Unfortunately, in only 60%-70% of surgical cases is the tumor completely resected^[1,3]. Debulking surgery should also be considered in the presence of metastatic secondaries because this may lead to improved survival and quality of life, especially in those with somatostatinoma syndrome^[1,21]. Indeed, palliation for bile duct obstruction, pain or hormonal excess is beneficial in most unresectable cases^[1].

For patients with liver secondaries that are not amenable to resection or ablation, hepatic artery embolization or chemoembolization may be an effective therapy for symptomatic palliation^[22]. Adjuvant chemotherapy is not advocated after complete resection^[1], however, in locally unresectable cases or in metastatic somatostatinoma, chemotherapeutic agents have been used with moderate clinical responses^[1,23].

Somatostatinomas are slow-growing lesions and long-term survival is possible^[11], even with no intervention. Unfavorable prognostic predictors include tumor size > 3 cm, poor cytological differentiation, regional and/or portal vein metastases, a non-functioning tumor, and incomplete surgical resection^[1].

Ultimately, patients with localized disease and a successful resection are the most likely to achieve a cure^[2], however, even in the presence of metastases, the 5-year

survival for patients undergoing surgical resection with adjuvant chemotherapy approaches 40%^[1].

REFERENCES

- 1 **House MG**, Yeo CJ, Schulick RD. Periampullary pancreatic somatostatinoma. *Ann Surg Oncol* 2002; **9**: 869-874
- 2 **Marakis G**, Ballas K, Rafailidis S, Alatsakis M, Patsiaoura K, Sakadamis A. Somatostatin-producing pancreatic endocrine carcinoma presented as relapsing cholangitis -- a case report. *Pancreatology* 2005; **5**: 295-299
- 3 **Choi YS**, Park JK, Lee SH, Yoon WJ, Lee JK, Ryu JK, Kim YT, Yoon YB. [A case of pancreatic somatostatinoma] *Korean J Gastroenterol* 2006; **48**: 351-354
- 4 **Ozbakir O**, Kelestimur F, Ozturk F, Sozuer E, Unal A, Patiroglu TE, Guven K. Carcinoid syndrome due to a malignant somatostatinoma. *Postgrad Med J* 1995; **71**: 695-698
- 5 **Semelka RC**, Custodio CM, Cem Balci N, Woosley JT. Neuroendocrine tumors of the pancreas: spectrum of appearances on MRI. *J Magn Reson Imaging* 2000; **11**: 141-148
- 6 **Roberts L Jr**, Dunnick NR, Foster WL Jr, Halvorsen RA, Gibbons RG, Meyers WC, Feldman JM, Thompson WM. Somatostatinoma of the endocrine pancreas: CT findings. *J Comput Assist Tomogr* 1984; **8**: 1015-1018
- 7 **Larsson LI**, Hirsch MA, Holst JJ, Ingemannson S, Kuhl C, Jensen SL, Lundqvist G, Rehfeld JF, Schwartz TW. Pancreatic somatostatinoma. Clinical features and physiological implications. *Lancet* 1977; **1**: 666-668
- 8 **Kaneko H**, Yanaihara N, Ito S, Kusumoto Y, Fujita T, Ishikawa S, Sumida T, Sekiya M. Somatostatinoma of the duodenum. *Cancer* 1979; **44**: 2273-2279
- 9 **Tanaka S**, Yamasaki S, Matsushita H, Ozawa Y, Kurosaki A, Takeuchi K, Hoshihara Y, Doi T, Watanabe G, Kawaminami K. Duodenal somatostatinoma: a case report and review of 31 cases with special reference to the relationship between tumor size and metastasis. *Pathol Int* 2000; **50**: 146-152
- 10 **Blaser A**, Vajda P, Rosset P. [Duodenal somatostatinomas associated with von Recklinghausen disease] *Schweiz Med Wochenschr* 1998; **128**: 1984-1987
- 11 **Moayedoddin B**, Booya F, Wermers RA, Lloyd RV, Rubin J, Thompson GB, Fatourechi V. Spectrum of malignant somatostatin-producing neuroendocrine tumors. *Endocr Pract* 2006; **12**: 394-400
- 12 **Čolović R**, Micev M, Grubor N, Radak V. [Somatostatinoma of the Vater's papilla in a patient with von Recklinghausen's disease] *Vojnosanit Pregl* 2007; **64**: 219-222
- 13 **Tjon A**, Tham RT, Jansen JB, Falke TH, Lamers CB. Imaging features of somatostatinoma: MR, CT, US, and angiography. *J Comput Assist Tomogr* 1994; **18**: 427-431
- 14 **Konomi K**, Chijiwa K, Katsuta T, Yamaguchi K. Pancreatic somatostatinoma: a case report and review of the literature. *J Surg Oncol* 1990; **43**: 259-265
- 15 **Wynick D**, Williams SJ, Bloom SR. Symptomatic secondary hormone syndromes in patients with established malignant pancreatic endocrine tumors. *N Engl J Med* 1988; **319**: 605-607
- 16 **Anene C**, Thompson JS, Saigh J, Badakhsh S, Ecklund RE. Somatostatinoma: atypical presentation of a rare pancreatic tumor. *Am J Gastroenterol* 1995; **90**: 819-821
- 17 **Guo M**, Lemos LB, Bigler S, Baliga M. Duodenal somatostatinoma of the ampulla of vater diagnosed by endoscopic fine needle aspiration biopsy: a case report. *Acta Cytol* 2001; **45**: 622-626
- 18 **Oberg K**, Eriksson B. Endocrine tumours of the pancreas. *Best Pract Res Clin Gastroenterol* 2005; **19**: 753-781
- 19 **Krausz Y**, Bar-Ziv J, de Jong RB, Ish-Shalom S, Chisin R, Shibley N, Glaser B. Somatostatin-receptor scintigraphy in the management of gastroenteropancreatic tumors. *Am J Gastroenterol* 1998; **93**: 66-70
- 20 **O'Brien TD**, Chejfec G, Prinz RA. Clinical features of duodenal somatostatinomas. *Surgery* 1993; **114**: 1144-1147
- 21 **Green BT**, Rockey DC. Duodenal somatostatinoma presenting with complete somatostatinoma syndrome. *J Clin Gastroenterol* 2001; **33**: 415-417
- 22 **Chamberlain RS**, Canes D, Brown KT, Saltz L, Jarnagin W, Fong Y, Blumgart LH. Hepatic neuroendocrine metastases: does intervention alter outcomes? *J Am Coll Surg* 2000; **190**: 432-445
- 23 **Harris GJ**, Tio F, Cruz AB Jr. Somatostatinoma: a case report and review of the literature. *J Surg Oncol* 1987; **36**: 8-16

S- Editor Tian L **L- Editor** Kerr C **E- Editor** Ma WH



CASE REPORT

Is iron overload in alcohol-related cirrhosis mediated by hepcidin?

Tariq Iqbal, Azzam Diab, Douglas G Ward, Matthew J Brookes, Chris Tselepis, Jim Murray, Elwyn Elias

Tariq Iqbal, Azzam Diab, Elwyn Elias, Department of Gastroenterology, University Hospital Birmingham, Vincent Drive, Birmingham B15 2TH, United Kingdom

Douglas G Ward, Matthew J Brookes, Chris Tselepis, Department of Cancer Studies, University of Birmingham, Vincent Drive, Birmingham B15 2TT, United Kingdom

Jim Murray, Department of Hematology, University Hospital Birmingham, Vincent Drive, Birmingham B15 2TH, United Kingdom

Author contributions: Iqbal T and Tselepis C designed the study and wrote the paper; Diab A collected the patient samples; Ward DG performed the analysis and analyzed the results; Murray J and Elias E provided expertise in hematology and hepatology in the preparation of the manuscript.

Supported by University Hospital Birmingham NHS Foundation Trust

Correspondence to: Dr. Tariq Iqbal, Department of Gastroenterology, University Hospital Birmingham, Vincent Drive, Birmingham B15 2TH, United Kingdom. t.h.iqbal@bham.ac.uk

Telephone: +44-121-4721311

Received: October 12, 2009 **Revised:** November 2, 2009

Accepted: November 9, 2009

Published online: December 14, 2009

Iqbal T, Diab A, Ward DG, Brookes MJ, Tselepis C, Murray J, Elias E. Is iron overload in alcohol-related cirrhosis mediated by hepcidin? *World J Gastroenterol* 2009; 15(46): 5864-5866 Available from: URL: <http://www.wjgnet.com/1007-9327/15/5864.asp> DOI: <http://dx.doi.org/10.3748/wjg.15.5864>

INTRODUCTION

Hepatic iron overload in alcohol related cirrhosis and the detrimental effect of excessive iron on hepatic tissues in this condition is well described^[1]. Previous studies investigating whole-body retention of iron showed a two-fold increase in intestinal iron absorption in chronic alcoholism, and the underlying mechanism has not been identified^[2].

Hepcidin, a 25 amino acid peptide, is the recently described body iron storage regulator. Under physiological conditions, hepcidin expression is stimulated by stored tissue iron, inflammatory stimuli and repressed by anemia and tissue hypoxia^[3]. Recently, interactions between various signals affecting hepcidin production by hepatocytes have been elucidated^[4]. Hepcidin binds to the iron exporter protein ferroportin on the basolateral aspect of macrophages and enterocytes and causes internalization and degradation of this molecule^[5], rendering cells iron-loaded. The two major systemic effects of elevated hepcidin production are therefore reduction of intestinal iron uptake and reticulo-endothelial sequestration of iron.

As the erythron is the main user of iron, its requirement for red cell production is paramount. In the presence of anemia due to ineffective erythropoiesis, animal experiments have shown that an unidentified signal from bone marrow seems able to override the stimulus of elevated body iron stores, repressing hepcidin and allowing duodenal iron absorption to continue even in the presence of elevated iron stores^[6].

Spur cell anemia (SCA) is an interesting clinical condition in which both erythropoiesis and tissue iron stores are altered by excessive alcohol consumption such that sufferers develop severe tissue iron overload and ongoing hemolysis^[7]. The hemolysis is due to structural abnormalities of red cell membranes, resulting in spiculated erythrocytes (acanthocytes) which undergo early splenic destruction^[8]. Treatment of SCA has been disappointing and it is commonly viewed as an indicator of end-stage liver disease^[9].

Abstract

In this case report we describe the relationship between ferritin levels and hepcidin in a patient with alcohol-related spur cell anemia who underwent liver transplantation. We demonstrate a reciprocal relationship between serum or urinary hepcidin and serum ferritin, which indicates that inadequate hepcidin production by the diseased liver is associated with elevated serum ferritin. The ferritin level falls with increasing hepcidin production after transplantation. Neither inflammatory indices (IL6) nor erythropoietin appear to be related to hepcidin expression in this case. We suggest that inappropriately low hepcidin production by the cirrhotic liver may contribute substantially to elevated tissue iron stores in cirrhosis and speculate that hepcidin replacement in these patients may be of therapeutic benefit in the future.

© 2009 The WJG Press and Baishideng. All rights reserved.

Key words: Alcohol; Iron; Anaemia; Hepcidin; Cirrhosis

Peer reviewer: Stefano Bellentani, Professor, Fondo Studio Malattie Fegato-ONLUS, Sezione di Campogalliano, Via R. Luxemburg, 29/N, 41011 Campogalliano, Italy

We postulate that reduced hepcidin production in the cirrhotic liver might be a significant factor contributing to the body iron excess in this patient with end stage alcohol-induced cirrhosis and SCA who underwent orthotopic liver transplantation (OLT).

CASE REPORT

The patient was a 55-year old female with a 10-year history of excessive alcohol consumption who, following hospitalization due to decompensation and alcoholic hepatitis, became abstinent in May 2005. She remained stable until March 2006 when she developed worsening jaundice. Hematological findings indicated that hemolysis was a significant contributory factor in the patient's jaundice. Subsequent investigations confirmed the diagnosis of SCA in the context of cirrhosis. She was referred for transplantation assessment in November 2006. She had an unconjugated hyperbilirubinaemia (230 U/L) and raised reticulocyte count ($125 \times 10^9/\text{L}$). Hepatic synthetic function was relatively preserved with an INR of 1.5 and serum albumin concentration of 38 g/L. A blood film showed many acanthocytes with polychromasia and spherocytes. A transjugular liver biopsy showed micronodular cirrhosis and grade 1 siderosis. Her serum ferritin level at this time was greatly elevated at 600 ng/mL.

The patient decompensated further and was listed for transplantation. The blood film immediately before transplantation showed a predominance of acanthocytes (70%-80% of total red blood cells (RBC), and there was a gradual reduction in acanthocytes over the 48 h following transplantation so that examination of a blood film at 48 h after surgery indicated that acanthocytes made up 50%-60% of total circulating RBCs.

The patient gave consent for blood and urine samples collection for the study (LREC 08/MRE09/2). Samples were taken immediately before and at 12, 36, 48 h and 2 mo after transplantation. Blood was analyzed for ferritin, hemoglobin, erythropoietin, IL-6 and CRP to assess the extent of hemolysis and inflammation. Hepcidin was measured by SELDI-TOF using Cu²⁺ loaded IMAC ProteinChip Arrays and stable isotope labeled hepcidin as an internal standard as previously described^[10] and available via <http://www.hepcidin.bham.ac.uk/>. Urine samples were normalized with respect to protein concentration (20 µg/mL, Bradford assay).

A sample of the explant liver was analyzed for hepcidin mRNA by q-RTPCR and this was compared with samples taken from 8 normal livers.

The hepcidin level in relation to hematological parameters is shown in Table 1. Hepcidin levels before transplantation were very low compared with the elevated ferritin. Following transplantation, hepcidin production rose with falling ferritin. At 2 mo after transplantation, the hepcidin production had fallen in the context of the normal serum ferritin. The urinary hepcidin/ferritin ratio rose progressively following transplantation.

Figure 1 shows that the rise and subsequent fall in urinary hepcidin following transplantation does not seem to be related to erythropoietin production which remains quite stable (except for one dip at 12 h coincident with a

Table 1 Urinary hepcidin levels in relation to haemoglobin and ferritin

Time	Urinary hepcidin (ng/mg)	Ferritin (ng/mL)	Hepcidin/ferritin ratio	Hb (g/dL)
0 h	5	542	0.009	7.0
12 h	8	349	0.023	10.7
36 h	100	404	0.248	9.8
48 h	112	413	0.272	9.3
2 mo	12	81	0.148	14.3

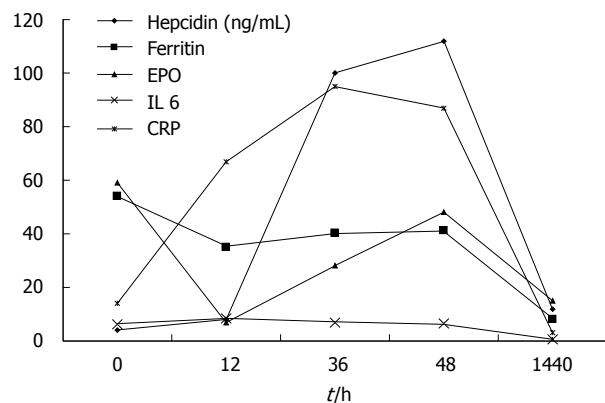


Figure 1 Variation in iron parameters with time.

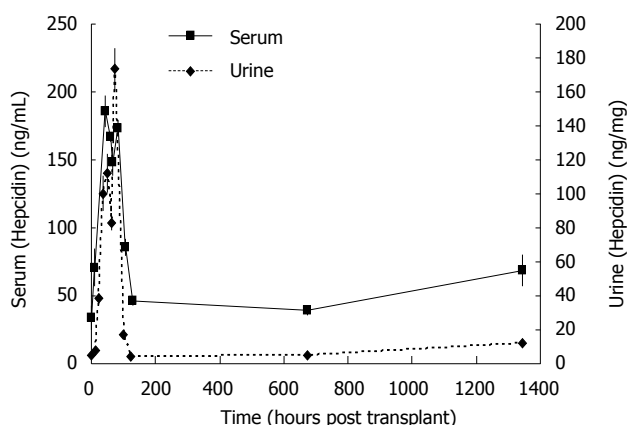


Figure 2 Correlation between urinary and serum ferritin.

two unit peri-operative blood transfusion). Similarly, IL6 levels did not vary greatly. CRP rose as expected in relation to the operation. This rise was not immediately accompanied with the dramatic rise in hepcidin production which was delayed for 12 h. Figure 2 illustrates a close correlation between urinary and serum hepcidin levels in this patient (Pearson correlation coefficient $r = 0.958$).

We compared hepcidin mRNA expression in the explant liver with that in 8 normal livers from transplant donor tissues. Hepcidin mRNA expression in the explant liver from our patient was significantly lower than that in normal liver (data not shown).

DISCUSSION

This case illustrates "inappropriate" low hepcidin production in an iron-over loaded cirrhotic patient with

alcohol-related SCA. Following successful transplantation, hepcidin production by the new liver increased accompanied with falling serum ferritin. "Appropriate" hepcidin production by the new liver would act to sequester iron in reticulo-endothelial stores and to repress duodenal iron uptake. At 2 mo after OLT, both hepcidin and ferritin fell to low levels.

One potential mechanism for pre-operative hepcidin repression would be high circulating erythropoietin level in the hemolyzing patient. Apart from a small reduction in EPO in the peri-operative period which co-incided with a blood transfusion, EPO remained relatively high in the post-operative period consistent with observed persistence of spur cells and the ongoing anemia. This hepcidin expression in the new liver increased progressively. It is likely that hepcidin production in the new liver during the early post-transplantation period remains somewhat muted in relation to the ongoing EPO stimulus.

IL6 stimulates hepcidin production acutely through the STAT pathway. In our patient IL6 was low before transplantation and did not rise in the peri-operative period. CRP did rise in the immediate post-transplantation period as expected. This may have had a bearing on the observed increase in hepcidin as inflammation is a major trigger to hepcidin production.

In our case, although the cirrhosis was undoubtedly alcohol-related, the patient had been abstinent for 2 years. This raises the possibility that, even in the absence of an ongoing stimulus, a persistent hepatic oxidative state, perhaps induced by iron overload, could trigger ongoing repression of hepcidin production. This illustrates potentially differential effects of acute stimulation of hepcidin perhaps *via* the IL6/STAT pathway and chronic repression mediated by oxidative stress^[1].

In summary, the cirrhotic liver in this patient with alcohol-induced spur cell anemia produced very little hepcidin in relation to circulating high ferritin levels and this deficiency was corrected by transplantation.

The mechanisms underlying reduced hepcidin production in this situation, in particular the role of oxidative stress as mediated through CHOP/CEBP, deserve further

studies in the setting of human alcohol-related cirrhosis. The influence of alcoholic cirrhosis on duodenal expression of iron transporter proteins and the influence of local effects related to oxidative stress and external factors such as erythropoiesis on human hepcidin production clearly deserve further prospective examinations.

REFERENCES

- 1 Yip WW, Burt AD. Alcoholic liver disease. *Semin Diagn Pathol* 2006; **23**: 149-160
- 2 Duane P, Raja KB, Simpson RJ, Peters TJ. Intestinal iron absorption in chronic alcoholics. *Alcohol Alcohol* 1992; **27**: 539-544
- 3 Andrews NC. Forging a field: the golden age of iron biology. *Blood* 2008; **112**: 219-230
- 4 De Domenico I, Ward DM, Kaplan J. Hepcidin regulation: ironing out the details. *J Clin Invest* 2007; **117**: 1755-1758
- 5 Nemeth E, Tuttle MS, Powelson J, Vaughn MB, Donovan A, Ward DM, Ganz T, Kaplan J. Hepcidin regulates cellular iron efflux by binding to ferroportin and inducing its internalization. *Science* 2004; **306**: 2090-2093
- 6 Pak M, Lopez MA, Gabayan V, Ganz T, Rivera S. Suppression of hepcidin during anemia requires erythropoietic activity. *Blood* 2006; **108**: 3730-3735
- 7 Chapman RW, Morgan MY, Laulicht M, Hoffbrand AV, Sherlock S. Hepatic iron stores and markers of iron overload in alcoholics and patients with idiopathic hemochromatosis. *Dig Dis Sci* 1982; **27**: 909-916
- 8 Takashimizu S, Shiraishi K, Watanabe N, Numata M, Kawazoe K, Miyachi H, Tokunaga M, Akatuka A, Matsuzaki S. Scanning electron microscopic studies on morphological abnormalities of erythrocytes in alcoholic liver diseases. *Alcohol Clin Exp Res* 2000; **24**: 81S-86S
- 9 Chitale AA, Sterling RK, Post AB, Silver BJ, Mulligan DC, Schulak JA. Resolution of spur cell anemia with liver transplantation: a case report and review of the literature. *Transplantation* 1998; **65**: 993-995
- 10 Kemna EH, Tjalsma H, Podust VN, Swinkels DW. Mass spectrometry-based hepcidin measurements in serum and urine: analytical aspects and clinical implications. *Clin Chem* 2007; **53**: 620-628
- 11 Nishina S, Hino K, Korenaga M, Vecchi C, Pietrangelo A, Mizukami Y, Furutani T, Sakai A, Okuda M, Hidaka I, Okita K, Sakaida I. Hepatitis C virus-induced reactive oxygen species raise hepatic iron level in mice by reducing hepcidin transcription. *Gastroenterology* 2008; **134**: 226-238

S- Editor Tian L L- Editor Ma JY E- Editor Ma WH



CASE REPORT

Neoadjuvant peptide receptor radionuclide therapy for an inoperable neuroendocrine pancreatic tumor

Daniel Kaemmerer, Vikas Prasad, Wolfgang Daffner, Dieter Hörsch, Günter Klöppel, Merten Hommann, Richard P Baum

Daniel Kaemmerer, Wolfgang Daffner, Merten Hommann, Department of General and Visceral Surgery, Zentralklinik Bad Berka, 99437 Bad Berka, Germany

Vikas Prasad, Richard P Baum, Department of Nuclear Medicine, Center for PET, Zentralklinik Bad Berka, 99437 Bad Berka, Germany

Dieter Hörsch, Department of Internal Medicine, Gastroenterology, Endocrinology and Oncology, Zentralklinik Bad Berka, 99437 Bad Berka, Germany

Günter Klöppel, Department of Pathology, University of Kiel, 24105 Kiel, Germany

Author contributions: Kaemmerer D researched the case, analyzed the data and wrote the paper; Prasad V and Baum RP performed the PRRT as neoadjuvant approach; Hommann M, Daffner W and Kaemmerer D accomplished the operation; Klöppel G and Hörsch D investigated the histology and critically revised the paper.

Correspondence to: Dr. Daniel Kaemmerer, Department of General and Visceral Surgery, Zentralklinik Bad Berka, 99437 Bad Berka, Germany. d.kaemmerer.avc@zentralklinik-bad-berka.de

Telephone: +49-364-5852700 Fax: +49-364-5853536

Received: August 26, 2009 Revised: October 26, 2009

Accepted: November 2, 2009

Published online: December 14, 2009

Graduate School of Medicine, University of Tokyo, 7-3-1 Hongo, Bunkyo-ku, Tokyo, 113-8655, Japan

Kaemmerer D, Prasad V, Daffner W, Hörsch D, Klöppel G, Hommann M, Baum RP. Neoadjuvant peptide receptor radionuclide therapy for an inoperable neuroendocrine pancreatic tumor. *World J Gastroenterol* 2009; 15(46): 5867-5870 Available from: URL: <http://www.wjgnet.com/1007-9327/15/5867.asp> DOI: <http://dx.doi.org/10.3748/wjg.15.5867>

INTRODUCTION

Although pancreatic endocrine tumors (pNETs) are rare, they are among the most common neuroendocrine neoplasms of the abdomen^[1]. pNETs account for less than 5% of all primary pancreatic malignancies. They are separated into functional (insulinomas, gastrinomas, glucagonomas, somatostatinomas) and non-functional pNETs. Non-functioning pNETs are pancreatic tumors with endocrine differentiation that lack a clinical syndrome of hormone hypersecretion. Up to 60% of non-functioning endocrine pancreatic tumors are already metastasized at diagnosis. In the advanced stage the pNETs still remains a interdisciplinary challenge. Pancreatic neuroendocrine tumors treatment by chemotherapy and radiation therapy has not demonstrated significant antitumoral effects. Because well differentiated neuroendocrine neoplasms usually express somatostatin receptors, they can be targeted with peptide receptor radionuclide therapy (PRRT) with palliative intention^[2,3]. Several studies showed promising results in patients with advanced neuroendocrine tumors, with a partial response or disease stabilisation in palliative treatment^[3,4]. But surgery still remains the gold standard in the management of pNETs^[5]. Aggressive surgical resection can be performed safely and may improve both symptomatic disease and overall survival^[6]. Prognostic indices such as tumor differentiation and the ability to achieve R0 resection have been linked to survival outcome. Here we describe the treatment of an initially inoperable pNET with peptide receptor radionuclides and show that this neoadjuvant treatment resulted in downstaging of the tumor and curative surgery.

CASE REPORT

A 33-year-old woman was admitted to an external hospital

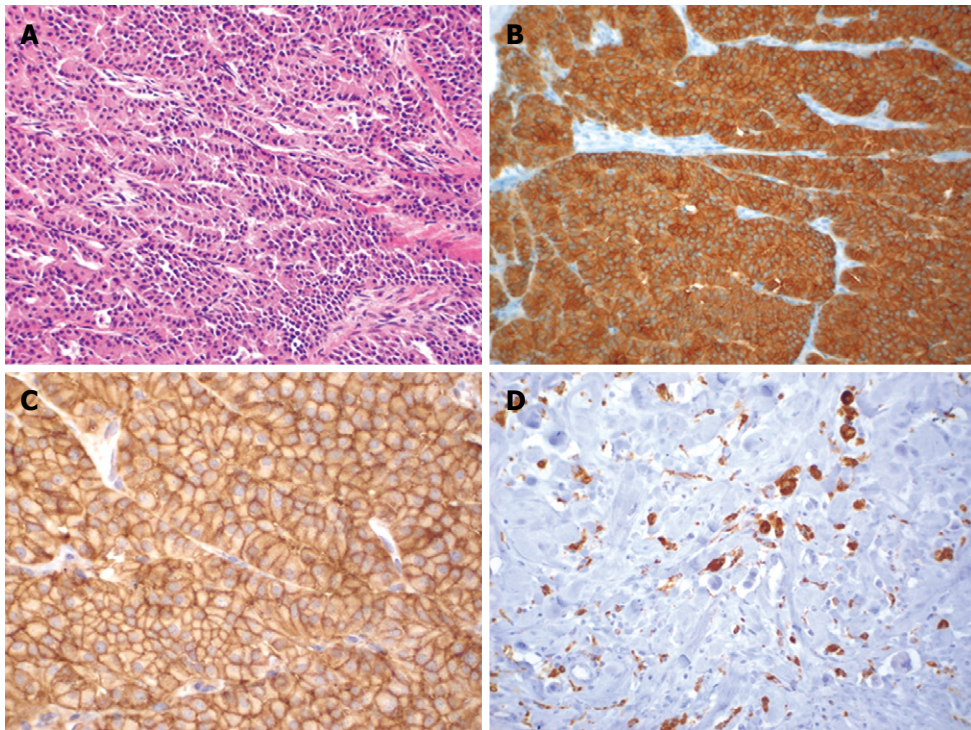
Abstract

Pancreatic endocrine tumors are rare but are among the most common neuroendocrine neoplasms of the abdomen. At diagnosis many of them are already advanced and difficult to treat. We report on an initially inoperable malignant pancreatic endocrine tumor in a 33-year-old woman, who received neoadjuvant peptide receptor radionuclide therapy (PRRT) as first-line treatment. This resulted in a significant downstaging of the tumor and allowed its subsequent complete surgical removal. Follow-up for eighteen months revealed a complete remission. This is the first report on neoadjuvant PRRT in a neuroendocrine neoplasm with subsequent successful complete resection.

© 2009 The WJG Press and Baishideng. All rights reserved.

Key words: Endocrine pancreatic carcinoma; Peptide receptor radionuclide therapy; Neodjuvant treatment; Pancreatic surgery; Molecular imaging; Receptor pancreatic endocrine tumor; Computed tomography

Peer reviewer: Taku Aoki, MD, Division of Hepato-Biliary-Pancreatic and Transplantation Surgery, Department of Surgery,

**Figure 1 Histological images.**

A: Lymph node metastasis of a high differentiated neuroendocrine carcinoma of the pancreas showing a trabecular pattern (HE, $\times 120$); B: The cells are positive for synaptophysin ($\times 120$); C: High membranous expression of somatostatin-receptor SSTR-2 ($\times 120$); D: Macrophages (CD68-positive) as a sign for tumor necrosis after PRRT ($\times 120$).

because of recurrent abdominal pain, flush attacks and diarrhea. CT revealed enlarged paraaortic lymph nodes, but no primary tumor. On exploratory laparotomy a tumor in the head of the pancreas was found and was thought to be a pancreatic ductal adenocarcinoma. This tumor was deemed inoperable because of the involvement of the mesenteric vessels and the paraaortic lymph nodes. Therefore only a lymph node biopsy was obtained. Histological investigation of the biopsy specimen revealed a lymph node metastasis (peripancreatic) of a highly differentiated neuroendocrine carcinoma that stained positive for chromogranin A and synaptophysin (Figure 1A and B). There was no expression of insulin, glucagon, somatostatin, or pancreatic polypeptide. The somatostatin receptor SSTR2 showed distinct membranous expression (Figure 1C). The tumor cells were only supported by small stromal tissue bands. A [^{68}Ga]DOTA-1-Nal 3 -octreotide (NOC) PET/CT was performed to evaluate the somatostatin receptor status. Chromogranin A and serotonin serum levels were normal at all times. Finally, the patient was diagnosed as having a highly differentiated neuroendocrine pancreatic carcinoma, stage IV. Biotherapy with a somatostatin analogue failed. The patient still complained about flushes and diarrhea.

As the patient resolutely refused any chemotherapy, but was willing to undergo radioreceptor therapy, two cycles of PRRT were administered intravenously. The first cycle, administering 6000 MBq (162.1 mCi) [^{90}Y]DOTA-TATE (DOTA-[Tyr 3] octreotate) was given in February 2007 and the second one, injecting 4500 MBq (121.6 mCi), in June 2007. To prevent nephrotoxicity, an amino acid infusion based on the protocol of Jamar *et al* $^{[7]}$ was used. Kidney function was measured by $^{99\text{m}}\text{Tc}$ -DTPA using the single sample plasma clearance method for GFR calculation. $^{99\text{m}}\text{Tc}$ -MAG3 was used for dynamic renal scintigraphy and for determination of

the tubular extraction rate (TER). The blood profile and routine laboratory parameters (electrolytes, liver function tests, creatinine, BUN *etc.*) were checked prior to therapy and then every month.

Mild grade 1 anemia and erythrocytopenia were noted as the only side effects. There was no other hematotoxicity or nephrotoxicity.

After 2 cycles the abdominal lymph node metastases had regressed significantly and PET/CT using [^{68}Ga]DOTA-NOC and ^{18}F -FDG ([^{18}F]fluor-2-deoxy-glucose) performed in October 2007 indicated that the patient was operable. After every PRRT cycle a partial remission (EORTC criteria 1999) was detected (Figure 2B and C).

In November 2007, a pylorus-preserving pancreateo-duodenectomy (Traverso-Longmire) was performed with en bloc resection of parts of the jejunum and its mesenterium and lymph nodes (Figure 3). The operation specimen revealed a tumor in the head of the pancreas that was more than 2 cm in diameter and had metastasized to one mesenteric lymph node. Histologically, the endocrine tumor formed a trabecular pattern. The cell structures were embedded in well developed hyaline connective tissue, some parts of which were myxomatous. In the myxomatous area there were aggregates of CD68 positive macrophages that were occasionally positive for iron (Figure 1D). The tumor tissue infiltrated the surrounding pancreatic and interstitial tissue and also showed perineural infiltration. Immunohistologically, about 5%-10% of the tumor cells expressed glucagon or somatostatin and were negative for insulin, serotonin and pancreatic polypeptide. The somatostatin receptor SSTR2 showed a distinct membranous staining pattern in all tumor cells. The lymph node was filled with tumor tissue. The final stage was ypT2 pN1 pM1(LYM) G3 R0 L0 V0 $^{[8]}$. The patient left the hospital 19 d after the operation. Six, twelve and

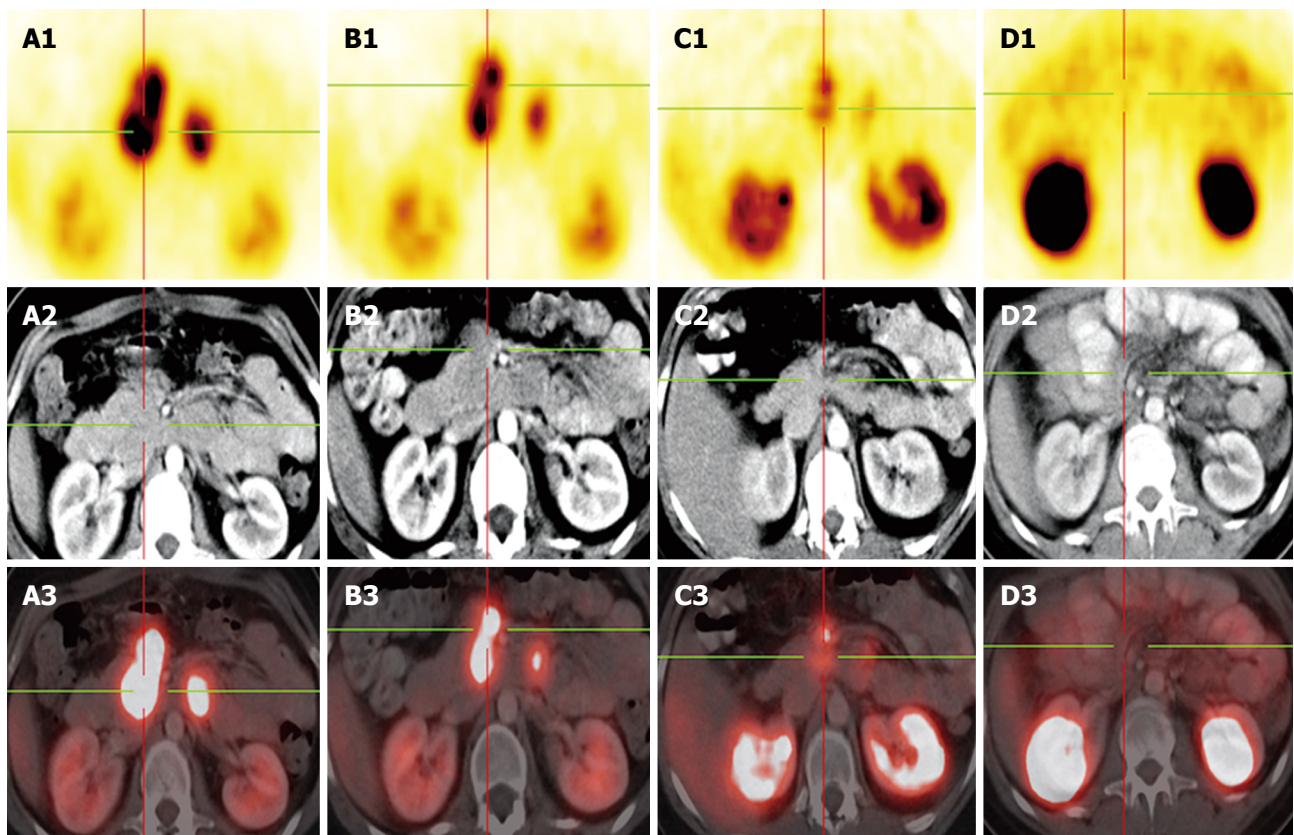


Figure 2 Gallium-68 DOTA-NOC PET-CT in the follow up. A: Octreotide scan prior to PRRT-1, Gallium-68 DOTA NOC PET-CT and prior operation, showing multiple paraaortal lymph nodes next to the pancreas head; B: 3 mo after PRRT-1; C: 5 mo after PRRT-2 showing consistently decreasing mesenteric lymph nodes metastases with a decreasing SUV; D: Octreotide scan as follow up 18 mo after operation-complete remission.

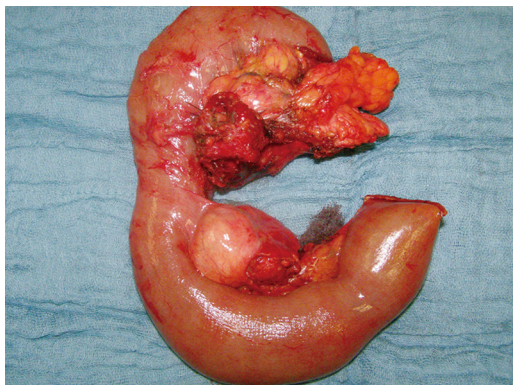


Figure 3 The pancreatic tumor with lymph node metastases (peripancreatic and one distal mesenteric lymph node metastasis) after pylorus-preserving duodenopancreatectomy and mesenteric lymphadenectomy *en bloc*.

eighteen months later a $[^{68}\text{Ga}]$ DOTA NOC PET/CT revealed a complete remission (Figure 2D).

DISCUSSION

Advanced malignant pNETs are difficult to treat^[9,10] and there are only a few studies on the resection of pNETs with extensive local spread. It seems, however, that patients with advanced malignant pNETs benefit from resection, because postoperative actuarial 5-year survival rates of up to 80% have been reported after extended tumor resection, even with synchronous metastasis^[11,12].

Nonetheless, the presence of liver or distant metastases is the prognostic factor determining survival^[13]. In our patient, the diagnosis of a malignant well differentiated pNET was made on a biopsy specimen obtained during an explorative laparotomy. Tumor tissue showed a high expression of the somatostatin receptor SSTR2. Since the patient refused any chemotherapy, treatment with PRRT was performed. In the course of therapy an excellent downstaging of the initially inoperable tumor was reached. The oncology concept was changed from palliative to curative intent considering operability. PRRT is usually used as a palliative treatment^[14]. Currently, there are no reports that deal with the use of radionuclide therapy as a neoadjuvant strategy in oncological surgery. Our case indicates that this therapy may be useful for downstaging and downsizing well differentiated neuroendocrine tumors, thereby achieving a higher operability rate. We recommend first performing $[^{68}\text{Ga}]$ DOTA-NOC PET/CT to evaluate the somatostatin receptor status^[15,16]. If there is high SSTR expression PRRT will be effective^[17]. In addition, staging of the patient after every cycle is required in order to evaluate the response and the operability. The tumor should be downsized to an extent in which a R0-resection should be feasible. In case of a relapse, which is not unlikely^[11], another course of PRRT is again a therapeutic option.

In conclusion, based on the encouraging results obtained in this case we believe that neoadjuvant PRRT is a novel approach in the treatment of surgically unrese-

ctable pNETs in patients with positive somatostatin receptor status.

REFERENCES

- 1 Anlauf M, Sipos B, Kloppel G. [Tumors of the endocrine pancreas] *Pathologe* 2005; **26**: 46-51
- 2 Gulec SA, Baum R. Radio-guided surgery in neuroendocrine tumors. *J Surg Oncol* 2007; **96**: 309-315
- 3 Kwekkeboom DJ, de Herder WW, Kam BL, van Eijck CH, van Essen M, Kooij PP, Feelders RA, van Aken MO, Krenning EP. Treatment with the radiolabeled somatostatin analog [177 Lu-DOTA 0,Tyr3]octreotide: toxicity, efficacy, and survival. *J Clin Oncol* 2008; **26**: 2124-2130
- 4 Muros MA, Varsavsky M, Iglesias Rozas P, Valdivia J, Delgado JR, Forrer F, Bodei L, Paganelli G. Outcome of treating advanced neuroendocrine tumours with radiolabelled somatostatin analogues. *Clin Transl Oncol* 2009; **11**: 48-53
- 5 O'Grady HL, Conlon KC. Pancreatic neuroendocrine tumours. *Eur J Surg Oncol* 2008; **34**: 324-332
- 6 Nomura N, Fujii T, Kanazumi N, Takeda S, Nomoto S, Kasuya H, Sugimoto H, Yamada S, Nakao A. Nonfunctioning neuroendocrine pancreatic tumors: our experience and management. *J Hepatobiliary Pancreat Surg* 2009; **16**: 639-647
- 7 Jamar F, Barone R, Mathieu I, Walrand S, Labar D, Carlier P, de Camps J, Schran H, Chen T, Smith MC, Bouterfa H, Valkema R, Krenning EP, Kvols LK, Pauwels S. 86Y-DOTA0)-D-Phe1-Tyr3-octreotide (SMT487)--a phase 1 clinical study: pharmacokinetics, biodistribution and renal protective effect of different regimens of amino acid co-infusion. *Eur J Nucl Med Mol Imaging* 2003; **30**: 510-518
- 8 Rindi G, Kloppel G, Alhman H, Caplin M, Couvelard A, de Herder WW, Eriksson B, Falchetti A, Falconi M, Komminoth P, Korner M, Lopes JM, McNicol AM, Nilsson O, Perren A, Scarpa A, Scoazec JY, Wiedenmann B. TNM staging of foregut (neuro)endocrine tumors: a consensus proposal including a grading system. *Virchows Arch* 2006; **449**: 395-401
- 9 Dralle H, Krohn SL, Karges W, Boehm BO, Brauckhoff M, Gimm O. Surgery of resectable nonfunctioning neuroendocrine pancreatic tumors. *World J Surg* 2004; **28**: 1248-1260
- 10 Norton JA, Warren RS, Kelly MG, Zuraek MB, Jensen RT. Aggressive surgery for metastatic liver neuroendocrine tumors. *Surgery* 2003; **134**: 1057-1063; discussion 1063-1065
- 11 Norton JA, Kivlen M, Li M, Schneider D, Chuter T, Jensen RT. Morbidity and mortality of aggressive resection in patients with advanced neuroendocrine tumors. *Arch Surg* 2003; **138**: 859-866
- 12 Kazanjian KK, Reber HA, Hines OJ. Resection of pancreatic neuroendocrine tumors: results of 70 cases. *Arch Surg* 2006; **141**: 765-769; discussion 769-770
- 13 Rindi G, D'Adda T, Froio E, Fellegara G, Bordi C. Prognostic factors in gastrointestinal endocrine tumors. *Endocr Pathol* 2007; **18**: 145-149
- 14 Wehrmann C, Senftleben S, Zachert C, Muller D, Baum RP. Results of individual patient dosimetry in peptide receptor radionuclide therapy with 177Lu DOTA-TATE and 177Lu DOTA-NOC. *Cancer Biother Radiopharm* 2007; **22**: 406-416
- 15 Wild D, Schmitt JS, Gijn M, Macke HR, Bernard BF, Krenning E, De Jong M, Wenger S, Reubi JC. DOTA-NOC, a high-affinity ligand of somatostatin receptor subtypes 2, 3 and 5 for labelling with various radiometals. *Eur J Nucl Med Mol Imaging* 2003; **30**: 1338-1347
- 16 Zhernosekov K, Aschoff P, Filosofov D, Jahn M, Jennewein M, Adrian HJ, Bihl H, Rosch F. Visualisation of a somatostatin receptor-expressing tumour with 67Ga-DOTATOC SPECT. *Eur J Nucl Med Mol Imaging* 2005; **32**: 1129
- 17 Baum RP, Prasad V, Hommann M, Horsch D. Receptor PET/CT imaging of neuroendocrine tumors. *Recent Results Cancer Res* 2008; **170**: 225-242

S- Editor Wang JL L- Editor O'Neill M E- Editor Ma WH



Cronkhite-Canada syndrome associated with myelodysplastic syndrome

Rei Suzuki, Atsushi Irisawa, Takuto Hikichi, Yuta Takahashi, Hiroko Kobayashi, Hiromi Kumakawa, Hiromasa Ohira

Rei Suzuki, Atsushi Irisawa, Takuto Hikichi, Hiroko Kobayashi, Hiromasa Ohira, Department of Internal Medicine II, Fukushima Medical University, 1 Hikarigaoka, Fukushima 960-1295, Japan

Yuta Takahashi, Hiromi Kumakawa, Internal Medicine, Soma Public Hospital, 142 Niinuma aza tubogasaku, Soma 976-0011, Japan

Author contributions: Suzuki R and Irisawa A wrote the paper; Suzuki R, Hikichi T, Takahashi Y, and Kumakawa H contributed to this work by direct participation in the work; Irisawa A, Kobayashi H and Ohira H designed, performed the work and revised it critically for important intellectual content.

Correspondence to: Rei Suzuki, MD, Department of Internal Medicine II, Fukushima Medical University, 1 Hikarigaoka, Fukushima 960-1295, Japan. enterotube@hotmail.com

Telephone: +81-24-5471202 **Fax:** +81-24-5472055

Received: September 21, 2009 **Revised:** October 20, 2009

Accepted: October 27, 2009

Published online: December 14, 2009

Suzuki R, Irisawa A, Hikichi T, Takahashi Y, Kobayashi H, Kumakawa H, Ohira H. Cronkhite-Canada syndrome associated with myelodysplastic syndrome. *World J Gastroenterol* 2009; 15(46): 5871-5874 Available from: URL: <http://www.wjgnet.com/1007-9327/15/5871.asp> DOI: <http://dx.doi.org/10.3748/wjg.15.5871>

INTRODUCTION

Cronkhite-Canada syndrome (CCS), first described by Cronkhite and Canada in 1955^[1], is a rare, acquired, nonfamilial syndrome with diffuse gastrointestinal (GI) polyposis, atrophic nail change, alopecia, cutaneous hyperpigmentation, diarrhea, abdominal pain, and other GI complications such as protein-losing enteropathy and malnutrition. Goto^[2] and Takeuchi *et al*^[3] reviewed 278 cases of CCS patients up to 1993 and found that 212 (76.3%) of them were Japanese. Except for cases of anemia caused by malnutrition, CCS with hematologic disorder has not been reported. This report is the first to describe a case of CCS in a patient with myelodysplastic syndrome (MDS).

Abstract

We report a case of Cronkhite-Canada syndrome (CCS) associated with myelodysplastic syndrome (MDS). A 54-year-old woman, diagnosed as MDS the prior year after evaluation of anemia, visited our hospital with the chief complaint of epigastric discomfort. She also had dysgeusia, alopecia, atrophic nail change, and pigmentation of the palm, all of which began several months ago. Blood tests revealed severe hypoalbuminemia. Colonoscopy (CS) showed numerous, dense, red polyps throughout the colon and rectum. Biopsy specimens showed stromal edema, infiltration of lymphocytes, and cystic dilatation of the crypt. Her clinical manifestations and histology were consistent with CCS. We prescribed corticosteroids, which dramatically improved her physical findings, laboratory data, and endoscopic findings. This is the first report of CCS in a patient with MDS.

© 2009 The WJG Press and Baishideng. All rights reserved.

Key words: Cronkhite-Canada syndrome; Myelodysplastic syndrome; Polyposis; Steroid therapy

Peer reviewer: Dr. Luca Morelli, MD, U.O., Anatomia e Istologia Patologica, Ospedale S. Chiara, largo Medaglie d'Oro 9, Trento, 38100, Italy

CASE REPORT

A 54-year-old woman visited our hospital with the chief complaint of epigastric discomfort for a month. She was diagnosed as MDS the prior year after evaluation of anemia following a routine check-up. She also suffered from dysgeusia, alopecia, and pigmentation of the palms several months ago. She and her family had no history of GI disease. Physical examination revealed a partial loss of capillus and supercilia, with blackish brown pigmentation in both palms (Figure 1).

Partial loss of body hair including capillus and supercilia (Figure 1A) with blackish brown pigmentation was found in both palms (Figure 1B). Atrophic nail change was observed later (Figure 1C). Laboratory test showed that her white blood cell (WBC) count was 6400/ μ L (3000-6000), red blood cell (RBC) count was $349 \times 10^6/\mu\text{L}$ (380-500 $\times 10^6$), platelet count was $9.7 \times 10^4/\mu\text{L}$ (12-38 $\times 10^4$), C-reactive protein (CRP) was negative and erythrocyte sedimentation rate (ESR) was 40 mm/1 h, total protein was 5.7 g/dL (6.5-8.0), and serum albumin was 3.2 g/dL

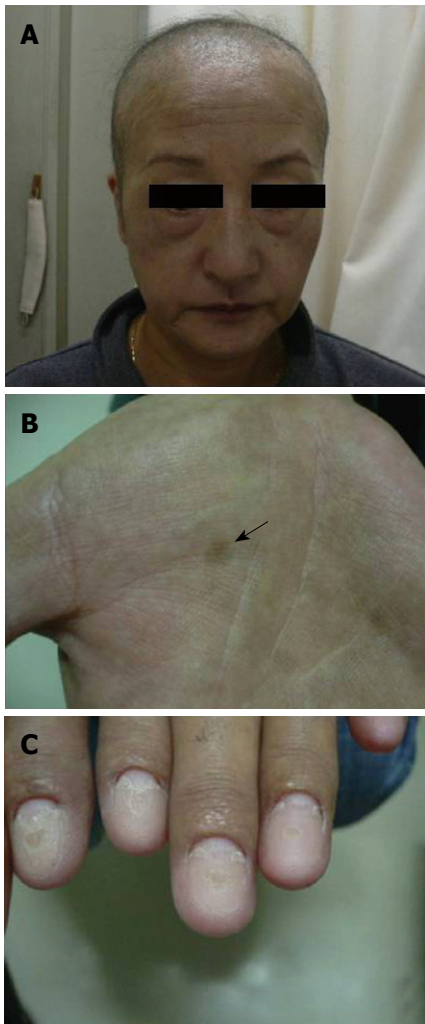


Figure 1 Physical findings in our case at her first visit. A: Partial loss of the capillus and supercilia; B: Blackish brown pigmentation in both palms (black arrow); C: Atrophic nail change.

(4.0–5.0). Esophagogastroduodenoscopy (EGD), performed for further evaluation of the GI tract, revealed red and edematous granular polyps with giant folds, the so-called red-carpet-like polyposis of the stomach (Figure 2). A biopsy specimen displayed proliferation of connective tissue, edema, and infiltration of lymphocytes in the lamina propria. Since these findings could not confirm the diagnosis, we prescribed famotidine (20 mg per day) for nonspecific gastritis. Watery diarrhea gradually worsened, occurring up to 7 times per day at 2 wk after her first visit. Then, alopecia also worsened and atrophic nail change was observed.

Laboratory test displayed not only elevated CRP and ESR, but also hypoalbuminemia (Alb 3.2 g/dL). We suspected protein-losing enteropathy and performed colonoscopy (CS) for differential diagnosis, which showed numerous, dense, red polyps throughout the colon and rectum (Figure 3A). Biopsy specimens from the colon displayed cystic dilation of crypts and edematous stroma with inflammatory cell infiltration (Figure 3B). These physical and endoscopic findings were consistent with CCS, but CS findings did not exclude ulcerative colitis. We added salazosulfapyridine (3 g per day) and probiot-

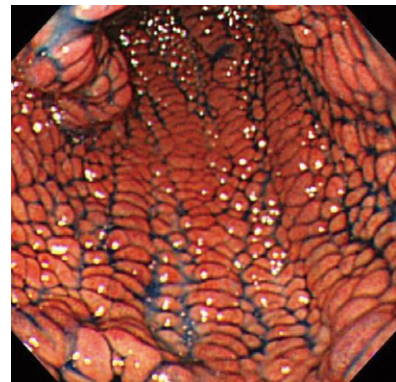


Figure 2 Esophagogastroduodenoscopy. Red and edematous granular polyps with giant folds, the so-called red-carpet-like polyposis of the stomach before treatment.

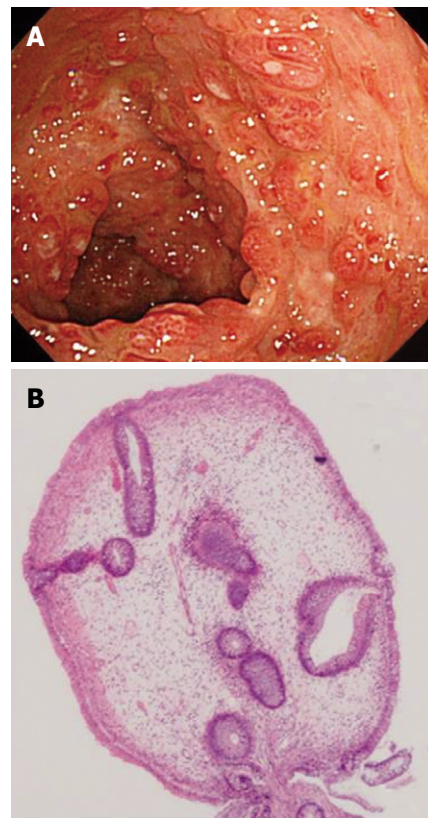


Figure 3 Colonoscopy (CS) findings. A: Numerous, dense, red polyps throughout the colon and rectum; B: Biopsy specimen from colon displaying cystic dilation of crypts and edematous stroma with inflammatory cell infiltration before treatment (HE, $\times 100$).

ics for diagnostic therapy. Diarrhea and alopecia were gradually relieved, but hypoalbuminemia increased to 1.8 g/dL. Three months after salazosulfapyridine treatment, we started corticosteroid therapy with intravenous prednisolone (40 mg per day) and then exchanged salazosulfapyridine to mesalazine (1500 mg per day). We tapered the dosage of prednisolone at two-week intervals in consideration of the clinical and laboratory changes in our patient. Diarrhea gradually became solid and the serum albumin level increased steadily to 2.5 g/dL one month later. At three months after treatment, we tapered prednisolone to 2.5 mg/d. Her clinical manifestations were



Figure 4 Clinical manifestations of the patient after treatment.

dramatically relieved (Figure 4). The CS findings were relieved and no neoplastic change was observed (Figure 5). The clinical course of this patient is depicted in Figure 6.

DISCUSSION

CCS, first described by Cronkhite and Canada in 1955^[1], is a rare, acquired, nonfamilial syndrome with diffuse GI polyposis, atrophic nail change, alopecia, and cutaneous hyperpigmentation. Its etiology is apparently associated with the ectoderm abnormality^[2,3].

Therapeutic options comprise nutrition support, steroid therapy^[4-6], antiplasmin therapy^[4,7], mesalazine^[8] and surgery^[9]. Numerous cases for which corticosteroid treatment was effective have been reported, but corticosteroid therapy is regarded as a first-line therapy. In this case, although an insufficient effect of salazosulfapyridine and antiplasmin agents was observed, steroid therapy was also found to have dramatic effects.

The etiology of CCS remains unknown. Infection, mental stress, concomitant neoplasm, and immune abnormalities are regarded as triggering factors for CCS^[3,10]. In addition, MDS has a high incidence (10%-20%) ac-

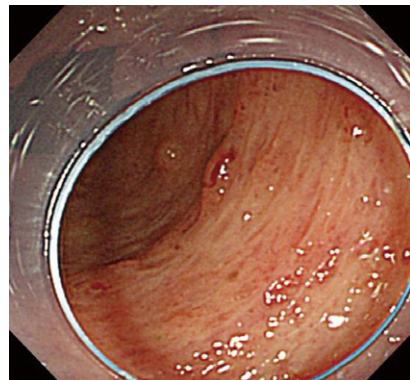


Figure 5 CS image after treatment.

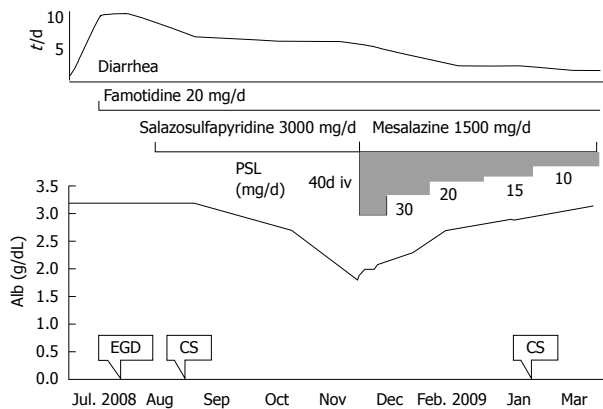


Figure 6 Clinical course of the patient.

companying autoimmune diseases, such as systemic lupus erythematosus and aortitis^[11-13]. It is particularly interesting that GI autoimmune diseases, such as inflammatory bowel disease (IBD) and Behcet's disease, are also reported in patients with MDS. The etiology is considered to be an imbalance of various cytokines attributable to the abnormal level of multipotent stem cells. Reportedly, up-regulation of cytokines, such as TGF- β , TGF- β receptor, IL-6, and IL-7 receptors mapped to chromosome 8, related to inflammation and cell proliferation, plays an important role in the pathogenesis of patients having Behcet's disease with MDS and trisomy^[14-16].

This case was consistent with CCS, considering its typical clinical manifestations and histology. We infer the possibility that cytokine abnormalities induced by earlier MDS may have caused CCS in this case. However, the karyotype was not trisomy 8, 46, XX, or i(7) (q10). Moreover, inflammatory cytokine levels (IFN γ , IL-6, IL-10, TNF- α) were within normal limits. These results suggest that the etiology of this case is not associated with cytokine imbalance, as reported for Behcet's disease with MDS of trisomy 8.

In conclusion, we report a case of CCS in a patient with MDS. Although the association of CCS and MDS in this case remains uncertain, clarification of the CCS etiology is possible through accumulation of similar cases and results of further studies of the pathogenesis of MDS associated with autoimmune disease.

REFERENCES

- 1 Cronkhite LW Jr, Canada WJ. Generalized gastrointestinal polyposis; an unusual syndrome of polyposis, pigmentation, alopecia and onychotrophia. *N Engl J Med* 1955; **252**: 1011-1015
- 2 Goto A. Cronkhite-Canada syndrome: epidemiological study of 110 cases reported in Japan. *Nippon Geka Hokan* 1995; **64**: 3-14
- 3 Takeuchi Y, Yoshikawa M, Tsukamoto N, Shiroi A, Hoshida Y, Enomoto Y, Kimura T, Yamamoto K, Shiiki H, Kikuchi E, Fukui H. Cronkhite-Canada syndrome with colon cancer, portal thrombosis, high titer of antinuclear antibodies, and membranous glomerulonephritis. *J Gastroenterol* 2003; **38**: 791-795
- 4 Yamashita T, Miyazawa M, Suzuki H. A case of Cronkhite-Canada syndrome improved markedly with antiplasmin agent and steroid (In Japanese, Abstract in English). *Gastroenterol Endosc* 1996; **38**: 45-50
- 5 Futagami K, Tanaka S, Haruma K, Yoshihara M, Sumii K, Kajiyama G. Five cases of Cronkhite-Canada syndrome treated by steroid pulse therapy (In Japanese, Abstract in English). *Digestion and Absorption* 1998; **21**: 151-154
- 6 Koishi T. A case of Cronkhite-Canada syndrome (In Japanese). *Nippon Naika Gakkai Zasshi* (J Jpn Soc Int Med) 1976; **65**: 1060
- 7 Goto A. Cronkhite-Canada syndrome: observations about treatment course and prognosis of 123 cases reported in Japan (In Japanese). *Nippon Geka Hokan* (Arch Jpn Chir) 1988; **57**: 427-433
- 8 Takakura M, Adachi H, Tsuchihashi N, Miyazaki E, Yoshioka Y, Yoshida K, Oryo F, Sawada T. A Case of Cronkhite-Canada Syndrome markedly improved with mesalazine therapy. *Digestive Endoscopy* 2004; **16**: 74-78
- 9 Kabeshima Y, Izawa N, Yano K, Toizumi A, Tamura Y, Kageyama T, Kaneko K. A case report of Cronkhite-Canada syndrome successfully remitted by surgical treatment (In Japanese). *Jpn J Gastroenterol Surg* 2007; **40**: 227-232
- 10 Hirasaki S, Tanimizu M, Moriwaki T, Kajihara T, Nishina T, Hyoudou K. A case of Cronkhite-Canada syndrome associated with cholangiocellular carcinoma (In Japanese). *Nippon Shokakibyo Gakkai Zasshi* 2005; **102**: 583-588
- 11 Funato K, Kuriyama Y, Uchida Y, Suzuki A, Miyazawa K, Ohyashiki K. Myelodysplastic syndrome accompanied by Addison's disease and multiple autoimmune phenomena: steroid therapy resolved cytopenias and all immune disorders. *Intern Med* 2001; **40**: 1041-1044
- 12 Lopez FF, Vaidyan PB, Mega AE, Schiffman FJ. Aortitis as a manifestation of myelodysplastic syndrome. *Postgrad Med J* 2001; **77**: 116-118
- 13 Giannouli S, Voulgarelis M, Zintzaras E, Tzioufas AG, Moutsopoulos HM. Autoimmune phenomena in myelodysplastic syndromes: a 4-yr prospective study. *Rheumatology* (Oxford) 2004; **43**: 626-632
- 14 Tsubata R, Suzuki F, Sugihara T, Ogawa J, Hagiwara H, Nanki T, Kohsaka H, Kubota T, Miyasaka N. [An autopsy case of intestinal Behcet's disease with sacroiliitis accompanied by myelodysplastic syndrome with trisomy 8.] *Nihon Rinsho Meneki Gakkai Kaishi* 2005; **28**: 48-55
- 15 Hasegawa H, Iwamasa K, Hatta N, Fujita S. Behcet's disease associated with myelodysplastic syndrome with elevated levels of inflammatory cytokines. *Mod Rheumatol* 2003; **13**: 350-355
- 16 Adachi Y, Tsutsumi A, Murata H, Takemura H, Chino Y, Takahashi R, Ebisuka T, Sumida T. Behcet's disease accompanied by myelodysplastic syndrome with trisomy 8: two case reports and a review of 15 Japanese cases. *Mod Rheumatol* 2003; **13**: 90-94

S- Editor Tian L L- Editor Wang XL E- Editor Lin YP



Spontaneous liver rupture in hypereosinophilic syndrome: A rare but fatal complication

Yue-Sun Cheung, Shun Wong, Philip Koon-Ngai Lam, Kit-Fai Lee, John Wong, Paul Bo-San Lai

Yue-Sun Cheung, Kit-Fai Lee, John Wong, Paul Bo-San Lai,
Department of Surgery, Prince of Wales Hospital, The Chinese University of Hong Kong, Hong Kong, China

Shun Wong, Department of Pathology, Princess Margaret Hospital, Hong Kong, China

Philip Koon-Ngai Lam, Department of Anesthesia and Intensive Care, Prince of Wales Hospital, The Chinese University of Hong Kong, Hong Kong, China

Author contributions: Cheung YS, Lam PKN, Lee KF and Lai PBS designed the work; Cheung YS, Wong S, Lam PKN, Lee KF and Wong J performed the work; Cheung YS, Wong S, Lee KF and Wong J wrote the paper.

Correspondence to: Paul Bo-San Lai, Professor, Department of Surgery, Prince of Wales Hospital, The Chinese University of Hong Kong, Shatin, New Territories, Hong Kong, China. paullai@surgery.cuhk.edu.hk

Telephone: +852-26321411 Fax: +852-26377974

Received: August 16, 2009 Revised: October 1, 2009

Accepted: October 9, 2009

Published online: December 14, 2009

Cheung YS, Wong S, Lam PKN, Lee KF, Wong J, Lai PBS. Spontaneous liver rupture in hypereosinophilic syndrome: A rare but fatal complication. *World J Gastroenterol* 2009; 15(46): 5875-5878 Available from: URL: <http://www.wjgnet.com/1007-9327/15/5875.asp> DOI: <http://dx.doi.org/10.3748/wjg.15.5875>

INTRODUCTION

Spontaneous intrahepatic hemorrhage and liver rupture usually occur in patients with underlying hepatocellular carcinoma or adenoma^[1,2]. This has also been described in patients with HELLP syndrome, Ehlers Danlos disease and graft-vs-host disease^[3-6]. In this report, we described a rare case of spontaneous liver rupture in a patient with hypereosinophilic syndrome (HES), of which the diagnosis was delayed, resulting in a fatal outcome.

CASE REPORT

A 48-year-old man with good past health was admitted because of fever associated with flu-like symptoms and left loin pain for a few days. Initial physical examination showed mild suprapubic and left loin tenderness, and urine dipsticks revealed microscopic haematuria. The chest radiograph was normal and initial blood tests showed eosinophilia and mildly deranged liver function (Table 1). The patient had no clinical signs of allergic reaction. Ultrasound examination of the abdomen revealed no abnormality in the hepatobiliary and urinary system. Urine microscopy showed microscopic haematuria. Ova or parasites were not detected in stool samples. The cultures from blood, sputum and urine were all negative.

Five days after admission, while awaiting further investigations, the patient suddenly developed hypovolemic shock. He rapidly deteriorated to pulseless electrical activity. Cardiopulmonary resuscitation was initiated immediately. He was pale and his abdomen was distended. His pulse returned after resuscitation with 2 L gelofusine. His hemoglobin level dropped from 14.5 to 5 g/dL. In addition, ultrasound examination of the abdomen confirmed the presence of free intraperitoneal fluid. The patient was given six units of unmatched blood during resuscitation. Owing to the unstable hemodynamic state and the diagnosis of exsanguinating intra-abdominal pathology, emergency laparotomy was arranged.

Abstract

We report a rare case of spontaneous liver rupture in a patient with hypereosinophilic syndrome (HES), of which the diagnosis was delayed, resulting in a fatal outcome. The diagnostic criteria and treatment of HES with hepatic involvement were reviewed. The possible cause of spontaneous liver rupture in HES and its management were also discussed. To our knowledge, this is the first case report of spontaneous liver rupture in HES. We emphasized the need of a high index of suspicion in diagnosing HES, so that early treatment could be initiated.

© 2009 The WJG Press and Baishideng. All rights reserved.

Key words: Hypereosinophilic syndrome; Eosinophilia; Hemoperitoneum; Complication; Spontaneous liver rupture

Peer reviewers: Dr. Bijan Eghtesad, Associate Professor, Department of General Surgery, Cleveland Clinic Foundation, 9500 Euclid Avenue, Cleveland, OH 44195, United States; Salvatore Gruttadauria, MD, Assistant Professor, Abdominal Transplant Surgery, ISMETT, Via E. Tricomi, 190127 Palermo, Italy; Tadatoshi Takayama, Professor, Department of Digestive Surgery, Nihon University School of Medicine, 30-1 Oyaguchi-kamimachi, Itabashi-ku, Tokyo 173-8610, Japan

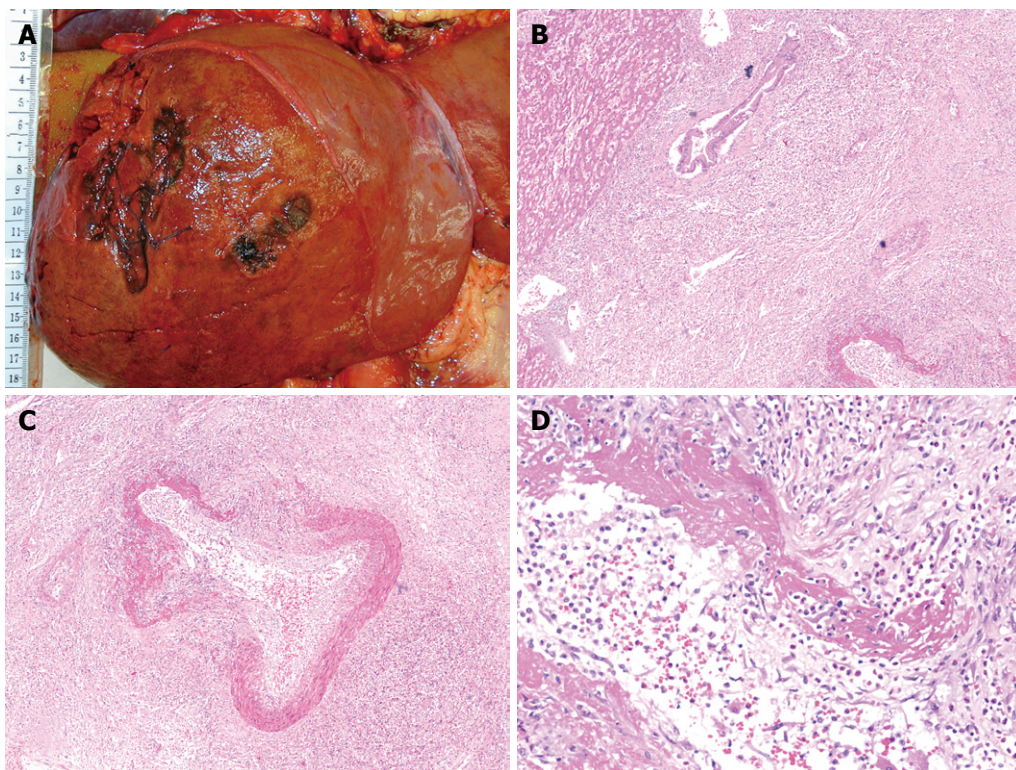


Figure 1 Post-mortem examination of liver. A: The ruptured site over the right lobe of liver; B: Expanded portal tracts with fibrosis and inflammation (microscopy, HE stain, 100 × magnification); C: Hepatic artery with fibrinoid necrosis (microscopy, HE stain, 200 × magnification); D: Eosinophilic infiltration of the hepatic artery (microscopy, HE stain, 400 × magnification).

Table 1 Blood tests on admission

Blood test	Value	Unit
WBC	22.6 ¹	10 ⁹ /L
Eosinophil	6.6 ¹	10 ⁹ /L
Haemoglobin	13.9	g/dL
Platelet	179	10 ⁹ /L
PT	12.9	s
INR	1.33	
APTT	38.7	s
Na	133	mmol/L
K	3.7	mmol/L
Urea	3.6	mmol/L
Creatinine	68	umol/L
Protein	74	g/L
Albumin	34	g/L
Bilirubin	25 ¹	umol/L
ALP	207 ¹	IU/L
ALT	55	IU/L
GGT	504 ¹	U/L
CRP	190.1 ¹	mg/L

¹Elevated values.

On laparotomy, 4 L of blood in the peritoneal cavity and a 10 cm ruptured subcapsular haematoma at anterior sector of right lobe with capsular tear were found. Active bleeding was found at a 9 cm laceration of 5 cm deep at segment VI/VII of the liver (Figure 1A). The liver was not cirrhotic with no palpable space occupying lesion. No abnormality and retroperitoneal haematoma were detected in other intra-abdominal organs. Hemostasis was attempted by suturing the liver laceration and packing. Bleeding from

the raw surface was coagulated with a TissueLink device (TissueLink Medical Inc, Dover, U.S.). However, the patient developed coagulopathy with diffuse oozing after massive transfusion with blood products (10 units of platelet concentrates, 16 units of fresh frozen plasma, and 16 units of pack cells). He required high dose trabecular support during operation. Perihepatic packing was performed and the abdomen was closed. He finally succumbed 1 h after the operation at the intensive care unit.

Post-mortem examination of the patient confirmed the diagnosis of HES with diffuse eosinophilic infiltration to the heart, liver, pancreas, mesentery, kidneys and urinary bladder. Microscopic examination of the liver showed marked eosinophilic expansion in the portal tracts and dilated sinusoids. The portal tract hepatic arteries showed fibrinoid necrosis with eosinophilic infiltration (Figure 1A-D). The lacerated areas showed extensive tissue necrosis and eosinophilic infiltration.

DISCUSSION

Eosinophilia, defined as an increased eosinophil count in peripheral blood and accumulation in various tissues^[7], can be caused by atopic disease, hypersensitivity reaction, parasitic infection, vasculitis and hematological disorders. It is also found in uncommon conditions, such as eosinophilic gastrointestinal disease, Churg-Strauss syndrome and HES^[8]. The diagnostic criteria for HES, first described by Chusid *et al*^[9] in 1975, include persistent peripheral blood eosinophilia for more than 6 mo with an absolute

eosinophil count greater than 1500 cells/ μL , the presence of organ involvement by eosinophilic infiltration, and exclusion of secondary causes of eosinophilia^[8].

The common organ systems involved in HES are hematologic (100%), cardiovascular (58%), cutaneous (56%), neurologic (54%) and pulmonary (49%) systems^[8]. Liver and gastrointestinal tract are involved in only 20%-30% of patients. Patients with hepatic involvement may develop chronic active hepatitis-like picture and some may suffer from Budd-Chiari syndrome secondary to strictures in inferior vena cava or hepatic veins as a result of eosinophilic infiltration^[10]. Spontaneous rupture of bladder and esophagus due to eosinophilic infiltration has been reported in the literature^[11,12]. To our knowledge, this is the first case report of spontaneous liver rupture in HES.

Patients with HES usually present with vague symptoms^[8], making its diagnosis difficult and delayed. In our case, the patient presented with fever and flu-like symptoms, which were not specific of any disease. Although his liver function was mildly deranged, the normal initial sonographic appearance of the hepatobiliary system gave further misleading reassurance to the clinicians in identifying the hepatic involvement. Without a high index of suspicion, it was difficult to diagnose HES early and to start treatment before the catastrophic event in our case, namely liver rupture and subsequent mortality.

In order to avoid end organ damage by HES, it is important to establish the diagnosis and start treatment accordingly. Secondary causes of eosinophilia, such as atopic disease, hypersensitivity reaction or parasitic infestation, should be excluded. For patients with deranged liver function, non-invasive investigations including ultrasound of the liver and biliary system and hepatitis serology should be performed to exclude common disorders of the hepatobiliary system. In patients suspicious of HES with hepatic involvement, liver biopsy can be performed to demonstrate eosinophilic infiltration of the liver^[13,14]. After the diagnosis of HES is confirmed, specific tests on Fip1-like-1 and platelet-derived growth factor receptor α (FIP1L1-PDGFR α) fusion gene mutation can guide further treatment using targeted therapy^[8].

Successful treatment using corticosteroids has been reported in patients with hepatic HES^[13,14]. Studies also showed that patients with HES have a good response to targeted therapy according to the result of FIP1L1-PDGFR α ^[15,16]. HES patients showing positive FIP1L1-PDGFR α have a good response to imatinib mesylate, resulting in a normal eosinophil count^[15]. For patients with negative FIP1L1-PDGFR α , mepolizumab (an anti-interleukin 5 antibody) can effectively stabilize the eosinophil count and reduce the daily steroid dose to less than approximately 7.5 mg prednisolone^[16].

The present case of liver rupture was likely caused by eosinophilic infiltration and fibrinoid necrosis of the vascular wall, leading to rupture of hepatic arteries as demonstrated in Figure 1B-D. Although reports are available on cardiopulmonary resuscitation (CPR)-related major liver injury^[16], this was unlikely in our case because

the event of deterioration occurred abruptly before the initiation of CPR. The right posterolateral located liver laceration in the absence of ribs fractures further made traumatic cause of the liver rupture unlikely. CPR-related liver trauma usually occurs in the left lobe where it is anatomically close to the point of chest compression^[17].

Management and prognosis of spontaneous liver rupture heavily depend on its severity and the hemodynamic stability of patients. For stable patients, non-operative management with transfusion or transarterial selective embolization of the feeding artery has been described with promising results^[1,4]. For patients with hemodynamic instability or failure in non-operative treatments, surgery for haemostasis is recommended as in our case. Hemostasis can be achieved by temporary tamponade of the liver using packs and portal triad occlusion (Pringle manoeuvre)^[18]. After initial operative resuscitation and identification of the site of bleeding, different surgical techniques, including direct suture ligation, hepatic resection, selective hepatic artery ligation and perihepatic packing, can be employed for hemostasis depending on the case scenario^[17]. Despite all these methods, if patients develop coagulopathy, acidosis and multi-organ failure, the chance of survival is low.

Although the clinical course of HES is highly variable and dependent on the degree of organ involvement, early diagnosis and initiation of treatment are of paramount importance. Delay in diagnosis may lead to catastrophic complications. A high index of suspicion is crucial in the management of patients with eosinophilia.

REFERENCES

- 1 Leung KL, Lau WY, Lai PB, Yiu RY, Meng WC, Leow CK. Spontaneous rupture of hepatocellular carcinoma: conservative management and selective intervention. *Arch Surg* 1999; **134**: 1103-1107
- 2 Erdogan D, Busch OR, van Delden OM, Ten Kate FJ, Gouma DJ, van Gulik TM. Management of spontaneous haemorrhage and rupture of hepatocellular adenomas. A single centre experience. *Liver Int* 2006; **26**: 433-438
- 3 Sheikh RA, Yasmeen S, Pauly MP, Riegler JL. Spontaneous intrahepatic hemorrhage and hepatic rupture in the HELLP syndrome: four cases and a review. *J Clin Gastroenterol* 1999; **28**: 323-328
- 4 Wicke C, Pereira PL, Neeser E, Flesch I, Rodegerdts EA, Becker HD. Subcapsular liver hematoma in HELLP syndrome: Evaluation of diagnostic and therapeutic options—a unicenter study. *Am J Obstet Gynecol* 2004; **190**: 106-112
- 5 Gelbmann CM, Kölninger M, Gmeinwieser J, Leser HG, Holstege A, Schölmerich J. Spontaneous rupture of liver in a patient with Ehlers Danlos disease type IV. *Dig Dis Sci* 1997; **42**: 1724-1730
- 6 Barnett SJ, Weisdorf-Schindle S, Baker KS, Saltzman DA. Spontaneous liver rupture in a child with graft-versus-host disease. *J Pediatr Surg* 2004; **39**: e1-e3
- 7 Sade K, Mysels A, Levo Y, Kivity S. Eosinophilia: A study of 100 hospitalized patients. *Eur J Intern Med* 2007; **18**: 196-201
- 8 Sheikh J, Weller PF. Clinical overview of hypereosinophilic syndromes. *Immunol Allergy Clin North Am* 2007; **27**: 333-355
- 9 Chusid MJ, Dale DC, West BC, Wolff SM. The hypereosinophilic syndrome: analysis of fourteen cases with review of the literature. *Medicine (Baltimore)* 1975; **54**: 1-27
- 10 Inoue A, Michitaka K, Shigematsu S, Konishi I, Hirooka M, Hiasa Y, Matsui H, Matsuura B, Horiiike N, Hato T,

- Miyaoka H, Onji M. Budd-Chiari syndrome associated with hypereosinophilic syndrome; a case report. *Intern Med* 2007; **46**: 1095-1100
- 11 **Hwang EC**, Kwon DD, Kim CJ, Kang TW, Park K, Ryu SB, Ma JS. Eosinophilic cystitis causing spontaneous rupture of the urinary bladder in a child. *Int J Urol* 2006; **13**: 449-450
- 12 **Cohen MS**, Kaufman A, DiMarino AJ Jr, Cohen S. Eosinophilic esophagitis presenting as spontaneous esophageal rupture (Boerhaave's syndrome). *Clin Gastroenterol Hepatol* 2007; **5**: A24
- 13 **Dillon JF**, Finlayson ND. Idiopathic hypereosinophilic syndrome presenting as intrahepatic cholestatic jaundice. *Am J Gastroenterol* 1994; **89**: 1254-1255
- 14 **Ung KA**, Remotti H, Olsson R. Eosinophilic hepatic necrosis in hypereosinophilic syndrome. *J Clin Gastroenterol* 2000; **31**: 323-327
- 15 **Baccarani M**, Cilloni D, Rondoni M, Ottaviani E, Messa F, Merante S, Tiribelli M, Buccisano F, Testoni N, Gottardi E, de Vivo A, Giugliano E, Iacobucci I, Paolini S, Soverini S, Rosti G, Rancati F, Astolfi C, Pane F, Saglio G, Martinelli G. The efficacy of imatinib mesylate in patients with FIP1L1-PDGFRalpha-positive hypereosinophilic syndrome. Results of a multicenter prospective study. *Haematologica* 2007; **92**: 1173-1179
- 16 **Rothenberg ME**, Klion AD, Roufosse FE, Kahn JE, Weller PF, Simon HU, Schwartz LB, Rosenwasser LJ, Ring J, Griffin EF, Haig AE, Frewer PI, Parkin JM, Gleich GJ. Treatment of patients with the hypereosinophilic syndrome with mepolizumab. *N Engl J Med* 2008; **358**: 1215-1228
- 17 **Meron G**, Kurkciyan I, Sterz F, Susani M, Domanovits H, Tobler K, Bohdjalian A, Laggner AN. Cardiopulmonary resuscitation-associated major liver injury. *Resuscitation* 2007; **75**: 445-453
- 18 **Parks RW**, Chrysos E, Diamond T. Management of liver trauma. *Br J Surg* 1999; **86**: 1121-1135

S- Editor Tian L **L- Editor** Wang XL **E- Editor** Zheng XM



Surgery for rare aneurysm associated with colorectal cancer

Pei-Hua Lu, Guo-Qing Tao, Wei Shen, Bin Cai, Zhi-Yang Jiang, Jian Sun

Pei-Hua Lu, Guo-Qing Tao, Wei Shen, Bin Cai, Zhi-Yang Jiang, Jian Sun, Department of General Surgery, Wuxi People's Hospital of Nanjing Medical University, No. 299, Qingyang Road, Wuxi 214023, Jiangsu Province, China

Author contributions: Lu PH and Shen W contributed equally to this work; Lu PH, Tao GQ and Shen W designed research; Lu PH, Tao GQ, Cai B, Jiang ZY and Sun J performed research; Tao GQ and Cai B contributed new reagents/analytic tools; Lu PH and Shen W wrote the paper.

Correspondence to: Pei-Hua Lu, MMSC, Department of General Surgery, Wuxi People's Hospital of Nanjing Medical University, No. 299, Qingyang Road, Wuxi 214023, Jiangsu Province, China. lphyt1_1@yahoo.com.cn

Telephone: +86-510-85350091 Fax: +86-510-82828435

Received: June 18, 2009 Revised: August 18, 2009

Accepted: August 25, 2009

Published online: December 14, 2009

Gastroenterol 2009; 15(46): 5879-5881 Available from: URL: <http://www.wjgnet.com/1007-9327/15/5879.asp> DOI: <http://dx.doi.org/10.3748/wjg.15.5879>

INTRODUCTION

The surgical treatment of coexistent aortic aneurysm and colorectal cancer (CRC) needs special consideration. The controversy is mainly whether to treat both diseases or treat either of them alone. If we choose to treat both, should we treat them simultaneously or as staged procedures? For a two-stage process, there is a significant risk of aortic aneurysm rupture, and a single-stage procedure has the disadvantages of technical difficulty and graft infection^[1-3]. Lin *et al*^[4] have proposed that the treatment priority should be given to life-threatening lesions. Such cases include the presence of an abdominal aorta aneurysm with a dangerously large diameter and synchronous obstructing or perforating CRC. Veraldi *et al*^[5] have indicated that a one-stage procedure reduces the length of stay, avoids further surgical and anesthetic trauma, and does not increase graft infection.

We report a case of rectal cancer and concomitant aneurysm from the descending aorta to the common iliac artery, which is similar to a DeBakey type I aortic dissecting aneurysm, with a maximum diameter of 4.06 cm in the abdominal aortic segment and 6.51 cm in thoracic aortic segment. The patient was treated with the Dixon operation under conditions of controlled hypotension, without aneurysm rupture. At 2 years follow-up, the patient remained free of CRC and his aneurysm was stable.

CASE REPORT

A 69-year-old man underwent anal examination after complaining of a change in bowel habits and rectal bleeding 2 years ago. Anal examination revealed a cauliflower-like lesion located 7 cm from the edge of the anus, which involved more than half of the rectal circumference. Abdominal computed tomography (CT) revealed the presence of a rectal tumor, which almost obstructed the bowel lumen (Figure 1). Medical history included smoking, diabetes, hypertension and thoracoabdominal aortic aneurysm for 6 years. After admission, the patient underwent chest radiography, which confirmed concomitant aneurysm and tracheal

Abstract

The occurrence of concomitant aortic aneurysm and colorectal cancer is a rare medical entity, and controversy surrounds its optimal treatment. We report a case of rectal cancer and concomitant aneurysm from the ascending aorta to the common iliac artery. As with DeBakey type I aortic dissecting aneurysm, our patient was treated by rectal cancer resection, with preservation of the anus (Dixon operation) under controlled hypotension. Blood pressure was maintained at 80-90/50-60 mmHg and the pulse at 70-90 beats/min. The pathological examination of the surgical specimen showed a poorly differentiated T3N0 tumor. The patient had an uneventful recovery without aneurysm rupture, and was discharged from hospital on postoperative day 15 after 3 d adjuvant chemotherapy with oxaliplatin combined with calcium folinate and fluorouracil. The patient was given six courses of adjuvant chemotherapy in 6 mo, without recurrence or metastasis, and the aneurysm was still stable after 2 years follow-up.

© 2009 The WJG Press and Baishideng. All rights reserved.

Key words: Colorectal cancer; DeBakey I aneurysm; Aortic aneurysm

Peer reviewer: Frank I Tovey, OBE, ChM, FRCS, Honorary Research Fellow, Department of Surgery, University College London, London, United Kingdom

Lu PH, Tao GQ, Shen W, Cai B, Jiang ZY, Sun J. Surgery for rare aneurysm associated with colorectal cancer. *World J Gastroenterol* 2009 December 14; 15(46): 5879-5881



Figure 1 Thickening of the rectal wall, with narrowing of the lumen.



Figure 2 Chest radiography confirmed concomitant aneurysm and tracheal compression.

compression (Figure 2). Advanced CT angiography revealed large ectasia of the ascending aorta, aortic arch and descending aorta, with a maximum diameter of 6.51 cm and mural thrombosis. In addition, the aneurysm extended to the abdominal aorta, internal-organ arteries and the right common iliac artery, with a length of 60 cm and a diameter of 4.06 cm in the abdominal aortic aneurysm (Figure 3). Elevation of carcinoembryonic antigen and blood urea nitrogen to 11.79 ng/mL and 13.60 mmol/L, respectively, allowed diagnosis of digestive tract tumor and renal inadequacy. A complete preoperative metastatic work-up was negative.

Complicating aneurysm increases the difficulty of managing advanced malignant disease. We treated this patient with the Dixon operation under conditions of controlled hypotension, with minimal blood pressure fluctuation, and renal function protection and blood sugar regulation. Intraoperative blood pressure was maintained at 80-90/50-60 mmHg and the pulse at 70-90 beats/min. The surgery was completed in 1.5 h. Postoperative blood pressure was < 100/60 mmHg and was maintained between 100/60 mmHg and 110/70 mmHg by glyceryl trinitrate administered by mini pump. The pathological examination of the surgical specimen showed a poorly differentiated T3N0 tumor.

The patient had an uneventful recovery, and he was discharged from hospital on postoperative day 15 after 3 d adjuvant chemotherapy with oxaliplatin combined with calcium folinate and fluorouracil. The patient was given six courses of adjuvant chemotherapy without

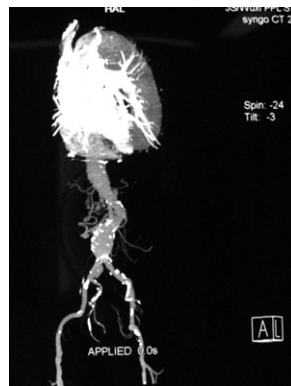


Figure 3 CT angiography of the aorta showed large ectasia from the ascending aorta to the right common iliac artery.

tumor recurrence or metastasis and the aneurysm was still stable after 2 years follow-up.

DISCUSSION

The concomitant occurrence of aortic aneurysm and CRC appears to be increasing, from 0.5% to 2%^[2], as a result of the increase in the two individual diseases, which is caused by increased life expectancy and improved imaging capability in revealing additional asymptomatic disease^[5]. Published studies are either small case series or limited retrospective reports^[3,6], therefore, the ideal treatment strategy represents a therapeutic dilemma^[2]. Initial aortic aneurysm repair followed by CRC resection exposes patients to the risk of tumor progression before resection, although no study has shown the oncological implications of such a delay. Resection of CRC followed by staged aneurysmorrhaphy carries a significant risk of aortic aneurysm rupture in the perioperative period, particularly when the aortic aneurysm is > 5 cm in diameter^[2]. Synchronous treatment of both lesions has been described but has the disadvantages of technical difficulties and graft infection, especially when the patient is in poor general condition.

Veraldi *et al*^[5] have found, from Medline 1987-2005, a total of 229 cases of associated aortic aneurysm and CRC. Four emergency operations have been reported, one for rupture of the aortic aneurysm, two for unstable aneurysm, and one for diastatic rupture of the cecum by the stenosing neoplasm in the sigmoid colon. Including these four, there were 25 patients in all with only one disease treated. In 24 of these, intervention was carried out for CRC because of the advanced stage of the disease or poor general condition of the patient. In the remaining case, because of postoperative death, only the aneurysm was treated. From January 1988 to May 2006, 14 patients with both diseases were observed and treated in the University of Verona^[5]. In one of these patients, only CRC was treated because of poor cardiac conditions, and the patient died after 2 mo from myocardial infarction.

Patients in poor general condition, who are treated for both diseases simultaneously or in stages face the risk of surgical fatality. Our patient had a rare true aneurysm similar to a dissecting aneurysm^[7]. Usually, dissecting aneurysm is caused by an intimal tear or interstitial hemorrhage and requires emergency surgery, and has

a low survival rate. He had been protected by blood pressure control since his aneurysm was diagnosed 8 years ago. CT revealed that the aneurysm was in a steady state, and the diameter and distribution of the aneurysm showed no obvious changes in these 8 years. The aneurysm in our patient began from the ascending aorta and extended to the common iliac artery, which is a very rare occurrence, and the prognosis was beyond our expectation. This kind of aneurysm usually requires Bentall's procedure and the elephant trunk technique for artificial blood vessel replacement. Bentall's procedure is a cardiac surgery technique that involves composite graft replacement of the aortic valve, aortic root and ascending aorta, with reimplantation of the coronary arteries into the graft. For the elephant trunk technique, excess tubular graft material is inserted during ascending aortic and arch repair, to facilitate the subsequent treatment of distal aortic aneurysms. These operations are extremely hazardous.

Davies *et al*^[8] have pointed out that treatment decisions should involve a balance between the risk of complications caused by the dilated aorta and those from the operation itself. The most devastating complication of an aneurysm is dissection, which leads to arterial occlusion and rupture and is almost invariably fatal. However, the risk of operation is also unmanageable. The risk of spinal cord injury, particularly in operations on the descending aorta^[9], is also significant. As a result of surgical risk and expense, our patient elected for conservative treatment for his aneurysm 8 years ago. When we were faced with the rare aortic aneurysm and CRC, we chose only to resect the CRC as a result of the great risks of the operation because of the patient's age, mural thrombosis, renal inadequacy, diabetes and hypertension. The postoperative recovery was satisfactory, with stable aneurysm and no cancer recurrence during follow-up.

Most surgeons agree that treatment priority should be focused on symptomatic or more life-threatening lesions in CRC and aneurysm. The largest retrospective study to date was reported by Lin *et al*^[4] in 2007. In that study, 108 patients with synchronous aortic aneurysm and CRC were identified, and 92 were treated for both lesions. Thirty-five patients had CRC removed first, following two patients with aneurysm rupture while 2/35 people with aneurysm rupture had CRC removed first. Twenty-three patients with endovascular aortic repair were associated with shorter recovery and lower postoperative mortality rate. This modality offered potential treatment benefits in patients with suitable anatomy who have concomitant CRC. However, the treatment should be offered with caution because of the risk of sigmoid ischemia caused by inferior mesenteric artery occlusion. Sometimes the

single operation decision may be a better one. In the study of Lin *et al*^[4], 16 patients were treated for only one disease, because of advanced CRC, hepatic metastasis or ruptured aneurysm, and these patients had a good prognosis. The most important thing is that treatment decisions should involve striking a balance between the risk of the disease itself and the complications of the operation. However, likely aneurysm rupture presents a great challenge, and urgent aneurysm repair is required to preserve the patient's life.

In summary, in patients with aortic aneurysm and CRC, priority should be given to the more life-threatening lesion. If patients have heart disease or are in poor general condition, attempting to treat both CRC and aneurysm carries a great risk, and it may be possible only to treat one of the conditions.

REFERENCES

- 1 Rivolta N, Piffaretti G, Tozzi M, Lomazzi C, Riva F, Alunno A, Boni L, Castelli P. Management of simultaneous abdominal aortic aneurysm and colorectal cancer: the rationale of minimally invasive approach. *Surg Oncol* 2007; **16** Suppl 1: S165-S167
- 2 Baxter NN, Noel AA, Cherry K, Wolff BG. Management of patients with colorectal cancer and concomitant abdominal aortic aneurysm. *Dis Colon Rectum* 2002; **45**: 165-170
- 3 Kiskinis D, Spanos C, Melas N, Eftymiopoulos G, Saratzis N, Lazaridis I, Gkinis G. Priority of resection in concomitant abdominal aortic aneurysm (AAA) and colorectal cancer (CRC): review of the literature and experience of our clinic. *Tech Coloproctol* 2004; **8** Suppl 1: s19-s21
- 4 Lin PH, Barshefs NR, Albo D, Kougias P, Berger DH, Huynh TT, LeMaire SA, Dardik A, Lee WA, Coselli JS. Concomitant colorectal cancer and abdominal aortic aneurysm: evolution of treatment paradigm in the endovascular era. *J Am Coll Surg* 2008; **206**: 1065-1073; discussion 1074-1075
- 5 Veraldi GF, Minicozzi AM, Leopardi F, Cipriani V, Genco B, Pacca R. Treatment of abdominal aortic aneurysm associated with colorectal cancer: presentation of 14 cases and literature review. *Int J Colorectal Dis* 2008; **23**: 425-430
- 6 Illuminati G, Calio' FG, D'Urso A, Lorusso R, Ceccanei G, Vietri F. Simultaneous repair of abdominal aortic aneurysm and resection of unexpected, associated abdominal malignancies. *J Surg Oncol* 2004; **88**: 234-239
- 7 Sayer D, Bratby M, Brooks M, Loftus I, Morgan R, Thompson M. Aortic morphology following endovascular repair of acute and chronic type B aortic dissection: implications for management. *Eur J Vasc Endovasc Surg* 2008; **36**: 522-529
- 8 Davies RR, Goldstein LJ, Coady MA, Tittle SL, Rizzo JA, Kopf GS, Elefteriades JA. Yearly rupture or dissection rates for thoracic aortic aneurysms: simple prediction based on size. *Ann Thorac Surg* 2002; **73**: 17-27; discussion 27-28
- 9 Griep RB, Ergin MA, Galla JD, Lansman S, Khan N, Quintana C, McCollough J, Bodian C. Looking for the artery of Adamkiewicz: a quest to minimize paraplegia after operations for aneurysms of the descending thoracic and thoracoabdominal aorta. *J Thorac Cardiovasc Surg* 1996; **112**: 1202-1213; discussion 1213-1215

S- Editor Tian L L- Editor O'Neill M E- Editor Zheng XM



LETTERS TO THE EDITOR

Lethal neuroendocrine carcinoma in ulcerative colitis

Hugh J Freeman, Ken Berean

Hugh J Freeman, Department of Medicine (Gastroenterology), University of British Columbia, Vancouver, BC, V6T 1W5, Canada

Ken Berean, Department of Pathology, University of British Columbia, Vancouver, BC, V6T 1W5, Canada

Author contributions: Freeman HJ and Berean K contributed equally to this work.

Correspondence to: Hugh J Freeman, MD, Professor, Department of Medicine (Gastroenterology), UBC Hospital, 2211 Wesbrook Mall, Vancouver, BC, V6T 1W5, Canada. hugfree@shaw.ca

Telephone: +1-604-8227216 **Fax:** +1-604-8227236

Received: October 19, 2009 **Revised:** November 7, 2009

Accepted: November 14, 2009

Published online: December 14, 2009

Abstract

A 48-year old male with longstanding and extensive pancolitis developed a high grade and rapidly lethal malignant lesion in the ascending colon characterized by a neuroendocrine carcinoma. Prior biopsies obtained from multiple sites in the colon during endoscopic surveillance were reported to show only inflammatory changes without dysplasia. Although operator-dependent, repeated endoscopic studies may have limitations during surveillance programs because the biological behavior of some colonic neoplastic lesions may have a rapid and very aggressive clinical course.

© 2009 The WJG Press and Baishideng. All rights reserved.

Key words: Colorectal cancer; Neuroendocrine carcinoma; Ulcerative colitis; Surveillance colonoscopy; Dysplasia

Peer reviewer: Boris Kirshtein, MD, Department of Surgery A, Soroka University Medical Center, POB 151, Beer Sheva 84101, Israel

Freeman HJ, Berean K. Lethal neuroendocrine carcinoma in ulcerative colitis. *World J Gastroenterol* 2009; 15(46): 5882-5883 Available from: URL: <http://www.wjgnet.com/1007-9327/15/5882.asp> DOI: <http://dx.doi.org/10.3748/wjg.15.5882>

TO THE EDITOR

An article recently published in *World Journal of Gastroenterology* concerning two patients, aged 35 and 77 years

respectively, with left-sided ulcerative colitis, was of special importance^[1]. In spite of colonoscopic and histologic follow-up in the previous year, both developed large neuroendocrine carcinomas in the rectum, and one patient was reported to have died due to multiple liver metastases.

We had a similar experience in a 48-year old male with longstanding extensive pan-ulcerative colitis for 16 years, first diagnosed in 1992. During the clinical course, his symptoms were initially treated and controlled with 5-aminosalicylates and corticosteroids. Endoscopic studies eventually showed virtually complete mucosal healing and biopsies showed only minimal inflammatory changes. No other immunosuppressive drugs or biological agents were used. During the last decade, he continued to use 5-aminosalicylates alone and remained completely asymptomatic. He underwent repeated surveillance colonoscopies with multiple site biopsies throughout the colon, which showed minimal inflammatory changes. Dysplasia was not reported in any colonic biopsy specimen. Approximately ten months after his last endoscopic procedure, he developed right upper quadrant abdominal pain. Blood studies, including liver chemistry tests, were normal, but an ultrasound and a computerized tomographic (CT) scan suggested possible liver metastases. In addition, the CT suggested a focal thickening area in the ascending colon. Colonoscopy confirmed an ulcerated sessile lesion. Histologic examination of the endoscopic biopsies showed an ulcerating tumor with predominant trabecular architecture and vascular stroma. The tumor cells had hyperchromatic nuclei with small nucleoli and scant pale-stained cytoplasm. Mitoses were numerous and there was abundant apoptosis, consistent with a high grade malignancy. Immunohistochemical stain for chromogranin and synaptophysin showed moderately intense staining of a neuroendocrine carcinoma. Tumor cells were positive for CK7 and negative for CK-20. Subsequent studies also showed pulmonary metastases and palliative chemotherapy was provided with FOLFOX B (12 cycles), but the disease remained progressive so FOLFIRI (10 cycles) was given. He died fourteen months after diagnosis.

Neuroendocrine carcinomas of the colon and rectum, accounting for less than 1% of colon and rectal cancers reported over more than a decade from Memorial Sloan-Kettering in New York, United States^[2], are very distinct from well-differentiated carcinoid tumors (or neuroendocrine tumors, using the World Health Organization schema discussed elsewhere^[3]) seen with inflammatory bowel disease but often detected incidentally during surgi-

cal treatment^[4,5]. About 70% of those classified as neuroendocrine carcinomas present with metastatic disease and appear to have a dismal prognosis with a reported overall mean survival of about ten months^[2]. These carcinomas have been subdivided into small and large cell types based on their histological and immunohistochemical features, similar to those of pulmonary neuroendocrine cancers with most positively stained for neuroendocrine markers, such as chromogranin, synaptophysin and/or neuron-specific enolase^[2]. Interestingly, in a report from Taiwan, there were 2 patients with small cell carcinomas that were believed to represent gastrointestinal metastases from a primary pulmonary site, possibly emphasizing the difficulty in defining their origin in some cases^[6].

Scattered reports are available on poorly differentiated neuroendocrine carcinoma with inflammatory bowel disease have been noted with an equally dismal outcome^[7-9]. In a recent report by Grassia *et al*^[1], however, surveillance studies were completed during the preceding year, and yet, large lesions in the most distal colon were eventually detected later. Although the present case of pancolitis developed a carcinoma in the ascending colon, the surveillance efforts for longstanding extensive colitis failed, in spite of multiple site endoscopic biopsies for dysplasia over many years. While colonoscopic evaluation, especially in surveillance programs, remains operator-dependent, these cases emphasize that repeated and systematic endoscopic and histological evaluations have limits because the underlying biological behavior of some colonic neoplastic lesions

may result in a rapidly developing and aggressive clinical course.

REFERENCES

- 1 Grassia R, Bodini P, Dizioli P, Staiano T, Iiritano E, Bianchi G, Buffoli F. Neuroendocrine carcinomas arising in ulcerative colitis: coincidences or possible correlations? *World J Gastroenterol* 2009; **15**: 4193-4195
- 2 Bernick PE, Klimstra DS, Shia J, Minsky B, Saltz L, Shi W, Thaler H, Guillem J, Paty P, Cohen AM, Wong WD. Neuroendocrine carcinomas of the colon and rectum. *Dis Colon Rectum* 2004; **47**: 163-169
- 3 Chetty R. Requiem for the term 'carcinoid tumour' in the gastrointestinal tract? *Can J Gastroenterol* 2008; **22**: 357-358
- 4 Greenstein AJ, Balasubramanian S, Harpaz N, Rizwan M, Sachar DB. Carcinoid tumor and inflammatory bowel disease: a study of eleven cases and review of the literature. *Am J Gastroenterol* 1997; **92**: 682-685
- 5 Freeman HJ. Appendiceal carcinoids in Crohn's disease. *Can J Gastroenterol* 2003; **17**: 43-46
- 6 Yang CJ, Hwang JJ, Kang WY, Chong IW, Wang TH, Sheu CC, Tsai JR, Huang MS. Gastro-intestinal metastasis of primary lung carcinoma: clinical presentations and outcome. *Lung Cancer* 2006; **54**: 319-323
- 7 Rubin A, Pandya PP. Small cell neuroendocrine carcinoma of the rectum associated with chronic ulcerative colitis. *Histopathology* 1990; **16**: 95-97
- 8 Yaziji H, Broghamer WL Jr. Primary small cell undifferentiated carcinoma of the rectum associated with ulcerative colitis. *South Med J* 1996; **89**: 921-924
- 9 Sigel JE, Goldblum JR. Neuroendocrine neoplasms arising in inflammatory bowel disease: a report of 14 cases. *Mod Pathol* 1998; **11**: 537-542

S-Editor Wang JL L-Editor Wang XL E-Editor Lin YP



ACKNOWLEDGMENTS

Acknowledgments to reviewers of *World Journal of Gastroenterology*

Many reviewers have contributed their expertise and time to the peer review, a critical process to ensure the quality of *World Journal of Gastroenterology*. The editors and authors of the articles submitted to the journal are grateful to the following reviewers for evaluating the articles (including those published in this issue and those rejected for this issue) during the last editing time period.

Luigi E Adinolfi, Professor, Division of Internal Medicine & Hepatology, Seconda Università di Napoli, Facoltà di Medicina e Chirurgia, Via Cotugno, 1 (c/o Ospedale Gesù e Maria), 80135 Naples, Italy

Alastair D Burt, Professor, Dean of Clinical Medicine, Faculty of Medical Sciences, Newcastle University, Room 13, Peacock Hall, Royal Victoria Infirmary, Newcastle upon Tyne NE1 4LP, United Kingdom

Dario Conte, Professor, GI Unit - IRCCS Osp. Maggiore, Chair of Gastroenterology, Via F. Sforza, 35, Milano 20122, Italy

William Dickey, Altnagelvin Hospital, Londonderry, BT47 6SB, Northern Ireland, United Kingdom

Abdellah Essaid, Professor, Hospital Ibn Sina, Rabat 10100, Morocco

Kazuhiko Hanazaki, MD, Professor and Chairman, Department of Surgery, Kochi Medical School, Kochi University, Kohasu, Okohcho, Nankoku, Kochi 783-8505, Japan

Marek Hartleb, Professor, Department of Gastroenterology, Silesian Medical School, ul. Medyków 14, Katowice 40-752, Poland

Imran Hassan, MD, Assistant Professor, Department of Surgery, SIU School of Medicine, 701 North Rutledge, PO Box 19638, Springfield, IL 62794, United States

Keiji Hirata, MD, Surgery 1, University of Occupational and Environmental Health, 1-1 Iseigaoka, Yahatanishi-ku, Kitakyushu 807-8555, Japan

Kevin Cheng-Wen Hsiao, MD, Assistant Professor, Colon and rectal surgery, Tri-Service General Hospital, No. 325, Sec. 2, Cheng-Kung Rd, Nei-Hu district, 114 Taipei, Taiwan, China

Dr. Limas Kupcinskas, Professor, Gastroenterology of Kaunas University of Medicine, Miekevicius 9, Kaunas LT 44307, Lithuania

Giovanni Maconi, MD, Department of Gastroenterology, 'L.Sacco' University Hospital, Via G.B. Grassi, 74, Milan 20157, Italy

Giulio Marchesini, Professor, Department of Internal Medicine and Gastroenterology, "Alma Mater Studiorum" University of Bologna, Policlinico S. Orsola, Via Massarenti 9, Bologna 40138, Italy

Sri P Misra, Professor, Gastroenterology, Moti Lal Nehru Medical College, Allahabad 211001, India

Emiko Mizoguchi, MD, PhD, Department of Medicine, Gastrointestinal Unit, GRJ 702, Massachusetts General Hospital, Boston, MA 02114, United States

Dr. Valerio Nobili, Liver Unit, Research Institute, Bambino Gesù Children's Hospital, S. Onofrio 4 Square, 00165 Rome, Italy

Josep M Pique, MD, Department of Gastroenterology, Hospital Clínic of Barcelona, Villarroel, 170, Barcelona 08036, Spain

Henning Schulze-Bergkamen, MD, Henning Schulze-Bergkamen, First Medical Department, University of Mainz, Langenbeckstr, 1, 55101 Mainz, Germany

Mitsuo Shimada, Professor, Department of Digestive and Pediatric Surgery, Tokushima University, Kuramoto 3-18-15, Tokushima 770-8503, Japan

Tadashi Shimoyama, MD, Hirosaki University, 5 Zaifu-cho, Hirosaki 036-8562, Japan

Rudolf E Stauber, Professor, Department of Internal Medicine, Medical University Graz, Division of Gastroenterology and Hepatology, Auenbruggerplatz 15, A-8036 Graz, Austria

Dr. Stefan Wirth, Professor, Children's Hospital, Heusnerstr. 40, Wuppertal 42349, Germany

Ming-Lung Yu, MD, PhD, Professor, Division of Hepatology, Department of Medicine, Kaohsiung Medical University Hospital, 100 Tzyou 1st Rd, Kaohsiung 807, Taiwan, China



Meetings

Events Calendar 2009

January 12-15, 2009
Hyatt Regency San Francisco, San Francisco, CA
Mouse Models of Cancer

January 21-24, 2009
Westin San Diego Hotel, San Diego, CA
Advances in Prostate Cancer Research

February 3-6, 2009
Carefree Resort and Villas, Carefree, AZ (Greater Phoenix Area)
Second AACR Conference
The Science of Cancer Health
Disparities in Racial/Ethnic Minorities and the Medically Underserved

February 7-10, 2009
Hyatt Regency Boston, Boston, MA
Translation of the Cancer Genome

February 8-11, 2009
Westin New Orleans Canal Place, New Orleans, LA
Chemistry in Cancer Research: A Vital Partnership in Cancer Drug Discovery and Development

February 13-16, 2009
Hong Kong Convention and Exhibition Centre, Hong Kong, China
19th Conference of the APASL
<http://www.apasl2009hongkong.org/en/home.aspx>

February 27-28, 2009
Orlando, Florida
AGAI/AASLD/ASGE/ACG Training Directors' Workshop

February 27-Mar 1, 2009
Vienna, Austria
EASL/AASLD Monothematic: Nuclear Receptors and Liver Disease
www.easl.ch/vienna2009

March 13-14, 2009
Phoenix, Arizona
AGAI/AASLD Academic Skills Workshop

March 20-24, 2009
Marriott Wardman Park Hotel
Washington, DC
13th International Symposium on Viral Hepatitis and Liver Disease

March 23-26, 2009
Glasgow, Scotland
British Society of Gastroenterology (BSC) Annual Meeting
Email: bsg@mailbox.ulcc.ac.uk

April 8-9, 2009
Silver Spring, Maryland
2009 Hepatotoxicity Special Interest Group Meeting

April 18-22, 2009
Colorado Convention Center, Denver, CO
AACR 100th Annual Meeting 2009

April 22-26, 2009
Copenhagen, Denmark
the 44th Annual Meeting of the European Association for the Study of the Liver (EASL)
<http://www.easl.ch/>

May 17-20, 2009
Denver, Colorado, USA
Digestive Disease Week 2009

May 29-June 2, 2009
Orange County Convention Center Orlando, Florida
45th ASCO Annual Meeting
www.asco.org/annualmeeting

May 30, 2009
Chicago, Illinois
Endpoints Workshop: NASH

May 30-June 4, 2009
McCormick Place, Chicago, IL
DDW 2009
<http://www.ddw.org>

June 17-19, 2009
North Bethesda, MD
Accelerating Anticancer Agent Development

June 20-26, 2009
Flims, Switzerland
Methods in Clinical Cancer Research (Europe)

June 24-27 2009
Barcelona, Spain
ESMO Conference: 11th World Congress on Gastrointestinal Cancer
www.worldgicancer.com

June 25-28, 2009
Beijing International Convention Center (BICC), Beijing, China
World Conference on Interventional Oncology
<http://www.chinamed.com.cn/wcio2009/>

July 5-12, 2009
Snowmass, CO, United States
Pathobiology of Cancer: The Edward A. Smuckler Memorial Workshop

July 17-24, 2009
Aspen, CO, United States
Molecular Biology in Clinical Oncology

August 1-7, 2009
Vail Marriott Mountain Resort, Vail, CO, United States
Methods in Clinical Cancer Research

August 14-16, 2009
Bell Harbor Conference Center, Seattle, Washington, United States
Practical Solutions for Successful Management
<http://www.asge.org/index.aspx?id=5040>

September 23-26, 2009
Beijing International Convention Center (BICC), Beijing, China
19th World Congress of the International Association of Surgeons, Gastroenterologists and Oncologists (IASGO)
<http://iasgo2009.org/en/index.shtml>

September 27-30, 2009
Taipei, China
Asian Pacific Digestive Week
<http://www.apdwcongress.org/2009/index.shtml>

October 7-11, 2009
Boston Park Plaza Hotel and Towers, Boston, MA, United States
Frontiers in Basic Cancer Research

October 13-16, 2009
Hyatt Regency Mission Bay Spa and Marina, San Diego, CA, United States
Advances in Breast Cancer Research: Genetics, Biology, and Clinical Applications

October 20-24, 2009
Versailles, France
Fifth International Conference on Tumor Microenvironment: Progression, Therapy, and Prevention

October 30-November 3, 2009
Boston, MA, United States
The Liver Meeting

November 15-19, 2009
John B. Hynes Veterans Memorial Convention Center, Boston, MA, United States
AACR-NCI-EORTC Molecular Targets and Cancer Therapeutics

November 21-25, 2009
London, UK
Gastro 2009 UEGW/World Congress of Gastroenterology
www.gastro2009.org



Global Collaboration for Gastroenterology

For the first time in the history of gastroenterology, an international conference will take place which joins together the forces of four pre-eminent organisations: Gastro 2009, UEGW/WCOG London. The United European Gastroenterology Federation (UEGF) and the World Gastroenterology Organisation (WGO), together with the World Organisation of Digestive Endoscopy (OMED) and the British Society of Gastroenterology (BSG), are jointly organising a landmark meeting in London from November 21-25, 2009. This collaboration will ensure the perfect balance of basic science and clinical practice, will cover all disciplines in gastroenterology (endoscopy, digestive oncology, nutrition, digestive surgery, hepatology, gastroenterology) and ensure a truly global context; all presented in the exciting setting of the city of London. Attendance is expected to reach record heights as participants are provided with a compact "all-in-one" programme merging the best of several GI meetings. Faculty and participants from all corners of the earth will merge to provide a truly global environment conducive to the exchange of ideas and the forming of friendships and collaborations.



Instructions to authors

GENERAL INFORMATION

World Journal of Gastroenterology (*World J Gastroenterol*) ISSN 1007-9327, DOI: 10.3748) is a weekly, peer-reviewed, online, open-access (OA) journal supported by an editorial board of 1126 experts in gastroenterology and hepatology from 60 countries.

The biggest advantage of the OA model is that it provides free, full-text articles in PDF and other formats for experts and the public without registration, which eliminates the obstacle that traditional journals possess and usually delays the speed of the propagation and communication of scientific research results. The open access model has been proven to be a true approach that may achieve the ultimate goal of the journals, i.e. the maximization of the value to the readers, authors and society.

Maximization of the value of the readers can be comprehended in two ways. First, the journal publishes articles that can be directly read or downloaded free of charge at any time, which attracts more readers. Second, the readers can apply the knowledge in clinical practice without delay after reading and understanding the information in their fields. In addition, the readers are encouraged to propose new ideas based on those of the authors, or to provide viewpoints that are different from those of the authors. Such discussions or debates among different schools of thought will definitely boost advancements and developments in the fields. Maximization of the value of the authors refers to the fact that these journals provide a platform that promotes the speed of propagation and communication to a maximum extent. This is also what the authors really need. Maximization of the value of the society refers to the maximal extent of the social influences and impacts produced by the high quality original articles published in the journal. This is also the main purpose of many journals around the world.

The major task of *WJG* is to report rapidly the most recent results in basic and clinical research on esophageal, gastrointestinal, liver, pancreas and biliary tract diseases, *Helicobacter pylori*, endoscopy and gastrointestinal surgery, including: gastrolesophageal reflux disease, gastrointestinal bleeding, infection and tumors; gastric and duodenal disorders; intestinal inflammation, microflora and immunity; celiac disease, dyspepsia and nutrition; viral hepatitis, portal hypertension, liver fibrosis, liver cirrhosis, liver transplantation, and metabolic liver disease; molecular and cell biology; geriatric and pediatric gastroenterology; diagnosis and screening, imaging and advanced technology.

The columns in *WJG* will include the following. (1) Editorial: to introduce and comment on major advances in rapidly developing areas and their importance. (2) Frontier: to review recent developments and comment on current research status in important fields, and propose directions for future research. (3) Topic Highlight: this column consists of three formats, including: (a) 10 invited review articles on a hot topic; (b) a commentary on common issues associated with this hot topic; and (c) a commentary on the 10 individual articles. (4) Observation: to update the development of old and new questions, highlight unsolved problems, and provide strategies for their resolution. (5) Guidelines for Basic Research: as suggested by the title. (6) Guidelines for Clinical Practice: to provide guidelines for clinical diagnosis and treatment. (7) Review: to review systematically the most representative progress and unsolved problems, comment on current research status, and make suggestions for future work. (8) Original Article: to report original and innovative findings. (9) Brief Article: to report briefly on novel and innovative findings. (10) Case Report: To report a rare or typical case. (11) Letters to the Editor: to discuss and reply to contributions published in *WJG*, or to introduce and comment on a controversial issue of general interest. (12) Book Reviews: to introduce and comment on quality monographs. (13) Guidelines: To introduce consensuses and guidelines reached by international and national academic authorities on basic research and clinical practice.

Indexed and abstracted in

Current Contents®/Clinical Medicine, Science Citation Index Expanded (also known as SciSearch®), Journal Citation Reports/Science Edition, Index Medicus, MEDLINE, PubMed, Chemical Abstracts, EMBASE/Excerpta Medica, Abstracts Journals, PubMed Central, Digital Object Identifier, CAB Abstracts, and Global Health. ISI, Thomson Reuters, 2008 Impact Factor: 2.081 (32/55 Gastroenterology and Hepatology).

Published by

The WJG Press and Baishideng

SUBMISSION OF MANUSCRIPTS

Manuscripts should be typed in 1.5 line spacing and 12 pt. Book Antiqua with ample margins. Number all pages consecutively, and start each of the following sections on a new page: Title Page, Abstract, Introduction, Materials and Methods, Results, Discussion, Acknowledgments,

References, Tables, Figures, and Figure Legends. Neither the editors nor the publisher are responsible for the opinions expressed by contributors. Manuscripts formally accepted for publication become the permanent property of The WJG Press and Baishideng, and may not be reproduced by any means, in whole or in part, without the written permission of both the authors and the publisher. We reserve the right to copy-edit and put onto our website accepted manuscripts. Authors should follow the relevant guidelines for the care and use of laboratory animals of their institution or national animal welfare committee. For the sake of transparency in regard to the performance and reporting of clinical trials, we endorse the policy of the International Committee of Medical Journal Editors to refuse to publish papers on clinical trial results if the trial was not recorded in a publicly-accessible registry at its outset. The only register now available, to our knowledge, is <http://www.clinicaltrials.gov> sponsored by the United States National Library of Medicine, and we encourage all potential contributors to register with it. However, in the event that other registers become available, you will be duly notified. A letter of recommendation from each author's organization should be provided with the contributed article to ensure the privacy and secrecy of research is protected.

Authors should retain one copy of the text, tables, photographs and illustrations because rejected manuscripts will not be returned to the corresponding author(s) and the editors will not be responsible for loss or damage to photographs and illustrations sustained during mailing.

Online submissions

Manuscripts should be submitted through the Online Submission System at: <http://wjg.wjgnet.com/wjg>. Authors are highly recommended to consult the ONLINE INSTRUCTIONS TO AUTHORS (<http://www.wjgnet.com/wjg/help/instructions.jsp>) before attempting to submit online. For assistance, authors encountering problems with the Online Submission System may send an email describing the problem to submission@wjgnet.com, or by telephone: +86-10-85381892. If you submit your manuscript online, do not make a postal contribution. Repeated online submission for the same manuscript is strictly prohibited.

MANUSCRIPT PREPARATION

All contributions should be written in English. All articles must be submitted using word-processing software. All submissions must be typed in 1.5 line spacing and 12 pt. Book Antiqua with ample margins. Style should conform to our house format. Required information for each of the manuscript sections is as follows:

Title page

Title: Title should be less than 12 words.

Running title: A short running title of less than 6 words should be provided.

Authorship: Authorship credit should be in accordance with the standard proposed by International Committee of Medical Journal Editors, based on (1) substantial contributions to conception and design, acquisition of data, or analysis and interpretation of data; (2) drafting the article or revising it critically for important intellectual content; and (3) final approval of the version to be published. Authors should meet conditions 1, 2, and 3.

Institution: Author names should be given first, then the complete name of institution, city, province and postcode. For example, Xu-Chen Zhang, Li-Xin Mei, Department of Pathology, Chengde Medical College, Chengde 067000, Hebei Province, China. One author may be represented from two institutions, for example, George Sgourakis, Department of General, Visceral, and Transplantation Surgery, Essen 45122, Germany; George Sgourakis, 2nd Surgical Department, Korgialenio-Benakio Red Cross Hospital, Athens 15451, Greece

Author contributions: The format of this section should be: Author contributions: Wang CL and Liang L contributed equally to this work; Wang CL, Liang L, Fu JF, Zou CC, Hong F and Wu XM designed the research; Wang CL, Zou CC, Hong F and Wu XM performed the research; Xue JZ and Lu JR contributed new reagents/analytic tools; Wang CL, Liang L and Fu JF analyzed the data; and Wang CL, Liang L and Fu JF wrote the paper.

Supportive foundations: The complete name and number of supportive foundations should be provided, e.g., Supported by National Natural Science Foundation of China, No. 30224801

Correspondence to: Only one corresponding address should be

provided. Author names should be given first, then author title, affiliation, the complete name of institution, city, postcode, province, country, and email. All the letters in the email should be in lower case. A space interval should be inserted between country name and email address. For example, Montgomery Bissell, MD, Professor of Medicine, Chief, Liver Center, Gastroenterology Division, University of California, Box 0538, San Francisco, CA 94143, United States. montgomery.bissell@ucsf.edu

Telephone and fax: Telephone and fax should consist of +, country number, district number and telephone or fax number, e.g., Telephone: +86-10-59080039, Fax: +86-10-85381893

Peer reviewers: All articles received are subject to peer review. Normally, three experts are invited for each article. Decision for acceptance is made only when at least two experts recommend an article for publication. Reviewers for accepted manuscripts are acknowledged in each manuscript, and reviewers of articles which were not accepted will be acknowledged at the end of each issue. To ensure the quality of the articles published in *WJG*, reviewers of accepted manuscripts will be announced by publishing the name, title/position and institution of the reviewer in the footnote accompanying the printed article. For example, reviewers: Professor Jing-Yuan Fang, Shanghai Institute of Digestive Disease, Shanghai, Affiliated Renji Hospital, Medical Faculty, Shanghai Jiaotong University, Shanghai, China; Professor Xin-Wei Han, Department of Radiology, The First Affiliated Hospital, Zhengzhou University, Zhengzhou, Henan Province, China; and Professor Anren Kuang, Department of Nuclear Medicine, Huaxi Hospital, Sichuan University, Chengdu, Sichuan Province, China.

Abstract

There are unstructured abstracts (no more than 256 words) and structured abstracts (no more than 480). The specific requirements for structured abstracts are as follows:

An informative, structured abstracts of no more than 480 words should accompany each manuscript. Abstracts for original contributions should be structured into the following sections. AIM (no more than 20 words): Only the purpose should be included. Please write the aim as the form of "To investigate/study/...; MATERIALS AND METHODS (no more than 140 words); RESULTS (no more than 294 words): You should present *P* values where appropriate and must provide relevant data to illustrate how they were obtained, e.g. 6.92 ± 3.86 vs 3.61 ± 1.67 , $P < 0.001$; CONCLUSION (no more than 26 words). Available from: <http://www.wjgnet.com/wjg/help/8.doc>

Key words

Please list 5-10 key words, selected mainly from *Index Medicus*, which reflect the content of the study.

Text

For articles of these sections, original articles, rapid communication and case reports, the main text should be structured into the following sections: INTRODUCTION, MATERIALS AND METHODS, RESULTS and DISCUSSION, and should include appropriate Figures and Tables. Data should be presented in the main text or in Figures and Tables, but not in both. The main text format of these sections, editorial, topic highlight, case report, letters to the editors, can be found at: <http://www.wjgnet.com/wjg/help/instructions.jsp>.

Illustrations

Figures should be numbered as 1, 2, 3, etc., and mentioned clearly in the main text. Provide a brief title for each figure on a separate page. Detailed legends should not be provided under the figures. This part should be added into the text where the figures are applicable. Figures should be either Photoshop or Illustrator files (in tiff, eps, jpeg formats) at high-resolution. Examples can be found at: <http://www.wjgnet.com/1007-9327/13/4520.pdf>; <http://www.wjgnet.com/1007-9327/13/4554.pdf>; <http://www.wjgnet.com/1007-9327/13/4891.pdf>; <http://www.wjgnet.com/1007-9327/13/4986.pdf>; <http://www.wjgnet.com/1007-9327/13/4498.pdf>. Keeping all elements compiled is necessary in line-art image. Scale bars should be used rather than magnification factors, with the length of the bar defined in the legend rather than on the bar itself. File names should identify the figure and panel. Avoid layering type directly over shaded or textured areas. Please use uniform legends for the same subjects. For example: Figure 1 Pathological changes in atrophic gastritis after treatment. A: ...; B: ...; C: ...; D: ...; E: ...; F: ...; G: ...etc. It is our principle to publish high resolution-figures for the printed and E-versions.

Tables

Three-line tables should be numbered 1, 2, 3, etc., and mentioned clearly in the main text. Provide a brief title for each table. Detailed legends should not be included under tables, but rather added into the text where applicable. The information should complement, but not duplicate the text. Use one horizontal line under the title, a second under column heads, and a third below the Table, above any footnotes. Vertical and italic lines should be omitted.

Notes in tables and illustrations

Data that are not statistically significant should not be noted. ^a*P* < 0.05, ^b*P* < 0.01 should be noted (*P* > 0.05 should not be noted). If there are other series of *P* values, ^c*P* < 0.05 and ^d*P* < 0.01 are used. A third series of *P* values can be expressed as ^e*P* < 0.05 and ^f*P* < 0.01. Other notes in tables or under illustrations should be expressed as ¹F, ²F, ³F; or sometimes as other symbols with a superscript (Arabic numerals) in the upper left corner. In a multi-curve illustration, each curve should be labeled with ●, ○, ■, □, ▲, △, etc., in a certain sequence.

Acknowledgments

Brief acknowledgments of persons who have made genuine contributions to the manuscript and who endorse the data and conclusions should be included. Authors are responsible for obtaining written permission to use any copyrighted text and/or illustrations.

REFERENCES

Coding system

The author should number the references in Arabic numerals according to the citation order in the text. Put reference numbers in square brackets in superscript at the end of citation content or after the cited author's name. For citation content which is part of the narration, the coding number and square brackets should be typeset normally. For example, "Crohn's disease (CD) is associated with increased intestinal permeability^[12,21]". If references are cited directly in the text, they should be put together within the text, for example, "From references^[19,22-24], we know that..."

When the authors write the references, please ensure that the order in text is the same as in the references section, and also ensure the spelling accuracy of the first author's name. Do not list the same citation twice.

PMID and DOI

Please provide PubMed citation numbers to the reference list, e.g. PMID and DOI, which can be found at <http://www.ncbi.nlm.nih.gov/sites/entrez?db=pubmed> and <http://www.crossref.org/SimpleTextQuery/>, respectively. The numbers will be used in E-version of this journal.

Style for journal references

Authors: the name of the first author should be typed in bold-faced letters. The family name of all authors should be typed with the initial letter capitalized, followed by their abbreviated first and middle initials. (For example, Lian-Sheng Ma is abbreviated as Ma LS, Bo-Rong Pan as Pan BR). The title of the cited article and italicized journal title (journal title should be in its abbreviated form as shown in PubMed), publication date, volume number (in black), start page, and end page [PMID: 11819634 DOI: 10.3748/wjg13.5396].

Style for book references

Authors: the name of the first author should be typed in bold-faced letters. The surname of all authors should be typed with the initial letter capitalized, followed by their abbreviated middle and first initials. (For example, Lian-Sheng Ma is abbreviated as Ma LS, Bo-Rong Pan as Pan BR) Book title. Publication number. Publication place: Publication press, Year: start page and end page.

Format

Journals

English journal article (list all authors and include the PMID where applicable)

- 1 Jung EM, Clevert DA, Schreyer AG, Schmitt S, Rennert J, Kubale R, Feuerbach S, Jung F. Evaluation of quantitative contrast harmonic imaging to assess malignancy of liver tumors: A prospective controlled two-center study. *World J Gastroenterol* 2007; **13**: 6356-6364 [PMID: 18081224 DOI: 10.3748/wjg13.6356]

Chinese journal article (list all authors and include the PMID where applicable)

- 2 Lin GZ, Wang XZ, Wang P, Lin J, Yang FD. Immunologic effect of Jianpi Yishen decoction in treatment of Pixu-diarrhoea. *Shijie Huaren Xiaohua Zazhi* 1999; **7**: 285-287

In press

- 3 Tian D, Araki H, Stahl E, Bergelson J, Kreitman M. Signature of

balancing selection in Arabidopsis. *Proc Natl Acad Sci USA* 2006; In press

Organization as author

- 4 **Diabetes Prevention Program Research Group.** Hypertension, insulin, and proinsulin in participants with impaired glucose tolerance. *Hypertension* 2002; **40**: 679-686 [PMID: 12411462 PMCID:2516377 DOI:10.1161/01.HYP.0000035706.28494.09]

Both personal authors and an organization as author

- 5 **Vallancien G**, Emberton M, Harving N, van Moorselaar RJ; Alf-One Study Group. Sexual dysfunction in 1274 European men suffering from lower urinary tract symptoms. *J Urol* 2003; **169**: 2257-2261 [PMID: 12771764 DOI:10.1097/01.ju.0000067940.76090.73]

No author given

- 6 21st century heart solution may have a sting in the tail. *BMJ* 2002; **325**: 184 [PMID: 12142303 DOI:10.1136/bmj.325.7357.184]

Volume with supplement

- 7 **Geraud G**, Spierings EL, Keywood C. Tolerability and safety of frovatriptan with short- and long-term use for treatment of migraine and in comparison with sumatriptan. *Headache* 2002; **42** Suppl 2: S93-99 [PMID: 12028325 DOI:10.1046/j.1526-4610.42.s2.7.x]

Issue with no volume

- 8 **Banit DM**, Kaufer H, Hartford JM. Intraoperative frozen section analysis in revision total joint arthroplasty. *Clin Orthop Relat Res* 2002; **(401)**: 230-238 [PMID: 12151900 DOI:10.1097/00003086-200208000-00026]

No volume or issue

- 9 Outreach: Bringing HIV-positive individuals into care. *HRSA Careaction* 2002; 1-6 [PMID: 12154804]

Books

Personal author(s)

- 10 **Sherlock S**, Dooley J. Diseases of the liver and biliary system. 9th ed. Oxford: Blackwell Sci Pub, 1993: 258-296

Chapter in a book (list all authors)

- 11 **Lam SK**. Academic investigator's perspectives of medical treatment for peptic ulcer. In: Swabb EA, Azabo S. Ulcer disease: investigation and basis for therapy. New York: Marcel Dekker, 1991: 431-450

Author(s) and editor(s)

- 12 **Breedlove GK**, Schorfheide AM. Adolescent pregnancy. 2nd ed. Wieczorek RR, editor. White Plains (NY): March of Dimes Education Services, 2001: 20-34

Conference proceedings

- 13 **Harnden P**, Joffe JK, Jones WG, editors. Germ cell tumours V. Proceedings of the 5th Germ cell tumours Conference; 2001 Sep 13-15; Leeds, UK. New York: Springer, 2002: 30-56

Conference paper

- 14 **Christensen S**, Oppacher F. An analysis of Koza's computational effort statistic for genetic programming. In: Foster JA, Lutton E, Miller J, Ryan C, Tettamanzi AG, editors. Genetic programming-EuroGP 2002: Proceedings of the 5th European Conference on Genetic Programming; 2002 Apr 3-5; Kinsdale, Ireland. Berlin: Springer, 2002: 182-191

Electronic journal (list all authors)

- 15 Morse SS. Factors in the emergence of infectious diseases. *Emerg Infect Dis* serial online, 1995-01-03, cited 1996-06-05; 1(1): 24 screens. Available from: URL: <http://www.cdc.gov/ncidod/EID/eid.htm>

Patent (list all authors)

- 16 **Pagedas AC**, inventor; Ancel Surgical R&D Inc, assignee. Flexible endoscopic grasping and cutting device and positioning tool assembly. United States patent US 20020103498. 2002 Aug 1

Statistical data

Write as mean \pm SD or mean \pm SE.

Statistical expression

Express *t* test as *t* (in italics), *F* test as *F* (in italics), chi square test as χ^2 (in Greek), related coefficient as *r* (in italics), degree of freedom as *v* (in Greek), sample number as *n* (in italics), and probability as *P* (in italics).

Units

Use SI units. For example: body mass, *m* (B) = 78 kg; blood pressure, *p* (B) = 16.2/12.3 kPa; incubation time, *t* (incubation) = 96 h, blood glucose concentration, *c* (glucose) 6.4 ± 2.1 mmol/L; blood CEA mass concentration, *p* (CEA) = 8.6 ± 24.5 μ g/L; CO₂ volume fraction, 50 mL/L CO₂, not 5% CO₂; likewise for 40 g/L formaldehyde, not 10% formalin; and mass fraction, 8 ng/g, etc. Arabic numerals such as 23, 243, 641 should be read 23243641.

The format for how to accurately write common units and quantums can be found at: <http://www.wjgnet.com/wjg/help/14.doc>.

Abbreviations

Standard abbreviations should be defined in the abstract and on first mention in the text. In general, terms should not be abbreviated unless they are used repeatedly and the abbreviation is helpful to the reader. Permissible abbreviations are listed in Units, Symbols and Abbreviations: A Guide for Biological and Medical Editors and Authors (Ed. Baron DN, 1988) published by The Royal Society of Medicine, London. Certain commonly used abbreviations, such as DNA, RNA, HIV, LD50, PCR, HBV, ECG, WBC, RBC, CT, ESR, CSF, IgG, ELISA, PBS, ATP, EDTA, mAb, can be used directly without further explanation.

Italics

Quantities: *t* time or temperature, *c* concentration, *A* area, *l* length, *m* mass, *V* volume.

Genotypes: *gyrA*, *arg I*, *c myc*, *c fos*, etc.

Restriction enzymes: *EcoRI*, *HindI*, *BamHI*, *Kbo I*, *Kpn I*, etc.

Biology: *H. pylori*, *E. coli*, etc.

SUBMISSION OF THE REVISED MANUSCRIPTS AFTER ACCEPTED

Please revise your article according to the revision policies of *WJG*. The revised version including manuscript and high-resolution image figures (if any) should be copied on a floppy or compact disk. The author should send the revised manuscript, along with printed high-resolution color or black and white photos, copyright transfer letter, and responses to the reviewers by courier (such as EMS/DHL).

Editorial Office

World Journal of Gastroenterology

Editorial Department: Room 903, Building D, Ocean International Center,

No.62 Dongsihuan Zhonglu, Chaoyang District, Beijing 100025, China

Telephone: +86-10-59080039

Fax: +86-10-85381893

E-mail: wjg@wjgnet.com

<http://www.wjgnet.com>

Language evaluation

The language of a manuscript will be graded before it is sent for revision.

- (1) Grade A: priority publishing;
- (2) Grade B: minor language polishing;
- (3) Grade C: a great deal of language polishing needed;
- (4) Grade D: rejected. Revised articles should reach Grade A or B.

Copyright assignment form

Please download a Copyright assignment form from <http://www.wjgnet.com/wjg/help/10.doc>.

Responses to reviewers

Please revise your article according to the comments/suggestions provided by the reviewers. The format for responses to the reviewers' comments can be found at: <http://www.wjgnet.com/wjg/help/9.doc>.

Proof of financial support

For paper supported by a foundation, authors should provide a copy of the document and serial number of the foundation.

Links to documents related to the manuscript

WJG will be initiating a platform to promote dynamic interactions between the editors, peer reviewers, readers and authors. After a manuscript is published online, links to the PDF version of the submitted manuscript, the peer-reviewers' report and the revised manuscript will be put online. Readers can make comments on the peer reviewer's report, authors' responses to peer reviewers, and the revised manuscript. We hope that authors will benefit from this feedback and be able to revise the manuscript accordingly in a timely manner.

Science news releases

Authors of accepted manuscripts are suggested to write a science news item to promote their articles. The news will be released rapidly at EurekAlert/AAAS (<http://www.eurekalert.org>). The title for news items should be less than 90 characters; the summary should be less than 75 words; and main body less than 500 words. Science news items should be lawful, ethical, and strictly based on your original content with an attractive title and interesting pictures.

Publication fee

Authors of accepted articles must pay a publication fee.

EDITORIAL, TOPIC HIGHLIGHTS, BOOK REVIEWS and LETTERS TO THE EDITOR are published free of charge.